

N77-79521

NASA CR-114715

**FOR EARLY DOMESTIC DISSEMINATION**

Because of its significant early commercial potential, this information, which has been developed under a U.S. Government program, is being disseminated within the United States in advance of general publication. This information may be duplicated and used by the recipient with the express limitation that it not be published. Release of this information to other domestic parties by the recipient shall be made subject to these limitations. Foreign release may be made only with prior NASA approval and appropriate export licenses. This legend shall be marked on any reproduction of this information in whole or in part. Date for general release May 1, 1977.

**A METHOD FOR PREDICTING THE STABILITY CHARACTERISTICS  
OF AN ELASTIC AIRPLANE**

**Volume IV—FLEXSTAB 1.02.00 Demonstration Cases and Results**

By G. M. Dornfeld, K. G. Bhatia, R. E. Maier,  
R. N. Snow, and D. A. Van Rossum

D6-41064-4  
October 1974

Distribution of this report is provided in the interest of information exchange. Responsibility for the contents resides in the author or organization that prepared it.

Prepared Under Contract No. NAS2-5006, and  
NAS2-7729 by

Boeing Commercial Airplane Company  
Seattle, Washington 98124

and

Boeing Computer Services, Inc.  
Seattle, Washington 98124

for

**AMES RESEARCH CENTER  
NATIONAL AERONAUTICS AND SPACE ADMINISTRATION**



.

.

.

.

.

1. Report No. NAS2-5006, NAS2-7729	2. Government Accession No.	3. Recipient's Catalog No.	
4. Title and Subtitle <b>A METHOD FOR PREDICTING THE STABILITY CHARACTERISTICS OF AN ELASTIC AIRPLANE—Volume IV: FLEXSTAB 1.02.00 Demonstration Cases and Results</b>		5. Report Date October 1974	6. Performing Organization Code
		8. Performing Organization Report No. D6-41064-4	
7. Author(s) G. M. Dornfeld, K. G. Bhatia, R. E. Maier, R. N. Snow, and D. A. Van Rossum		10. Work Unit No. NAS2-5006, NAS2-7729	11. Contract or Grant No. NAS2-5006
9. Performing Organization Name and Address Boeing Commercial Airplane Company Seattle, Washington 98124 and Boeing Computer Services, Inc. Seattle, Washington 98124		13. Type of Report and Period Covered Contractor Report	
		14. Sponsoring Agency Code	
12. Sponsoring Agency Name and Address National Aeronautics and Space Administration Washington, D.C. 20546		15. Supplementary Notes	
16. Abstract The application of the FLEXSTAB system to analyze airplane configurations is explained with examples of demonstration cases: Dart Model I, Dart Model II, the Boeing 707-320B, the Boeing 2707-300PT(SST), and the Lockheed YF-12A. The Dart Models I and II are two very simple configurations used to illustrate the program input and usage. The modeling and the preparation of input data for the 707, SST and YF-12A configurations is discussed, and the selected results are presented in a tabular form. A comparison of results with other sources is included for the 707 and SST models. In addition, a comparison of the FLEXSTAB results for pressure and force distribution with the experimental results for an arrow-wing configuration (obtained under NASA Contract NAS1-12875) are included.			
17. Key Words (Suggested by Author(s)) Aerodynamics, Aeroelasticity, Dynamics, Flexibility, Stability and Control, Stability, Structures		18. Distribution Statement Unclassified—Unlimited	
19. Security Classif. (of this report) Unclassified	20. Security Classif. (of this page) Unclassified	21. No. of Pages 248	22. Price*



## CONTENTS

	Page
1.0 INTRODUCTION . . . . .	1-1
2.0 USE OF THE SOLUTION-ORIENTED INPUT OPTIONS . . . . .	2-1
2.1 Discussion of Each Solution-oriented Option . . . . .	2-1
2.1.1 GD Program Solution-oriented Options . . . . .	2-1
2.1.2 AIC Program Solution-oriented Options . . . . .	2-1
2.1.3 ISIC Program Solution-oriented Options . . . . .	2-10
2.1.4 NM Program Solution-oriented Options . . . . .	2-10
2.1.5 ESIC Program Solution-oriented Options . . . . .	2-11
2.1.6 SD&SS Program Solution-oriented Options . . . . .	2-11
2.1.7 TH Program Solution-oriented Options . . . . .	2-14
2.1.8 ALOADS Program Solution-oriented Options . . . . .	2-15
3.0 AIRPLANE DEFINITION PROGRAMS . . . . .	3-1
3.1 Summary of Input Requirements . . . . .	3-3
3.1.1 Geometry Definition (GD) Program . . . . .	3-3
Slender Body input . . . . .	3-3
Interference Body input . . . . .	3-3
Thin Body input . . . . .	3-4
3.1.2 Geometry Definition Plot (GD PLOT) Program . . . . .	3-4
3.1.3 Aerodynamic Influence Coefficient (AIC) Program . . . . .	3-4
AIC input . . . . .	3-4
3.1.4 AIC Matrix Correction (CAIC) Program . . . . .	3-5
3.1.5 Internal Structural Influence Coefficient (ISIC) Program . . . . .	3-5
General information . . . . .	3-5
Slender Body input . . . . .	3-5
Thin Body input . . . . .	3-6
3.1.6 Elastic Axis Plot (EAPLOT) Program . . . . .	3-6
3.1.7 Normal Modes (NM) Program . . . . .	3-6
3.1.8 Normal Modes Plot (NMPLOT) Program . . . . .	3-6
3.1.9 External Structural Influence Coefficient (ESIC) Program . . . . .	3-6
General information . . . . .	3-7
Slender Body input . . . . .	3-7
Thin Body input . . . . .	3-7
3.2 Dart Model I Demonstration Case . . . . .	3-8
3.2.1 Geometry Definition Program—GD-1 . . . . .	3-8
Reference Axis System placement . . . . .	3-8
Fuselage definition . . . . .	3-11
Wing definition . . . . .	3-14
Fuselage Interference Body . . . . .	3-18
Geometry Definition Plot . . . . .	3-21

## CONTENTS—Continued

	Page
3.2.2 Aerodynamic Influence Coefficient Program—AIC-1 . . . . .	3-25
AIC input . . . . .	3-25
3.2.3 Internal Structural Influence Coefficient Program—ISIC-1 . . . . .	3-24
General information . . . . .	3-25
Fuselage definition . . . . .	3-27
Wing definition . . . . .	3-27
3.2.4 Normal Modes Program—NM-1 . . . . .	3-29
3.2.5 External Structural Influence Coefficient Program—ESIC-1 . . . . .	3-29
General information . . . . .	3-33
Fuselage definition . . . . .	3-33
Wing definition . . . . .	3-34
3.3 Dart Model II Demonstration Case . . . . .	3-35
3.3.1 Geometry Definition Program—GD-2 . . . . .	3-35
Fuselage definition . . . . .	3-35
Wing pod definition . . . . .	3-35
Fuselage Interference Body . . . . .	3-35
Wing pod Interference Bodies . . . . .	3-39
Wing definition . . . . .	3-42
Geometry Definition Plot . . . . .	3-44
3.3.2 Aerodynamic Influence Coefficient Program—AIC-2 . . . . .	3-44
AIC input . . . . .	3-44
3.4 Boeing 707-320B Demonstration Case . . . . .	3-47
3.4.1 Geometry Definition Program—GD-3A and GD-3B . . . . .	3-47
Fuselage definition . . . . .	3-47
Wing definition . . . . .	3-49
Fuselage Interference Body . . . . .	3-54
Horizontal stabilizer . . . . .	3-56
Vertical tail . . . . .	3-59
Struts . . . . .	3-59
Nacelle definition . . . . .	3-62
Nacelle Interference Bodies . . . . .	3-64
3.4.2 Geometry Definition Plot Program—GD PLOT-3 . . . . .	3-65
3.4.3 Aerodynamic Influence Coefficient Program—AIC-3 . . . . .	3-65
AIC input . . . . .	3-65
3.4.4 Internal Structural Influence Coefficient Program—ISIC-3 . . . . .	3-65
General information . . . . .	3-65
Fuselage definition . . . . .	3-68
Wing definition . . . . .	3-68
Vertical tail and horizontal stabilizer definitions . . . . .	3-70
Strut definitions . . . . .	3-73
Nacelle definitions . . . . .	3-75
Refinement of the 707-320B mass data . . . . .	3-76

## CONTENTS—Continued

	Page
3.4.5 Elastic Axis Plot Program—EAPLOT-3 . . . . .	3-76
3.4.6 Normal Modes Program—NM-3 . . . . .	3-76
3.4.7 Normal Modes Plot Program—NMPLOT-3 . . . . .	3-76
3.5 Boeing 2707-300PT (SST) Demonstration Case . . . . .	3-87
3.5.1 Geometry Definition Program—GD-4 . . . . .	3-87
Fuselage definition . . . . .	3-87
Wing definition . . . . .	3-88
Fuselage Interference Body definition . . . . .	3-90
Horizontal stabilizer definition . . . . .	3-92
Nacelle definition . . . . .	3-95
3.5.2 Geometry Definition Plot Program—GDPLLOT-4 . . . . .	3-95
3.5.3 Aerodynamic Influence Coefficient Program—AIC-4 . . . . .	3-96
AIC input . . . . .	3-96
3.5.4 AIC Matrix Correction Program—CAIC-4 . . . . .	3-96
3.5.5 External Structural Influence Coefficient Program—ESIC-4 . . . . .	3-97
General information . . . . .	3-97
Fuselage definition . . . . .	3-100
Wing definition . . . . .	3-100
Horizontal stabilizer definition . . . . .	3-103
Nacelle definitions . . . . .	3-104
Airplane mass data . . . . .	3-104
3.6 Lockheed YF-12A Demonstration Case . . . . .	3-105
3.6.1 Geometry Definition Program—GD-5A and GD-5B . . . . .	3-105
Fuselage definition . . . . .	3-105
Nacelle definition . . . . .	3-107
Fuselage Interference Body . . . . .	3-108
Nacelle Interference Body . . . . .	3-108
Chine definition . . . . .	3-110
Inboard wing definition . . . . .	3-112
Outboard wing definition . . . . .	3-112
Vertical tail definition . . . . .	3-113
Nacelle ventral fin definition . . . . .	3-113
Supersonic fuselage definition . . . . .	3-114
Supersonic nacelle definition . . . . .	3-114
3.6.2 Geometry Definition Plot Program . . . . .	3-114
3.6.3 Aerodynamic Influence Coefficient Program—AIC-5A and AIC-5B . . . . .	3-116
AIC input . . . . .	3-116

## CONTENTS—Continued

	Page
3.6.4 External Structural Influence Coefficient Program—ESIC-5A and ESIC-5B . . . . .	3-116
General information . . . . .	3-118
Fuselage definition . . . . .	3-118
Nacelle definition . . . . .	3-119
Wing definition . . . . .	3-119
Vertical tail and ventral fin definition . . . . .	3-119
Supersonic structural definition . . . . .	3-120
 4.0 AIRPLANE ANALYSIS PROGRAMS . . . . .	 4-1
4.1 Summary of Input Requirements . . . . .	4-1
4.1.1 Stability Derivatives and Static Stability (SD&SS) Program . . . . .	4-1
\$General Specifications . . . . .	4-1
\$Matrix Print List . . . . .	4-3
\$SDSS Matrix Output List . . . . .	4-3
\$Thrust Data . . . . .	4-3
\$Gyroscopic Data . . . . .	4-3
\$Control Surface Data . . . . .	4-3
\$Stability Problem Data . . . . .	4-3
\$Wind Tunnel Data . . . . .	4-4
\$Perturbation Data . . . . .	4-5
\$Dynamic Analysis . . . . .	4-5
\$Exterior Influence Data . . . . .	4-5
\$Structural Data . . . . .	4-5
\$Pressure Data . . . . .	4-5
\$Area Ratio Data . . . . .	4-5
\$Recycle Data . . . . .	4-5
4.1.2 Pressure Distribution Plot (PD PLOT) Program . . . . .	4-6
4.1.3 Time Histories (TH) Program . . . . .	4-6
\$Integration Specifications . . . . .	4-6
\$Initial Conditions . . . . .	4-6
\$Accuracy Criteria . . . . .	4-6
\$Print Specifications . . . . .	4-6
\$Plot Specifications . . . . .	4-6
\$Maximum Euler Angles . . . . .	4-6
\$Elastic Perturbation Data . . . . .	4-6
\$Tabular Wind Tunnel Data . . . . .	4-6
\$Gust Data . . . . .	4-7
4.1.4 Time Histories Plot (TH PLOT) Program . . . . .	4-7
4.1.5 Structural Loads (SLOADS) Program . . . . .	4-7
4.1.6 Air Loads (ALOADS) Program . . . . .	4-7



**CONTENTS—Continued**

	Page
4.2 Dart Model I Demonstration Case . . . . .	4-8
4.2.1 Stability Derivatives and Static Stability Program—SDSS-1A . . . . .	4-8
\$General Specifications . . . . .	4-8
\$Matrix Print List . . . . .	4-9
\$Control Surface Data . . . . .	4-9
\$Stability Problem Data . . . . .	4-9
\$Perturbation Data . . . . .	4-10
4.2.2 Stability Derivatives and Static Stability Program—SDSS-1B . . . . .	4-10
\$General Specifications . . . . .	4-10
4.2.3 Stability Derivatives and Static Stability Program—SDSS-1C . . . . .	4-10
\$General Specifications . . . . .	4-10
\$Matrix Print List . . . . .	4-10
\$Perturbation Data . . . . .	4-10
4.2.4 Stability Derivatives and Static Stability Program—SDSS-1D . . . . .	4-10
\$General Specifications . . . . .	4-11
4.2.5 Time Histories Program—TH-1 . . . . .	4-11
\$Integration Specifications . . . . .	4-11
\$Initial Conditions . . . . .	4-11
\$Print Specifications . . . . .	4-11
\$Gust Data . . . . .	4-11
4.2.6 Structural Loads Program—SLOADS-1 . . . . .	4-11
4.2.7 Air Loads Program—ALoads-1 . . . . .	4-11
4.3 Dart Model II Demonstration Case . . . . .	4-12
4.3.1 Stability Derivatives and Static Stability Program—SDSS-2 . . . . .	4-12
\$General Specifications . . . . .	4-12
\$Control Surface Data . . . . .	4-12
\$Stability Problem Data . . . . .	4-12
\$Perturbation Data . . . . .	4-13
\$Structural Data . . . . .	4-13
4.4 Boeing 707-320B Demonstration Case . . . . .	4-14
4.4.1 Stability Derivatives and Static Stability Program—SDSS-3A . . . . .	4-14
\$General Specifications . . . . .	4-14
\$Matrix Print List . . . . .	4-14
\$Thrust Data . . . . .	4-14
\$Control Surface Data . . . . .	4-15
\$Stability Problem Data . . . . .	4-15
\$Perturbation Data . . . . .	4-15
\$Dynamic Analysis . . . . .	4-16
\$Recycle Data . . . . .	4-16

## CONTENTS—Continued

	Page
4.4.2 Stability Derivatives and Static Stability Program—SDSS-3B . . .	4-16
\$General Specifications . . . . .	4-16
\$Matrix Print List . . . . .	4-16
\$Thrust Data . . . . .	4-16
\$Control Surface Data . . . . .	4-16
\$Stability Problem Data . . . . .	4-17
\$Wind Tunnel Data . . . . .	4-17
\$Perturbation Data . . . . .	4-17
\$Dynamic Analysis . . . . .	4-18
\$Structural Data . . . . .	4-18
4.4.3 Pressure Distribution Plot Program—PDLOT-3 . . . . .	4-18
4.4.4 Time Histories Program—TH-3 . . . . .	4-18
\$Integration Specifications . . . . .	4-18
\$Initial Conditions . . . . .	4-18
\$Print Specifications . . . . .	4-18
\$Plot Specifications . . . . .	4-18
\$Integration Specifications . . . . .	4-19
\$Initial Conditions . . . . .	4-19
\$Print Specifications . . . . .	4-19
\$Plot Specifications . . . . .	4-19
\$Elastic Perturbation Data . . . . .	4-19
\$Integration Specifications . . . . .	4-19
\$Initial Conditions . . . . .	4-19
\$Print Specifications . . . . .	4-19
\$Plot Specifications . . . . .	4-19
\$Elastic Perturbation Data . . . . .	4-19
\$Integration Specifications . . . . .	4-19
\$Initial Conditions . . . . .	4-19
\$Print Specifications . . . . .	4-19
\$Plot Specifications . . . . .	4-19
\$Elastic Perturbation Data . . . . .	4-20
\$Integration Specifications . . . . .	4-20
\$Initial Conditions . . . . .	4-20
\$Print Specifications . . . . .	4-20
\$Plot Specifications . . . . .	4-20
\$Elastic Perturbation Data . . . . .	4-20
\$Gust Data . . . . .	4-20
4.4.5 Time Histories Plot Program—THPLOT-3 . . . . .	4-20
4.4.6 Structural Loads Program—SLOADS-3 . . . . .	4-20

## CONTENTS—Continued

	Page
4.5 Boeing 2707-300PT (SST) Demonstration Case . . . . .	4-21
4.5.1 Stability Derivatives and Static Stability Program—SDSS-4A . . . . .	4-21
\$General Specifications . . . . .	4-21
\$Matrix Print List . . . . .	4-21
\$Thrust Data . . . . .	4-21
\$Control Surface Data . . . . .	4-22
\$Stability Problem Data . . . . .	4-22
4.5.2 Stability Derivatives and Static Stability Program—SDSS-4B . . . . .	4-22
\$General Specifications . . . . .	4-22
\$Matrix Print List . . . . .	4-22
\$Thrust Data . . . . .	4-22
\$Control Surface Data . . . . .	4-23
\$Stability Problem Data . . . . .	4-23
\$Perturbation Data . . . . .	4-23
\$Dynamic Analysis . . . . .	4-23
4.5.3 Stability Derivatives and Static Stability Program—SDSS-4C . . . . .	4-23
4.5.4 Air Loads Program—ALoads-4 . . . . .	4-24
4.6 YF-12A Demonstration Case . . . . .	4-25
4.6.1 Stability Derivatives and Static Stability Program—SDSS-5A . . . . .	4-25
\$General Specifications . . . . .	4-25
\$Matrix Print List . . . . .	4-25
\$Thrust Data . . . . .	4-25
\$Control Surface Data . . . . .	4-26
\$Stability Problem Data . . . . .	4-26
\$Area Ratio Data . . . . .	4-26
\$Recycle Data . . . . .	4-26
4.6.2 Stability Derivatives and Static Stability Program—SDSS-5B . . . . .	4-27
\$General Specifications . . . . .	4-27
\$Matrix Print List . . . . .	4-27
\$Thrust Data . . . . .	4-27
\$Control Surface Data . . . . .	4-27
\$Stability Problem Data . . . . .	4-27
\$Area Ratio Data . . . . .	4-27
\$Recycle Data . . . . .	4-27
4.6.3 Air Loads Program—ALoads-5A . . . . .	4-28
4.6.4 Air Loads Program—ALoads-5B . . . . .	4-29

## CONTENTS—Continued

	Page
5.0 TIMING FOR THE DEMONSTRATION CASES . . . . .	5-1
6.0 DEMONSTRATION CASE RESULTS, OTHER FLEXSTAB RESULTS AND COMPARISONS . . . . .	6-1
6.1 Results and Comparisons of the Boeing 707-320B Demonstration Case . . . . .	6-3
6.2 Results and Comparisons of Boeing 2707-300 (SST) Demonstration Case . . . . .	6-38
6.3 Results of the Lockheed YF-12A Demonstration Case . . . . .	6-53
6.4 Results and Comparisons of the Arrow-Wing Configuration. . . . .	6-60
7.0 GLOSSARY . . . . .	7-1
APPENDIX A—Dart Model I Demonstration Case Input Listings . . . . .	A-1
APPENDIX B—Transformation Matrix Used in the Dart Model I ESIC Structural Definition . . . . .	B-1
APPENDIX C—Demonstration Case Usage of Flexstab Input Options and Modeling Techniques . . . . .	C-1
REFERENCES . . . . .	R-1

## FIGURES

No.		Page
3.2-1	Geometry of Dart Model I . . . . .	3-9
3.2-2	Placement of Reference Axis System--Dart Model I . . . . .	3-10
3.2-3	Placement of Local Slender Body Coordinate System--Dart Model I . . . . .	3-12
3.2-4	Slender Body Nose, Tail, and Control Point Locations . . . . .	3-13
3.2-5	Region Influenced by Thin Bodies--Dart Model I . . . . .	3-13
3.2-6	Placement of Local Thin Body Coordinate System--Dart Model I . . . . .	3-15
3.2-7	Planform Definition--Dart Model I . . . . .	3-16
3.2-8	Paneling Scheme and Control Point Locations--Dart Model I . . . . .	3-17
3.2-9	Placement of Local Interference Body Coordinate System--Dart Model I . . . . .	3-19
3.2-10	Interference Body Cross-Sectional Definition--Dart Model I . . . . .	3-20
3.2-11	Interference Body Geometry--Dart Model I . . . . .	3-22
3.2-12	Final Geometry Definition--Dart Model I . . . . .	3-23
3.2-13	Calcomp Plot of DART Model I . . . . .	3-24
3.2-14	Elastic Axis Representation of Dart Model I Structure . . . . .	3-26
3.2-15	Fuselage Structural Representation--Dart Model I--ISIC . . . . .	3-28
3.2-16	Wing Structural Representation--Dart Model I--ISIC . . . . .	3-30
3.2-17	ESIC Structural Representation--Dart Model I . . . . .	3-32
3.3-1	Geometry of Dart Model II . . . . .	3-36
3.3-2	Placement of Reference Axis System--Dart Model II . . . . .	3-37
3.3-3	Placement of Wing Pod Local Slender Body Coordinate Systems--Dart Model II . . . . .	3-38
3.3-4	Fuselage Interference Body (IB1) Cross-Sectional Panel Corner Point Locations--Dart Model II . . . . .	3-40
3.3-5	Wing Pod Interference Body Cross-Sectional Panel Corner Point Locations-- Dart Model II . . . . .	3-41
3.3-6	Wing Definitions--Dart Model II . . . . .	3-43
3.3-7	Calcomp Plot of DART Model II . . . . .	3-45
3.4-1	Fuselage Geometric Definition--707-320B . . . . .	3-48
3.4-2	Wing Planform Definition--707-320B . . . . .	3-50
3.4-3	Determination of the X-Coordinate of the Origin of Inwing--707-320B . . . . .	3-51
3.4-4	Determination of the Z-Coordinate of the Origin of Inwing--707-320B . . . . .	3-52
3.4-5	Planform Modifications--707-320B . . . . .	3-53
3.4-6	Determination of Model Wing-Body Intersection Point--707-320B . . . . .	3-55
3.4-7	Interference Body Transverse Panel Edge Locations--707-320B . . . . .	3-56
3.4-8	Determination of Model Horizontal Stabilizer Location--707-320B . . . . .	3-57
3.4-9	Model Horizontal Stabilizer Planform--707-320B . . . . .	3-58
3.4-10	Vertical Tail Modeling--707-320B . . . . .	3-60
3.4-11	Nacelle Strut Planform Definition--707-320B . . . . .	3-61
3.4-12	Nacelle Model Definition--707-320B . . . . .	3-63
3.4-13	Geometry Definition Plot--707-320B . . . . .	3-66
3.4-14	Elastic Axis Representation of 707-320B Structure . . . . .	3-67
3.4-15	Stiffness Modeling for the 707-320B Fuselage . . . . .	3-69
3.4-16	Wing Structural Model--707-320B . . . . .	3-71
3.4-17	Model Mass Distribution--707-320B . . . . .	3-72
3.4-18	Structural Models of the 707-320B Struts . . . . .	3-74

## FIGURES—Continued

No.		Page
3.4-19	Elastic Axis Plot 707-320B . . . . .	3-77
3.4-20	Normal Modes Plot—707-320B . . . . .	3-78
3.5-1	Planform Definition—SST . . . . .	3-89
3.5-2	Fuselage Interference Body Cross Section—SST . . . . .	3-91
3.5-3	Geometry Definition Plot—SST . . . . .	3-93
3.5-4	SAMECS Structural Grids for SST Wing and Horizontal Stabilizer Showing Original Nodes to be Used by FLEXSTAB . . . . .	3-98
3.5-5	SAMECS Structural Grid for SST Wing Showing Nodes Used by FLEXSTAB . . . . .	3-101
3.5-6	ESIC Structural Paneling for SST Wing and Horizontal Stabilizer . . . . .	3-102
3.6-1	YF-12A Configuration . . . . .	3-106
3.6-2	Fuselage Interference Body Definition—YF-12A . . . . .	3-109
3.6-3	Nacelle Interference Body Definition—YF-12A . . . . .	3-111
3.6-4	Geometry Definition Plot—YF-12A . . . . .	3-115
6.1-1	707-320B, THPLOT-3, u-PERTURBATION = 600 IPS, u Vs Time; Based on SDSS-3A (Residual Elastic) Data . . . . .	6-18
6.1-2	707-320B, THPLOT-3, u-PERTURBATION = 600 IPS, $\theta_p$ Vs Time; Based on SDSS-3A (Residual Elastic) Data . . . . .	6-19
6.1-3	707-320B, THPLOT-3, u-PERTURBATION = 600 IPS, $N_p$ Vs Time; Based on SDSS-3A (Residual Elastic) Data . . . . .	6-20
6.1-4	707-320B, THPLOT-3, v-PERTURBATION = 600 IPS, $\beta_p$ Vs Time; Based on SDSS-3A (Residual Elastic) Data . . . . .	6-21
6.1-5	707-320B, THPLOT-3, v-PERTURBATION = 600 IPS, $\phi_p$ Vs Time; Based on SDSS-3A (Residual Elastic) Data . . . . .	6-22
6.1-6	707-320B, THPLOT-3, v-PERTURBATION = 600 IPS, $\psi_p$ Vs Time; Based on SDSS-3A (Residual Elastic) Data . . . . .	6-23
6.1-7	707-320B, THPLOT-3, w-PERTURBATION = 600 IPS, $\alpha_p$ Vs Time; Based on SDSS-3A (Residual Elastic) Data . . . . .	6-24
6.1-8	707-320B, THPLOT-3, w-PERTURBATION = 600 IPS, $\theta_p$ Vs Time; Based on SDSS-3A (Residual Elastic) Data . . . . .	6-25
6.1-9	707-320B, THPLOT-3, w-PERTURBATION = 600 IPS, $N_p$ Vs Time; Based on SDSS-3A (Residual Elastic) Data . . . . .	6-26
6.1-10	707-320B, THPLOT-3, p-PERTURBATION = 0.50 RAD/SEC, $\phi_p$ Vs Time; Based on SDSS-3A (Residual Elastic) Data . . . . .	6-27
6.1-11	707-320B, THPLOT-3, p-PERTURBATION = 0.50 RAD/SEC, p Vs Time; Based on SDSS-3A (Residual Elastic) Data . . . . .	6-28
6.1-12	707-320B, THPLOT-3, One Minus Cosine Gust, w = -12.0 IPS, Length = 30.0 $\bar{c}$ , $\theta_p$ Vs Time; Based on SDSS-3A (Residual Elastic) Data . . . . .	6-29
6.1-13	707-320B, THPLOT-3, One Minus Cosine Gust, w = -12.0 IPS, Length = 30.0 $\bar{c}$ , $N_p$ Vs Time; Based on SDSS-3A (Residual Elastic) Data . . . . .	6-31
6.1-14	Pressure Distribution Plot—707-320B . . . . .	6-32
6.2-1	Variations of Lift and Pitching Moment With Angle of Attack for SST . . . . .	6-41
6.2-2	Effect of Mach Number on Lift Slope and Aerodynamic Center for SST, Tail-off . . . . .	6-43

**FIGURES—Continued**

No.		Page
6.2-3	Wing Pressure Comparisons for SST, Tail-off . . . . .	6-44
6.2-4	Fuselage Pressure Distributions for SST . . . . .	6-48
6.2-5	2707-300PT (SST) SD&SS and ALOADS Programs Displacement Output and Reconciliation of the Two. . . . .	6-50
6.4-1	FLEXSTAB Aerodynamic Geometry of the Arrow-Wing Configuration . .	6-61
6.4-2	Analysis-To-Experiment Pressure Comparison for Arrow-Wing Configuration, Trailing Edge Flap Undeformed $M = 0.40, \alpha = 2.1^\circ$ . . . .	6-62
6.4-3	Analysis-To-Experiment Pressure Comparison for Arrow-Wing Configuration; Trailing Edge Flap Undeformed $M = 0.85, \alpha = 2.1^\circ$ . . . .	6-63
6.4-4	Analysis-To-Experiment Pressure Comparison for Arrow-Wing Configuration; Trailing Edge Flap Undeformed $M = 1.05, \alpha = 2.0^\circ$ . . . .	6-64
6.4-5	Analysis-To-Experiment Pressure Comparison for Arrow-Wing Configuration; Trailing Edge Flap Undeformed $M = 2.5, \alpha = 2.0^\circ$ . . . .	6-65
6.4-6	Analysis-To-Experiment Pressure Comparison for Arrow-Wing Configuration; Trailing Edge Flap Undeformed $M = 0.40, \alpha = 8.0^\circ$ . . . .	6-67
6.4-7	Analysis-To-Experiment Pressure Comparison for Arrow-Wing Configuration; Trailing Edge Flap Undeformed $M = 0.85, \alpha = 7.9^\circ$ . . . .	6-68
6.4-8	Analysis-To-Experiment Pressure Comparison for Arrow-Wing Configuration; Trailing Edge Flap Undeformed $M = 1.05, \alpha = 7.9^\circ$ . . . .	6-69
6.4-9	Analysis-To-Experiment Pressure Comparison for Arrow-Wing Configuration; Trailing Edge Flap Undeformed $M = 2.5, \alpha = 7.9^\circ$ . . . .	6-70
6.4-10	Analysis-To-Experiment Spanload Comparison for Arrow-Wing Configuration; Trailing Edge Flap = $0.0^\circ$ . . . . .	6-71
6.4-11	Analysis-To-Experiment Pressure Comparison for Arrow-Wing Configuration; Trailing Edge Flap = $8.3^\circ M = 0.40, \alpha = 0.1^\circ$ . . . . .	6-72
6.4-12	Analysis-To-Experiment Pressure Comparison for Arrow-Wing Configuration; Trailing Edge Flap = $8.3^\circ M = 1.05, \alpha = 0.0^\circ$ . . . . .	6-73
6.4-13	Analysis-To-Experiment Spanload Comparison for Arrow-Wing Configuration; Trailing Edge Flap = $8.3^\circ$ . . . . .	6-74
6.4-14	Analysis-To-Experiment Normal Force and Pitching Moment Comparison for Arrow-Wing Configuration $M = -.40$ . . . . .	6-75
6.4-15	Analysis-To-Experiment Normal Force and Pitching Moment Comparison for Arrow-Wing Configuration $M = 0.85$ . . . . .	6-76
6.4-16	Analysis-To-Experiment Normal Force and Pitching Moment Comparison for Arrow-Wing Configuration $M = 1.05$ . . . . .	6-77
6.4-17	Analysis-To-Experiment Normal Force and Pitching Moment Comparison for Arrow-Wing Configuration $M = 2.5$ . . . . .	6-78
B.0-1	ESIC Structural Representation—Dart Model I . . . . .	B-2
B.0-2	ISIC Structural Representation—Dart Model I . . . . .	B-4
B.0-3	Relationships Between Typical ESIC and ISIC Structural Nodes—Dart Model I . . . . .	B-6

## TABLES

No.		Page
2.0-1	Summary of Data Interrelationships for Solution Oriented Options . . .	2-2
3.0-1	Computer Run Identification–Airplane Definition Programs . . . . .	3-2
3.5-1	Arrangement of Input Flexibility Matrix for SST . . . . .	3-99
3.6-1	Arrangement of the Flexibility Matrix Input to the ESIC Program for YF-12A . . . . .	3-117
4.0-1	Computer Run Identification - Airplane Analysis Programs. . . . .	4-2
4.2-1	Input Differences for the Dart Model I SD&SS Runs . . . . .	4-8
4.6-1	Arrangement of the Flexibility Matrix Input to the ALOADS Program for YF-12A . . . . .	4-28
5.0-1	Timing for the Dart Model I Demonstration Case . . . . .	5-2
5.0-2	Timing for the Dart Model II Demonstration Case . . . . .	5-2
5.0-3	Timing for the Boeing 707-320B Demonstration Case . . . . .	5-3
5.0-4	Timing for the Boeing 2707-300PT (SST) Demonstration Case . . . . .	5-4
5.0-5	Timing for the Lockheed YF-12A Demonstration Case . . . . .	5-4
6.1-1	Comparison of Methods for Calculating Aerodynamic Stability and Control Data–Boeing 707-320B (Rigid) . . . . .	6-4
6.1-2	Comparison of Methods for Calculating Longitudinal Dynamic Characteristics–Boeing 707-320B (Rigid) . . . . .	6-7
6.1-3	Comparison of Methods for Calculating Lateral-Directional Dynamic Characteristics–Boeing 707-320B (Rigid) . . . . .	6-8
6.1-4	Comparison of Methods for Calculating Aerodynamic Stability and Control Data–Boeing 707-320B (Flexible) . . . . .	6-11
6.1-5	Comparison of Methods for Calculating Longitudinal Dynamic Characteristics–Boeing 707-320B (Flexible) . . . . .	6-16
6.1-6	Comparison of Methods of Calculating Lateral-Directional Dynamics Characteristics–Boeing 707-320B (Flexible) . . . . .	6-17
6.1-7	Comparison of Boeing 707-320B Rigid Body and Normal Modes Frequencies–SDSS-3A (Residual Elastic) . . . . .	6-17
6.1-8	Comparison of Boeing 707-320B Phugoid Characteristics from the TH-3 and SDSS-3A (Residual Elastic) . . . . .	6-30
6.1-9	Comparison of Boeing 707-320B Lateral-Directional Dynamic Characteristics from the TH-3 and SDSS-3A (Residual Elastic) . . . . .	6-30
6.2-1	Comparison of Methods for Calculating Aerodynamic Stability and Control Data-Boeing 2707-300PT (SST) . . . . .	6-39
6.2-2	Comparison of Methods for Calculating Longitudinal Dynamic Characteristics-Boeing 2707-300PT (SST) . . . . .	6-51
6.3-1	Aerodynamic Stability and Control Data–Lockheed YF-12A . . . . .	6-54
6.3-2	Aerodynamic Stability and Control Data–Lockheed YF-12A . . . . .	6-55
6.3-3	Aerodynamic Stability and Control Data–Lockheed YF-12A . . . . .	6-56
6.3-4	Aerodynamic Stability and Control Data–Lockheed YF-12A . . . . .	6-57
6.3-5	Aerodynamic Stability and Control Data –Lockheed YF-12A . . . . .	6-58
6.3-6	Aerodynamic Stability and Control Data–Lockheed YF-12A . . . . .	6-59



**TABLES—Continued**

No.		Page
A.0-1	Input Deck Listing for GD-1 . . . . .	A-2
A.0-2	Input Deck Listing for AIC-1 . . . . .	A-3
A.0-3	Input Deck Listing for ISIC-1 . . . . .	A-4
A.0-4	Input Deck Listing for NM-1 . . . . .	A-6
A.0-5	Input Deck Listing for SDSS-1A . . . . .	A-7
A.0-6	Input Deck Listing for SDSS-1B . . . . .	A-9
A.0-7	Input Deck Listing for TH-1 . . . . .	A-11
A.0-8	Input Deck Listing for SLOADS-1 . . . . .	A-12
A.0-9	Input Deck Listing for ESIC-1 . . . . .	A-13
A.0-10	Input Deck Listing for SDSS-1C . . . . .	A-14
A.0-11	Input Deck Listing for SDSS-1D . . . . .	A-16
A.0-12	Input Deck Listing for ALOADS-1 . . . . .	A-18
A.0-13	[CS] Matrix Input to ESIC-1 . . . . .	A-19
A.0-14	Transformation Matrix [T] Used to Create [CS] . . . . .	A-21
C.0-1	GD Program Input Option Usage . . . . .	C-2
C.0-2	AIC Program Input Option Usage . . . . .	C-4
C.0-3	ISIC Program Input Option Usage . . . . .	C-5
C.0-4	NM Program Input Option Usage . . . . .	C-6
C.0-5	ESIC Program Input Option Usage . . . . .	C-7
C.0-6	SD&SS Program Input Option Usage . . . . .	C-8
C.0-7	TH Program Input Option Usage . . . . .	C-18
C.0-8	SLOADS Program Input Option . . . . .	C-19
C.0-9	Modeling Technique Usage . . . . .	C-20

## SYMBOLS

With the exception of matrix names which are defined in appendix B of volume III, this list includes all symbols used in this report.

General:

$b$	wing span
$C_p$	pressure coefficient, $p - p_1 / \bar{q}_1$
$\Delta C_p$	Thin Body lifting pressure coefficient, $P_l - P_u / \bar{q}_1$
$C_L$	lift coefficient, lift / $\bar{q}_1 S_w$
$C_N$	normal force coefficient, total force normal to the airplane / $\bar{q}_1 S_w$
$C_D$	drag coefficient, drag / $\bar{q}_1 S_w$
$C_m$	pitching moment coefficient, pitching moment / $\bar{q}_1 \bar{c} S_w$
$C_Y$	side force coefficient, side force / $\bar{q}_1 S_w$
$C_\ell$	rolling moment coefficient, rolling moment / $\bar{q}_1 b S_w$
$C_n$	yawing moment coefficient, yawing moment / $\bar{q}_1 b S_w$ , section normal force coefficient
$C_{L_0}$	lift coefficient at $\alpha = \delta e = 0^\circ$
$C_{D_0}$	drag coefficient at $\alpha = \delta e = 0^\circ$
$C_{m_0}$	pitching moment coefficient at $\alpha = \delta e = 0^\circ$
$C_{1/2}$	number of cycles to damp to one-half amplitude
$C_2$	number of cycles to double amplitude
$c$	local section chord length
$\bar{c}$	reference chord
$\bar{c}_p$	panel mean aerodynamic chord
$c_R$	root chord of wing

cg	center of gravity
cps	cycles per second
D	distance
DY	modal shape displacement in the Y-direction
DZ	modal shape displacement in the Z-direction
DZ <sub>N</sub>	modal shape displacement in the Z <sub>N</sub> -direction
d <sub>i</sub>	structural deflection along i-axis
EI <sub>i</sub>	bending stiffness about i-axis
GJ	bending stiffness about an x-axis
h	altitude; nondimensional cg location, $(X_{CG}-X_{LE})/\bar{c}$
h <sub>m</sub>	maneuver point
h <sub>n</sub>	neutral point
h <sub>m</sub> -h	maneuver margin
h <sub>n</sub> -h	static margin
Δh <sub>n</sub>	elastic increment to neutral point, $h_{nE}-h_{nR}$
ΔT	temperature deviation from standard
I <sub>XX</sub> , I <sub>YY</sub> , I <sub>ZZ</sub> , I <sub>XZ</sub>	moments and product of inertia in the Body Axis System
JP	junction point
M	Mach number
m	lumped mass
NZ	normal load factor
P <sub>1</sub> , Q <sub>1</sub> , R <sub>1</sub>	steady-state values of the rotation rates about the X <sub>B</sub> , Y <sub>B</sub> , and Z <sub>B</sub> axes, respectively
p, q, r	perturbation values of the rotation rates about the X <sub>B</sub> , Y <sub>B</sub> , and Z <sub>B</sub> axes, respectively

$p, p_1$	local and freestream static pressure, respectively
$p_l, p_u$	static pressure on lower and upper surface, respectively, of a Thin Body panel
$\bar{q}_1$	dynamic pressure, $\rho U_1^2/2$
$R$	radius, reference point
$R_I$	nacelle inlet radius
$R_{\max}$	nacelle maximum radius
$R_{\text{ave}}$	nacelle average radius
$S_w$	wing area
$T$	thrust
$t$	time
$t_{1/2}$	time to damp to one-half amplitude
$t_2$	time to double amplitude
$U$	$X_B$ -component of velocity
$U_1, V_1, W_1$	components of reference freestream velocity expanded on $X_B, Y_B,$ and $Z_B$ -axes, respectively
$u, v, w$	perturbation values of airplane translation velocity in the Body Axis System
$V$	velocity; $Y_B$ -component of velocity
$W$	$Z_B$ -component of velocity
$wt$	airplane weight
$X_{LE}$	$X$ -coordinate of leading edge of reference chord
$x$	$x$ -coordinate
$x_N$	Slender Body nose location (in Slender Body Aerodynamic Coordinate System)
$x_T$	Slender Body tail location (in Slender Body Aerodynamic Coordinate System)

$X, Y, Z$	Reference Axis System
$X_B, Y_B, Z_B$	Body Axis System
$X_E, Y_E, Z_E$	ESIC Reference Coordinate System
$x_{E_n}, y_{E_n}, z_{E_n}$	ESIC Thin Body Structural Coordinate System
$X_{IB}, Y_{IB}, Z_{IB}$	Interference Body Coordinate System
$X_M, Y_M, Z_M$	Local Slender Body Aerodynamic Coordinate System
$X_N, Y_N, Z_N$	Local Thin Body Aerodynamic Coordinate System
$x_n, y_n, z_n$	Thin Body Structural Coordinate System
$x_{n_i}, y_{n_i}, z_{n_i}$	Thin Body Elastic Segment Coordinate System
$\alpha$	angle of attack, $\tan^{-1}(W/U)$
$\beta$	sideslip angle, $\tan^{-1}(V/U)$ ; Mach number parameter, $\sqrt{ 1 - M^2 }$
$\gamma$	flightpath angle
$\Delta$	increment
$\delta_e$	elevator angle
$\delta_a$	aileron angle
$\delta_r$	rudder angle
	} (see section 9.2.1, volume II)
$\theta$	pitch attitude (see section 3.5.11, volume II); elastic rotation; dihedral angle
$\phi$	roll angle (see section 3.5.11, volume II)
$\psi$	yaw angle (see section 3.5.11, volume II)

Subscripts:

B	body
C	camber line
CG	center of gravity

E	elastic, ESIC
I	ISIC
IB	Interference Body
i	index
JP	junction point
LE	leading edge
max	maximum
min	minimum
N	Thin Body
n	index
neg	negative
o	origin; $\alpha = \delta e = 0^\circ$
P	perturbation value
pos	positive
R	rigid
SB	Slender Body
T	trim value
TB	Thin Body
TE	trailing edge
l	steady-state, trim value

Superscripts:

·	$\partial/\partial t$
..	$\partial^2/\partial t^2$

Stability Derivatives:

$$C_{L\dot{Q}} = \frac{\partial C_L}{\partial (q\bar{c}/2U_1)}, \text{ lift coefficient due to pitch rate}$$

$$C_{D\dot{Q}} = \frac{\partial C_D}{\partial (q\bar{c}/2U_1)}, \text{ drag coefficient due to pitch rate}$$

$$C_{m\dot{Q}} = \frac{\partial C_m}{\partial (q\bar{c}/2U_1)}, \text{ pitching moment coefficient due to pitch rate}$$

$$C_{L\ddot{Q}} = \frac{\partial C_L}{\partial (\dot{q}\bar{c}^2/4U_1^2)}, \text{ lift coefficient due to pitch acceleration}$$

$$C_{D\ddot{Q}} = \frac{\partial C_D}{\partial (\dot{q}\bar{c}^2/4U_1^2)}, \text{ drag coefficient due to pitch acceleration}$$

$$C_{m\ddot{Q}} = \frac{\partial C_m}{\partial (\dot{q}\bar{c}^2/4U_1^2)}, \text{ pitching moment coefficient due to pitch acceleration}$$

$$C_{Y\dot{P}} = \frac{\partial C_Y}{\partial (p\bar{b}/2U_1)}, \text{ side force coefficient due to roll rate}$$

$$C_{\ell\dot{P}} = \frac{\partial C_\ell}{\partial (p\bar{b}/2U_1)}, \text{ rolling moment coefficient due to roll rate}$$

$$C_{n\dot{P}} = \frac{\partial C_n}{\partial (p\bar{b}/2U_1)}, \text{ yawing moment coefficient due to roll rate}$$

$$C_{Y\ddot{P}} = \frac{\partial C_Y}{\partial (\dot{p}\bar{b}^2/4U_1^2)}, \text{ side force coefficient due to roll acceleration}$$

$$C_{\ell\ddot{P}} = \frac{\partial C_\ell}{\partial (\dot{p}\bar{b}^2/4U_1^2)}, \text{ rolling moment coefficient due to roll acceleration}$$

$$C_{n\ddot{P}} = \frac{\partial C_n}{\partial (\dot{p}\bar{b}^2/4U_1^2)}, \text{ yawing moment coefficient due to roll acceleration}$$

$$C_{Y_R} = \frac{\partial C_Y}{\partial (rb/2U_1)}, \text{ side force coefficient due to yaw rate}$$

$$C_{\ell_R} = \frac{\partial C_\ell}{\partial (rb/2U_1)}, \text{ rolling moment coefficient due to yaw rate}$$

$$C_{n_R} = \frac{\partial C_n}{\partial (rb/2U_1)}, \text{ yawing moment coefficient due to yaw rate}$$

$$C_{Y\dot{R}} = \frac{\partial C_Y}{\partial (\dot{r}b^2/4U_1^2)}, \text{ side force coefficient due to yaw acceleration}$$

$$C_{\ell\dot{R}} = \frac{\partial C_\ell}{\partial (\dot{r}b^2/4U_1^2)}, \text{ rolling moment coefficient due to yaw acceleration}$$

$$C_{n\dot{R}} = \frac{\partial C_n}{\partial (\dot{r}b^2/4U_1^2)}, \text{ yawing moment coefficient due to yaw acceleration}$$

$$C_{L_u} = \frac{\partial C_L}{\partial (u/U_1)}, \text{ lift coefficient due to forward velocity}$$

$$C_{D_u} = \frac{\partial C_D}{\partial (u/U_1)}, \text{ drag coefficient due to forward velocity}$$

$$C_{m_u} = \frac{\partial C_m}{\partial (u/U_1)}, \text{ pitching moment coefficient due to forward velocity}$$

$$C_{L_\alpha} = \frac{\partial C_L}{\partial \alpha}, \text{ lift coefficient due to angle of attack}$$

$$C_{D_\alpha} = \frac{\partial C_D}{\partial \alpha}, \text{ drag coefficient due to angle of attack}$$

$$C_{m_\alpha} = \frac{\partial C_m}{\partial \alpha}, \text{ pitching moment coefficient due to angle of attack}$$

$$C_{L\dot{\alpha}} = \frac{\partial C_L}{\partial (\dot{\alpha}\bar{c}/2U_1)}, \text{ lift coefficient due to angle-of-attack rate}$$



$$C_{D\dot{\alpha}} = \frac{\partial C_D}{\partial(\dot{\alpha}\bar{c}/2U_1)}, \text{ drag coefficient due to angle-of-attack rate}$$

$$C_{m\dot{\alpha}} = \frac{\partial C_m}{\partial(\dot{\alpha}\bar{c}/2U_1)}, \text{ pitching moment coefficient due to angle-of-attack rate}$$

$$C_{Y\beta} = \frac{\partial C_Y}{\partial\beta}, \text{ side force coefficient due to sideslip}$$

$$C_{\ell\beta} = \frac{\partial C_\ell}{\partial\beta}, \text{ rolling moment coefficient due to sideslip}$$

$$C_{n\beta} = \frac{\partial C_n}{\partial\beta}, \text{ yawing moment coefficient due to sideslip}$$

$$C_{Y\dot{\beta}} = \frac{\partial C_Y}{\partial(\dot{\beta}b/2U_1)}, \text{ side force coefficient due to sideslip rate}$$

$$C_{\ell\dot{\beta}} = \frac{\partial C_\ell}{\partial(\dot{\beta}b/2U_1)}, \text{ rolling moment coefficient due to sideslip rate}$$

$$C_{n\dot{\beta}} = \frac{\partial C_n}{\partial(\dot{\beta}b/2U_1)}, \text{ yawing moment coefficient due to sideslip rate}$$

$$C_{L\delta e} = \frac{\partial C_L}{\partial\delta e}, \text{ lift coefficient due to stabilizer deflection}$$

$$C_{D\delta e} = \frac{\partial C_D}{\partial\delta e}, \text{ drag coefficient due to stabilizer deflection}$$

$$C_{m\delta e} = \frac{\partial C_m}{\partial\delta e}, \text{ pitching moment coefficient due to stabilizer deflection}$$

$$C_{Y\delta a} = \frac{\partial C_Y}{\partial\delta a}, \text{ side force coefficient due to aileron deflection}$$

$$C_{\ell\delta a} = \frac{\partial C_\ell}{\partial\delta a}, \text{ rolling moment coefficient due to aileron deflection}$$

$$C_{n\delta a} = \frac{\partial C_n}{\partial\delta a}, \text{ yawing moment coefficient due to aileron deflection}$$

$$C_{Y_{\delta r}} = \frac{\partial C_Y}{\partial \delta r}, \text{ side force coefficient due to rudder deflection}$$

$$C_{\ell_{\delta r}} = \frac{\partial C_\ell}{\partial \delta r}, \text{ rolling moment coefficient due to rudder deflection}$$

$$C_{n_{\delta r}} = \frac{\partial C_n}{\partial \delta r}, \text{ yawing moment coefficient due to rudder deflection}$$

$$C_{Z_\alpha} = \frac{\partial C_{Z_B}}{\partial \alpha}, \text{ normal force coefficient due to angle of attack}$$

Stability Parameters:

$$\frac{\partial \delta e}{\partial n} \quad \text{elevator angle per g}$$

$$\frac{\partial \delta e}{\partial V} \quad \text{stick speed stability}$$

## SUMMARY

The application of the FLEXSTAB system to analyze airplane configurations is explained with examples of demonstration cases: Dart Model I, Dart Model II, the Boeing 707-320B, the Boeing 2707-300PT (SST) and the Lockheed YF-12A. The Dart Models I and II are two very simple configurations used to illustrate the program input and usage. The modeling and the preparation of input data for the 707, SST and YF-12A configurations is discussed, and the selected results are presented in a tabular form. A comparison of results with other sources is included for the 707 and SST models. In addition, a comparison of the FLEXSTAB results for pressure and force distribution with the experimental results for an arrow-wing configuration (obtained under NASA Contract NAS1-12875) are included.

This volume describes the preparation of the input data decks for each demonstration case. These descriptions provide the new user of FLEXSTAB with some general methods which, in combination with Volume II (the User's Manual), should aid data preparation for other configurations. Computing times for each case are given for both the Boeing Computer Service's CDC 6600 and the Lawrence Berkeley Laboratories' CDC 7600 computers.

Included in the appendices are tables illustrating the usage of the various program input options within each of the demonstration cases, and input deck listings for the Dart Model I runs. A special section is included which describes the usage of the FLEXSTAB "solution-oriented" input options.



## 1.0 INTRODUCTION

FLEXSTAB is a system of computer programs designed to predict the stability characteristics of elastic aircraft. These characteristics are determined from geometry, mass distribution, and flexibility information using linear aerodynamic and structural influence coefficient theory.

The FLEXSTAB computer program system is documented by a series of reports which describe the theory, input formats, programming and demonstration cases. Volume I describes the detailed theoretical derivation used for the structures, aerodynamics, and dynamics calculations. Volume II enables the user to prepare input decks, execute programs, and interpret results. Volume III describes the FLEXSTAB computer programs through a sequence of diagrams and flowcharts.

FLEXSTAB has been demonstrated by analyzing the Boeing 707-320B, the Boeing 2707-300PT (SST), the Lockheed YF-12A, and two very simple configurations designated Dart Models I and II. This volume gives a detailed description of the preparation of the input decks for each of these demonstration cases. In addition, selected results from these cases are presented. The 707 and SST results are compared with other sources. In addition, a comparison of the FLEXSTAB results for pressure and force distribution with the experimental results for an arrow-wing configuration are included. These comparisons are obtained from a Boeing study under NASA Contract NAS1-12875.

The Dart models were used as very simple checkout cases and do not represent problems of physical significance. They do, however, offer the new user an opportunity to become familiar with input data preparation and to execute inexpensive checkout cases at his own computer installation. More realistic and complex modeling problems are illustrated in the 707, SST, and YF-12A demonstration cases. The aerodynamic modeling techniques described are based on experience with linearized aerodynamic theories. It is recognized that more data is needed to generate a better base for recommendations regarding aerodynamic modeling.

A special section (Sec. 2.0) has been included which gives a complete discussion of the FLEXSTAB "solution-oriented" options, i.e., those input options which directly affect the type and extent of results that can be obtained from FLEXSTAB. In addition, appendix C contains tables that indicate which of the various input options and modeling techniques of Volume II were used in the demonstration cases.

It is strongly suggested that the new user consult this volume as well as Volume II before attempting to execute any of the FLEXSTAB programs. Section 2.0 and the Dart Model I input data deck descriptions in Sections 3.0 and 4.0 should be particularly helpful. For convenience, listings of the input data decks for each of the Dart Model I demonstration case runs are given in appendix A. The complete input data deck and output listings for the part I and II 707 and SST demonstration cases are included on the tape that contains the FLEXSTAB source code.



## 2.0 USE OF THE SOLUTION-ORIENTED INPUT OPTIONS

Solution-oriented options may be defined as those options that directly or indirectly affect the type and extent of analysis performed by FLEXSTAB. Through proper use of these options, the user is offered a considerable amount of flexibility in controlling the calculations performed by FLEXSTAB so that an efficient solution to his particular category of problem may be obtained. Section 2.1 discusses each option on a program by program basis and the effect that one option has on another. A description of the overall use of the FLEXSTAB programs as related to these options is given. The information presented in this section supplements the summary of input requirements presented in sections 3.1 and 4.1 of this volume and that of the FLEXSTAB User's Manual -- Volume II. A summary of the overall problem solving capability is presented in reference 2-1.

### 2.1 DISCUSSION OF EACH SOLUTION-ORIENTED OPTION

For each of the FLEXSTAB programs except SLOADS,\* CAIC, and the PLOT programs, Table 2.0-1 presents (a) a list of solution-oriented input options,+ (b) related options both in the subject program and in all other programs, and (c) the corresponding input deck card numbers of Vol. II. These options are referred to repeatedly in Sections 2.1.1 - 2.1.8.

#### 2.1.1 GD Program Solution-oriented Options

The \$SLENDER BODY option is required for two reasons. First, if the ISIC structures program is used, the Reference Junction Point must be at the nose of the fuselage -- a Slender Body on the symmetry plane. Secondly, a Slender Body is required if it is desired that a thrust vector be defined in the SD&SS program. Only for gliding flight analyses not involving an ISIC structural model can Slender Bodies be omitted.

The \$THIN BODY option is required, since to execute FLEXSTAB through the SD&SS program a control surface (longitudinal control as a minimum) must be defined on a Thin Body. The Thin Body panels used as control surfaces are specified in SD&SS.

#### 2.1.2 AIC Program Solution-oriented Options

The  $\Delta M_1$  option must be switched on if either or both SD&SS options, Speed<sub>OP</sub> and Comp<sub>OP</sub> are desired. This option generates an AIC matrix to be used for compressibility calculations. The Speed<sub>OP</sub> option controls the calculation of stick-speed static stability. The Comp<sub>OP</sub> option calculates the compressibility terms for the speed derivatives,  $\partial(\dots)/\partial(\hat{u})$ , and the yaw rate derivatives,  $\partial(\dots)/\partial(\hat{r})$ , as part of the calculation of the perturbation stability derivatives.

\*SLOADS merely prints information computed in SD&SS. As noted in Section 17 of Vol. II, this information is of limited usefulness.

+These appear in the same order as their appearance in Vol. II.

TABLE 2.0-1.—SUMMARY OF DATA INTERRELATIONSHIPS FOR SOLUTION-ORIENTED OPTIONS

OPTION DESIRED			RELATED OPTIONS		
PROGRAM	OPTION	CARD	PROGRAM	OPTION	CARD
GD	\$SLENDER BODY	6	ISIC SD&SS	\$JUNCTION POINT \$THRUST	9 19
	\$THIN BODY	27	SD&SS	\$CONTROL SURFACE	28
	NAS	37	SD&SS	U <sub>press</sub> <sub>Op</sub> Thickness <sub>Op</sub>	59 6
AIC	$\Delta M_1$	4	SD&SS	Speed <sub>Op</sub> Comp <sub>Op</sub>	6 59
	Steady Motion <sub>REF</sub>	5	ISIC SD&SS	\$OPTION FOR ELASTIC FORMULATION Motion <sub>REF</sub> Motion <sub>PERT</sub> U <sub>press</sub> <sub>Op</sub>	6 5 59 59
	Unsteady <sub>Op</sub>	6	SD&SS	Unsteady <sub>Op</sub> \$PERTURBATION DATA Motion <sub>PERT</sub> U <sub>press</sub> <sub>Op</sub>	6 58 59 59
	Unsteady Motion <sub>REF</sub>	7	SD&SS	\$DYNAMIC ANALYSIS Motion <sub>REF</sub> Unsteady <sub>Op</sub> \$PERTURBATION DATA Motion <sub>PERT</sub> U <sub>press</sub> <sub>Op</sub>	73 5 6 58 59 59
ISIC	\$CASE FOR INTERNAL STRUCTURAL INFLUENCE COEFFICIENT PROGRAM	1	NM SD&SS	\$CASE FOR NORMAL MODES PROGRAM Loads <sub>Op</sub> \$STRUCTURAL DATA	1 59 81



TABLE 2.0-1.—CONTINUED

OPTION DESIRED			RELATED OPTIONS			
PROGRAM	OPTION	CARD	PROGRAM	OPTION	CARD	
ISIC	\$OPTION FOR ELASTIC FORMULATION	6	AIC	Steady Motion <sub>REF</sub>	5	
			NM	\$OPTION FOR ELASTICITY FORMULATION	4	
			SD&SS	Motion <sub>REF</sub>	5	
				Elastic <sub>OP</sub>	5	
				\$PERTURBATION DATA	58	
	Motion <sub>PERT</sub>	59				
	\$JUNCTION POINT	9	GD	\$SLENDER BODY DATA	6	
	\$GYROSCOPIC DATA	41	SD&SS	\$GYROSCOPIC DATA	23	
NM	\$CASE FOR NORMAL MODES PROGRAM	1	ISIC	\$CASE FOR INTERNAL STRUCTURAL INFLUENCE COEFFICIENTS PROGRAM	1	
	\$OPTION FOR ELASTICITY FORMULATION	4	ISIC	\$OPTION FOR ELASTIC FORMULATION	6	
			SD&SS	Elastic <sub>OP</sub>	5	
			Motion <sub>PERT</sub>	59		
	NEIG	7	SD&SS	\$DYNAMIC ANALYSIS	73	
			TH	\$CASE FOR TIME HISTORIES PROGRAM	1	
ESIC	\$CASE FOR EXTERNAL STRUCTURAL INFLUENCE COEFFICIENT PROGRAM	1	SD&SS	\$STRUCTURAL DATA	81	
			6	SD&SS	Motion <sub>REF</sub>	5
					Elastic <sub>OP</sub>	5
					\$GYROSCOPIC DATA	23
					\$PERTURBATION DATA	58
	Motion <sub>PERT</sub>	59				

TABLE 2.0-1.—CONTINUED

OPTION DESIRED			RELATED OPTIONS					
PROGRAM	OPTION	CARD	PROGRAM	OPTION	CARD			
ESIC	\$CATALOG OF INPUT EXTERNAL MATRICES AND GEOMETRY DATA	6	ALOADS	\$CASE FOR ALOADS PROGRAM	1			
SD&SS	Motion <sub>REF</sub>	5	AIC	Steady Motion <sub>REF</sub>	5			
				Unsteady Motion <sub>REF</sub>	7			
			ISIC	\$OPTION FOR ELASTIC FORMULATION	6			
			ESIC	\$CATALOG OF INPUT EXTERNAL MATRICES AND GEOMETRY DATA	6			
		Elastic <sub>OP</sub>	5	SD&SS	\$GYROSCOPIC DATA	23		
	ALOADS			\$CASE FOR ALOADS PROGRAM	1			
	ISIC			\$OPTION FOR ELASTIC FORMULATION	6			
	NM			\$OPTION FOR ELASTICITY FORMULATION	4			
	ESIC			\$CATALOG OF INPUT EXTERNAL MATRICES AND GEOMETRY DATA	6			
	SD&SS			Shape <sub>OP</sub>	36			
				Disp <sub>IN</sub>	37			
				Unsteady <sub>OP</sub>	6	AIC	Unsteady <sub>OP</sub>	6
						Unsteady Motion <sub>REF</sub>	7	
	SD&SS					\$PERTURBATION DATA	58	
	Thickness <sub>OP</sub>	6		U <sub>press</sub> <sub>OP</sub>	59			
			GD	NAS	73			
					37			

TABLE 2.0-1.—CONTINUED

OPTION DESIRED			RELATED OPTIONS		
PROGRAM	OPTION	CARD	PROGRAM	OPTION	CARD
SD&SS	LE Thrust <sub>OP</sub>	6	SD&SS	\$STABILITY DATA	34
				\$PERTURBATION DATA	58
	Speed <sub>OP</sub>	6	AIC	$\Delta M_1$	4
	Gust <sub>OP</sub>	6	SD&SS	Motion <sub>PERT</sub>	59
			TH	\$GUST DATA	31
	\$THRUST DATA	19	GD	\$SLENDER BODY DATA	6
			SD&SS	\$GYROSCOPIC DATA	23
	\$GYROSCOPIC DATA	23	ISIC	\$GYROSCOPIC DATA	41
			ESIC	\$CATALOG OF INPUT EXTERNAL MATRICES AND GEOMETRY DATA	6
			SD&SS	Motion <sub>REF</sub>	5
				\$THRUST DATA	19
	\$CONTROL SURFACE	28	GD	\$THIN BODY	27
			SD&SS	Coneff <sub>OP</sub>	59
	\$STABILITY DATA	34	SD&SS	LE Thrust <sub>OP</sub>	6
	Problem	35	SD&SS	\$WIND TUNNEL DATA	47
	Shape <sub>OP</sub>	36	SD&SS	Elastic <sub>OP</sub>	5
				Shape <sub>OUT</sub>	37
			Disp <sub>IN</sub>	37	
			Disp <sub>OUT</sub>	37	
Shape <sub>OUT</sub>	37	SD&SS	Shape <sub>OP</sub>	36	
Disp <sub>IN</sub>	37	SD&SS	Elastic <sub>OP</sub>	5	
			Shape <sub>OP</sub>	36	
Disp <sub>OUT</sub>	37	SD&SS	Shape <sub>OP</sub>	36	

TABLE 2.0-1.—CONTINUED

OPTION DESIRED			RELATED OPTIONS		
PROGRAM	OPTION	CARD	PROGRAM	OPTION	CARD
SD&SS	Loads <sub>Op</sub>	37	ALOADS	\$CASE FOR ALOADS PROGRAM	1
			SLOADS	\$CASE FOR STRUCTURAL LOADS PROGRAM	1
	\$WIND TUNNEL DATA	47	SD&SS	Problem	35
			\$PERTURBATION DATA	58	AIC
	Motion <sub>PERT</sub>	59		Unsteady Motion <sub>REF</sub>	7
			ISIC	\$OPTION FOR ELASTIC FORMULATION	6
			ESIC	\$CATALOG OF INPUT EXTERNAL MATRICES AND GEOMETRY DATA	6
			SD&SS	Unsteady <sub>Op</sub>	6
				LE Thrust <sub>Op</sub>	6
			AIC	Steady Motion <sub>REF</sub>	5
				Unsteady <sub>Op</sub>	6
			ISIC	Unsteady Motion <sub>REF</sub>	7
				\$OPTION FOR ELASTIC FORMULATION	6
			NM	\$OPTION FOR ELASTICITY FORMULATION	4
	SD&SS	Gust <sub>Op</sub>	6		
		Steady <sub>Op</sub>	60		
	Comp <sub>Op</sub>	59	AIC	$\Delta M_1$	4
	Up <sub>ressOp</sub>	59	GD	\$THIN BODY	27
			AIC	Steady Motion <sub>REF</sub>	5
				Unsteady <sub>Op</sub>	6
SD&SS			Unsteady <sub>Op</sub>	6	

TABLE 2.0-1.—CONTINUED

OPTION DESIRED			RELATED OPTIONS		
PROGRAM	OPTION	CARD	PROGRAM	OPTION	CARD
SD&SS	Coeff. <sub>Op</sub>	59	SD&SS	\$CONTROL SURFACE DATA	28
	Loads <sub>Op</sub>	59	ISIC	\$CASE FOR INTERNAL STRUCTURAL INFLUENCE COEFFICIENT PROGRAM	1
			SLOADS	\$CASE FOR STRUCTURAL LOADS PROGRAM	1
	Steady <sub>Op</sub>	60	SD&SS	Motion <sub>PERT</sub>	59
				\$DYNAMIC ANALYSIS	73
			TH	\$CASE FOR TIME HISTORIES PROGRAM	1
	Unsteady <sub>Op</sub>	67	SD&SS	Motion <sub>PERT</sub>	59
				\$DYNAMIC ANALYSIS	73
			TH	\$CASE FOR TIME HISTORIES PROGRAM	1
	\$DYNAMIC ANALYSIS	73	AIC	Unsteady <sub>Op</sub>	6
			NM	NEIG	7
			SD&SS	Unsteady <sub>Op</sub>	6
				Motion <sub>PERT</sub>	59
				Steady <sub>Op</sub>	60
\$STRUCTURAL DATA	81	ISIC	\$CASE FOR INTERNAL STRUCTURAL INFLUENCE COEFFICIENT PROGRAM	1	
		ESIC	\$CASE FOR EXTERNAL STRUCTURAL INFLUENCE COEFFICIENT PROGRAM	1	
\$RECYCLE	4	TH	\$CASE FOR TIME HISTORIES PROGRAM	1	
		ALOADS	\$CASE FOR ALOADS PROGRAM	1	

TABLE 2.0-1.—CONCLUDED

OPTION DESIRED			RELATED OPTIONS		
PROGRAM	OPTION	CARD	PROGRAM	OPTION	CARD
TH	\$CASE FOR TIME HISTORIES PROGRAM	1	NM	NEIG	7
			SD&SS	Motion <sub>PERT</sub>	59
				Steady <sub>Op</sub>	60
	\$PLOT SPECIFICATIONS	13	THPLOT	Paper <sub>Op</sub>	1
	\$GUST DATA	31	SD&SS	Gust <sub>Op</sub>	6
ALoads	\$CASE FOR ALoads PROGRAM	1	ESIC	\$CATALOG OF INPUT EXTERNAL MATRICES AND GEOMETRY DATA	6
			SD&SS	Motion <sub>REF</sub>	5
				Loads <sub>Op</sub>	37
SLOADS	\$CASE FOR STRUCTURAL LOADS PROGRAM	1	SD&SS	Loads <sub>Op</sub>	37
				Loads <sub>Op</sub>	59
THPLOT	Paper <sub>Op</sub>	1	TH	\$PLOT SPECIFICATIONS	13

The Steady Motion<sub>REF</sub> option can be set by the user to calculate the steady aerodynamic matrices for symmetric motion only, or for both symmetric and antisymmetric motion. This solution-oriented option is therefore tied to the SD&SS program options Motion<sub>REF</sub> (card 5) and Motion<sub>PERT</sub> (card 59). The Motion<sub>REF</sub> option determines whether the *static* stability problem analysis\* is to be made for symmetric or coupled reference motion. The Motion<sub>PERT</sub> option of the \$PERTURBATION DATA section of the SD&SS input deck determines whether the stability derivatives, and the coefficients for the dynamic equations of motion, should be calculated for the symmetric, antisymmetric or coupled motion problem. The user can choose the symmetric reference motion option (e.g., steady level trimmed flight, Motion<sub>REF</sub> = Symmetric Reference Motion) and *still* select the coupled perturbation motion option (Motion<sub>PERT</sub> = Both) in order to compute both longitudinal and lateral/directional stability characteristics. If the TH program is to be executed however, coupled dynamic equations of motion must be set up, consequently Motion<sub>PERT</sub> = BOTH must be selected to generate derivatives for both symmetric and antisymmetric motion. The calculation of these quantities requires that Steady Motion<sub>REF</sub> = ASYMMETRIC must have been previously requested in the AIC program to compute steady aerodynamic matrices for both symmetric and antisymmetric motion.

The Unsteady<sub>OP</sub> option is tied directly to, or influences the results provided by, three other SD&SS options -- Unsteady<sub>OP</sub>, \$PERTURBATION DATA, and \$DYNAMIC ANALYSIS. This option allows the user to specify that steady, or steady and unsteady, aerodynamic matrices be calculated. If Unsteady<sub>OP</sub> = UNSTEADY is selected in the AIC program, setting Unsteady<sub>OP</sub> = UNSTEADY in the SD&SS program and including the \$PERTURBATION DATA section will cause the unsteady stability derivatives to be calculated. If the \$DYNAMIC *analysis* option is also chosen, these unsteady derivatives will then be used in the calculation of the airplane's dynamic stability characteristics. It should be noted that selecting Unsteady<sub>OP</sub> = UNSTEADY in the AIC program does not require the user to select the Unsteady<sub>OP</sub> option and \$PERTURBATION DATA section in the SD&SS program. Thus the user must exercise some judgment in deciding whether or not to select the Unsteady<sub>OP</sub> option in the SD&SS program because this decision will determine whether unsteady aerodynamic effects are retained in the calculation of both stability derivatives and dynamic stability characteristics. For example, if the \$PERTURBATION DATA and \$DYNAMIC ANALYSIS options are chosen, and the SD&SS Unsteady<sub>OP</sub> option is not, unsteady stability derivatives will *not* be computed and the dynamic stability characteristics will be computed on the basis of steady aerodynamic forces only.

The unsteady Motion<sub>REF</sub> option (card 7) allows the user to calculate the matrices for unsteady symmetric motion only, or for both symmetric and antisymmetric motion. This solution-oriented option is connected indirectly with the SD&SS \$PERTURBATION DATA section. If in that portion of the SD&SS input deck Unsteady<sub>OP</sub> = UNSTEADY is specified together with Motion<sub>PERT</sub> = BOTH, matrices for both symmetric and

---

\*See Table 9.2.1 for description of the three types of static stability problems allowed.

antisymmetric unsteady motion must be provided (i.e.,  $\text{Unsteady Motion}_{\text{REF}} = \text{ASYMMETRIC}$  must be selected in the AIC program). If matrices for symmetric steady and unsteady motion together with a matrix just for antisymmetric steady motion (no matrix for antisymmetric unsteady motion) are input to the SD&SS program, a fatal error will result if  $\text{Motion}_{\text{PERT}} = \text{BOTH}$  is specified in the \$PERTURBATION DATA section. The AIC program options  $\text{Steady Motion}_{\text{REF}}$ ,  $\text{Unsteady}_{\text{OP}}$  and  $\text{Unsteady Motion}_{\text{REF}}$  do make it possible, however, to calculate this latter set of three matrices with no warning or fatal message output from the AIC program. The AIC options also allow a user, again without warning, to calculate an aerodynamic matrix for antisymmetric unsteady motion without providing the corresponding matrix for steady motion. This limited set of data will also result in a fatal error if the  $\text{Motion}_{\text{PERT}}$  option of the SD&SS \$PERTURBATION DATA section is set to ASYMMETRIC.

### 2.1.3 ISIC Program Solution-oriented Options

The \$OPTION FOR ELASTIC FORMULATION section (cards 6 and 7) allows the user to select a rigid, static-elastic or residual-elastic elasticity formulation and to decide whether the corresponding structural matrices should be computed for the symmetric, the antisymmetric or both cases. Clearly, what is specified for this option must be coordinated with the total problem analysis and will involve a consideration of several other program options. The AIC program  $\text{Steady Motion}_{\text{REF}}$  option, which determines whether AIC matrices for symmetric motion only, or matrices for both symmetric and antisymmetric motion will be generated, will normally correspond to the data input to this ISIC section.

Analyses to be conducted in the SD&SS program must also be considered before the user decides upon the input data for \$OPTION FOR ELASTIC FORMULATION. The SD&SS options of concern are  $\text{Motion}_{\text{REF}}$  (SYMMETRIC REFERENCE MOTION or COUPLED REFERENCE MOTION),  $\text{Elastic}_{\text{OP}}$  (RIGID MODEL, STATIC-ELASTIC MODEL or RESIDUAL-ELASTIC MODEL) and  $\text{Motion}_{\text{PERT}}$  (SYMMETRIC, ASYMMETRIC, or BOTH). If option RESIDUAL-ELASTIC MODEL is chosen, the \$OPTION FOR ELASTIC FORMULATION data must also request the structural matrices sufficient for the NM program. For instance, the NM \$OPTION FOR ELASTICITY FORMULATION may request only an antisymmetric modal analysis, but the ISIC \$OPTION FOR ELASTIC FORMULATION could have data requesting both a symmetric and antisymmetric residual-elastic analysis. The reverse situation will, during execution of the NM program result in a fatal error.

The \$GYROSCOPIC DATA (ISIC card 41) option can be selected only if the user has angular momenta data for each engine, which is input to the SD&SS program via the section headed by \$GYROSCOPIC DATA (card 23).

### 2.1.4 NM Program Solution-oriented Options

As stated in section 2.1.3, the \$OPTION FOR ELASTICITY FORMULATION input data must be coordinated between the ISIC and NM programs. The input request made to \$OPTION FOR ELASTICITY FORMULATION in NM must be a subset of the requests



made to the ISIC program. Section 7.2.2 of Volume II should be consulted for a discussion of this option. Also, the information supplied by the \$OPTION FOR ELASTICITY FORMULATION data cards is associated with the MotionPERT option on card 59 of the SD&SS program. This option must be selected properly such that the perturbation motion selected in MotionPERT may be analyzed.

The option NEIG is considered a solution-oriented option because the number of eigenvalues selected is limited if either the TH program or \$DYNAMIC ANALYSIS section of the SD&SS program is used for the stability analysis. Although the NM program does not have any restrictions on the number of eigenvalues computed, the SD&SS and TH programs can accept no more than 20. Therefore, the restriction  $NEIG \leq 20.0$  ( $\leq 10.0$  if symmetric and antisymmetric motion are chosen) must be observed if output data are to be used by these latter two programs. Also, if NEIG is greater than the total number of structural dynamic degrees of freedom embodied in the ISIC calculations, the NM program will set NEIG equal to the total number of structural dynamic degrees of freedom (cf., Vol. I, sec. 6.0).

#### 2.1.5 ESIC Program Solution-oriented Options

The \$CATALOG OF INPUT EXTERNAL MATRICES AND GEOMETRY DATA section basically controls the computations in the program. Depending upon the input matrices available, identified by card section \$CATALOG OF INPUT EXTERNAL MATRICES AND GEOMETRY DATA (card 6), certain output is produced. The set of matrices produced are related to, or influence the choice of, certain options in the SD&SS program. These SD&SS options are MotionREF (SYMMETRIC REFERENCE MOTION or COUPLED REFERENCE MOTION), ElasticOp (RIGID MODEL, STATIC-ELASTIC MODEL, or RESIDUAL-ELASTIC MODEL), \$PERTURBATION DATA (type of perturbation motion) and \$GYROSCOPIC DATA (an analysis utilizing engine gyroscopic moments requires the input of  $[\Delta_G^S]$  or,  $[\Delta_G^S]$  and  $[\Delta_G^A]$ ).

#### 2.1.6 SD&SS Program Solution-oriented Options

The majority of the solution-oriented options impact in one way or another the options chosen in the SD&SS program. Some of these options and their relationship to the SD&SS program were previously described in the sections discussing the GD, AIC, ISIC, NM and ESIC programs. They are cross referenced in table 2.0-1 under the SD&SS program.

The option MotionREF is related to the AIC option Steady MotionREF in that if coupled reference motion is desired, Steady MotionREF must be set to ASYMMETRIC. Also, MotionREF is tied to the ISIC program through the \$OPTION FOR ELASTIC FORMULATION section and to the ESIC program through the \$CATALOG OF INPUT EXTERNAL MATRICES AND GEOMETRY DATA section. These two sections determine the type of motion for which the structural matrices are to be calculated. If gyroscopic effects are included, requiring the use of the \$GYROSCOPIC DATA section, the MotionREF option should be selected as COUPLED REFERENCE MOTION, unless the engine rotations on the right and left hand sides of the aircraft are opposite (also see section 4.1.1).

The Elastic<sub>OP</sub> option is directly related to options and matrices produced in the structures programs, viz. ISIC (\$OPTION FOR ELASTIC FORMULATION), NM (\$OPTION FOR ELASTICITY FORMULATION), and ESIC (\$CATALOG OF INPUT EXTERNAL MATRICES AND GEOMETRY DATA) which have been discussed previously.

As discussed in section 2.1.2, the Unsteady<sub>OP</sub> options in the AIC and SD&SS programs are related, as are also the SD&SS Unsteady<sub>OP</sub> option and the AIC option Unsteady Motion<sub>REF</sub>. Section 2.1.2 also discussed the interrelationships between the SD&SS options Unsteady<sub>OP</sub>, \$PERTURBATION DATA, and \$DYNAMIC ANALYSIS.

The thickness option includes only Slender Body thickness effects if airfoils have not been input to the GD program (parameter NAS on card 37). The thickness aerodynamic effects are important both for the aerodynamic coefficients  $C_{L0}$ ,  $C_{D0}$  and  $C_{m0}$ , and for the speed and yaw-rate stability derivatives. (The coefficients  $C_{L0}$ ,  $C_{D0}$  and  $C_{m0}$  affect aircraft trim and consequently they indirectly affect the stability derivatives.)

The LE Thrust<sub>OP</sub> option (card 6) also affects aircraft trim and certain of the stability derivatives. The derivatives and coefficients primarily affected are  $C_{D0}$ ,  $C_{m0}$ ,  $C_{D\hat{u}}$ ,  $C_{D\alpha}$  and  $C_{n\hat{p}}$ . This option, however, which is fairly expensive in terms of computer time, need only be used for wings with blunt leading edges having a subsonic leading edge.

The Speed<sub>OP</sub> option calculates the static stability parameter stick speed stability. This option requires the selection of the  $\Delta M_1$  option in the AIC program. This is an expensive option for an elastic aircraft having a large number of aerodynamic singularities.

The Gust<sub>OP</sub> option is related to use of the TH program. If the response to the passage of an aircraft through a discrete gust profile is desired, it is required. This option generates the gust aerodynamic matrices for  $W_g$  and/or  $V_g$  gust components. The particular gust component matrices constructed depend upon the Motion<sub>PERT</sub> option used. The  $W_g$  matrix requires that either the SYMMETRIC or BOTH parameter be input, and the  $V_g$  matrix requires the ASYMMETRIC or BOTH parameter. The requirements of the TH program, however, dictate that coupled motion perturbations be analyzed, consequently Motion<sub>PERT</sub> = BOTH is required. This choice will construct both the  $W_g$  and  $V_g$  matrices, whether or not both are required. (The unsteady gust effects,  $W_g$  and  $V_g$ , are dependent on the unsteady options in the AIC program, as well as the Unsteady<sub>OP</sub> option in SD&SS.)

The \$THRUST DATA section can only be selected if a Slender Body has been defined in the GD program (\$SLENDER BODY). If gyroscopic effects are to be analyzed, (i.e. the \$GYROSCOPIC DATA section is included) the \$THRUST DATA section is also required. Gliding flight is the only situation for which the \$THRUST DATA section can be omitted.

If the aircraft is modeled as a flexible structure, the \$GYROSCOPIC DATA section in the SD&SS program is tied to the two structures programs, which must in turn include the proper options for gyroscopic effects. ISIC program data must include the \$GYROSCOPIC DATA section, and the ESIC program must specify the proper  $\Delta G$  matrices in the SCATALOG OF INPUT EXTERNAL MATRICES AND GEOMETRY DATA section.

The stability Problem option (card 35) for which one of the three parameters CONSTANT, ITERATION, or SPECIFIED must be chosen, is discussed in Volume II, section 9.2.1. When Problem = CONSTANT the engine gyroscopic data input via \$GYROSCOPIC DATA must be chosen so that  $H_{OP} = \text{CONSTANT}$  will accurately model the problem, i.e. the angular momentum cannot be a function of the angular velocity of the engine. The ITERATION parameter is used in conjunction with the optional data set \$WIND TUNNEL DATA. Finally, when Problem = SPECIFIED is used the Shape<sub>OP</sub> option parameters can be only REFERENCE OR JIG (DESIGN cannot be used) and THRUST = CONSTANT. Further details of the interplay between the Problem option (card 35) and the Shape<sub>OP</sub> (card 36) are summarized in table 9.2-1 of Vol. II.

The contents of the \$CONTROL SURFACE DATA section depends directly on the GD program paneling. A Thin Body and its panels must be input in the GD program (\$THIN BODY section) in order to define a surface. A longitudinal control surface must be included in every configuration to be analyzed by the SD&SS program.

When Shape<sub>OP</sub> = DESIGN (card 36) it is recommended that the Shape<sub>OUT</sub> and Disp<sub>OUT</sub> option parameters (card 37) be set to 1.0 or 2.0 to print or punch the camber slope and position vectors of the jig shape.

The static Loads<sub>OP</sub> must be chosen if either the SLOADS or ALOADS programs are to be executed. Input to the SLOADS program is output by the ISIC program, and input to the ALOADS program by ESIC.

The other programs and options related to the solution-oriented option Motion<sub>PERT</sub> shown in table 2.0-1 have been previously discussed in conjunction with other solution-oriented options.

The Comp<sub>OP</sub> option is dependent on the selection of the  $\Delta M$  option in the AIC program to calculate aerodynamic matrices suitable for use in compressibility calculations for the speed and yaw-rate stability derivatives.

The Upress<sub>OP</sub> option controls the mode of output of the unsteady lifting pressures on thin bodies (i.e. those pressures arising from  $\dot{W}$ ,  $\dot{Q}$ ,  $\dot{P}$ ,  $\dot{V}$ ,  $\dot{R}$ ,  $\dot{u}_{e_i}$  and  $\dot{u}_{e_j}$ , where  $u_{e_i}$  is the  $i$ -th generalized coordinate used in the residual-elastic structural dynamic model). Its use, therefore, depends upon the unsteady analysis made, which is determined by the AIC options Unsteady<sub>OP</sub> and Unsteady Motion<sub>REF</sub> and the SD&SS Unsteady<sub>OP</sub> option.

The Coneff<sub>OP</sub> option governs the calculation of the control effectiveness derivatives for the trim controls defined in the \$CONTROL SURFACE DATA section. If the Elastic<sub>OP</sub> option is set to either RIGID or STATIC-ELASTIC the values obtained for these derivatives will be the same as those produced by the static stability derivatives section. However, the Coneff<sub>OP</sub> option is tied to the Motion<sub>PERT</sub> option instead of to the Motion<sub>REF</sub> option, so that control derivatives can be calculated for the aileron and rudder, as well as for the elevator, even though Motion<sub>REF</sub> = SYMMETRIC. If Elastic<sub>OP</sub> = RESIDUAL ELASTIC use of the Coneff<sub>OP</sub> option provides airplane control derivatives plus the generalized aerodynamic control derivatives for each elastic mode. These results, however,

yield nothing of value in Level 1.02.00 FLEXSTAB because they are not programmed for use either in the \$DYNAMIC ANALYSIS section or in the TH program.

Setting Loads<sub>OP</sub> = LOADS (card 59) results in the calculation and storage on tape of dynamic load matrices based on the ISIC program formulation for later printout by the SLOADS program. Section 17.2.1 of Volume II should be consulted for a discussion of the usefulness of these results.

The \$WIND TUNNEL DATA section (cards 47-57) is included only for the SD&SS option Problem = ITERATION. Using this option, the program trims the airplane by iteration using wind tunnel and/or handbook data supplied by the user. Any data not specified by the user in \$WIND TUNNEL DATA, but required for the trim solution, are calculated using linear theory.

User-supplied stability derivatives can be entered into the program through use of the options Steady<sub>OP</sub> and Unsteady<sub>OP</sub> appearing in the \$PERTURBATION DATA section. These options are related to the Motion<sub>PERT</sub> option—if Motion<sub>PERT</sub> = SYMMETRIC only symmetric stability derivatives can be input as empirical data. The empirical data input directly influences the dynamic analyses which can be made via \$DYNAMIC ANALYSIS section of SD&SS and by the TH program.

The \$STRUCTURAL DATA section must be included if a rigid model is being analyzed and neither the ISIC nor ESIC programs were executed. It is also necessary to leave blanks in the SIC Tape and IN/EX<sub>SIC</sub> fields of SD&SS card 7.

The analysis controlled by the \$DYNAMIC ANALYSIS section can be applied to the symmetric, antisymmetric, or coupled set of equations. The set selected is determined by the choice made for the SD&SS option Motion<sub>PERT</sub>.

In a recycle computer run through the SD&SS program (by use of the \$RECYCLE DATA section) multiple data sets are created on the output tape. The ALOADS program can analyze each recycle case, however the TH program can analyze results only from the initial case.

### 2.1.7 TH Program Solution-oriented Options

The solution-oriented option \$GUST DATA is related to two SD&SS options — Gust<sub>OP</sub> and Motion<sub>PERT</sub>. The Gust<sub>OP</sub> option must be selected to calculate the gust aerodynamic matrices, and the Motion<sub>PERT</sub> option must be selected as BOTH (coupled perturbation motion). This latter requirement (coupled perturbation motion) exists because the TH program always solves the six rigid body equations of motion: and, if the residual elastic option is selected, equations equal in number to the number of elastic (structural dynamic) modes selected must also be solved. (Although the effects of these modes on the rigid body degrees of freedom are included, the time histories of the structural dynamic degrees of freedom are neither printed nor plotted.)

The optional card section \$PLOT SPECIFICATIONS must be selected and appropriate data input if a plot tape containing time history information needed by the TH PLOT program is to be created.

#### 2.1.8 ALOADS Program Solution-oriented Options

As mentioned previously, the ALOADS program can be used only in conjunction with the ESIC program. A further restriction stems from the fact that an ALOADS computer run can be made only for symmetric reference flight, hence the SD&SS option Motion<sub>REF</sub> must be selected as SYMMETRIC. This program can, however, analyze multiple cases obtained from a \$RECYCLE DATA SD&SS computer run.



### 3.0 AIRPLANE DEFINITION PROGRAMS

This section describes the procedures used to create the FLEXSTAB definitions of Dart Models I and II, the Boeing 707-320B, the Boeing 2707-300PT (SST), and the Lockheed YF-12A. The Dart models do not represent problems of physical significance; rather, they were used as very simple checkout cases. They offer the new user an opportunity to a.) become familiar with input data preparation and b.) execute relatively inexpensive checkout cases at his own computer installation. The 707, SST, and YF-12A illustrate more realistic and more complex modeling problems.

The information used to develop the inputs for the 707-320B and the SST was obtained from Boeing documents that are not generally available. They are referred to as "company documents," without specified document numbers.

This section summarizes the input data requirements for each of the airplane definition programs and describes the input data decks used in the demonstration cases. Names are used throughout this volume to identify each of the airplane definition program computer runs. These names, along with the corresponding deck numbers which appear on the first card of each run, are given in table 3.0-1.

TABLE 3.0-1.—COMPUTER RUN IDENTIFICATION—AIRPLANE DEFINITION PROGRAMS

Program	Dart Model I		Dart Model II		707-320B		SST		YF-12A	
	Run name	Deck number	Run name	Deck number	Run name	Deck number	Run name	Deck number	Run name	Deck number
GD	GD-1	01-01	GD-2	02-01	GD-3A GD-3B	03-01 03-08	GD-4	04-01	GD-5A GD-5B	05-01 05-06
GDPLOT					GDPLOT-3	03-10	GDPLOT-4	04-09		
AIC	AIC-1	01-02	AIC-2	02-02	AIC-3	03-02	AIC-4	04-02	AIC-5A AIC-5B	05-02 05-07
CAIC							CAIC-4	04-07		
ISIC	ISIC-1	01-03			ISIC-3	03-03				
EAPLOT					EAPLOT-3	03-11				
NM	NM-1	01-04			NM-3	03-04				
NMPLOT					NMPLOT-3	03-12				
ESIC	ESIC-1	01-09					ESIC-4	04-03	ESIC-5A ESIC-5B	05-03 05-08



### 3.1 SUMMARY OF INPUT REQUIREMENTS

An airplane's shape is modeled by using the Geometry Definition Program, its aerodynamics by the Aerodynamic Influence Coefficient program, and its structure by either the Internal or External Structural Influence Coefficient program. This section summarizes the most important input requirements for these and all other airplane definition programs (see table 3.0-1, vol. II). Where possible, Volume II card numbers are given with each input requirement.

#### 3.1.1 Geometry Definition (GD) Program

The GD program requires an input data deck describing the external shape of the airplane. The program processes the data and assembles it on output tape GDTAPE for use by subsequent programs.

*Slender Body input.* – Slender Bodies are used to simulate airplane components such as fuselages, nacelles, and wing pods. When defining a Slender Body, the following information is required:

- Name of Slender Body (CARD 7)
- Slender Body origin (CARD 8)
- Nose and aft end locations (CARD 11)
- Regions influenced by Thin Bodies (CARDS 9-10)
- Number and placement of control points<sup>a</sup> (CARDS 11 and 15)
- Area or radius distribution (CARDS 12-14)
- Camber line definition (CARDS 16-17)

*Interference Body input.* – Interference bodies are used to cancel the interference effects experienced by Slender Bodies in a multiple wing/body configuration. The program requires the following information:

- Name of Interference Body and reference body (CARD 19)
- Interference Body origin (CARD 20)
- Region where Thin Bodies affect the referenced Slender Body (CARD 21)
- Wing-body intersection line

---

<sup>a</sup>The definition of Slender Body control points given in Volume II (see sec. 4.2.1) applies throughout this volume.

- Number and location of cross-sectional panel corner points (CARDS 22-23)
- Interference Body transverse panel edge locations (CARDS 22 and 24)
- Thin Body intersection data (CARD SET 25)
- Interference Body panel control point locations (CARD 26)

*Thin Body input.*—Thin Bodies are used to represent planar components such as wings and tail surfaces. The required input is:

- Name of Thin Body and reference body (CARD 28)
- Thin Body origin and dihedral (CARD 29)
- Planform definition (CARDS 30-32)
- Paneling scheme (CARDS 33-35)
- Panel control point locations (CARD SET 36)
- Airfoil definition (CARDS 37-39)
- Twist definition (CARDS 40-41)

### 3.1.2 Geometry Definition Plot (GD PLOT) Program

The GD PLOT program requires a GD program output tape (GDTAPE) and an input deck in which various plotting options are specified. From this information a three-view CalComp drawing of the model is produced (individual bodies can also be plotted if desired). Identified on the drawing (optional) are the Thin Body panel centroids and panel control points as well as the Slender Body control points.

### 3.1.3 Aerodynamic Influence Coefficient (AIC) Program

The AIC program uses data from the geometry definition output tape, GDTAPE, and an input deck to compute various steady and unsteady (if desired) aerodynamic matrices. These matrices are stored on output tape AICTAP for use in the SD&SS program.

*AIC input.*—The information required in the input data deck consists of:

- Type of reference motion—symmetric or coupled (CARD 5)
- Mach number (CARD 4)
- Perturbation delta Mach number—for Mach derivatives (CARD 4)
- Steady/unsteady option (CARDS 6-7)

- Near field–far field data (CARDS 11-15)

#### 3.1.4 AIC Matrix Correction (CAIC) Program

The CAIC program may be used to alter any or all elements of the [LSC] matrices computed by the AIC program. The information required as input consists of:

- Type of reference motion–symmetric or coupled (CARD 4)
- Method of altering the [LSC] matrices (CARD 4)
- Values used to alter the [LSC] matrices (CARDS 5-6)

#### 3.1.5 Internal Structural Influence Coefficient (ISIC) Program

The ISIC program requires a GD program output tape (GDTAPE) and a data deck defining stiffness and mass properties as input. From these data it generates input for the EAPLOT, NM, and SD&SS programs.

*General information.*—Certain information about program options and body coupling is required prior to the actual structural definitions of each body. This information includes:

- Problem type (CARDS 7-8)
- General Junction Point X-locations (CARD SET 11)
- General Junction Point symmetry code (CARD SET 11)
- Junction Point Paths (CARD 12)
- Gyroscopic effects option (CARDS 41-43)

*Slender Body input.*—Bodies defined as Slender Bodies in the GD program require the following structural data:

- Number of parts
- Associated General Junction Points (CARD 17)
- Number and locations of segments (CARDS 17 and 19)
- Number of interior structural nodes per segment (CARD SET 21)
- Segment stiffness properties (CARD SET 21)
- Lumped mass distribution and scale factors (CARDS 23-26)

*Thin Body input.* -- Bodies defined as Thin Bodies in the GD program require the following structural data:

- Associated General Junction Points (CARD 28)
- Number of parts
- Number and locations of segments (CARDS 30 and 32)
- Number of interior structural nodes per segment (CARD SET 34)
- Segment stiffness properties (CARD SET 34)
- Lumped mass distribution and scale factors (CARDS 37-40)

#### 3.1.6 Elastic Axis Plot (EAPLOT) Program

EAPLOT requires an ISIC program output tape (EATAPE) and an input data deck. From the tape input the EAPLOT program creates a three-view CalComp drawing of the elastic axes. Individual bodies can also be plotted. The General Junction Points, structural nodes, and lumped masses are identified on the drawing.

#### 3.1.7 Normal Modes (NM) Program

The NM program accepts data from an ISIC program output tape (SICTP1) and an input data deck. From these data the NM program computes the natural frequencies and modal shapes of the structural model. The information required in the input data deck includes:

- Structural option (CARD 5)
- Number of modal shapes desired (CARD 7)

#### 3.1.8 Normal Modes Plot (NMPLLOT) Program

The NMPLLOT program accepts the information computed by the NM program (stored on NMTAPE) and creates a CalComp drawing of the modal shapes of the structural model. The user specifies the type (symmetric and/or antisymmetric) and number of modal shapes to be plotted via an NMPLLOT input data deck. For each body on the model, the rotations and normalized displacements associated with each modal shape selected are indicated on the drawing.

#### 3.1.9 External Structural Influence Coefficient (ESIC) Program

The ESIC program uses a GD program output tape (GDTAPE), matrices from a structures program external to FLEXSTAB, and an input data deck defining the structural geometry of the model to generate structural matrices for the SD&SS program.

*General information.* –The following general information is required in the ESIC input deck:

- Catalog of input matrices (CARDS 7-9)
- Reference point location (CARD 11)
- Moment data option (CARDS 13-14)
- Structural geometry data input option—cards or tape (CARDS 15-16)
- Degrees of freedom option—cards or tape (CARDS 17-18)
- Submatrix position (CARDS 19-20)

*Slender Body input.* –Bodies defined as Slender Bodies in the GD program require the following structural data:

- Number and location of structural nodes (CARD 22)
- Lumped mass distribution and scale factors (CARDS 23-26)

*Thin Body input.* –Bodies defined as Thin Bodies in the GD program require the following input:

- Thin Body structural origin and dihedral (CARD 28)
- Number of structural nodes and panels (CARD 28)
- Structural node locations (CARD SET 29)
- Lumped mass distribution and scale factors (CARDS 30 and 33)
- Structural panel definitions (CARD SET 31)

## 3.2 DART MODEL I DEMONSTRATION CASE

Dart Model I is a wing-body configuration that serves to demonstrate the preparation of input data for the airplane definition programs. Special attention is given to those input requirements that are easily misunderstood.

In order to demonstrate internal and external structural modeling, a structural definition was provided by the ISIC and NM programs and another by using the ESIC program. Listings of the input decks for each of the Dart Model I definition program runs are given in appendix A.

This section is organized so that each of the input requirements brought out in section 3.1 is discussed individually. Dimensions of all lengths are in meters.

### 3.2.1 Geometry Definition Program—GD-1

Figure 3.2-1 illustrates the geometry of Dart Model I. It is composed of a “fuselage” with a conical nose and tail and a cylindrical midsection, and a rectangular, low-aspect-ratio wing with no thickness. This wing-body combination was modeled by representing the fuselage with a Slender Body and the wing with a Thin Body. An Interference Body, which cancels the velocities induced by the wing on the fuselage, was also defined (not shown in fig. 3.2-1).

This section discusses how these bodies were defined and input to the GD program. The bodies are discussed in an order which differs from that required by the GD program. Normally, it is advisable to first define the bodies in some natural sequence and then, once the input requirements for each are satisfied, rearrange their order to that prescribed by the GD program.

*Reference Axis System placement.*—First, the location of the Reference Axis System is specified. Although this is not an input requirement, the location and orientation of the Reference Axis System in relation to some component of the airplane (normally the fuselage) is of fundamental importance. It is with respect to this axis system that all bodies and local coordinate systems (structural as well as aerodynamic) are defined (see sec. 3.5, vol. II). The X-Z plane of the Reference Axis System must coincide with the airplane’s vertical plane of symmetry and the Y-axis must increase positively from the plane of symmetry toward the right wing tip. Within these criteria, placement of the Reference Axis System is arbitrary. However, as stated in section 3.5.1 of Volume II, the X-axis should be oriented so that it is parallel to (or nearly parallel to) the straight line which most closely approximates the locus of the fuselage cross-sectional area centroids. This ensures a good aerodynamic representation of the configuration.

In the case of Dart Model I, the origin of the Reference Axis System was placed at the nose of the fuselage (see fig. 3.2-2). The X-axis was aligned with the axis of revolution of the fuselage. (Note that from this point on, only those portions of the configuration lying on or to the right of the X-Z plane are defined.)

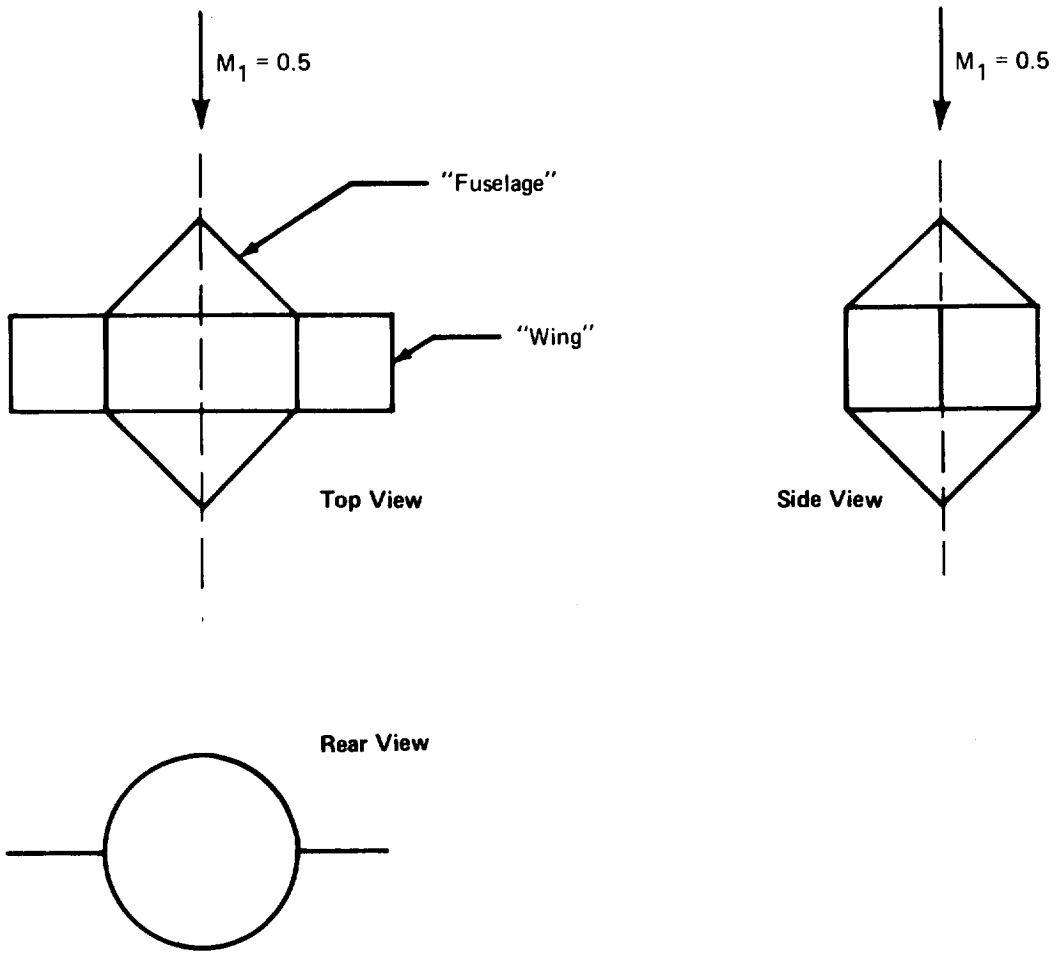


FIGURE 3.2-1.—GEOMETRY OF DART MODEL I

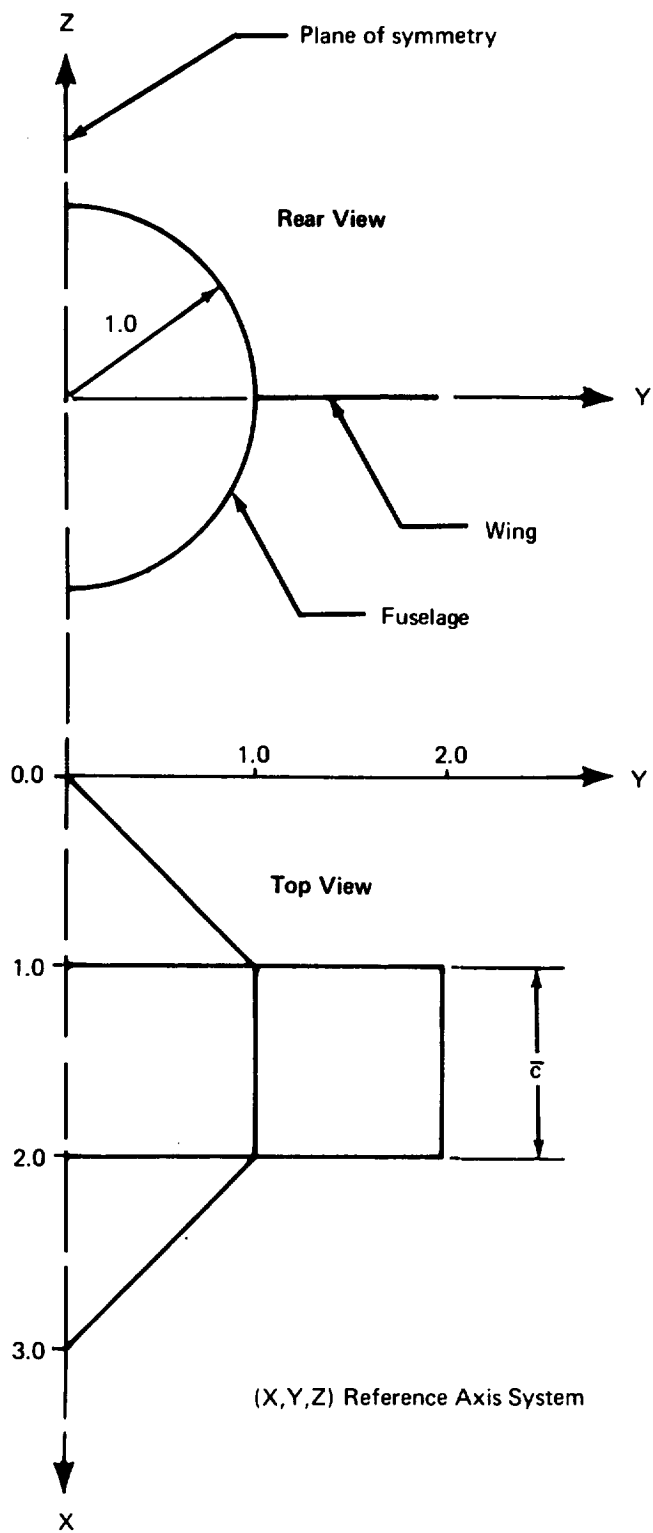


FIGURE 3.2-2.—PLACEMENT OF REFERENCE AXIS SYSTEM—DART MODEL I



After placement of the Reference Axis System, definition of the various components of the configuration followed.

*Fuselage definition.* –The Dart Model I fuselage has no camber and is circular in cross section.

- Name of Slender Body: The Dart Model I fuselage was given the name DART.
- Slender Body origin: The origin of the Local Slender Body Coordinate System was chosen to coincide with the origin of the Reference Axis System (see fig. 3.2-3). Note that the X-location of this origin is arbitrary since the location of the Slender Body is specified later. The Y- and Z-locations, however, determine the position of the  $X_M$ -axis about which the Slender Body is defined. These locations must be consistent with the Reference Axis System placement.
- Nose and aft end locations: Since the origin of the Local Slender Body Coordinate System coincided with the nose of the fuselage, the nose location,  $x_N$ , was set to zero. The length of the fuselage was assumed to be 3 meters; therefore,  $x_T = 3.0$  (see fig. 3.2-4).
- Regions influenced by Thin Bodies: This input defines the X-locations of the leading and trailing edges of the Interference Body associated with this Slender Body. In this case, the region was assumed to extend from the leading edge to the trailing edge of the wing, i.e., from  $X = 1.0$  to  $X = 2.0$  (see fig. 3.2-5). For more realistic configurations, the procedure recommended in section 4.2.1 of volume II should be followed.
- Number and placement of control points: Since a small checkout case was desired, only three control points were used. These were evenly distributed along the length of the fuselage by using the automatic placement option in the GD input. This option divides the Slender Body length into equal segments and places the control points at the midpoints of each (see fig. 3.2-4).
- Area or radius distribution: The fuselage radius distribution was specified by inputting body radii at four  $X_M$ -locations. Body radii of 0.0, 1.0, 1.0, and 0.0 were input at  $X_M = 0.0, 1.0, 2.0, \text{ and } 3.0$ , respectively.
- Camber line definition: The fuselage had no camber.

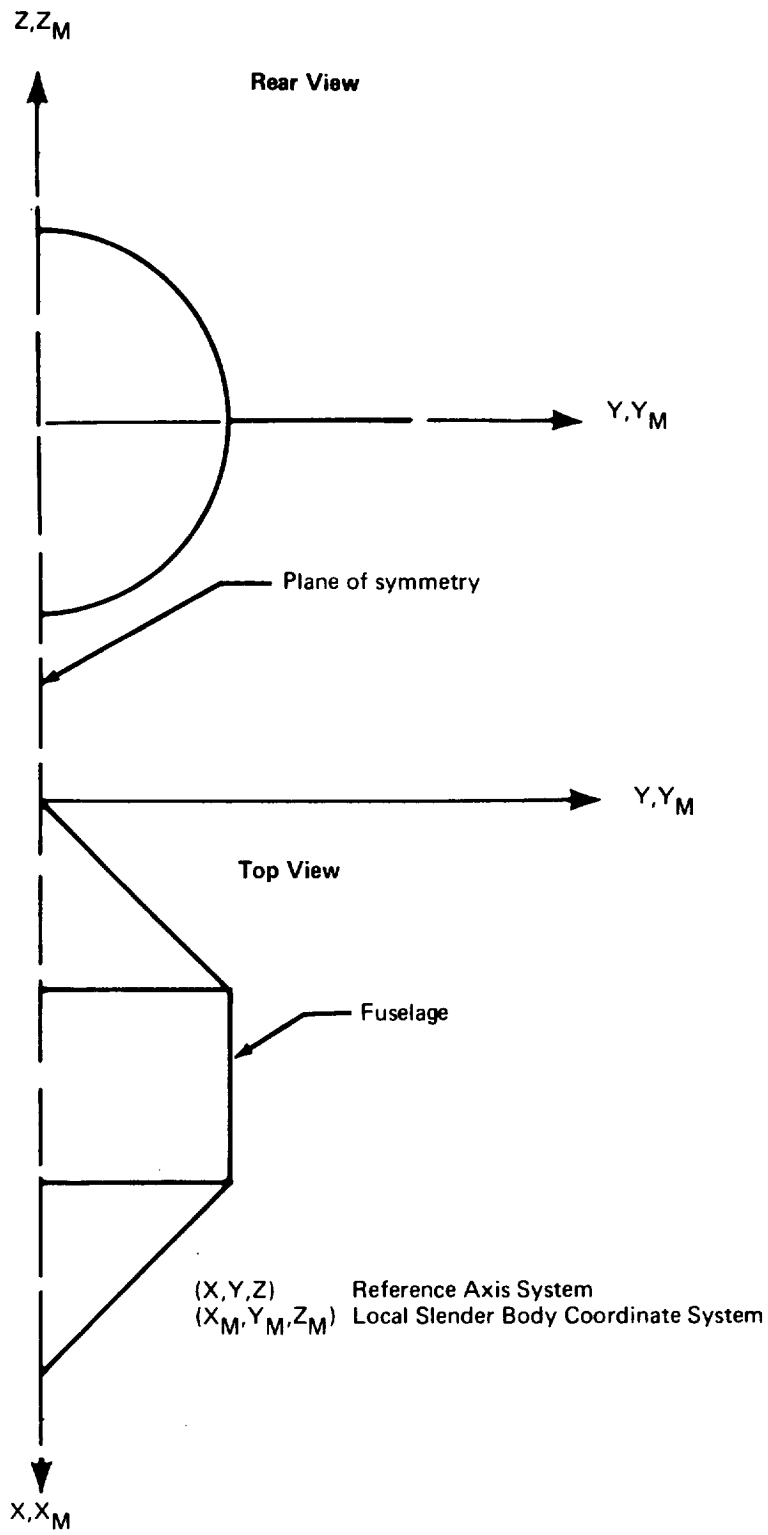


FIGURE 3.2-3.—PLACEMENT OF LOCAL SLENDER BODY COORDINATE SYSTEM—DART MODEL I

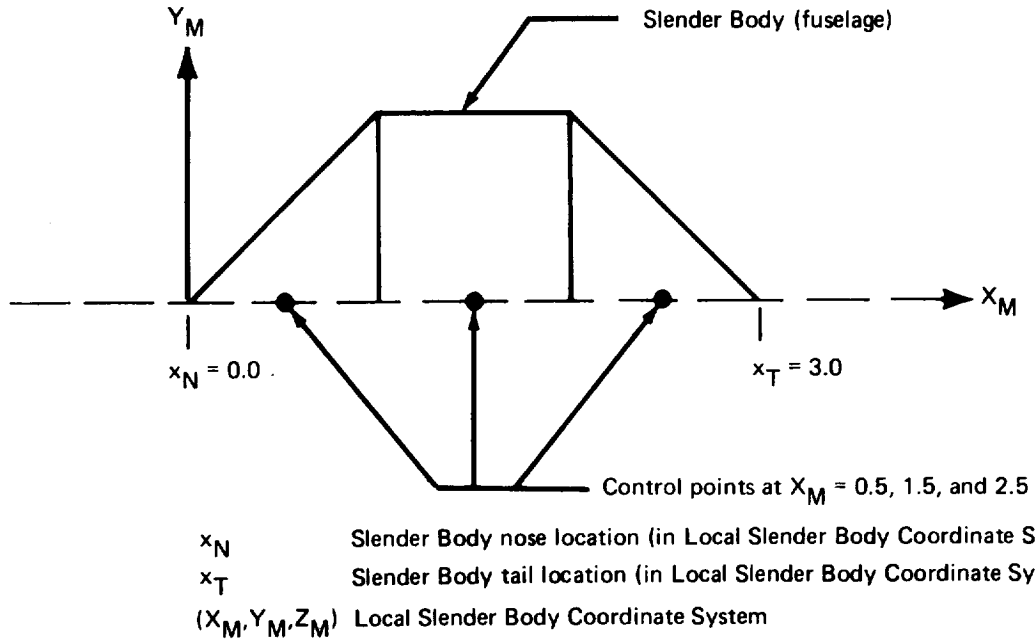


FIGURE 3.2.4.—SLENDER BODY NOSE, TAIL, AND CONTROL POINT LOCATIONS—  
DART MODEL I

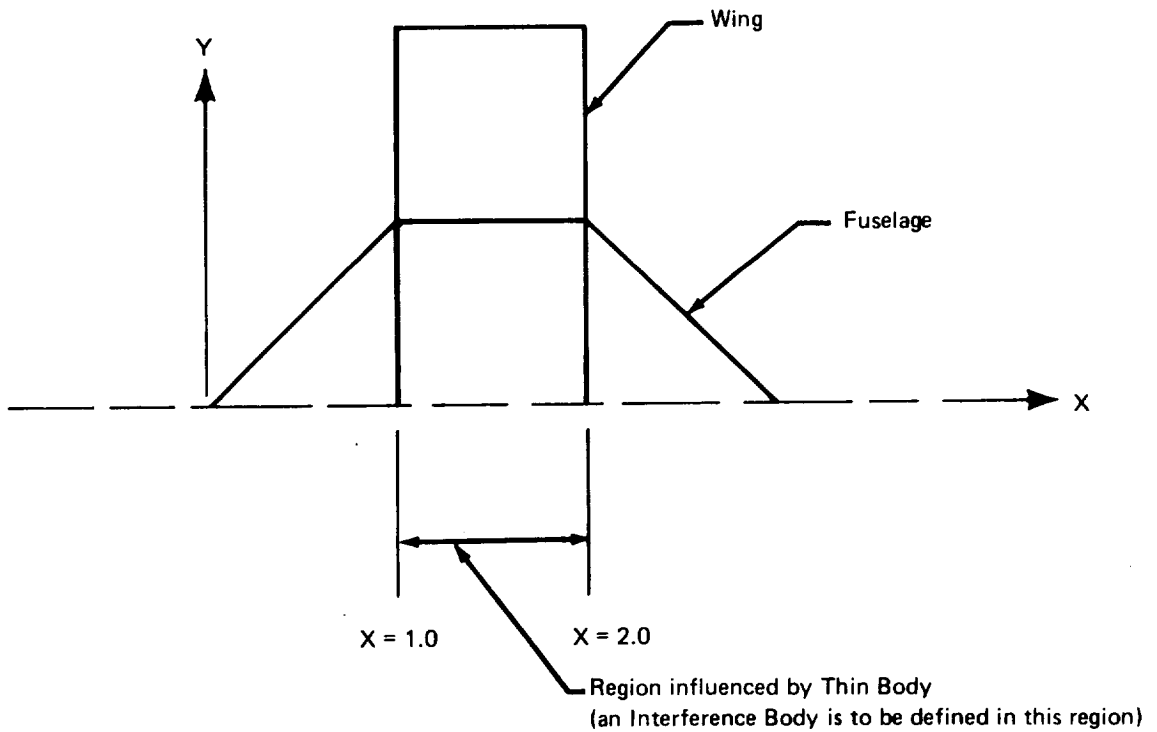
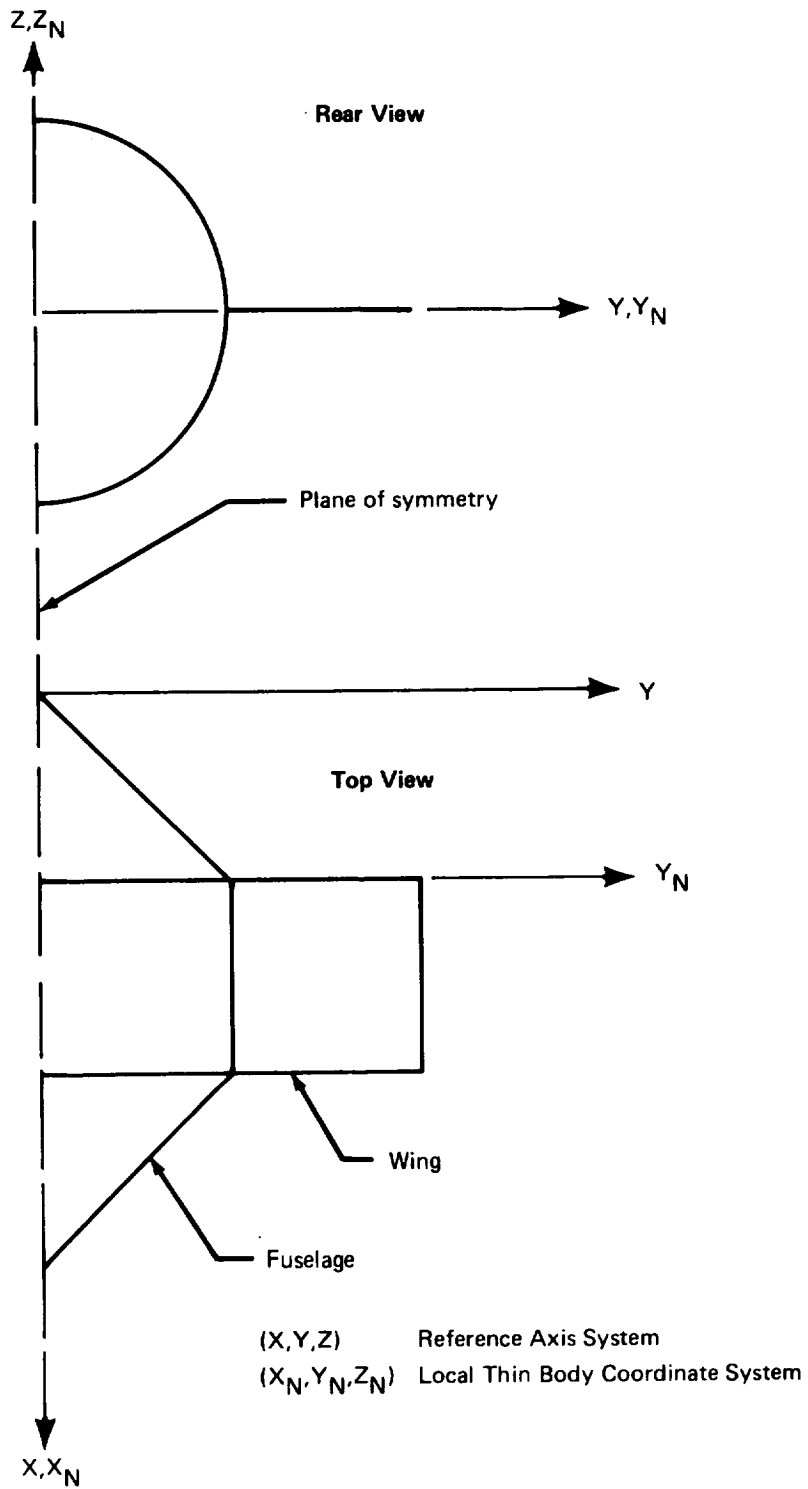


FIGURE 3.2.5.—REGION INFLUENCED BY THIN BODIES—DART MODEL I

*Wing definition.* –The wing of Dart Model I was defined with one Thin Body.

- Name of Thin Body and reference body: The wing of Dart Model I was named WING. Its reference body was IB1 (see “Fuselage Interference Body” below).
- Thin Body origin and dihedral: The planform of a Thin Body must be defined in a Local Thin Body Coordinate System (see sec. 3.5.5, vol. II). The origin of this coordinate system may be arbitrarily placed in the plane in which the Thin Body will lie. In the case of Dart Model I, the origin was placed at the point defined by the intersection of the extrapolated wing leading-edge line with the plane of symmetry, i.e., at  $X = 1.0$ ,  $Y = 0.0$ , and  $Z = 0.0$  (see fig. 3.2-6). The wing dihedral angle is zero degrees.
- Planform definition: The planform of a Thin Body is defined by specifying the  $X_N$ ,  $Y_N$ -coordinates of the planform break points (see CARD 30, sec. 4.2.2, vol. II). Figure 3.2-7 shows the planform chosen for the Thin Body used to represent the wing of Dart Model I. The planform break points and break point coordinates are also shown in the figure. Note that part of the wing planform lies *within* the Slender Body which represents the fuselage. This is acceptable since the GD program will automatically remove this portion of the Thin Body by making use of the fuselage Interference Body definition (see fig. 4.2-15, vol. II).
- Paneling scheme: For simplicity, the minimum number of panels that can be used on one Thin Body was specified. That is, one streamwise row containing two panels (see fig. 3.2-8).
- Panel control point locations: The panel control points were placed at the location recommended in volume II, i.e., at the 85% panel chord point along a line passing through the  $Y_N$ -centroid of the panel row (see fig. 3.2-8).
- Airfoil definition: The Dart Model I wing has no thickness or camber.
- Twist definition: No twist or incidence was specified for the wing.



**FIGURE 3.2-6.—PLACEMENT OF LOCAL THIN BODY  
 COORDINATE SYSTEM—DART MODEL I**

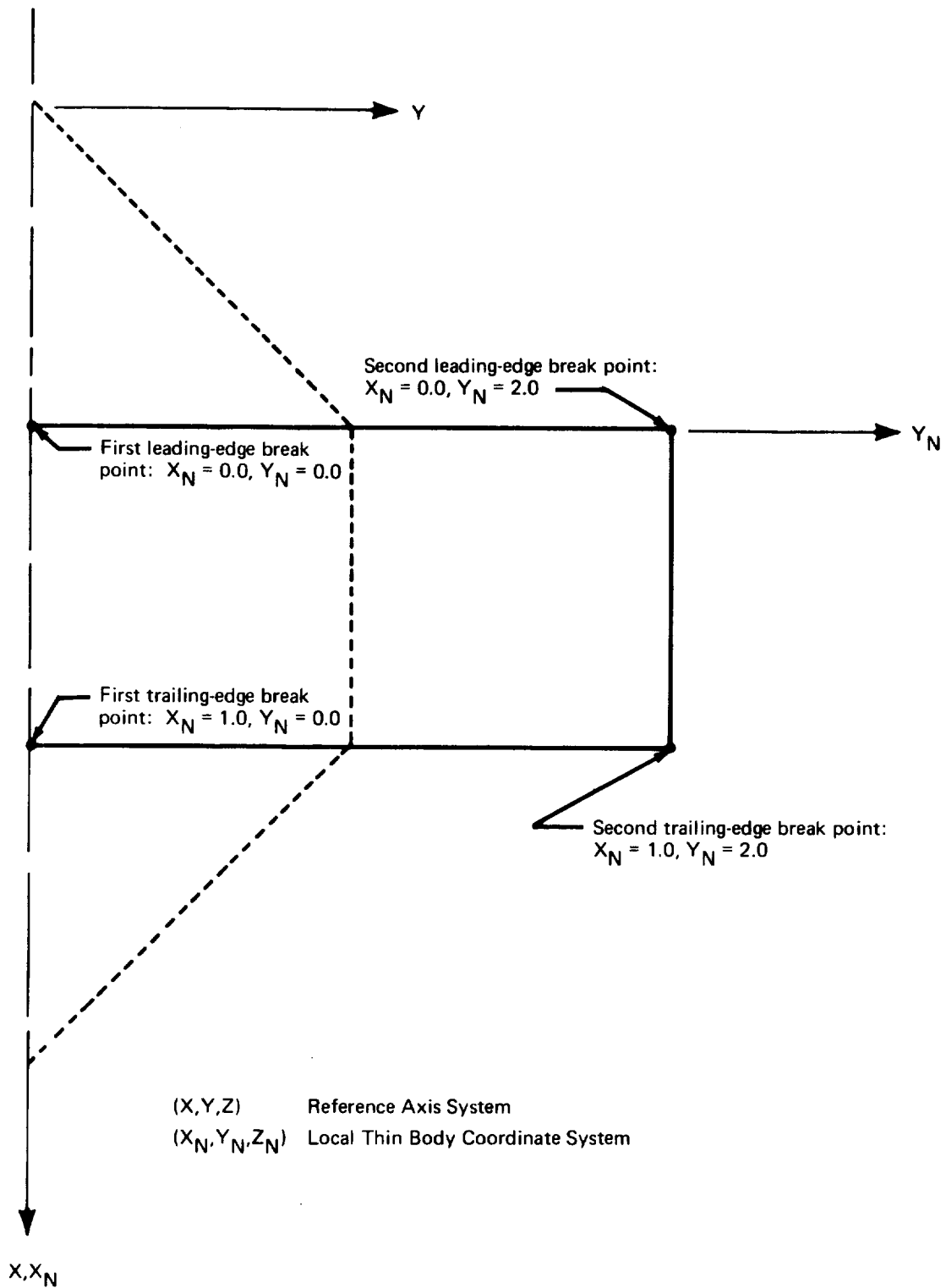


FIGURE 3.2-7.—PLANFORM DEFINITION—DART MODEL I

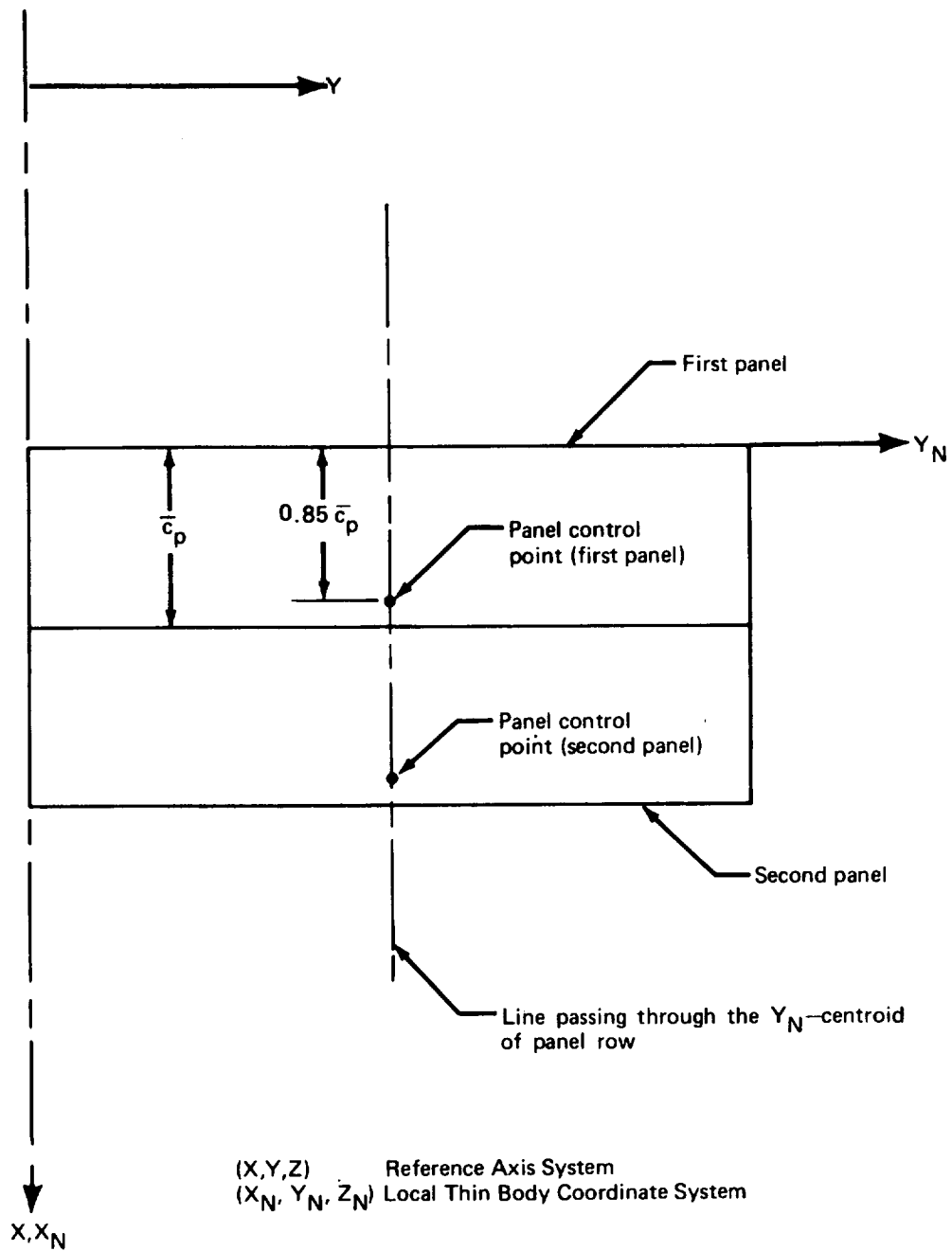
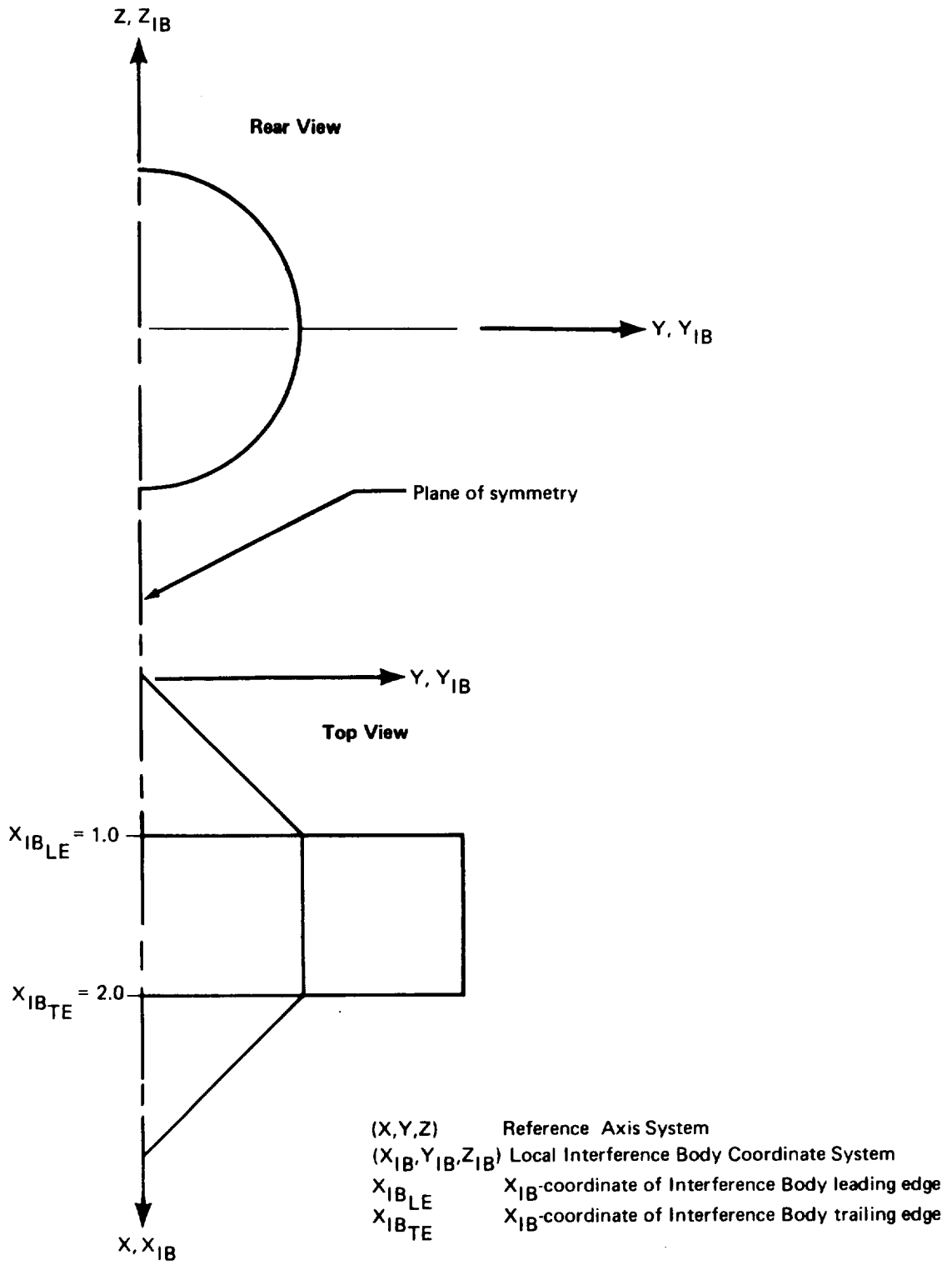


FIGURE 3.2-8.—PANELING SCHEME AND CONTROL POINT LOCATIONS—DART MODEL I

*Fuselage Interference Body.* –The purpose of an Interference Body is to cancel the flow field created by all Slender Bodies and Thin Bodies in the configuration (excluding the Slender Body with which the Interference Body is associated). An Interference Body normally assumes the form of a cylindrical shell of panels surrounding its associated Slender Body. The radius of this cylindrical shell should be approximately equal to the radius of its associated Slender Body in the region where the Thin Body intersections occur. In the case of Dart Model I, the fuselage Interference Body was kept as simple as possible. Its definition is described below.

- Name of Interference Body and reference body: IB1 was the name chosen for the fuselage Interference Body. Its reference body was DART.
- Interference Body origin: The origin of the Local Interference Body Coordinate System was chosen to coincide with that of the Reference Axis System (see fig. 3.2-9). Note that this was an arbitrary choice. The only restriction governing the placement of the origin of an Interference Body Coordinate System is that it must lie on the  $X_M$ -axis of the Local Slender Body Coordinate System of its associated Slender Body.
- Region where Thin Bodies affect the referenced Slender Body: This region was defined in the fuselage Slender Body data (in the Reference Axis System). It determines the location of the leading and trailing edges of the Interference Body. Here, these data are input in terms of the Local Interference Body Coordinate System, i.e.,  $X_{IBLE} = 1.0$  and  $X_{IBTE} = 2.0$  (see fig. 3.2-9).
- Wing-body intersection line: This is not an input requirement as such; however, before defining the Interference Body paneling specifications, it is necessary to consider the location of the line formed by the intersection of the Thin Body (wing) and Slender Body (fuselage). In general, this will not be a straight line since the fuselage Slender Body cross section will be varying in the region of the intersection. A *mean* wing-body intersection line may be defined as the straight line which is parallel to the X-axis and which deviates the least from the true wing-body intersection line. The  $(Y_{IB}, Z_{IB})$  coordinates of this line should be used as one of the Interference Body corner points (see below). (Note that this line should also lie in the  $X_N$ - $Y_N$  Thin Body plane.) In the case of Dart Model I, the wing-body intersection line is located at  $Y_{IB} = 1.0$ ,  $Z_{IB} = 0.0$ .
- Number and location of cross-sectional panel corner points: In keeping with the goal of a small numerical model, only two panels were placed around the defined half of the fuselage (see fig. 3.2-10). This meant that the locations of three cross-sectional corner points had to be specified. One corner point was chosen to correspond to the location of the mean wing-body intersection line defined above. The perpendicular distance from this line to the  $X_{IB}$ -axis defined an Interference Body “radius,”  $R_{IB}$ , which was used to determine the locations of the other corner points. For Interference Bodies associated with Slender Bodies *on* the plane of symmetry, it is recommended that two cross-sectional panel corner points be placed on the X-Z plane in order to “close” the interference shell. Using





**FIGURE 3.2-9—PLACEMENT OF LOCAL INTERFERENCE BODY COORDINATE SYSTEM—DART MODEL I**

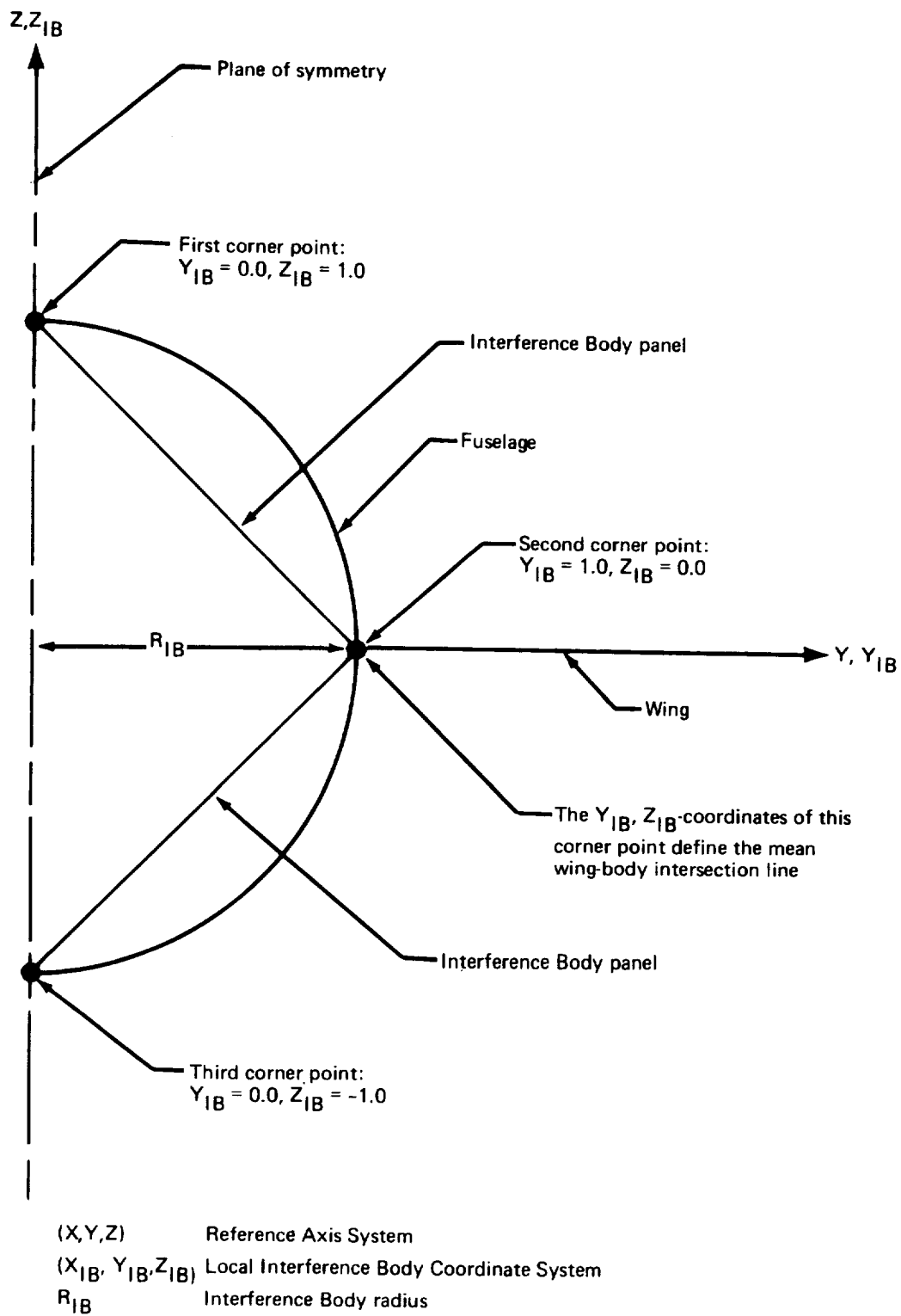


FIGURE 3.2-10.—INTERFERENCE BODY CROSS-SECTIONAL DEFINITION—DART MODEL I

the above criteria resulted in placing the two remaining corner points at  $Y_{IB} = 0.0$ ,  $Z_{IB} = 1.0$ , and  $Y_{IB} = 0.0$ ,  $Z_{IB} = 1.0$ , respectively (see fig. 3.2-10). The automatic paneling option was used to input the locations of these corner points.

- Interference Body transverse panel edge locations: Again, in the interest of simplicity, the Interference Body was specified to have only one panel in its streamwise direction. Its transverse panel edge locations (which in this case were simply the leading and trailing edges of the Interference Body) were specified by using the EQ. SPACE option. Figure 3.2-11 shows the isolated Interference Body geometry that has been completely defined at this point.
- Thin Body intersection data: The location of the end (root or tip) of each intersecting Thin Body is specified in this input. Note that this location *must* agree with the planform shape defined in the Thin Body data and should not be confused with the wing-body intersection line discussed above. In this case, since the Thin Body root coincided with the X-axis (see fig 3.2-7), a root location of  $Y_{IB} = 0.0$ ,  $Z_{IB} = 0.0$  was input. The dihedral was again set to zero. As mentioned previously, the GD program will automatically remove any portion of a Thin Body planform which lies inside an Interference Body (see fig. 4.2-15, vol. II). The mean wing-body intersection line becomes the redefined planform root (or tip) with the inboard (or outboard) row of Thin Body panels being changed accordingly. Figure 3.2-12 shows the geometry definition of Dart Model I after redefinition of the Thin Body (wing) has occurred. Note that the Thin Body panel control points are also shifted so that they are located properly with respect to the newly defined panel row.
- Interference Body panel control point locations: The panel control points were placed at the 85% panel chord points as shown in figure 3.2-11. This is the recommended location.

*Geometry Definition Plot.* -- Figure 3.2-13 shows the three-view plots of the Dart Model I as produced by the GD program plotting routine using the Calcomp machine. The top and side views of Figure 3.2-13 do not look like those shown in Figures 3.2-1 and 3.2-12. The discrepancy is in the plots obtained from the GD plot routine and involve the description of slender bodies (Dart Model I "fuselage"). The information file input to the plot routine does not contain the user's input description of the radius distribution at the defining points, but rather the radius,  $R_1$ , and slope,  $dR_1/dx$ , at the computed control points. Thus, instead of a "fuselage" composed of a conical nose and tail and a cylindrical midsection, the shape shown in figure 3.2-13 is plotted. The fuselage shown in the latter figure is not closed at the nose and tail, but rather the "shape" begins at the first control point and terminates at the last control point. The discrepancy noted above is minimized for models which have a large number of control points.

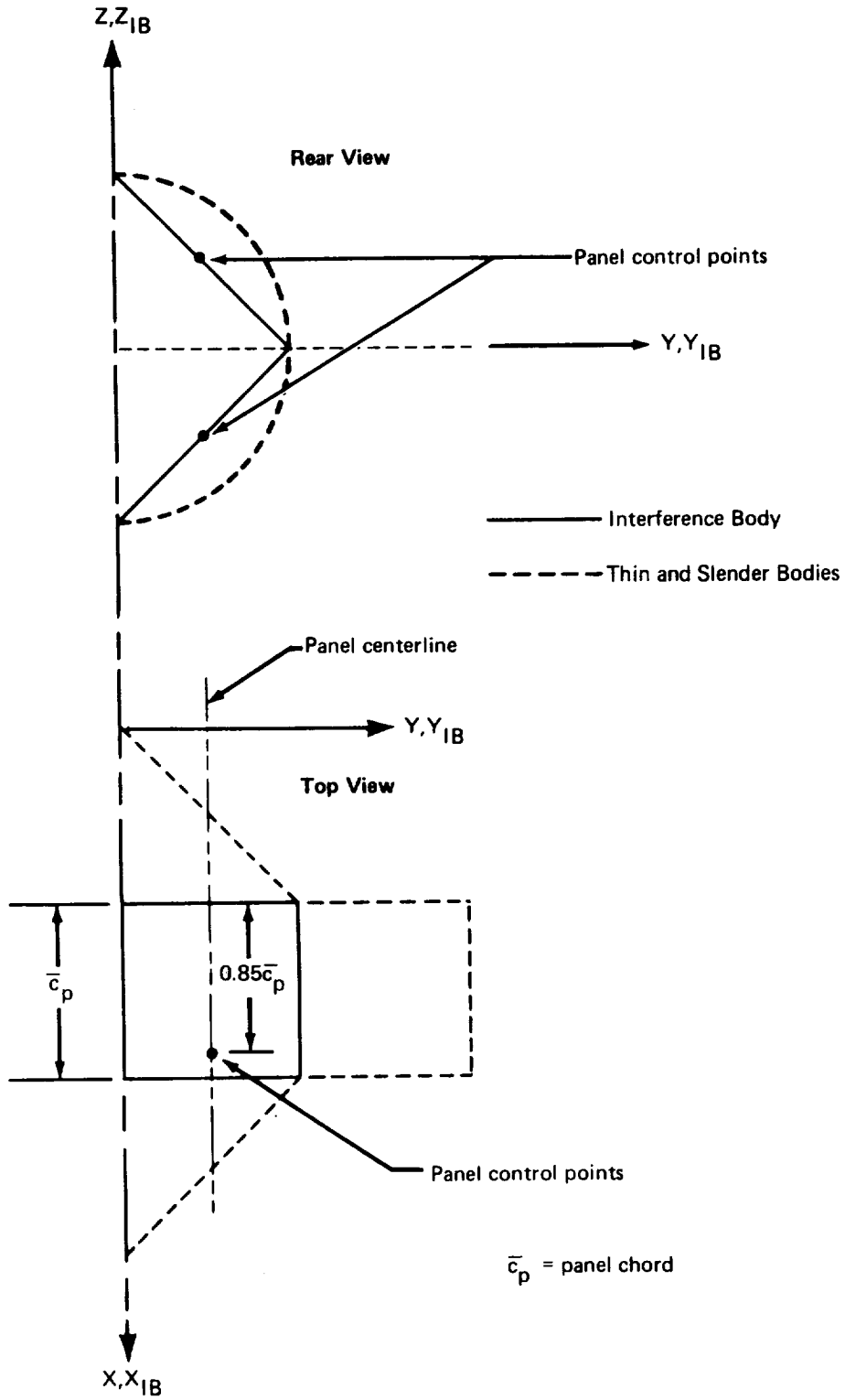


FIGURE 3.2-11.—INTERFERENCE BODY GEOMETRY—DART MODEL I

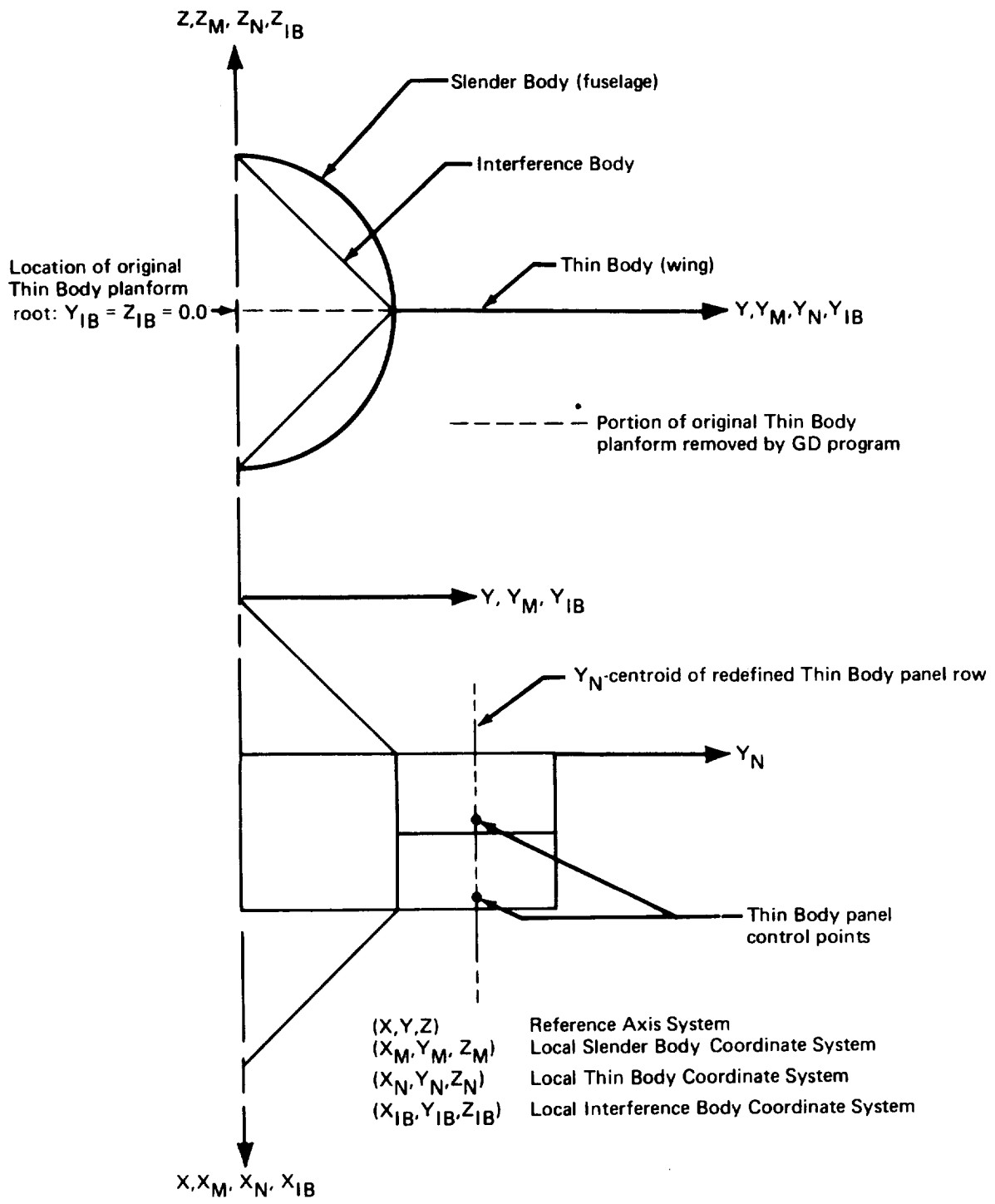


FIGURE 3.2-12.—FINAL GEOMETRY DEFINITION—DART MODEL I

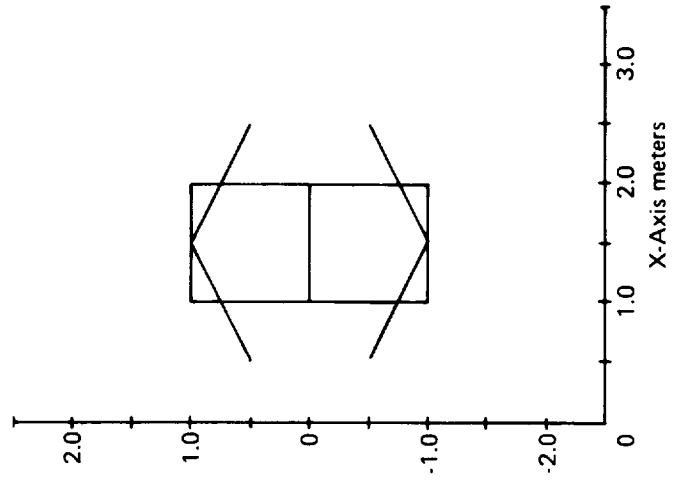
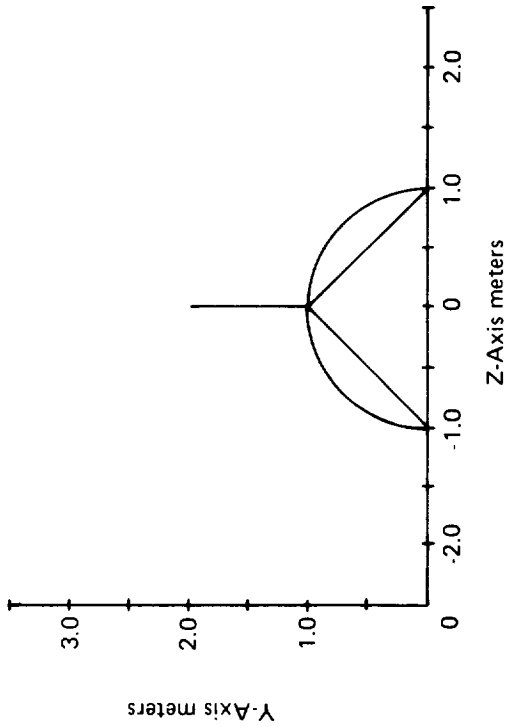
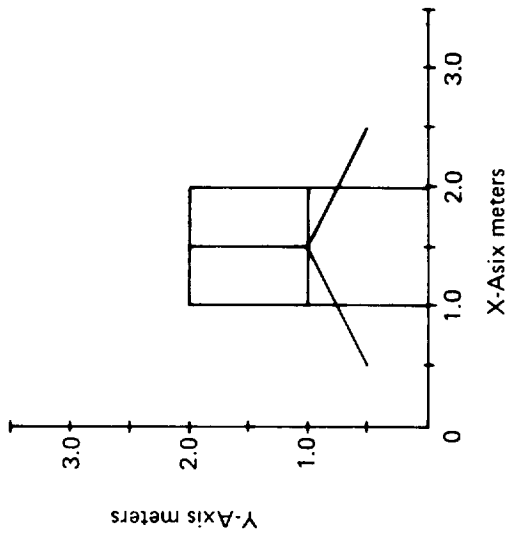


FIGURE 3.2.13. —CALCOMP PLOT OF DART MODEL I

### 3.2.2 Aerodynamic Influence Coefficient Program—AIC-1

The output tape from GD-1 and an input data deck were required in order to execute AIC-1.

*AIC input.*—Included in the AIC input data deck was the following general information.

- Type of reference motion. Both symmetric and antisymmetric reference motions were specified since coupled reference motion was to be analyzed in the SD&SS program.
- Mach number: The Mach number was set to 0.5.
- Perturbation delta Mach number: A perturbation delta Mach number was specified for exemplary reasons. Its value was arbitrarily set to 0.01.
- Steady/unsteady motion: Unsteady aerodynamics was requested for both symmetric and antisymmetric motion since both symmetric and antisymmetric unsteady calculations were to be made in SD&SS.

### 3.2.3 Internal Structural Influence Coefficient Program—ISIC-1

The first of two structural definitions was provided by the ISIC program. The Dart Model I structural definition was chosen to be very simple yet it required the use of most of the important ISIC input options. A description of the Dart Model I structural model follows.

*General Information.*—Figure 3.2-14 shows the elastic axes used for Dart Model I. The following input quantities were specified.

- Problem type: Since the effects of structural vibration modes were to be included in the analysis programs, the residual-elastic option was chosen. This option was chosen for both symmetric and antisymmetric loading conditions since coupled reference motion was to be analyzed in SD&SS.
- General Junction Point X-locations: As shown in Figure 3.2-14, two elastic axes define the Dart Model I structure. The Slender Body elastic axis coincides with the X-axis. The Thin Body elastic axis is parallel to the Y-axis and intersects the Slender Body axis at  $X = 1.2$ . This intersection defines one General Junction Point, namely,  $JP_{II}$ . The Reference Junction Point of the entire structure *must* be located at the nose of the configuration and is *always* the first General Junction Point assigned. Therefore,  $JP_I$  is at  $X = 0.0$ .
- General Junction Point symmetry code: Both General Junction Points are on the plane of symmetry (see fig. 3.2-14).

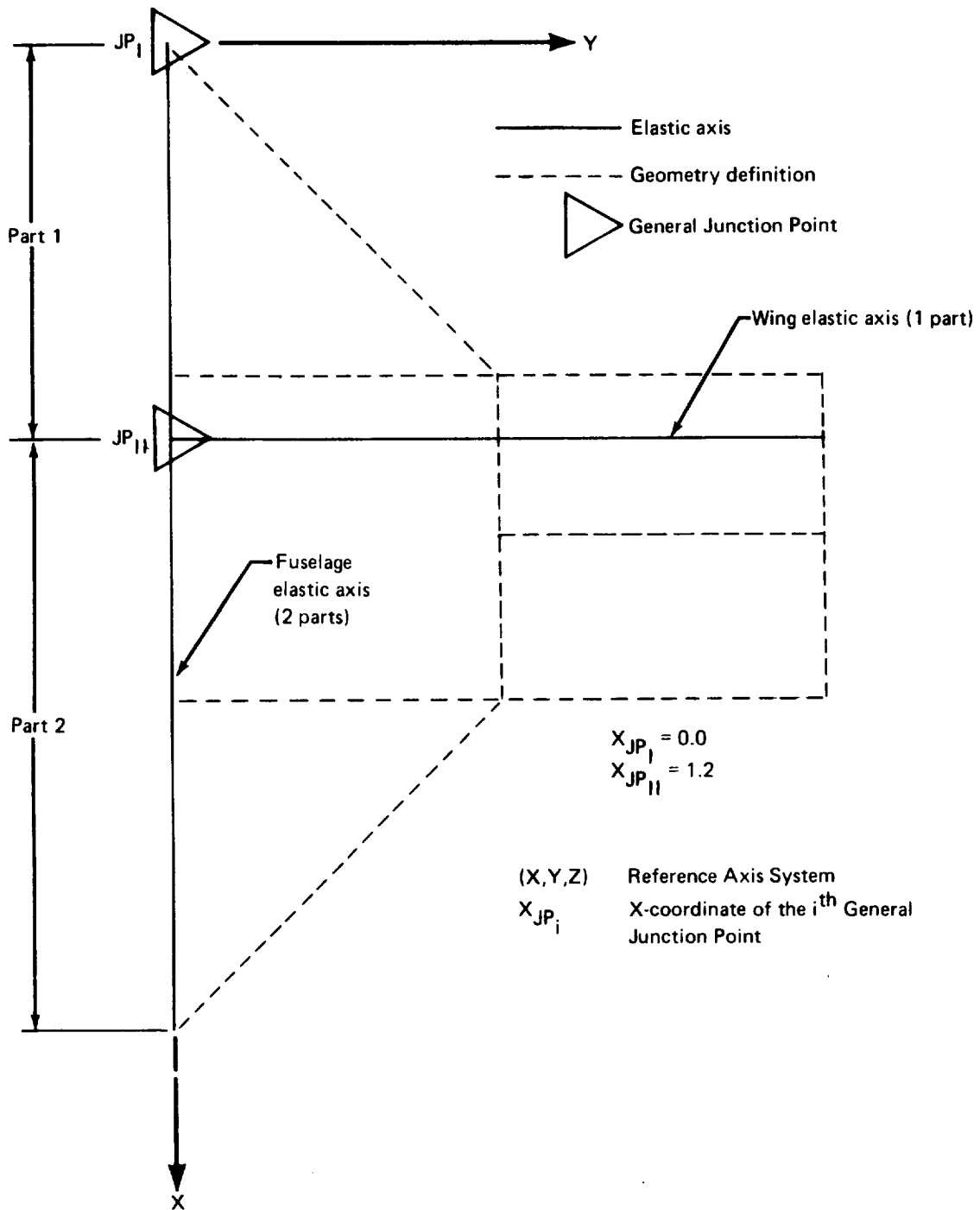


FIGURE 3.2-14.—ELASTIC AXIS REPRESENTATION OF DART MODEL I STRUCTURE



- Junction Point Paths: There is only one independent Junction Point Path; namely, JP<sub>I</sub>, JP<sub>II</sub>.
- Gyroscopic effects option: These cards were not included since Dart Model I had no engines.

*Fuselage definition.*—The elastic axis definition of figure 3.2-14 and some arbitrarily specified stiffness and mass values comprised the data used to generate the following information.

- Number of parts: The fuselage elastic axis was divided into two parts by the wing intersection (General Junction Point II; see fig. 3.2-14).
- Associated General Junction Points: Junction points I and II were the General Junction Points associated with the fuselage Slender Body.
- Number and locations of segments: The first part of the fuselage Slender Body consisted of one segment. The second part had three segments (see fig. 3.2-15). The coordinates of the ends of these segments are shown in figure 3.2-15.
- Number of interior structural nodes per segment: One interior node was specified for the first (and only) segment of Part 1. None were defined for the segments of Part 2.
- Segment stiffness properties: The  $EI_{YM}$ ,  $EI_{ZM}$ , and GJ values were arbitrarily set to 31420, 31420, and 1704 newton-meters squared, respectively, for each segment of the Slender Body. (Note: The *full* stiffness is input *even* when the fuselage elastic axis is on the plane of symmetry.)
- Lumped mass distribution and scale factors: A mass of one kilogram was placed at the location of the interior node on Slender Body Part 1 (see fig. 3.2-15). Another mass of one kilogram was placed at the final node of Part 2. Note: For masses which lie on the plane of symmetry *one half* the actual mass is input. The data therefore represents masses of two kilograms on the plane of symmetry. The \$SCALE FACTORS card section was not used.

*Wing definition.*—The wing input data were generated by using the elastic axis definition in figure 3.2-13 and arbitrarily specified stiffness and mass values.

- Associated General Junction Points: General Junction Point II was the only junction point associated with the wing (see fig. 3.2-14).
- Number of parts: The wing elastic axis had only one part.

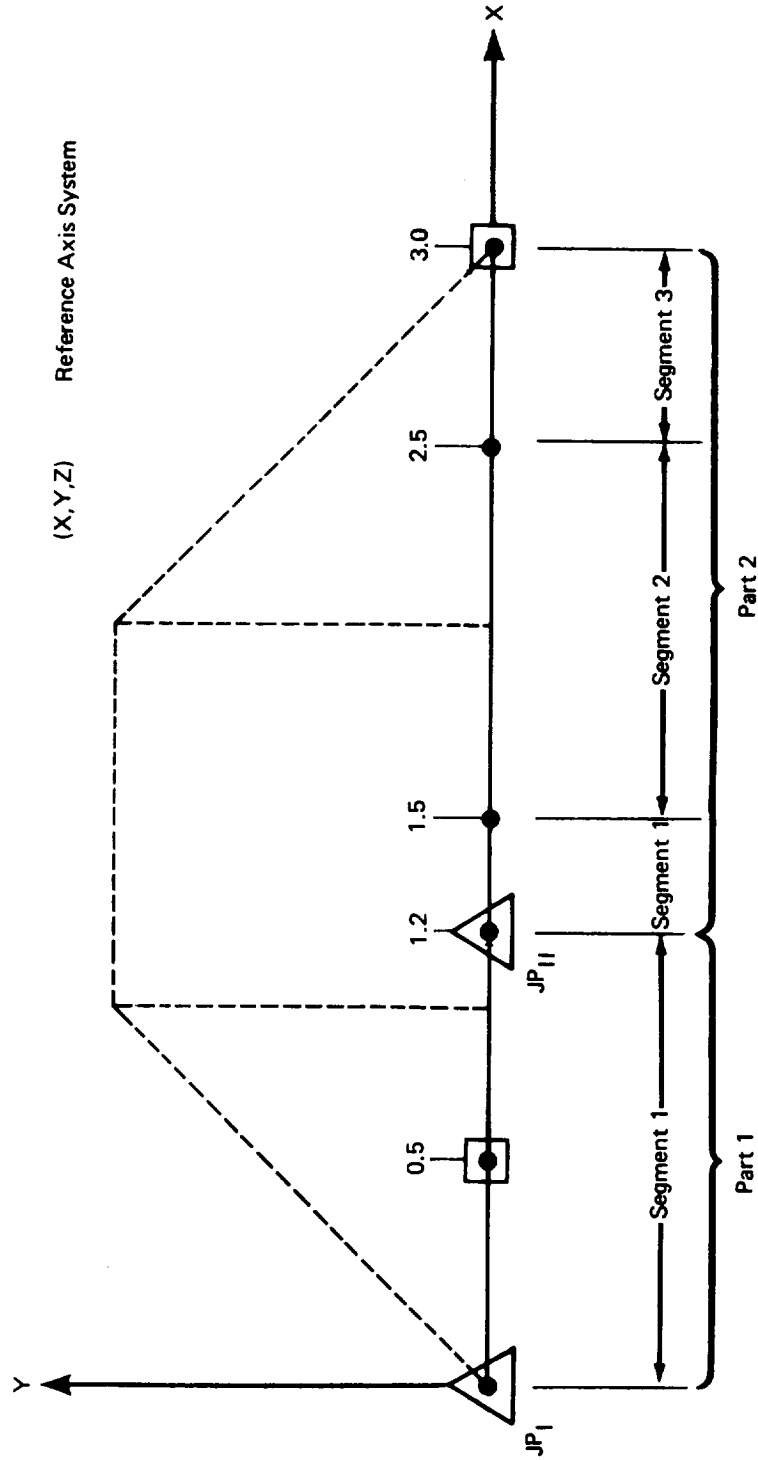
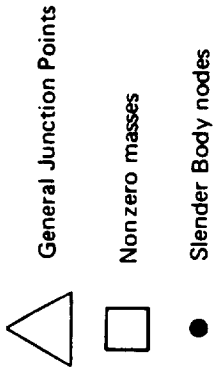


FIGURE 3.2-15.—FUSELAGE STRUCTURAL REPRESENTATION—DART MODEL I—ISIC

- Number and location of segments: The Thin Body representing the wing was specified to have two elastic segments (see fig. 3.2-16). Before the coordinates of the outboard ends of these segments could be specified, the location of the Thin Body Structural Coordinate System ( $x_n, y_n, z_n$ ) had to be determined. The X-coordinate of the origin of this system is the same as the X-coordinate of the Reference General Junction Point identified in the first field of CARD 28 (see sec. 6.2.2, vol. II); i.e., JP<sub>II</sub>. The  $x_n$ -axis coincides with the root structural intersection line calculated in the GD program (see sec 4.3, vol II) and the  $y_n$ -axis is parallel to the  $Y_N$ -axis of the Thin Body Aerodynamic Coordinate System. Having determined the orientation of this coordinate system, the coordinates of the outboard ends of the segments (shown in fig. 3.2-16) were input.
- Number of interior nodes per segment: One interior node was defined for the second Thin Body segment.
- Segment stiffness properties: The values of  $EI_{x_{n_i}}$  and GJ were arbitrarily set to 10.0 and 10.85 newton-meters squared, respectively, for each segment of the Thin Body.
- Lumped mass distribution and scale factors: Two lumped masses were specified to be associated with the first node of segment 2 (see fig. 3.2-16). The first mass was set equal to 1.0 kilogram and was located at  $x_{n_2} = -0.2$  meter. The second mass had a value of 0.1 kilogram and was placed at  $x_{n_2} = 0.1$ . The remaining two nodes had no masses associated with them. Scale factors were not used. (See sec. 3.5.8, vol. II, for a description of the Thin Body Elastic Segment Coordinate Systems.)

#### 3.2.4 Normal Modes Program—NM-1

The NM program was executed for Dart Model I solely for demonstration purposes. Normally, its execution is required only when performing a residual-elastic analysis in SD&SS in conjunction with an ISIC structural model. The NM-1 input consisted of the following information:

- Structural option: The residual-elastic structural option was chosen for both symmetric and antisymmetric motions. (This option must be chosen if eigenvalues and modal shapes are to be calculated.
- Number of modal shapes desired: It was requested that the first two symmetric and first two antisymmetric eigenvalues and modal shapes be calculated.

#### 3.2.5 External Structural Influence Coefficient Program—ESIC-1

A second structural definition of Dart Model I was obtained by executing the ESIC program. The reason for executing both ISIC and ESIC was to demonstrate that identical structural definitions could be obtained from each program. By comparing the results from an SD&SS run which used the structural definition produced by ISIC with the results from a run which used the ESIC definition, the equivalence of the two definitions was verified (see sec. 4.2).



It should be pointed out that in order to obtain an equivalent structural definition from the ESIC program, reference was made to the definition produced by ISIC-1. That is, the structural properties of Dart Model I as expressed by the ISIC definition were looked upon as though they were the structural properties of some actual configuration. Thus, the ESIC-1 input data were prepared by modeling the "given" Dart Model I structural definition.

The purpose of the ESIC program is to transform structural matrices produced external to FLEXSTAB by a finite-element structures program into matrices which are compatible with FLEXSTAB. No such matrices were available for Dart Model I. In order to use ESIC, it is a minimum requirement that the clamped flexibility matrix for symmetric motion,  $[CS]$ , to input on the ESIC input tape, NASTAP (see sec. 8, vol. II). Therefore, a  $[CS]$  matrix had to be generated for Dart Model I that would be compatible with ESIC and at the same time be an equivalent representation of the structure defined by ISIC-1.

The first step in generating a suitable  $[CS]$  matrix was to define the ESIC structural node locations. Sixteen ESIC structural nodes (see fig. 3.2-17) were chosen according to the following criteria:

- It is an ESIC requirement that at least one structural panel be specified for each Thin Body. Therefore, nodes were arbitrarily placed at the four corners of the wing. (It was later specified in the ESIC input deck (CARD 31) that these nodes defined the corner points of a Thin Body structural panel.)
- In order to represent inertia properties correctly, masses would have to be specified in the input data deck which would be identical in value and location to those used in the ISIC definition. Since masses in ESIC can only be specified at node locations, ESIC nodes were placed at locations corresponding to the ISIC lumped masses.
- The ISIC fuselage nodes had two degrees of freedom for symmetric motion:  $d_z$  and  $\theta_Y$ . In order to duplicate these degrees of freedom, *two* ESIC fuselage nodes, each with a  $d_z$  degree of freedom, were defined for each ISIC node. (It is a feature of the ESIC program that the Slender Body elastic rotation,  $\theta_Y$ , is calculated from the  $d_z$  displacements of the two nearest nodes. Therefore, the pairs of ESIC nodes which replaced each original ISIC node were placed close enough to the original locations to ensure that the desired  $\theta_Y$ 's would be calculated.) Note that the ISIC "node" at the nose of the fuselage is the clamped point (see sec. 6.2.1, vol. II) and has no degrees of freedom. Therefore, ESIC nodes corresponding to this node point were not required.

Having defined the ESIC structural nodes, the flexibility matrix was generated as follows. A transformation matrix  $[T]$ , was created which related the displacements at the ESIC nodes,  $\{d\}_E$ , to the displacements and rotations corresponding to the ISIC degrees of freedom,  $\{d\}_I$ , i.e.,

$$\{d\}_E = [T] \{d\}_I.$$

$(X, Y, Z)$  Reference Axis System  
 $(X_E, Y_E, Z_E)$  ESIC Reference Coordinate System  
 $(x_E, y_E, z_E)$  ESIC Thin Body Structural Coordinate System

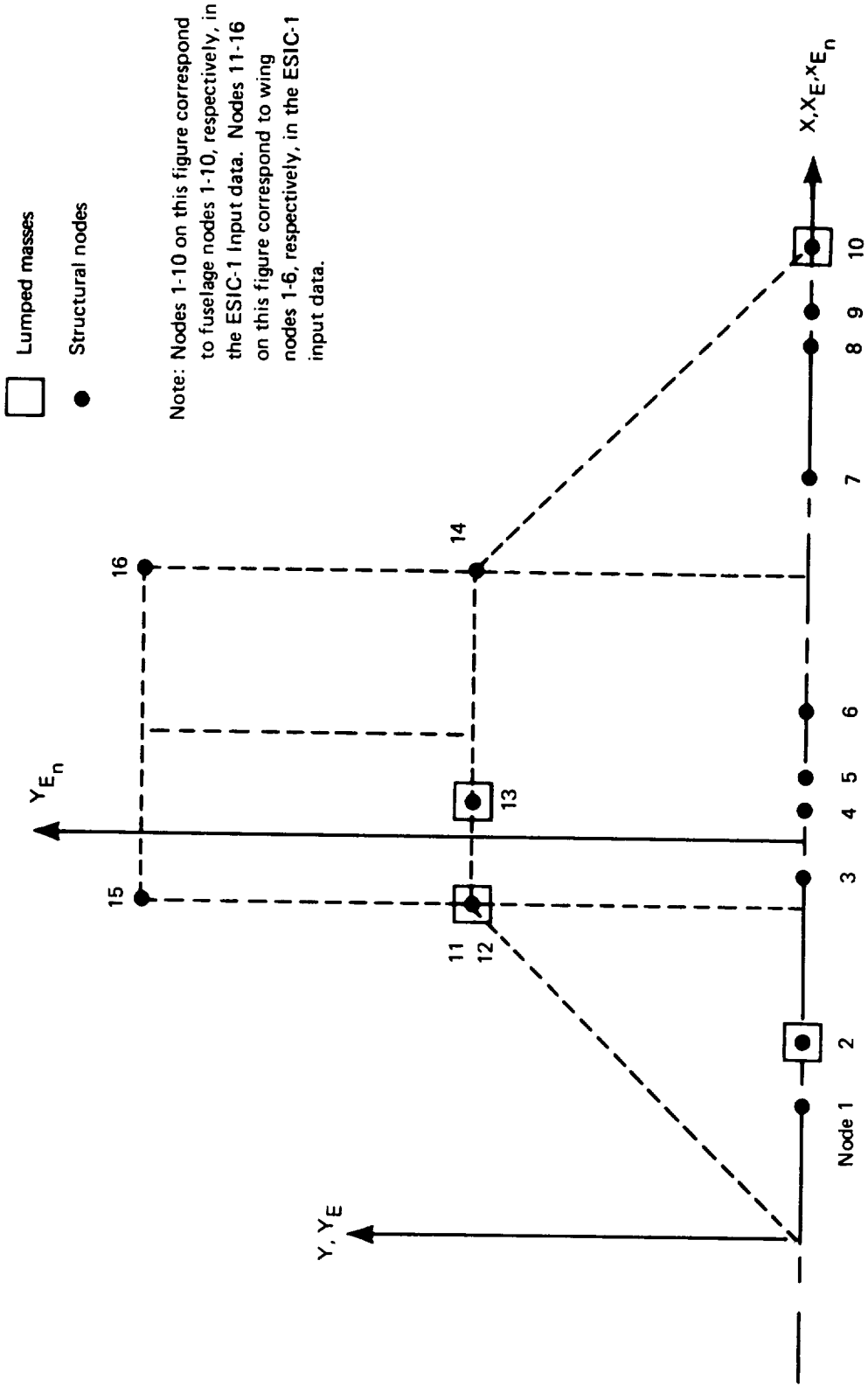


FIGURE 3.2-17. —ESIC STRUCTURAL REPRESENTATION—DART MODEL I

Once the [T] matrix was found, the desired clamped flexibility matrix, [CS], was found using the principle of virtual work, viz.,

$$[CS] = [T] [CS]_I [T]^T$$

where [CS]<sub>I</sub> is the corresponding clamped flexibility matrix for symmetric motion calculated by the ISIC program. The details of the formation of the transformation matrix, [T], are given in appendix B. [CS] and [T] are listed in appendices A.0-13 and A.0-14, respectively.

After generating the [CS] matrix and storing it on input tape NASTAP, the ESIC-1 input data deck was prepared. This input data followed directly from figure 3.2-17.

*General information.*—The majority of this information involved the data described above.

- Catalog of input matrices: It was specified that the [CS] matrix occupied file 1 of the input tape, NASTAP.
- Reference point location: This input specifies the location of the origin of the ESIC Reference Coordinate System. In this case, it was chosen to coincide with the origin of the Reference Axis System (see fig. 3.2-17), and therefore, CARDS 10 and 11 were omitted.
- Moment data option: The \$MOMENT DATA card section was omitted. This indicated that the moments of inertia, total mass, and center-of-gravity location were to be calculated by the program from the lumped mass card input.
- Structural geometry data input option: The \$TAPE INPUT OF STRUCTURAL GEOMETRIC DATA card section was not included since the structural geometry was to be input on cards.
- Degrees of freedom option: This option was used to inform the ESIC program that the displacements corresponding to the elements of [CS] are for the Z degree of freedom only for each Slender Body and Thin Body structural node.
- Submatrix position: The \$POSITION card section was omitted since the order of the bodies in the [CS] matrix agreed with that used in the GD program.

*Fuselage definition.*—The fuselage data were taken directly from figure 3.2-17.

- Number and location of structural nodes: Ten Slender Body nodes were specified to lie along the X<sub>E</sub>-axis. Nodes 1-10 (see fig. 3.2-17) were located at X<sub>E</sub> = 0.4, 0.6, 1.1, 1.3, 1.4, 1.6, 2.3, 2.7, 2.8, and 3.0 meters, respectively.

- Lumped mass distribution and scale factors: It is required that each structural node be assigned a mass in the ESIC input deck. Nodes at which masses are not desired must be assigned a mass equal to zero. For the Dart Model I fuselage, a lumped mass of 1.0 kilogram was specified for nodes 2 and 10. All other Slender Body nodes were assigned a zero mass. Scale factors were not used.

*Wing definition.*—Again, reference was made to figure 3.2-17 for most of the input data.

- Thin Body structural origin and dihedral: The origin of the ESIC Thin Body Structural Coordinate System ( $x_{E_n}$ ,  $y_{E_n}$ ,  $z_{E_n}$ ) was placed arbitrarily at  $X_E = 1.2$ ,  $Y_E = 0.0$ , and  $Z_E = 0.0$  (see fig. 3.2-17). The thin Body dihedral was set to zero since the Thin Body degrees of freedom,  $d_{z_{E_n}}$ , represented by  $[C^S]$  are parallel to the  $Z_E$ -axis.
- Number of structural nodes and panels: One Thin Body structural panel was used to model the wing. A total of six nodes were specified. (Note that although nodes 11 and 12 occupy the same physical location, they are distinct. Node 11 is used for locating a lumped mass whereas node 12 is part of the Thin Body structural panel. See appendix B.)
- Structural node locations: The Thin Body structural node locations were specified by inputting their ( $x_{E_n}$ ,  $y_{E_n}$ ) coordinates. These coordinates were taken directly from figure 3.2-17.
- Lumped mass distribution and scale factors: A lumped mass of 1.0 kilogram was placed at node 11. The mass at node 13 was set at 0.1 kilogram. Zero masses were specified for nodes 12, 14, 15, and 16. The \$SCALE FACTORS card section was not used.
- Structural panel definitions: There was only one structural panel defined for the Dart Model I wing. It was a quadrilateral panel with corner points defined by nodes 12, 14, 15, and 16 (see fig. 3.2-17).



### 3.3 DART MODEL II DEMONSTRATION CASE

Dart Model II is a symmetric cruciform configuration which should yield identical (in absolute value, at least) symmetric and antisymmetric properties when analyzed by SD&SS. For example, its rate of change of normal force coefficient with angle of attack,  $CZ_\alpha$ , should be equal to its rate of change of side force coefficient with sideslip angle,  $CY_\beta$  (cf., qualifying remarks made in sect 6.0). Thus, besides serving as a good example of input data handling for the definition programs, Dart Model II is a useful checkout for the SD&SS program.

Dart Model II was to be analyzed by the SD&SS program as a RIGID model only, hence an elastic structural representation was not necessary.

#### 3.3.1 Geometry Definition Program—GD-2

The geometry of Dart Model II is illustrated in figure 3.3-1. Note that its “fuselage” and four “wing pods” have the same shape and dimensions as the fuselage of Dart Model I. Dart Model II has two “wings” which have dihedral angles of plus and minus  $45^\circ$ , respectively. Thus the FLEXSTAB modeling of the geometric components consisted of the three Slender Bodies (SB1, SB2, and SB3) and two Thin Bodies (TB1 and TB2) shown in figure 3.3-2. Three Interference Bodies were also defined, one for each Slender Body.

The input data are discussed in the order in which the bodies were input into the program. Because of the similarities between Dart Models I and II, descriptions are brief and fewer illustrations are used. Dimensions of all lengths are in meters.

*Fuselage definition.*—For Dart Model II, the Reference Axis System was placed so that its origin coincided with the nose of the fuselage (see fig. 3.3-2). The Slender Body input data for the fuselage (SB1) were the same as those for Dart Model I (see sec. 3.2.1) and are not repeated here.

*Wing pod definition.*—Except for their relative locations in the Reference Axis System, the input data for each wing pod were identical to that of the fuselage. The upper wing pod (SB2) had its Local Slender Body Coordinate System origin placed at  $X = 0.0$ ,  $Y = 3/\sqrt{2}$ , and  $Z = 3/\sqrt{2}$  meters (see fig. 3.3-3). That of the lower wing pod (SB3) was placed at  $X = 0.0$ ,  $Y = 3/\sqrt{2}$ , and  $Z = -3/\sqrt{2}$  meters.

*Fuselage Interference Body.*—Since the Slender Body representing the fuselage lies on the plane of symmetry, it was only necessary to define the right half of the interference shell.

- Name of Interference Body and reference body: The fuselage Interference Body was named IB1. Its reference body was SB1.
- Interference Body origin: The origin of the Local Interference Body Coordinate System was placed at  $X = 1.0$ ,  $Y = 0.0$ , and  $Z = 0.0$  meters.
- Region where Thin Bodies affect the referenced Slender Body: This region was defined in the fuselage Slender Body data (CARD SET 10) to extend from  $X = 1.0$  to  $X = 2.0$ . Thus, in the Local Interference Body Coordinate System,  $X_{IB1LE} = 0.0$  and  $X_{IB1TE} = 1.0$ .

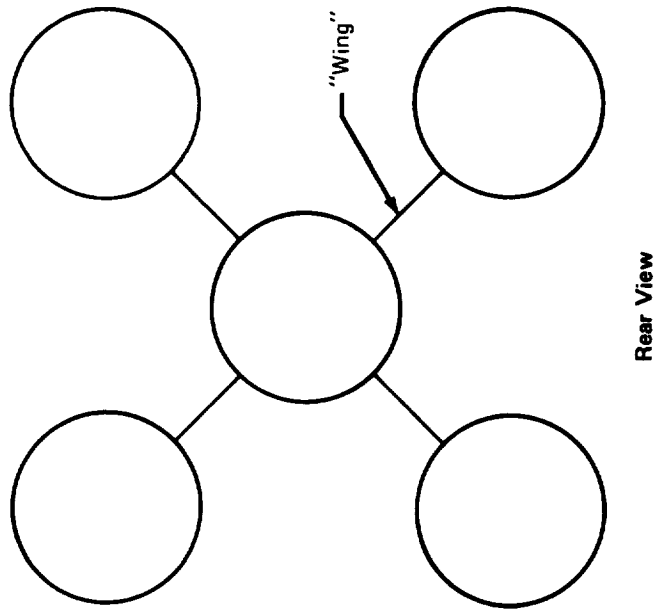
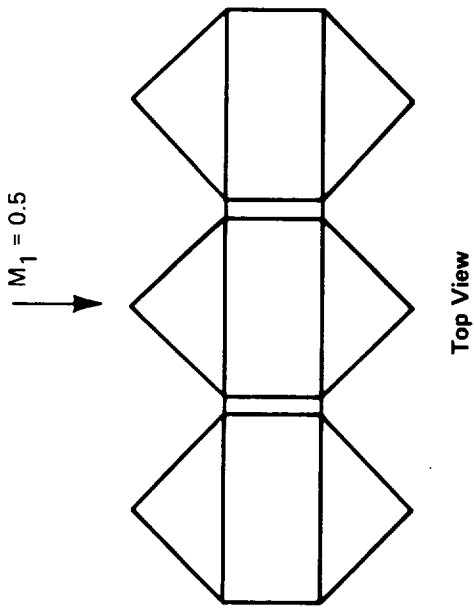
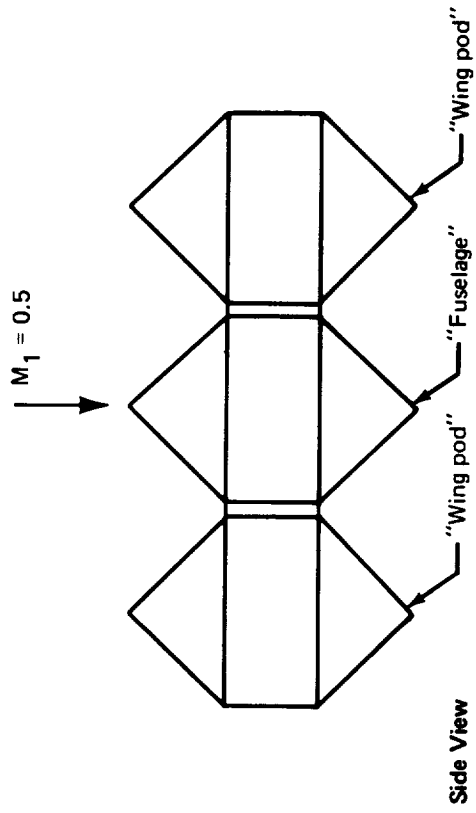


FIGURE 3.3-1.—GEOMETRY OF DART MODEL II

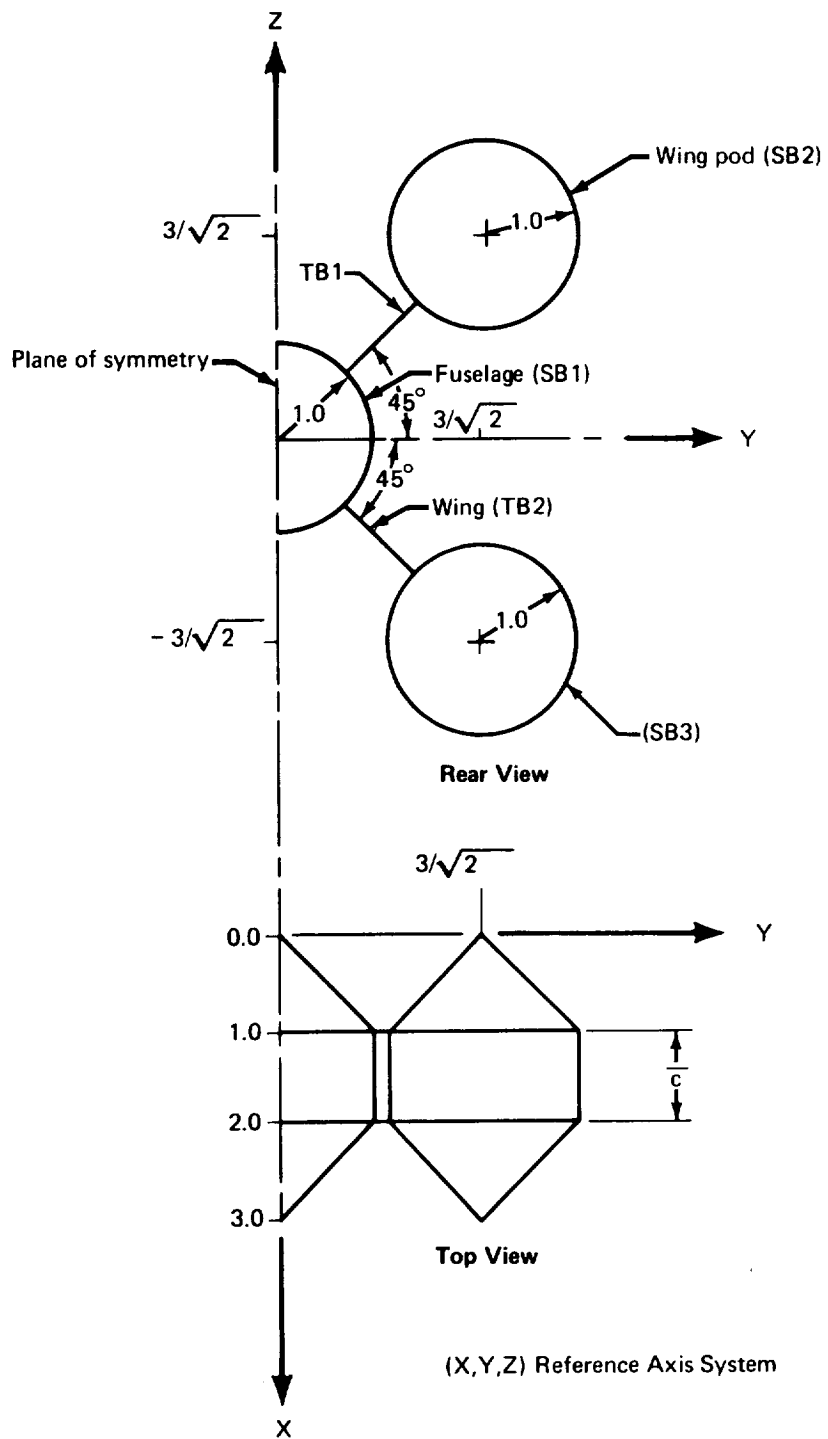


FIGURE 3.3-2.—PLACEMENT OF REFERENCE AXIS SYSTEM—DART MODEL II

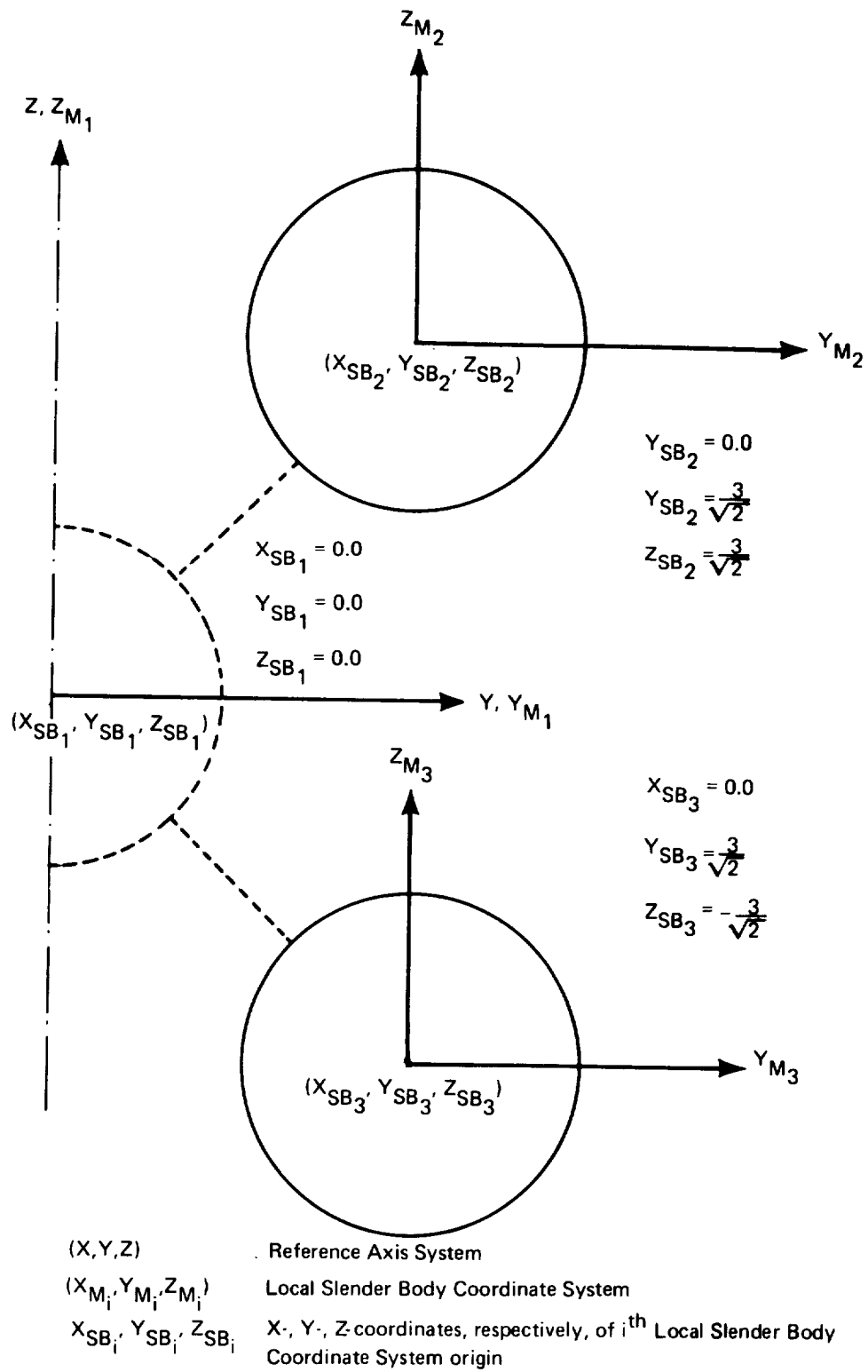


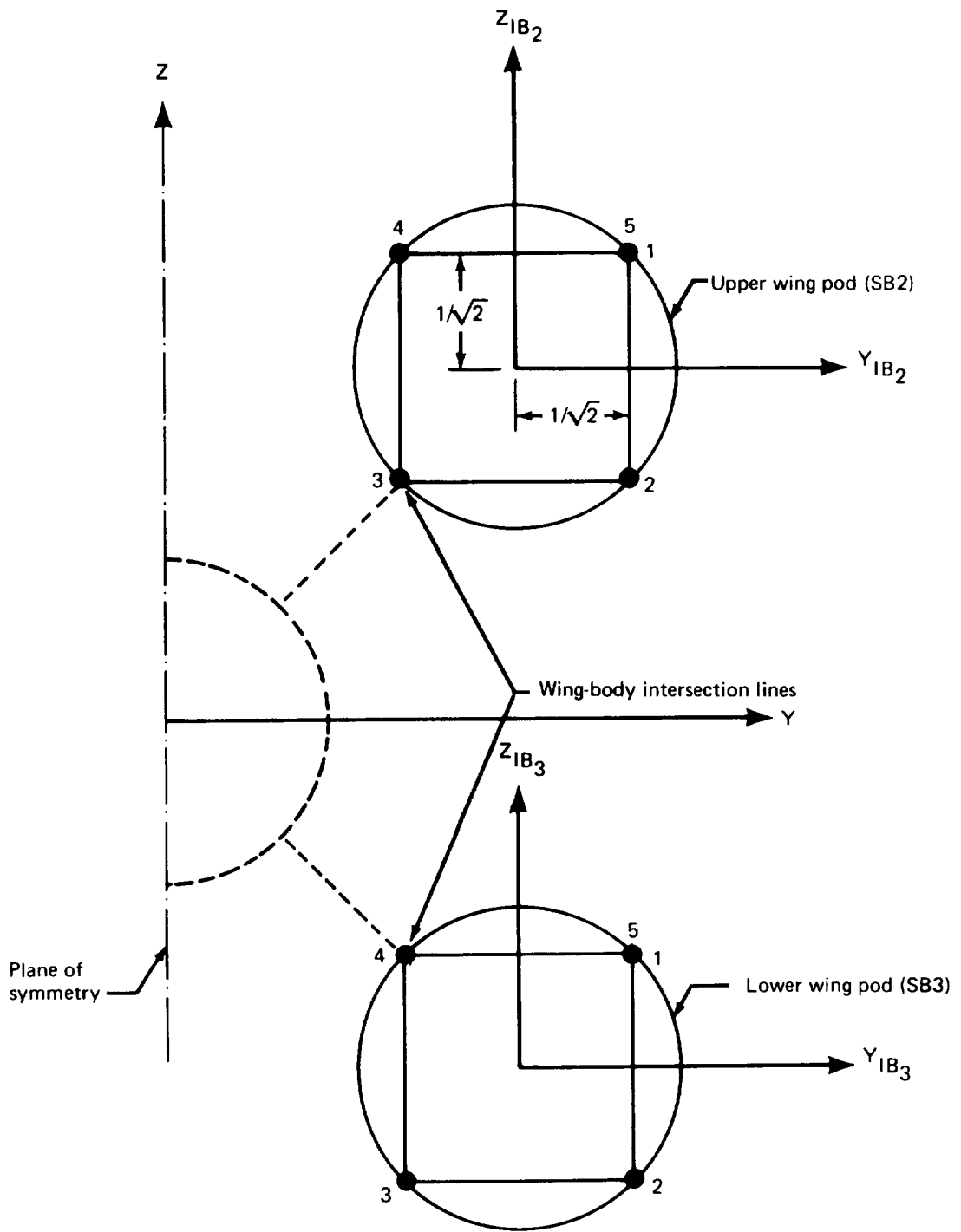
FIGURE 3.3-3.—PLACEMENT OF WING POD LOCAL SLENDER BODY COORDINATE SYSTEMS—DART MODEL II

- Wing-body intersection line: It can be seen from the physical geometry of Dart Model II (fig. 3.3-1) that the wings are in planes which pass through the fuselage axis having dihedral angles equal to plus and minus  $45^\circ$ . Therefore, the wing-body intersection line for the upper wing is at  $Y_{IB1} = 1/\sqrt{2}$  and  $Z_{IB1} = 1/\sqrt{2}$ ; that of the lower wing is at  $Y_{IB1} = 1/\sqrt{2}$  and  $Z_{IB1} = -1/\sqrt{2}$  (see fig. 3.3-4).
- Number and location of cross-sectional panel corner points: Five cross-sectional corner points were specified using the Y-Z paneling option (see fig. 3.3-4). Note that corner points 2 and 4 correspond to the wing-body intersection lines. (The locations of these corner points was arbitrary. Five were used since this is the minimum number which will yield symmetry with respect to both the X-Y and X-Z planes.)
- Interference Body transverse panel edge locations: There was only one panel per streamwise row; therefore, the already entered leading- and trailing-edge locations along with the EQ. SPACE option, defined the streamwise paneling.
- Thin Body intersection data: Both upper and lower wing roots coincided with the X-axis. Therefore, for the upper wing  $Y_{IB1} = Z_{IB1} = 0.0$  with the dihedral angle,  $\theta_{TB}$ , equal to  $45^\circ$ . For the lower wing,  $Y_{IB1} = 0.0$ ,  $Z_{IB1} = 0.0$ , and  $\theta_{TB} = -45^\circ$ .
- Interference Body panel control point locations: The panel control points were placed at the 85% panel chord points.

*Wing pod Interference Bodies.* – An Interference Body was defined for each of the two wing pods. With respect to their own Slender Bodies, these two Interference Bodies were defined identically. The discussion given below applies to both.

- Name of Interference Body and reference body: The upper wing pod Interference Body was named IB2; the lower was named IB3. The reference bodies were SB2 and SB3, respectively.
- Interference Body origin: The origin of the Local Interference Body Coordinate System for the upper wing pod Interference Body was placed at  $X = 1.0$ ,  $Y = 3/\sqrt{2}$ , and  $Z = 3/\sqrt{2}$ . That of the lower wing pod Interference Body was placed at  $X = 1.0$ ,  $Y = 3/\sqrt{2}$ , and  $Z = -3/\sqrt{2}$ .
- Region where Thin Bodies affect the referenced Slender Body: For both Interference Bodies it was specified that  $X_{IBLE} = 0.0$  and  $X_{IBTE} = 1.0$ , these data were specified previously in the wing pod Slender Body data as  $X_{LE} = 0.0$ ,  $X_{TE} = 1.0$ , respectively.
- Wing-body intersection line: For the upper wing pod Interference Body, the wing-body intersection line was located at  $Y_{IB2} = -1/\sqrt{2}$ ,  $Z_{IB2} = -1/\sqrt{2}$  (see fig. 3.3-5). The wing-body intersection line for the lower wing pod Interference Body occurred at  $Y_{IB3} = -1/\sqrt{2}$ ,  $Z_{IB3} = 1/\sqrt{2}$ .





- $(X, Y, Z)$  Reference Axis System
- $(X_{IB2}, Y_{IB2}, Z_{IB2})$  Local Interference Body Coordinate System (upper wing pod)
- $(X_{IB3}, Y_{IB3}, Z_{IB3})$  Local Interference Body Coordinate System (lower wing pod)

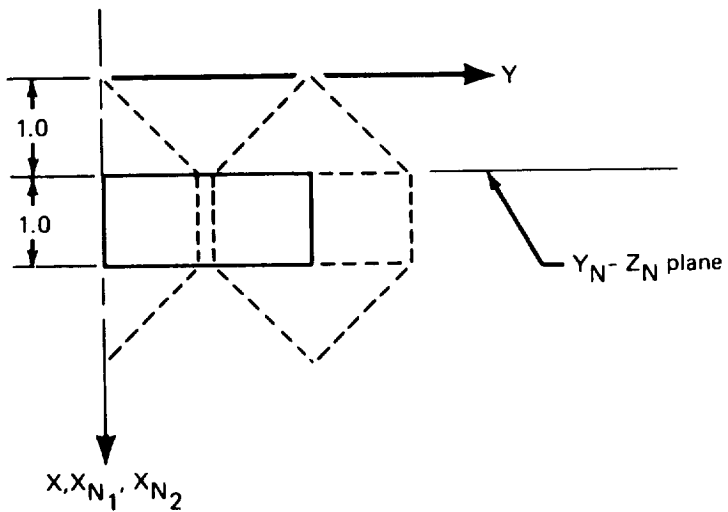
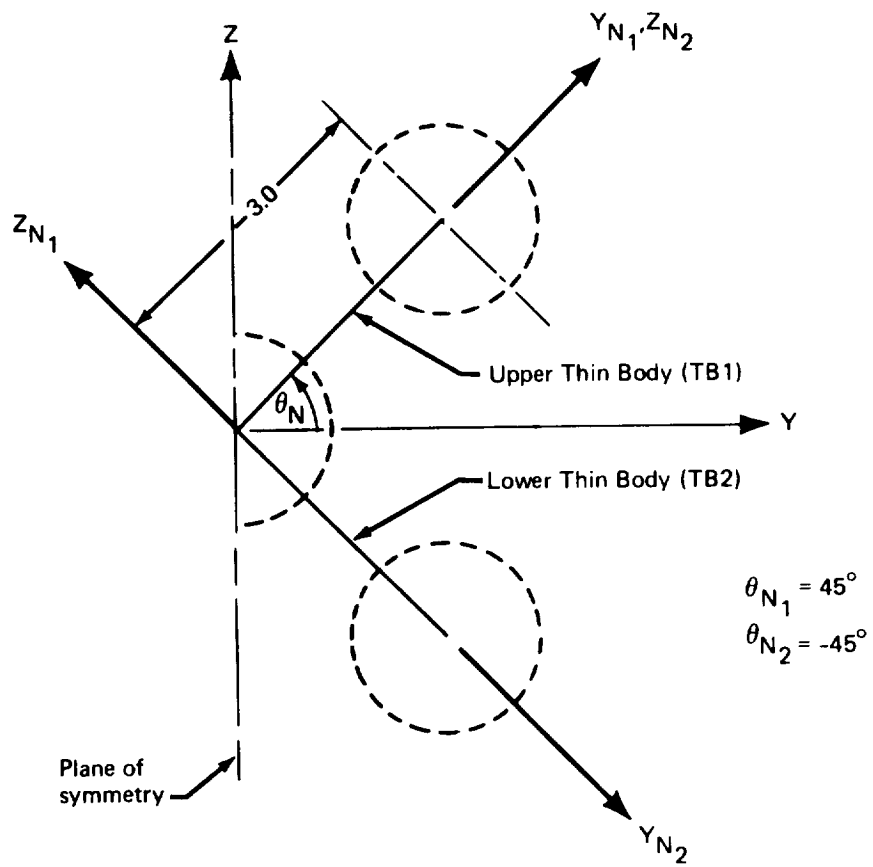
**FIGURE 3.3-5.—WING POD INTERFERENCE BODY CROSS-SECTIONAL PANEL CORNER POINT LOCATIONS—DART MODEL II**

- Number and location of cross-sectional panel corner points: Since the wing pods were represented by Slender Bodies lying off the plane of symmetry, the wing pod Interference Bodies were defined as complete shells of panels. In order to have the same cross-sectional shape as IB1, four panels were used for each Interference Body, which made necessary the definition of five cross-sectional panel corner points (fig. 3.3-5). (The coordinates of these corner points were entered using the Y-Z paneling option.)
- Interference Body transverse panel edge locations: The Interference Bodies contain only one panel in the streamwise direction; the previously specified leading and trailing edge locations, along with the EQ. SPACE option, defined the streamwise paneling.
- Thin Body intersection data: The tip of the upper wing planform coincided with the  $X_{IB2}$  axis of the upper wing pod. The location of this Thin Body tip in the Local Interference Body Coordinate System was  $Y_{IB2} = 0.0$ ,  $Z_{IB2} = 0.0$ . The Thin Body dihedral angle with respect to the local coordinate system,  $\theta_{TB}$ , was  $225^\circ$ . The corresponding input for the lower wing pod Interference Body was  $Y_{IB3} = 0.0$ ,  $Z_{IB3} = 0.0$ , and  $\theta_{TB} = 135^\circ$ .
- Interference Body panel control point locations: It was specified that the control points were to be located at the 85% panel chord points.

*Wing definition.*—The discussion below applies to both wings since they were modeled identically.

- Name of Thin Body and reference body: The upper and lower wings were named TB1 and TB2, respectively; the reference body was IB1 for both.
- Thin Body origin and dihedral: The origin of the Local Thin Body Coordinate System for the Thin Body representing the upper wing was placed at  $X = 1.0$ ,  $Y = 0.0$ , and  $Z = 0.0$ . A dihedral angle of  $45^\circ$  was specified. The origin of the local coordinate system for the lower wing was chosen to coincide with that of the upper wing; however, the dihedral angle of the lower wing was set to minus  $45^\circ$  (see fig. 3.3-6).
- Planform definition: The planform of the upper Thin Body was specified to be rectangular with a chord of 1.0 meter and a span of 3.0 meters. Its leading-edge root point coincided with the origin of its Local Thin Body Coordinate System. Within its own local coordinate system, the planform of the lower Thin Body was defined identically. Note that these definitions placed the tips of the Thin Bodies at the proper locations, i.e., the locations specified (on CARD SET 25) in the wing pod Interference Body input (see fig. 3.3-6).
- Paneling scheme: The same Thin Body paneling scheme that was used for Dart Model I was used here, i.e., one streamwise row containing two panels.





- (X, Y, Z) Reference Axis System
- ( $X_{N1}, Y_{N1}, Z_{N1}$ ) Local Thin Body Coordinate System (upper wing)
- ( $X_{N2}, Y_{N2}, Z_{N2}$ ) Local Thin Body Coordinate System (lower wing)

FIGURE 3.3-6.—WING DEFINITIONS—DART MODEL II

- Panel control point locations: The panel control points were placed at the 85% panel chord point along a line passing through the  $Y_N$ -centroid of the panel row.
- Airfoil definition: The wings of Dart Model II had no thickness of camber.
- Twist definition: No twist was specified for either wing.

*Geometry Definition Plot.* – Figure 3.3-7 shows the three-view plot of the Dart Model II as produced by the GD program plotting routine using the Calcomp machine. The top and side views of this latter figure do not agree with Figures 3.3-1 and 3.3-2. The reasons are identical with those given concerning the discussion of the Dart Model I plots. (Page 3-21.) As noted, the discrepancies involve the plot of the fuselage definition.

### 3.3.2 Aerodynamic Influence Coefficient Program–AIC-2

Input for the AIC program consisted of the output tape from GD-2 and the input data deck described below.

*AIC input.* –The following general information was specified in the AIC input data deck.

- Type of reference motion: Both symmetric and antisymmetric reference motions were requested since both symmetric and antisymmetric stability calculations were to be made in SD&SS.
- Mach number: A Mach number of 0.5 was arbitrarily specified.
- Perturbation delta Mach number: The value of this parameter was arbitrarily set to 0.02.
- Steady/unsteady motion: Unsteady aerodynamics was requested for both symmetric and antisymmetric motion so that unsteady calculations could be made in SD&SS.

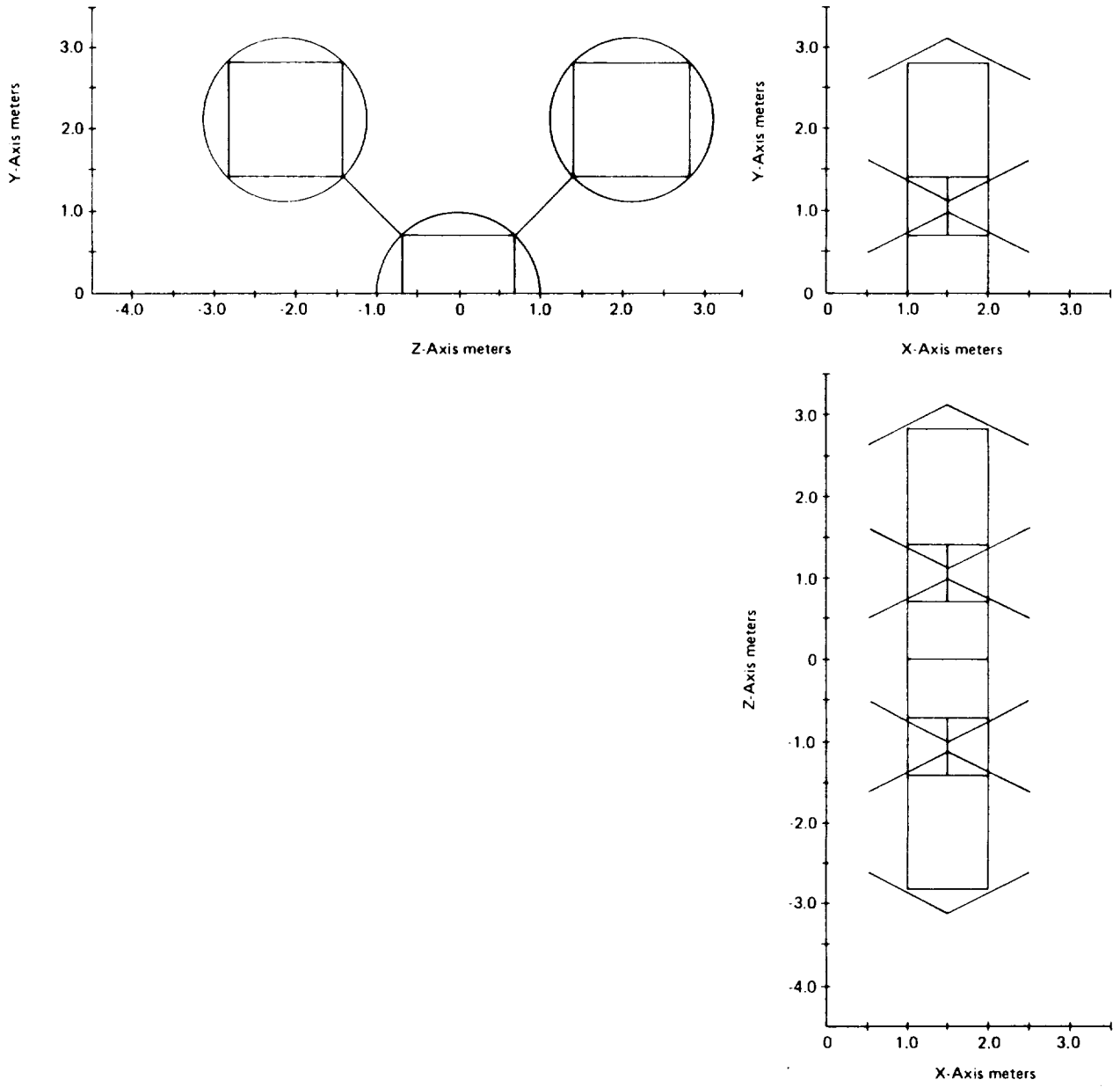


FIGURE 3.3.7.—CALCOMP PLOT OF DART MODEL II



### 3.4 BOEING 707-320B DEMONSTRATION CASE

The Boeing 707-320B provides a demonstration case that is typical of large, elastic, subsonic airplanes. The ISIC and NM programs were used to create the structural definition.

This section is organized in the same manner as section 3.2. Each of the input requirements summarized in section 3.1 is referenced and discussed. All linear dimensions shown are in inches.

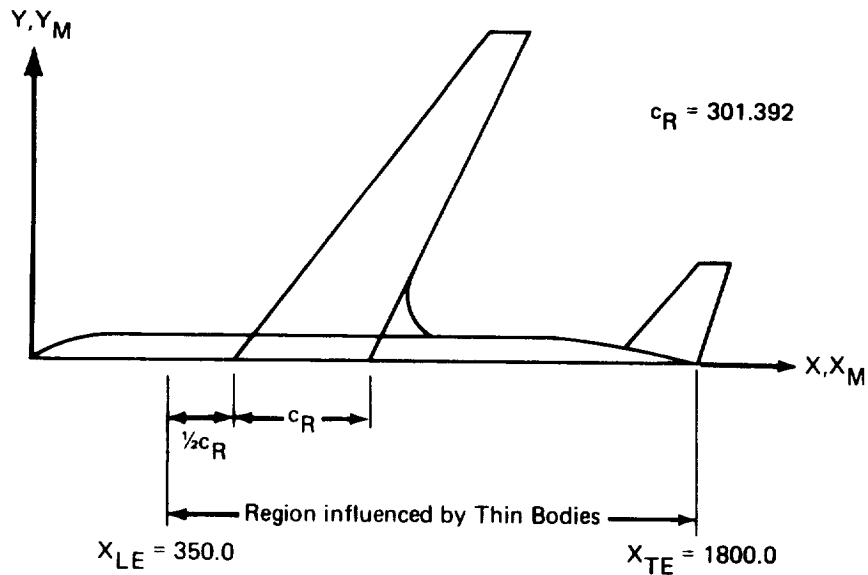
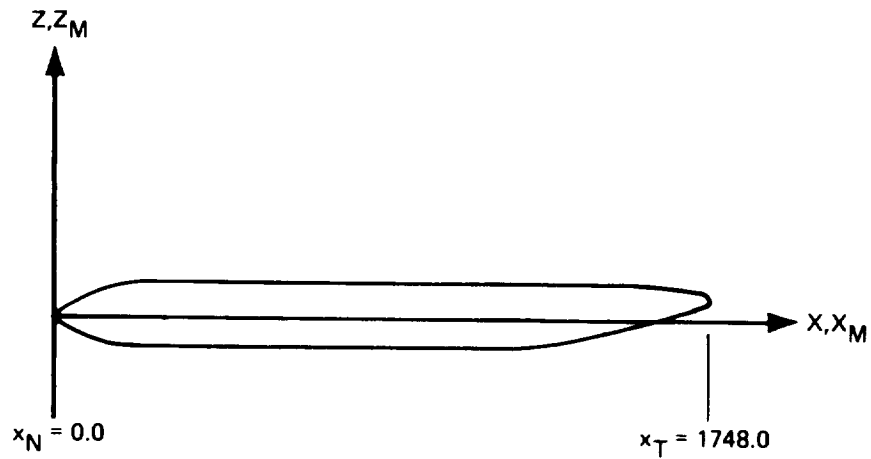
#### 3.4.1 Geometry Definition Program—GD-3A and GD-3B

The fuselage and nacelles were defined as Slender Bodies and the wing, horizontal stabilizer, vertical tail, and nacelle struts were defined as Thin Bodies. An Interference Body was used with each Slender Body. The GD program was executed twice to generate two definitions of the 707; GD-3B had zero wing twist to model the cruise shape of the airplane and GD-3A had  $1^\circ$  of linearly varying wing twist to model the jig shape.

This section describes the methods used to generate the definition of each body. The bodies are discussed in the order in which they were defined.

*Fuselage definition.*--A side-view of the fuselage, several cross-sectional views of the fuselage, and a plan-view of the entire configuration were used to generate the input data for the fuselage definition.

- Name of Slender Body: The fuselage was given the name FUSELAGE.
- Slender Body origin: The origin of the Reference Axis System was located at the nose of the fuselage. The X-axis was placed parallel to the fuselage coordinate axis prescribed on the available configuration drawings. This axis was a good approximation to the mean aerodynamic centerline (section 3.5.1 of vol II), and its use simplified the definition of the fuselage. The origin of the Local Slender Body Coordinate System was placed at the Reference Axis System origin (see fig. 3.4-1).
- Nose and aft end locations: Since the origin of the Local Slender Body Coordinate System coincided with the nose of the fuselage,  $x_N$  was set to zero. The length of the fuselage is 1748 inches; therefore,  $x_T = 1748.0$  (see fig. 3.4-1).
- Regions influenced by Thin Bodies: In subsonic flow the influence of the wing diminishes rapidly ahead of the wing leading edge. It is usually not necessary to extend the Interference Body to the nose of the fuselage. In this case, satisfactory results were obtained by extending the region of influence one-half the wing root chord length ahead of the leading edge of the wing root ( $X_{LE} = 350.0$ ). This region was extended to a point just slightly beyond the aft end of the fuselage ( $X_{TE} = 1800.0$ ) to account for effects from the horizontal stabilizer and the vertical tail (see fig. 3.4-1). This is consistent with the modeling technique described in section 4.2.1 of the User's Manual.



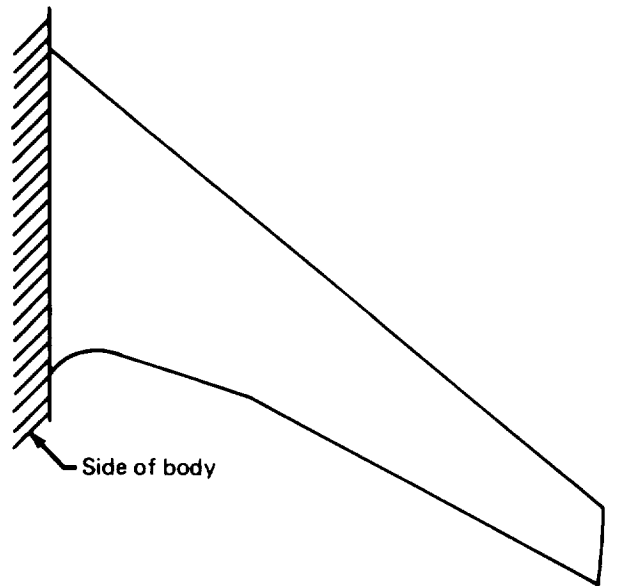
- |                   |   |
|-------------------|---|
| $(X, Y, Z)$       | Reference Axis System   |
| $(X_M, Y_M, Z_M)$ | Local Slender Body Coordinate System                                      |
| $c_R$             | Root chord of the wing  |
| $x_N, x_T$        | $X_M$ coordinates of the fuselage nose and tail                           |
| $X_{LE}, X_{TE}$  | X-coordinates of leading and trailing edges of fuselage Interference Body |

FIGURE 3.4-1.—FUSELAGE GEOMETRIC DEFINITION—707-320B

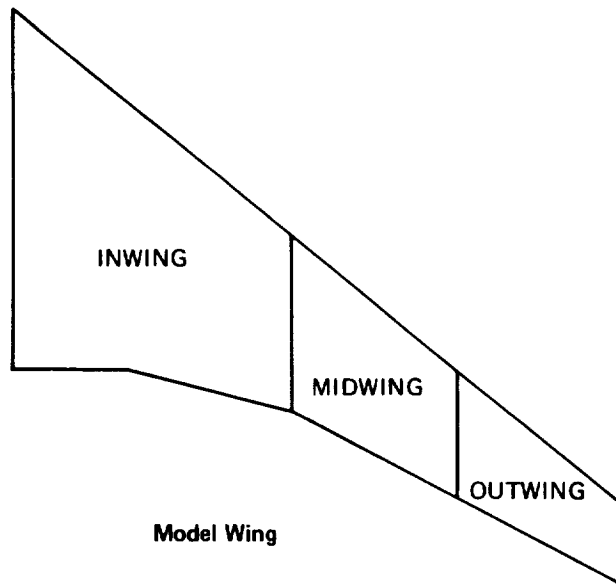
- Number and placement of control points: Using the automatic option in the GD input, 46 control points were evenly distributed along the length of the fuselage. Experience with similar programs has shown that about 50 line singularities give good results at reasonable cost.
- Area or radius distribution: The area distribution was determined by measuring several fuselage cross sections (with a planimeter) and plotting these areas versus  $X_M$ . This curve was then smoothed in regions where the area distribution changed rapidly (such as at the cab).
- Camber line definition: The camber line was determined (approximately) by drawing a line halfway between the upper and lower boundaries of the side-view drawing. Once again, irregularities were smoothed.

*Wing definition.*—The wing planform drawing, fuselage side-view and cross-sectional drawings, and the airfoil ordinates were used to define the wing. Because of the wing strut intersections it was necessary to define the wing as three Thin Bodies. The first, named INWING, extended from the plane of symmetry (X-Y plane) to the inboard strut. The second, MIDWING, extended from the inboard strut to the outboard strut, and the third, OUTWING, from the outboard strut to the tip (see fig. 3.4-2).

- Name of Thin Body and reference body: The reference bodies for INWING, MIDWING, and OUTWING were INTE (the fuselage Interference Body), INWING, and MIDWING, respectively.
- Thin Body origin and dihedral: The dihedral angle of each of the three Thin Bodies (INWING, MIDWING, and OUTWING) was  $7^\circ$ . The Y-coordinate of the origin of the Local Thin Body Coordinate System for INWING was taken to be zero (i.e., on the plane of symmetry). The X-coordinate was determined by extending the wing leading edge until it intersected the plane of symmetry (see fig. 3.4-3). To determine the Z-coordinate, a cross-sectional view of the fuselage located midway between the wing root leading and trailing edges was used. The intersections of the wing leading and trailing edges with the fuselage were placed on the drawing, and lines with  $7^\circ$  dihedral angles were extended from these points until they intersected the plane of symmetry (see fig. 3.4-4). The Z-coordinate of INWING's origin was then calculated by subtracting the Z-coordinate of the camber line at this same fuselage cross-section from the average value of the Z-coordinates of these intersections. This procedure ensured that the "low-wing" characteristics of the 707 would be represented in the model; that is, the vertical position and orientation of INWING with respect to the Slender Body representing the fuselage would be similar to that of the actual wing with respect to the actual fuselage. The origins of the Local Thin Body Coordinate Systems associated with MIDWING and OUTWING were set by using the Relocate option in the GD input (see CARD 29, sec. 4.2.2, vol II). This automatically placed the origin of MIDWING's Local Thin Body Coordinate System at the leading-edge tip of INWING, and the origin of OUTWING's Local Thin Body Coordinate System at the leading-edge tip of MIDWING (see fig. 3.4-5).



**Actual Wing**



**Model Wing**

**FIGURE 3.4-2.—WING PLANFORM DEFINITION—707-320B**



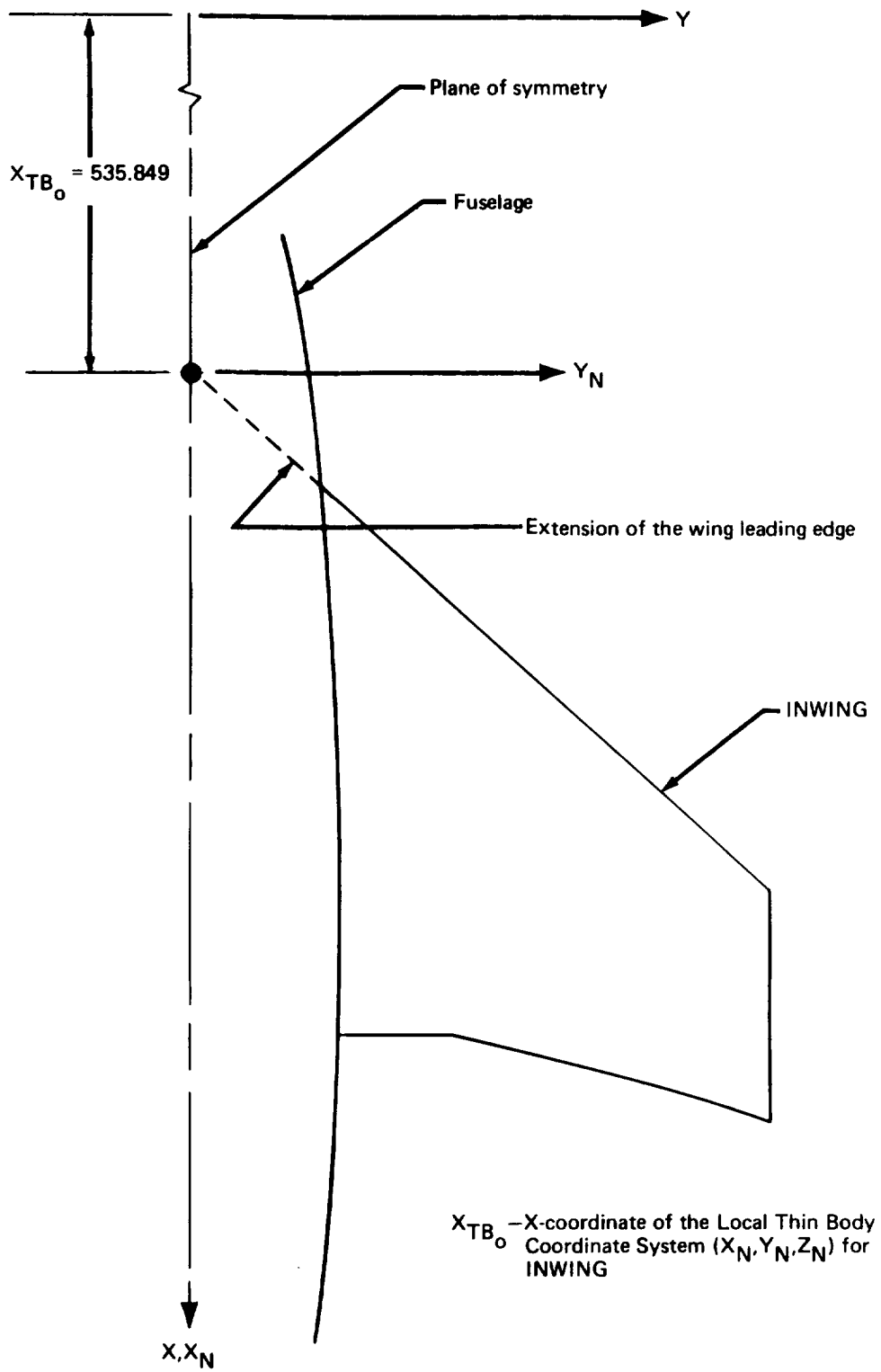
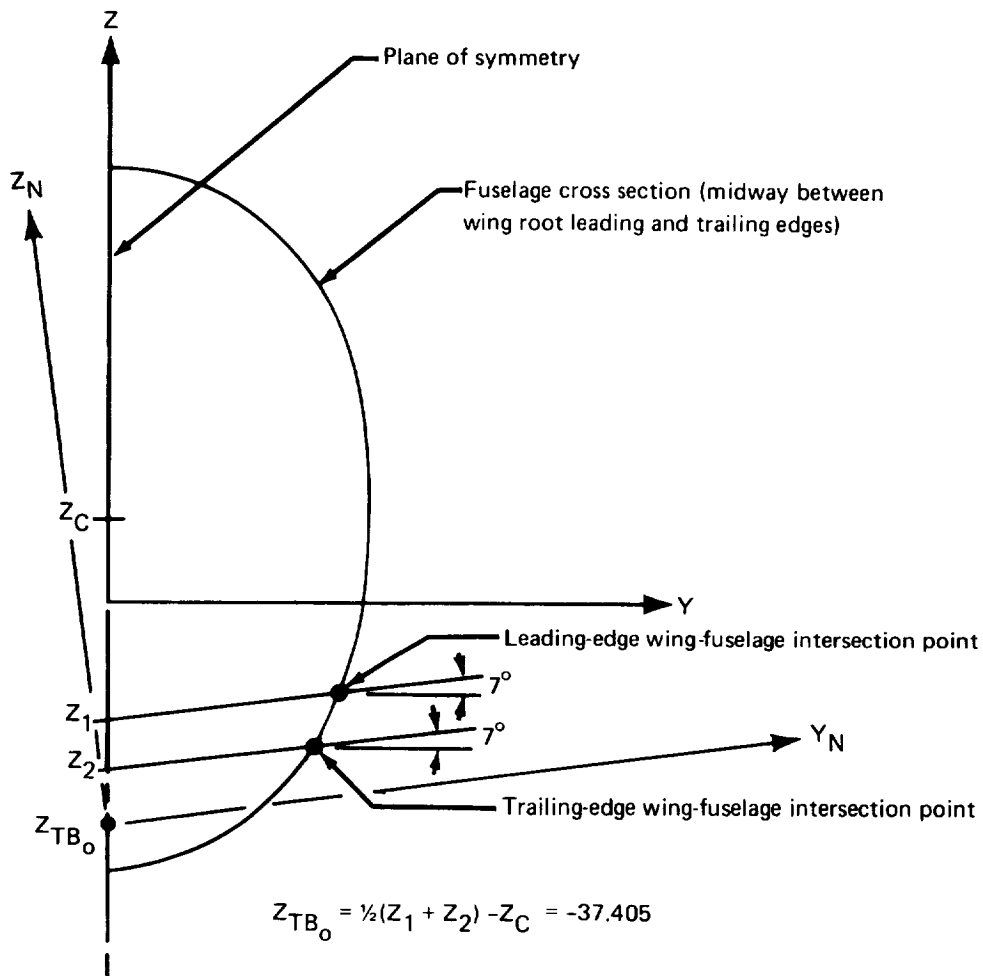


FIGURE 3.4-3.—DETERMINATION OF THE X-COORDINATE OF THE ORIGIN OF INWING—707-320B



- Where
- $Z_{TB_0}$  = Z-coordinate of INWING's Local Thin Body Coordinate System origin
  - $Z_1$  = Z-coordinate of the intersection of the extended wing leading edge with the plane of symmetry
  - $Z_2$  = Z-coordinate of the intersection of the extended wing trailing edge with the plane of symmetry
  - $Z_C$  = Z-coordinate of the fuselage camber line

**FIGURE 3.4.4.—DETERMINATION OF THE Z-COORDINATE OF THE ORIGIN OF INWING-707-320B**

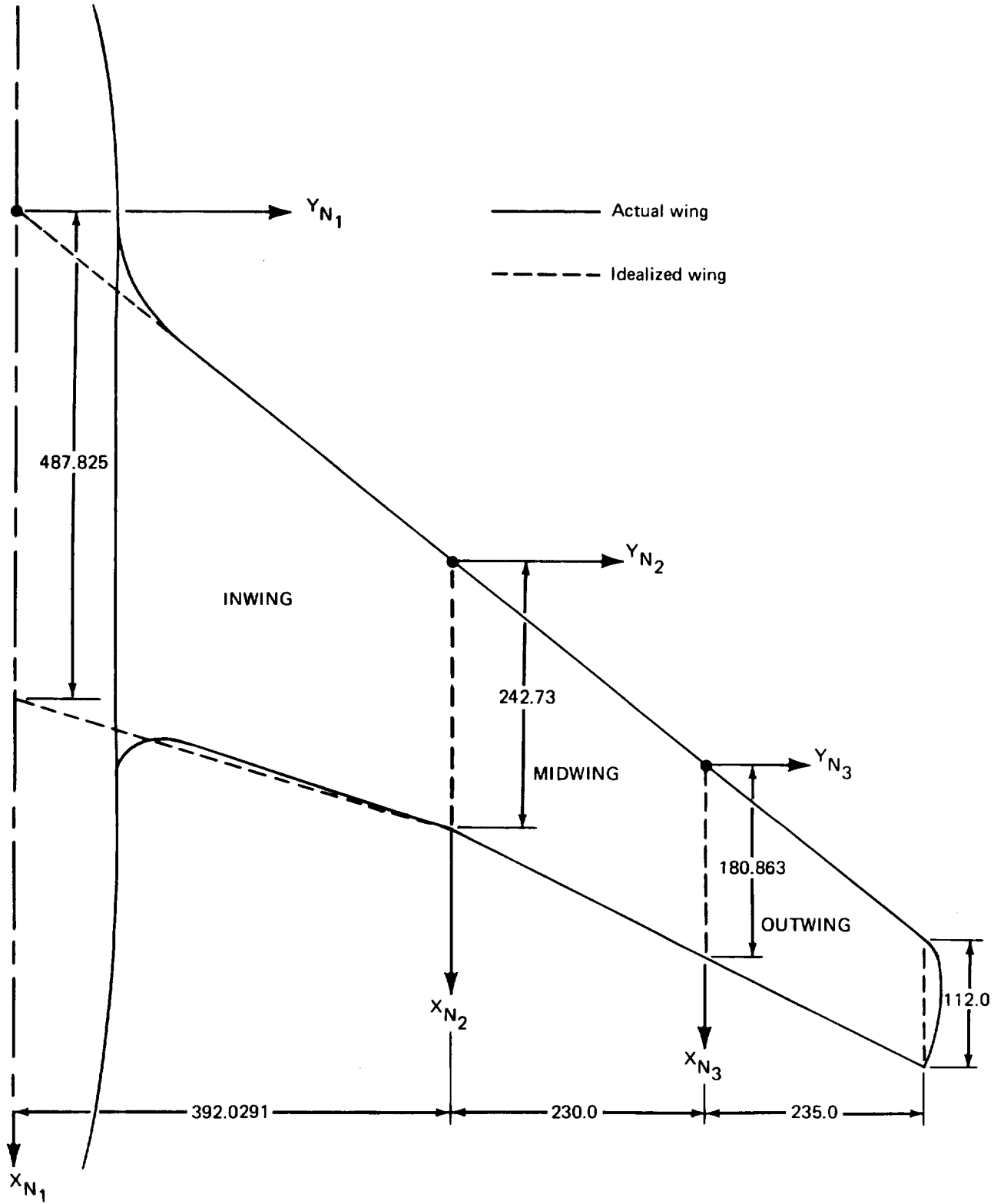


FIGURE 3.4-5.—PLANFORM MODIFICATIONS—707-320B

- **Planform definition:** The idealized wing planform is identical to the real planform except that the root fairings and the curved tip extension were not represented (see fig. 3.4-5).
- **Paneling scheme:** The wing planform was divided into five streamwise rows and eight spanwise rows (see sec. 3.4.2). The streamwise divisions were dictated by the locations of the nacelle struts and the fact that the wing and horizontal tail panel edges should occur at the same spanwise locations. (This requirement prevents wing trailing vortex legs from passing close to control points on the horizontal tail, which may cause unrealistic load distributions.) It is also very desirable to make the streamwise divisions of nearly equal width. This was not done because a large increase in the number of singularities would have been required.
- **Panel control point locations:** As recommended in volume II, the panel control points were placed at 85% of the panel chord on the streamwise lines that passed through the  $Y_N$ -centroid of each row of panels.
- **Airfoil definition:** The airfoils were defined at the root, tip, and three interior spanwise stations. These were linearly interpolated to provide definitions at six spanwise stations for INWING, three spanwise stations for MIDWING, and two spanwise stations for OUTWING.
- **Twist definition:** The GD program was executed twice in order to model the difference in twist between the cruise shape and the jig shape. In GD-3B, the cruise shape of the wing was specified as having zero twist. In GD-3A, the jig shape was modeled by inputting a twist that varied linearly from  $0^\circ$  at the root to  $1^\circ$  at the tip. The incidence of the wing, which is included in the twist input, was set at  $2^\circ$  for both runs.

*Fuselage Interference Body.* --Data required to define the fuselage Interference Body were a planform drawing of the entire configuration, wing and fuselage input data, and horizontal stabilizer data.

- **Name of Interference Body and reference body:** The fuselage Interference Body was given the name INTE; its reference body was FUSELAGE.
- **Interference Body origin:** The origin of this Local Interference Body Coordinate System was chosen to coincide with the origin of the Reference Axis System.
- **Region where Thin Bodies affect the referenced Slender Body:** This region was defined in the fuselage Slender Body data and determines the leading- and trailing-edge X-coordinates of the Interference Body. Therefore, the leading edge was located at a distance of one-half the root chord ahead of the leading edge of the root chord and the trailing edge was located at a point slightly beyond the aft end of the fuselage (see fig. 3.4-1). Here, these data are input in terms of the Local Interference Body Coordinate System, i.e.,  $X_{IBLE} = 350.0$ , and  $X_{IBTE} = 1800.0$ .

- Wing-body intersection line: The Y, Z-coordinates for this line were found from figure 3.4-6. A line with  $7^\circ$  dihedral angle was drawn from the average of the leading- and trailing-edge plane-of-symmetry intersection points (point  $Z_3$ ). The intersection of this line with the fuselage cross section at  $(Y_4, Z_4)$  defined the Y-coordinate of the wing-body intersection line. The Z-coordinate was set equal to the Z-coordinate of the intersection line,  $Z_4$ , minus the Z-coordinate of the camber line,  $Z_C$  (see fig. 3.4-6). The Y, Z-coordinates of the wing-body intersection line were used as the coordinates of one of the Interference Body corner points (see below).

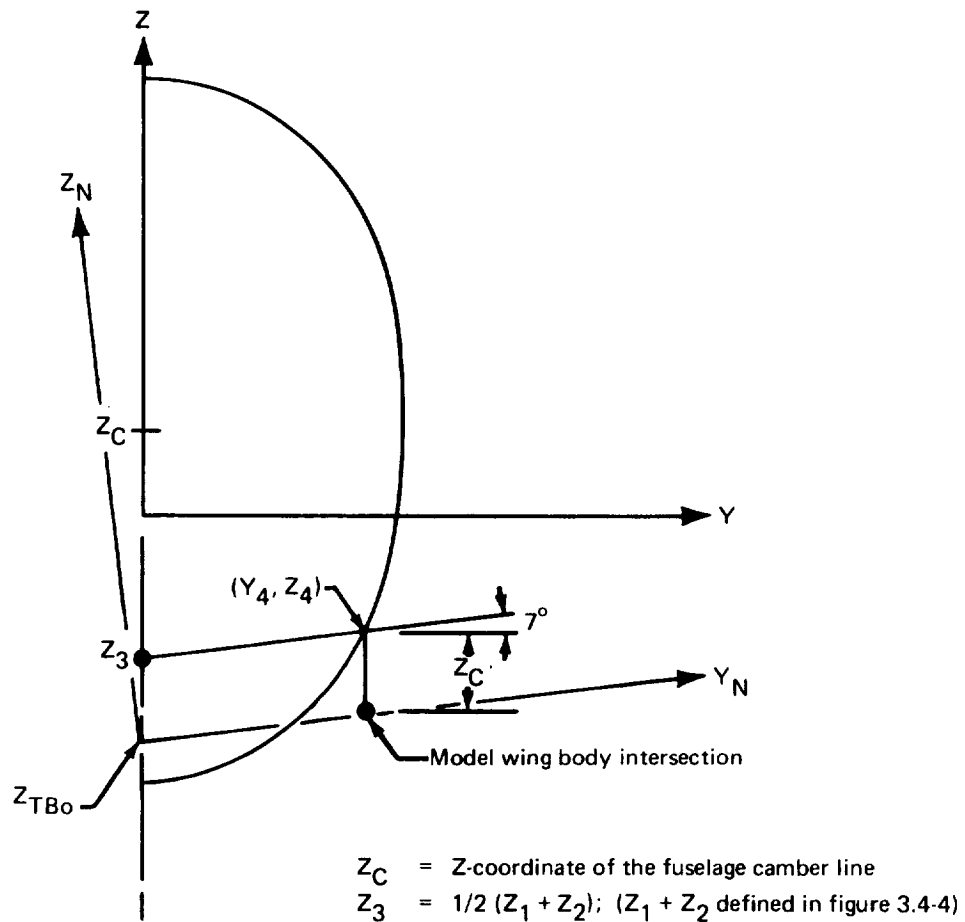


**FIGURE 3.4-6.—DETERMINATION OF MODEL WING-BODY INTERSECTION POINT—707-320B**

- Number and location of cross-sectional panel corner points: Three panels were placed around the defined half of the fuselage. (Four is the recommended minimum number of panels on an Interference Body half-shell). The wing-fuselage intersection line defined the location of one corner point ( $Y = 51.3076$ ,  $Z = 31.1052$ ) as well as an interference shell radius. In order to preserve this 60-inch radius, corner points were placed at  $Y = 0.0$  and  $Z = \pm 60.0$ . The Y-coordinate of the remaining corner point was arbitrarily chosen to be the same as that of the wing-fuselage intersection line, namely,  $Y = 51.3076$ . Its Z-coordinate was chosen so

that it would lie in the plane of the horizontal stabilizer Thin Body (see below), that is,  $Z = 6.2998$ . These four corner points were entered using the Y-Z input option. (The geometry of the Interference Body cross-section can be seen in figure 3.4-13.) If this model were redone, more than three interference body panels would be used.

- Interference Body transverse panel edge locations: The prime factor considered was the effect of Thin Bodies on the fuselage. The panel density was increased in regions where large pressure gradients might be expected (fig. 3.4-7). (The transverse panel edge locations were input manually in CARD SET 24.)

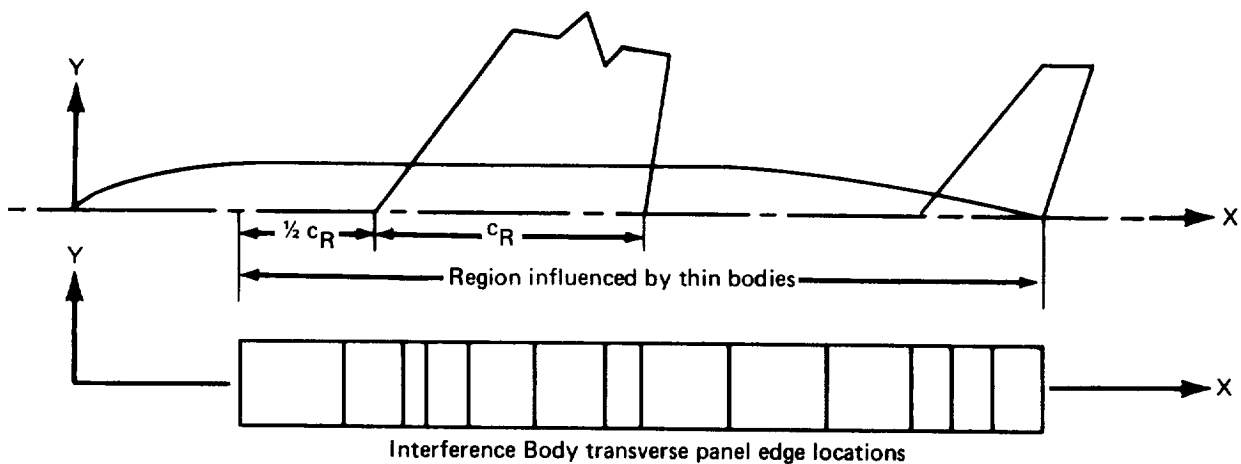
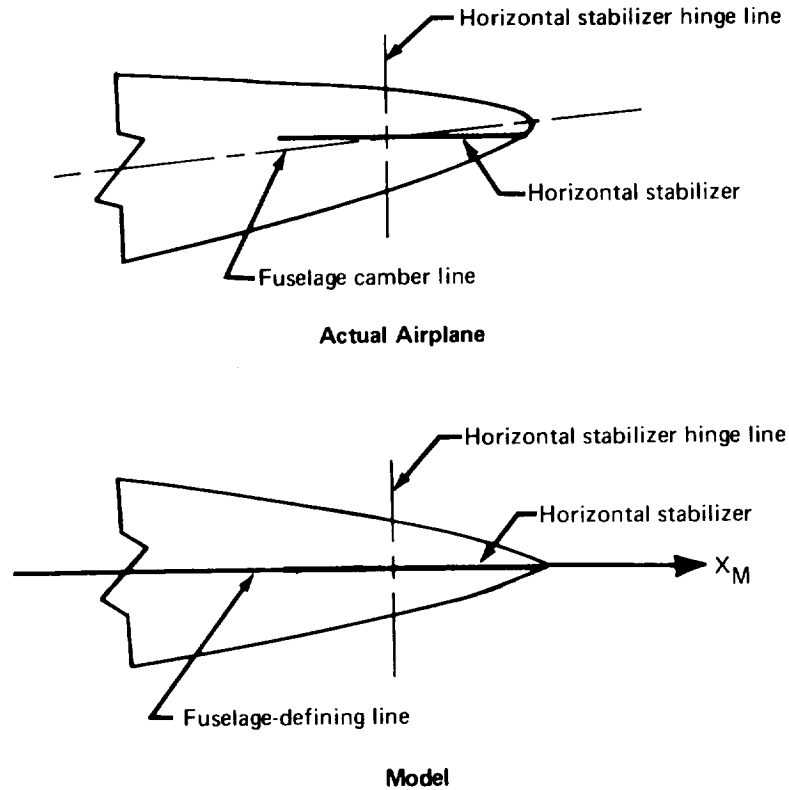


FIGURE 3.4-7.—INTERFERENCE BODY TRANSVERSE PANEL EDGE LOCATIONS—707-320B

- Thin Body intersection data: These data were taken directly from the inboard wing, horizontal stabilizer, and vertical tail input data.
- Interference Body panel control point locations: The panel control points were placed at the recommended location of 85% of the panel chord.

*Horizontal stabilizer.*—The data required to define the horizontal stabilizer were a plan-form drawing, a side-view drawing of the fuselage, the wing input data, and the airfoil ordinates.

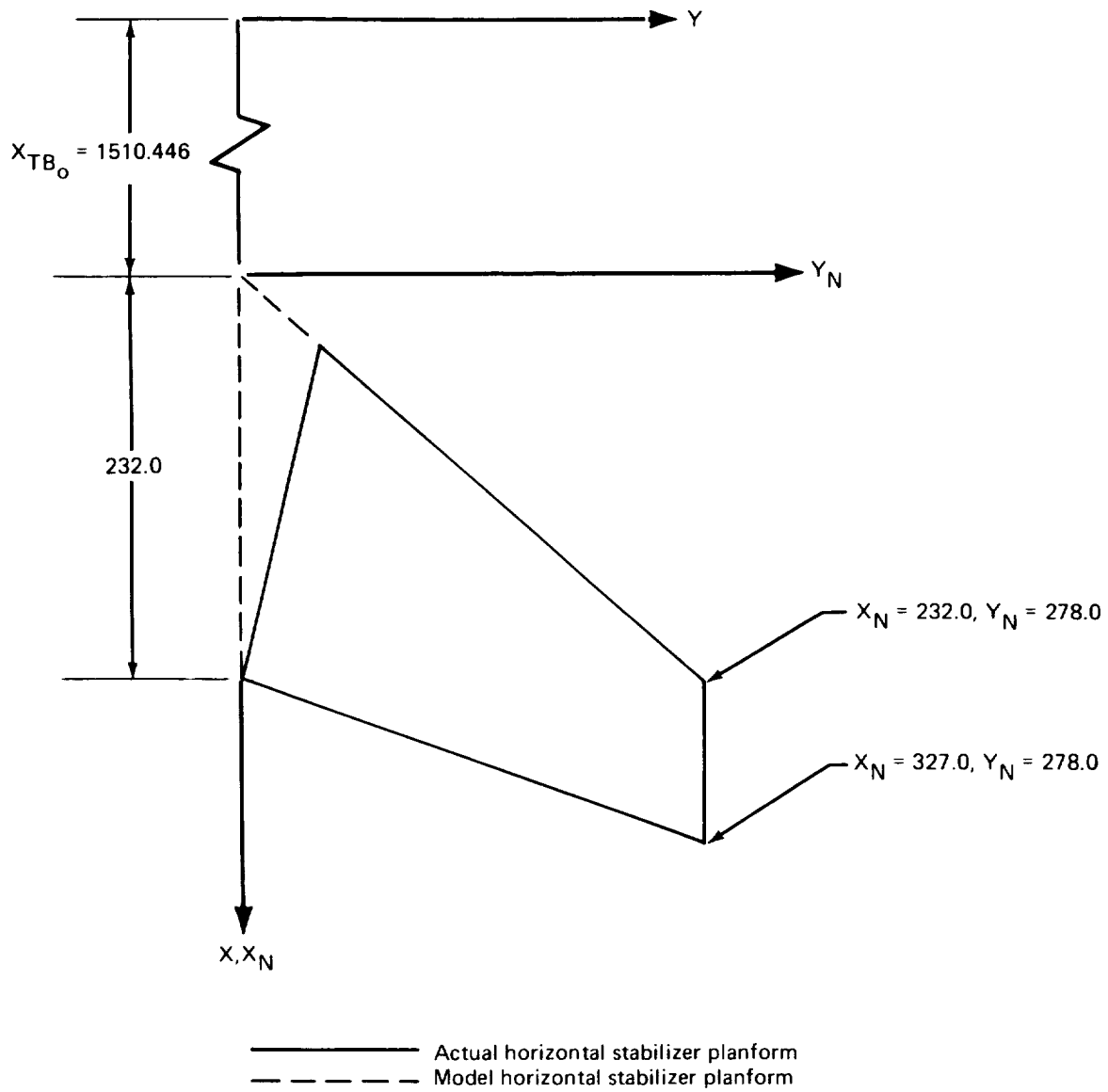
- Name of Thin Body and reference body: HOR was the name used for the horizontal stabilizer; its reference body was INTE.
- Thin Body origin and dihedral: The horizontal stabilizer was modeled with one Thin Body having  $7^\circ$  dihedral. The Z-coordinate of the Local Thin Body Coordinate System origin was chosen so that the distance from the horizontal tail to the fuselage camber line would be preserved. In this case, the horizontal hinge line coincided with the fuselage camber line, so the Z-coordinate was set to zero (see fig. 3.4-8). As a matter of convenience the Y-coordinate of the origin was also set to zero. The



**FIGURE 3.4-8.—DETERMINATION OF MODEL HORIZONTAL STABILIZER LOCATION—707-320B**

X-coordinate was then found by extending the leading edge of the horizontal stabilizer to the plane of symmetry (see fig. 3.4-9).

- **Planform definition:** The planform defined by the drawing was modified by extending the leading edge of the horizontal stabilizer to the plane of symmetry (see fig. 3.4-9).
- **Paneling scheme:** Force distribution was considered to be of secondary importance, so a very sparse paneling scheme was used. The streamwise panel edges were lined up with the streamwise panel edges of the wing (see “Wing definition”). The spanwise panel edges were arbitrarily placed at 40.8% and 74.0% of the chord.
- **Panel control point locations:** The panel control points were placed at the recommended 85% panel chord points.
- **Airfoil definition:** The airfoil ordinates were taken directly from Boeing documents.
- **Twist definition:** The horizontal stabilizer has no twist.



(X, Y, Z) Reference Axis System  
 ( $X_N, Y_N, Z_N$ ) Horizontal stabilizer's Local Thin Body Coordinate System  
 $X_{TB_0}$  X-coordinate of Local Thin Body Coordinate System origin

FIGURE 3.4-9.—MODEL HORIZONTAL STABILIZER PLANFORM—707-320B

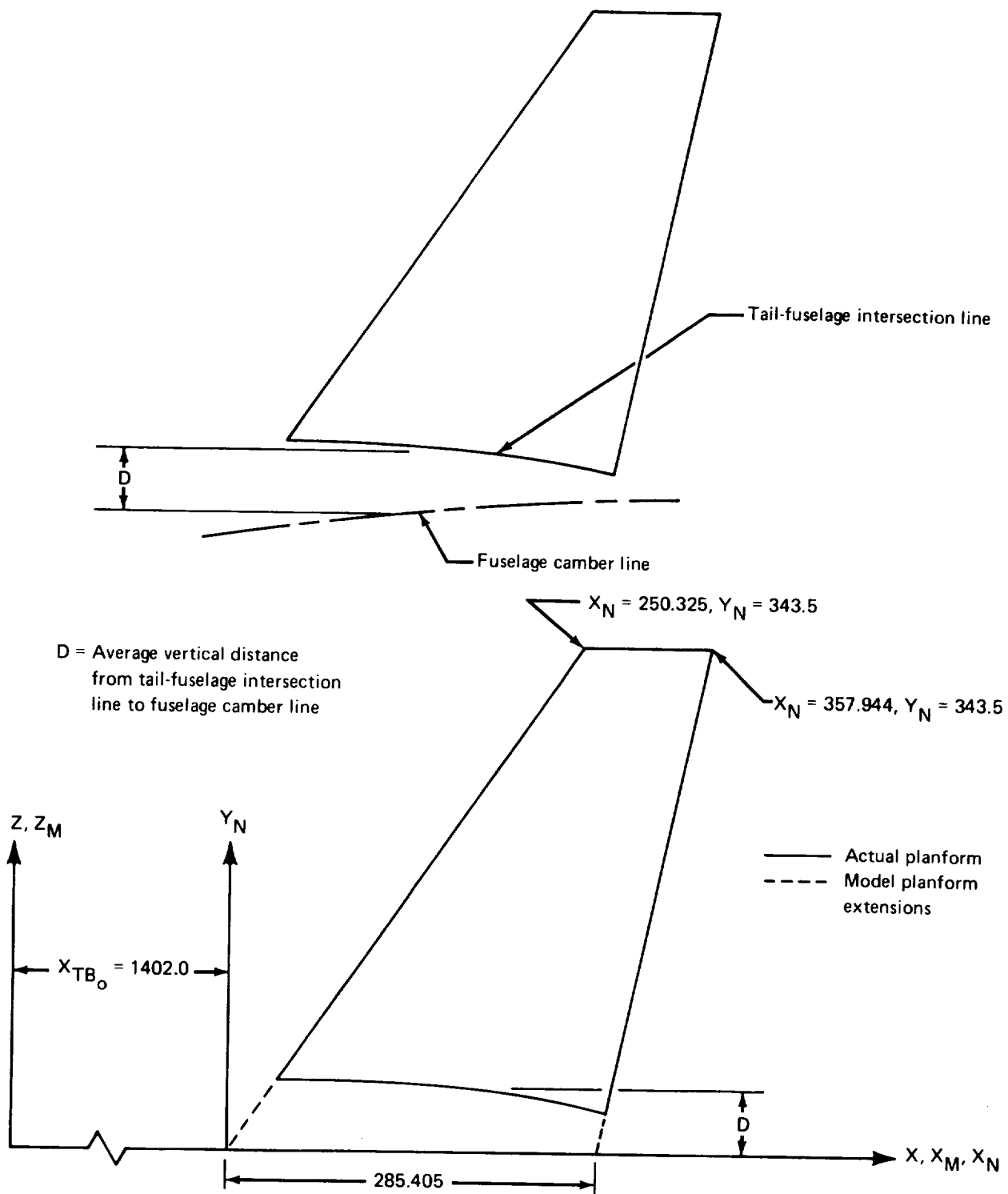


*Vertical tail.*—The data required to define the vertical tail were a planform drawing, a side-view drawing of the fuselage, and the vertical tail airfoil ordinates.

- Name of Thin Body and reference body: The vertical tail was named VERTICAL, its reference body was INTE.
- Thin Body origin and dihedral: The Y- and Z-coordinates of the vertical tail's Local Thin Body Coordinate System origin were specified to be 0.0. The X-coordinate,  $X_{TB0}$ , was found by extending the leading edge of the vertical tail until it intersected the X-axis (see next paragraph). The dihedral angle of the tail was set (by definition) to  $90^\circ$ .
- Planform definition: From the planform and fuselage side view drawings the average distance (in the Z-direction) from the tail-fuselage intersection line to the fuselage camber line, D, was found (see fig. 3.4-10). The planform was then shifted in the Z-direction such that the average distance from the tail-fuselage intersection line to the  $X_M$ -axis was equal to value of D determined above. The leading and trailing edges of this planform were then extended to the X-axis to complete the model planform definition (see fig. 3.4-10).
- Paneling scheme: Force distribution was considered to be relatively unimportant; therefore, a very sparse paneling arrangement was defined. Two streamwise panel rows (of approximately equal span) were specified, each containing three panels. The spanwise panel edges were placed at 40.8% and 74.0% of the chord. (The 74.0% line coincided with the leading edge line of the rudder.)
- Panel control point locations: The panel control points were placed at the recommended 85% panel chord points.
- Airfoil definition: The airfoil sections for the vertical tail were taken directly from Boeing documents.
- Twist definition: The vertical tail had no twist.

*Struts.*—The strut definitions required strut and nacelle planform drawings and each strut's airfoil ordinates. The discussion below applies to both the inboard and outboard struts.

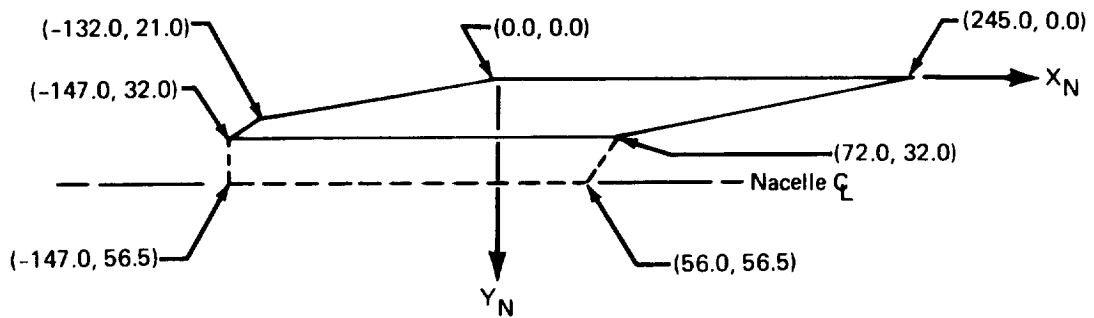
- Name of Thin Body and reference body: The inboard strut was named INSTRUT, the outboard strut, OUTSTRUT; their reference bodies were INWING and MIDWING, respectively.
- Thin Body origin and dihedral: The Relocate option was used to specify the locations of the origins of the Local Thin Body Coordinate Systems for the two struts. The origin of the coordinate system for INSTRUT was placed at the leading edge of the tip of INWING and the origin of the coordinate system for OUTSTRUT was placed at the leading edge of the tip of MIDWING. The dihedral angles of INSTRUT and OUTSTRUT are both  $-83.0^\circ$ .



$(X_M, Y_M, Z_M)$  Fuselage Local Slender Body Coordinate System  
 $(X_N, Y_N, Z_N)$  Vertical Tail Local Thin Body Coordinate System

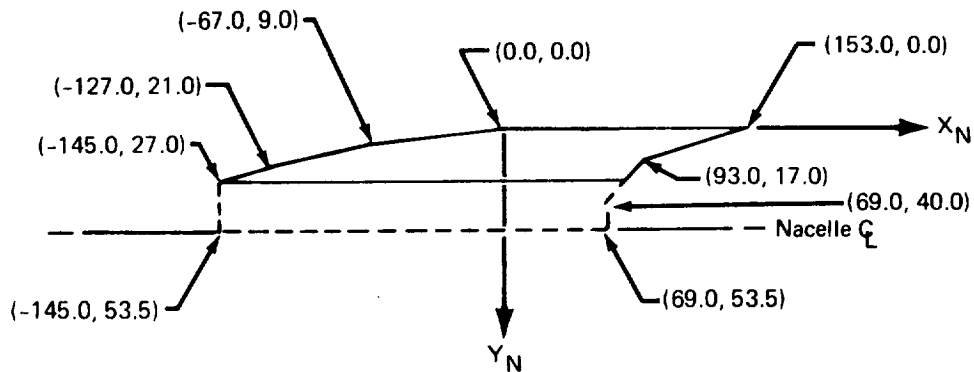
FIGURE 3.4-10.—VERTICAL TAIL MODELING—707-320B

- Planform definition: The planform of each strut was modified by extending the leading and trailing edges to the nacelle centerlines (see fig. 3.4-11). This procedure was used in order to determine the locations of the nacelle origins (see "Nacelle definition"). Planform break point coordinates are shown in figure 3.4.11.
- Paneling scheme: It was estimated that the struts would contribute very little to the aerodynamics of the entire configuration, so only three panels contained in one streamwise row were defined on each.
- Panel control point locations: The control points were placed at the 85% panel chord points.



**Inboard Strut**

— Actual strut planform  
 - - - Model strut planform extensions



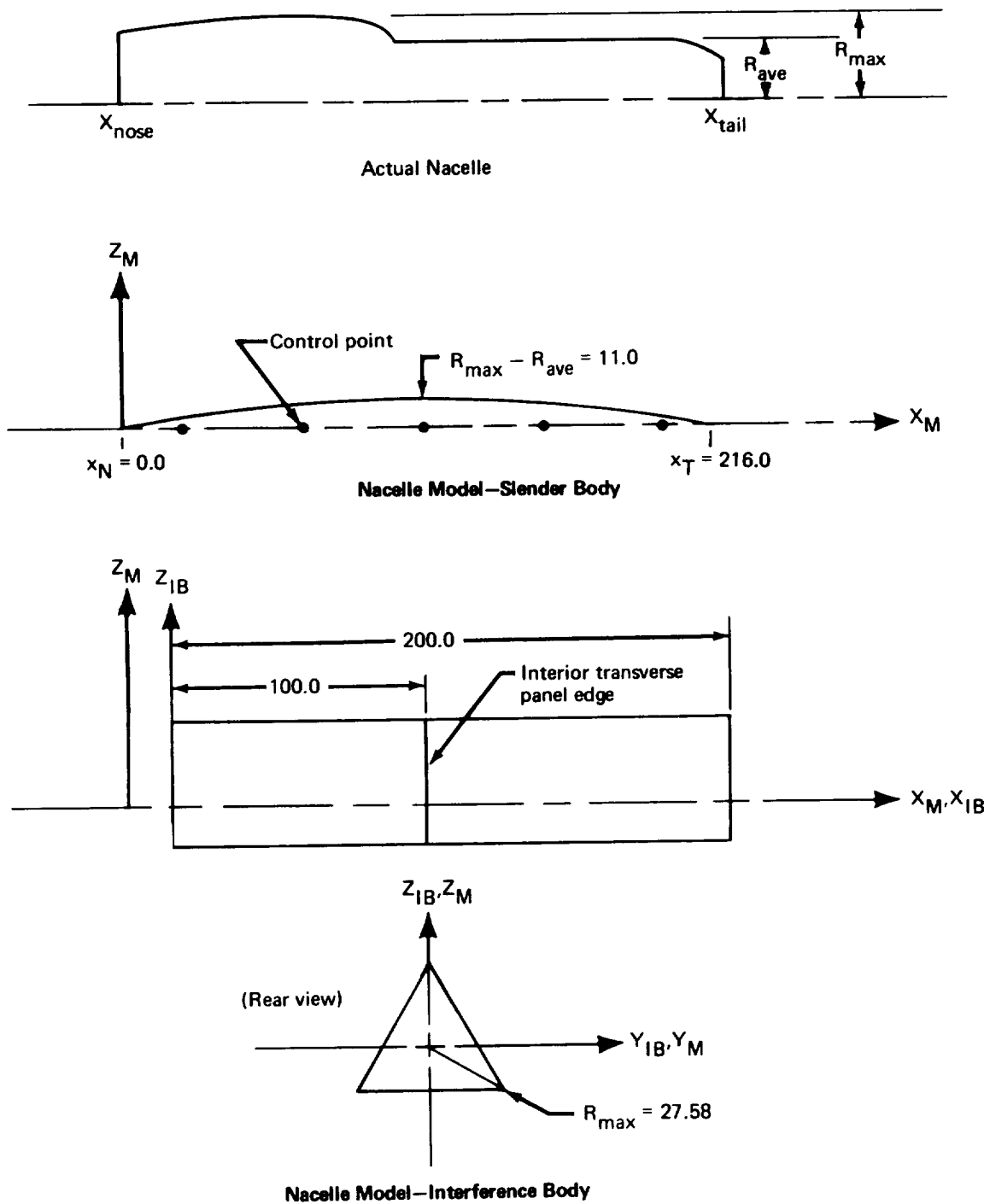
**Outboard Strut**

**FIGURE 3.4-11.—NACELLE STRUT PLANFORM DEFINITION—707-320B**

- Airfoil definition: The airfoil ordinates were taken directly from a company document.
- Twist definition: The struts had no twist.

*Nacelle definition.*—A side-view drawing of the nacelles and a general airplane configuration drawing were used to define the nacelle models. Each nacelle was represented by an Interference Body having a radius equal to the maximum radius of the actual nacelle and a Slender Body of much smaller radius to simulate nacelle thickness. The Slender Bodies are discussed first.

- Name of Slender Body: The inboard and outboard nacelles were named INNAC and OUTNAC, respectively.
- Slender Body origin: The X-coordinate of the Local Slender Body Coordinate System origin for INNAC was specified to be  $X = 670.101$ . The X-coordinate of OUTNAC's coordinate system origin was  $X = 851.928$ . The Y- and Z-coordinates were found by executing the GD program without nacelles, and then noting the Y- and Z-coordinates of the tips of INSTRUT and OUTSTRUT given in the printout (which, by definition, coincided with the nacelle centerlines). Using these coordinates ( $Y = 395.993$ ,  $Z = -45.7077$ , for INNAC, and  $Y = 623.9126$ ,  $Z = -14.7001$ , for OUTNAC) ensured that the Slender Bodies representing the nacelles would be located properly.
- Nose and aft end locations: These were taken directly from the side-view drawings of the nacelles (see fig. 3.4-12).
- Regions influenced by Thin Bodies: Because of the nacelles' close proximity to the wing and struts, it was specified that they would be influenced along their entire length.
- Number and placement of control points: Five control points were used to model each nacelle. They were evenly distributed between the nose and aft end locations by using the automatic placement option. This was considered an ample number since the nacelles are relatively small airplane components and their contribution to the overall stability characteristics of the airplane is probably minor.
- Area or radius distribution: The Slender Bodies were sized to represent the apparent thickness effects of the actual nacelles. The procedure used was to define each Slender Body as a parabola of revolution whose radius was equal to the maximum minus the average radius of the actual nacelle (see fig. 3.4-12). More recent experience shows that a better method is the one described in section 4.2.1 of volume II.
- Camber line definition: The nacelle models had no camber.



$(X_M, Y_M, Z_M)$  Local Slender Body Coordinate System  
 $(X_{IB}, Y_{IB}, Z_{IB})$  Local Interference Body Coordinate System

FIGURE 3.4-12.—NACELLE MODEL DEFINITION—707-320B

*Nacelle Interference Bodies.*—Information required to define these bodies consisted of side-view drawings of the nacelles and the nacelle Slender Body data. This description applies to both the inboard and outboard nacelle Interference Bodies.

- Name of Interference Body and reference body: The inboard and outboard nacelle Interference Bodies were given the names INTINNAC and INTOUT, respectively. Their reference bodies were INNAC and OUTNAC.
- Interference Body origin: The Y- and Z-coordinates of the Local Interference Body Coordinate System origin were identical to those of the corresponding nacelle Slender Body origin. The X-coordinate was just ahead of the first control point of the nacelle Slender Body.
- Regions where Thin Bodies affect the referenced Slender Body: This region extended from the Interference Body origin to a point slightly aft of the tail of the Slender Body (see fig. 3.4-12). (This region should have been terminated at the tail of the Slender Body.)
- Wing-body intersection line: In this case the corner points were input automatically (see below), and the program was allowed to make the paneling changes at the intersections of INSTRUT with INTINNAC and OUTSTRUT with INTOUT as shown in figure 4.2-15 in Volume II.
- Number and location of cross-sectional panel corner points: Only three panels were used in the interference shell (a larger number would be desirable if nacelle airloads were an important part of the analysis). The four panel corner points were placed at equal increments about the Slender Body by using the automatic input option. The radius of the shell was taken to be equal to the maximum radius of the actual nacelle (see fig. 3.4-12).
- Interference Body transverse panel edge locations: One interior transverse panel edge was placed halfway between the leading and trailing edges of the Interference Body by using the EQ. SPACE option (see fig. 3.4-12). (Again, a larger number of panels would be desirable if nacelle airloads were of primary interest.)
- Thin Body intersection data: This information was obtained from the strut input data. The tip of INSTRUT coincided with the  $X_{IB}$ -axis of INTINNAC's coordinate system; therefore  $Y_{IB} = Z_{IB} = 0.0$ . The same relationship existed between the tip of OUTSTRUT and INTOUT's  $X_{IB}$ -axis. The dihedral angle of both INSTRUT and OUTSTRUT (relative to the Local Interference Body Coordinate Systems) was  $97^\circ$ .
- Panel control point location: The control points were placed at the recommended location: 85% of the panel chord.

### 3.4.2 Geometry Definition Plot Program—GDPLLOT-3

The GDPLLOT program was used to obtain a graphic display of the aerodynamic model produced by GD-3A (see fig. 3.4-13). Note that only the paneling is shown. Indication of the panel centroid and/or control point locations was not requested.

### 3.4.3 Aerodynamic Influence Coefficient Program—AIC-3

Only one execution of the AIC program was necessary since the difference between the two geometric definitions involved only wing twist.

*AIC input.*—The following general information was specified in the AIC input data deck.

- Type of reference motion: Both symmetric and antisymmetric reference motions were requested since the airplane response to antisymmetric perturbations was to be calculated in SD&SS.
- Mach number: The freestream Mach number was set equal to 0.8.
- Perturbation delta Mach number: The perturbation delta Mach number was specified to be 0.06 (as calculated by the formula given in sec. 5.2.1, vol II).
- Steady/unsteady option: Unsteady aerodynamics was requested since dynamic stability calculations were to be made in SD&SS.

### 3.4.4 Internal Structural Influence Coefficient Program—ISIC-3

Only one structural definition of the 707-320B was necessary because the difference between the two geometric models did not affect the shape or paneling. This section describes the methods used to generate the input data deck. The bodies are discussed in the order in which they were defined.

*General information.*—The data required consisted of a complete elastic axis definition as shown in figure 3.4-14.

- Problem type: The residual-elastic option was chosen for both symmetric and antisymmetric motion so that all areas of the program would be exercised. Use of this option would allow a rigid, static-elastic or residual-elastic representation of the structure to be specified in the SD&SS program.
- General Junction Point X-locations: These locations were found from the available elastic axis data. There were no such data for the struts or nacelles so elastic axis positions were estimated. The General Junction Points were located at the nose of the fuselage and at each point where two elastic axes intersected (see fig. 3.4-14).
- General Junction Point symmetry code: From figure 3.4-14 it was noted that General Junction Points I, II, III, and IV were on the plane of symmetry and General Junction Points V, VI, VII, and VIII were off the plane of symmetry.

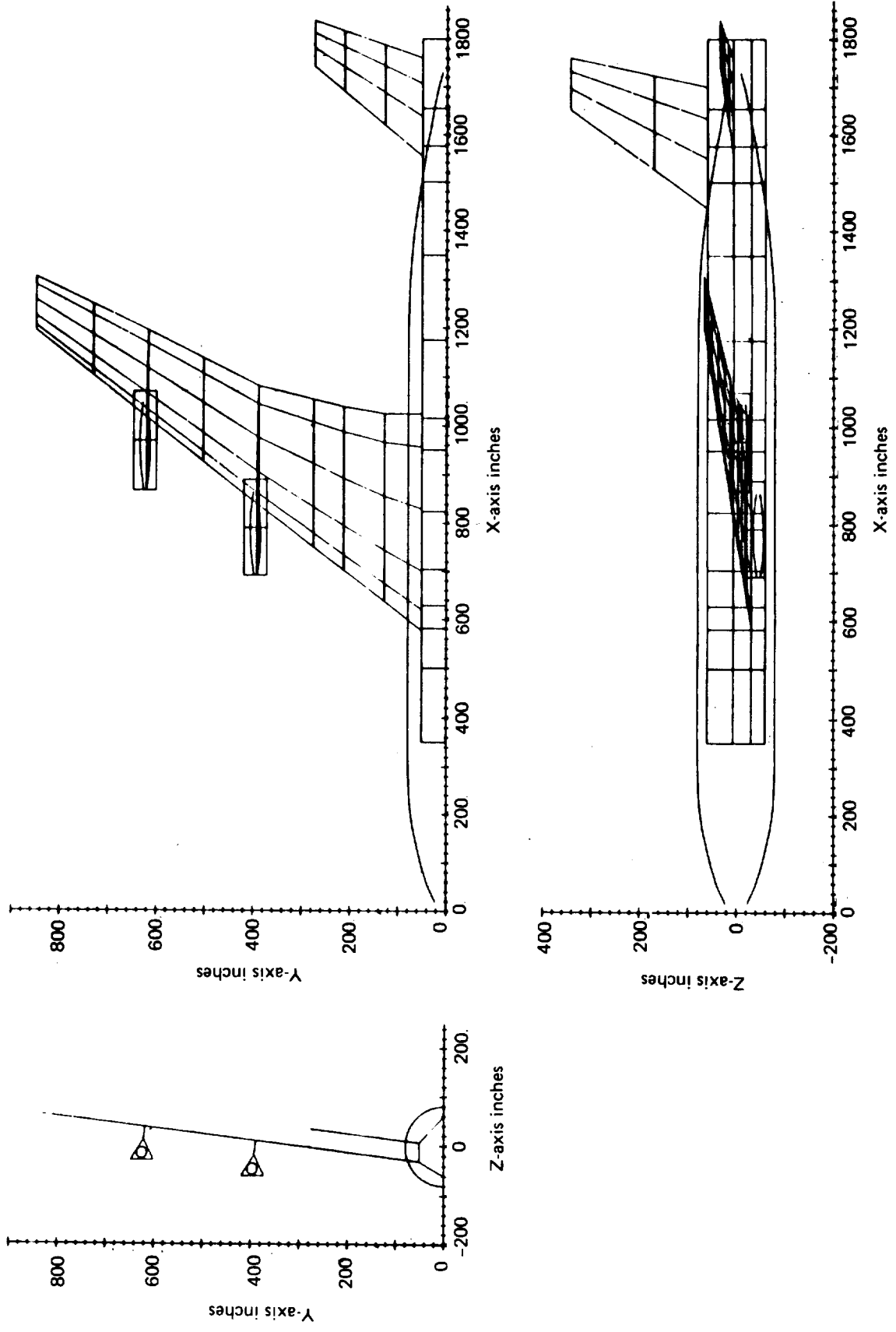


FIGURE 3.4-13.—GEOMETRY DEFINITION PLOT—707-320B





- **Junction Point Paths:** The independent Junction Point Paths defined by the elastic axes were found by tracing routes from each free end to the Reference Junction Point of the structural configuration at the nose (see fig. 3.4-14).
- **Gyroscopic effects option:** Gyroscopic moments due to the engines were specified to be associated with General Junction Points VII and VIII since these provided the structural connections for the nacelle.

*Fuselage definition.*—The airplane elastic axis drawing and the fuselage stiffness and mass properties were used to prepare the input data for the fuselage.

- **Number of parts:** The fuselage elastic axis was naturally divided into four parts by the wing, vertical tail, and horizontal stabilizer intersections (see fig. 3.4-14).
- **Associated General Junction Points:** Figure 3.4-14 shows that junction point I is located at the nose of the fuselage and that junction points II, III, and IV connect the Slender Body parts.
- **Number and locations of segments:** The fuselage was divided into segments by making a step function approximation of the  $EIY_M$  stiffness properties graph (see fig. 3.4-15). Each step represented a constant stiffness segment. The X-locations of the segment ends were taken directly from the graph.
- **Number of interior structural nodes per segment:** Because the stiffness properties of the fuselage varied so rapidly, there was no need to add interior structural nodes in any of the segments.
- **Segment stiffness properties:** The  $EIY_M$ ,  $EIZ_M$ , and GJ values for each segment were taken directly from the step approximations on the stiffness properties graphs. (Full stiffness values are input, even for elastic axes lying on the plane of symmetry.)
- **Lumped mass distribution and scale factors:** The raw mass data consisted of the locations of a number of point masses to represent the structural, passenger, cargo, and fuel masses. These masses were divided among the structural nodes in a manner that preserved the center of gravity of the fuselage. Some of these mass values were later altered when the total airplane mass, center of gravity, and moments of inertia were refined. These lumped masses were input in slugs, so no scale factors were required. (The mass values input were one-half the actual values since the fuselage elastic axis was on the plane of symmetry.)

*Wing definition.*—The wing was defined in the GD program by using three Thin Bodies. The structural input data were first determined by treating the wing as one body, and then dividing it into three pieces in order to make it consistent with the geometry definition. The GD program output, wing planform drawing, elastic axis definition, and stiffness and mass properties were required to prepare the input data.

- **Number of parts:** Each Thin Body had only one part.

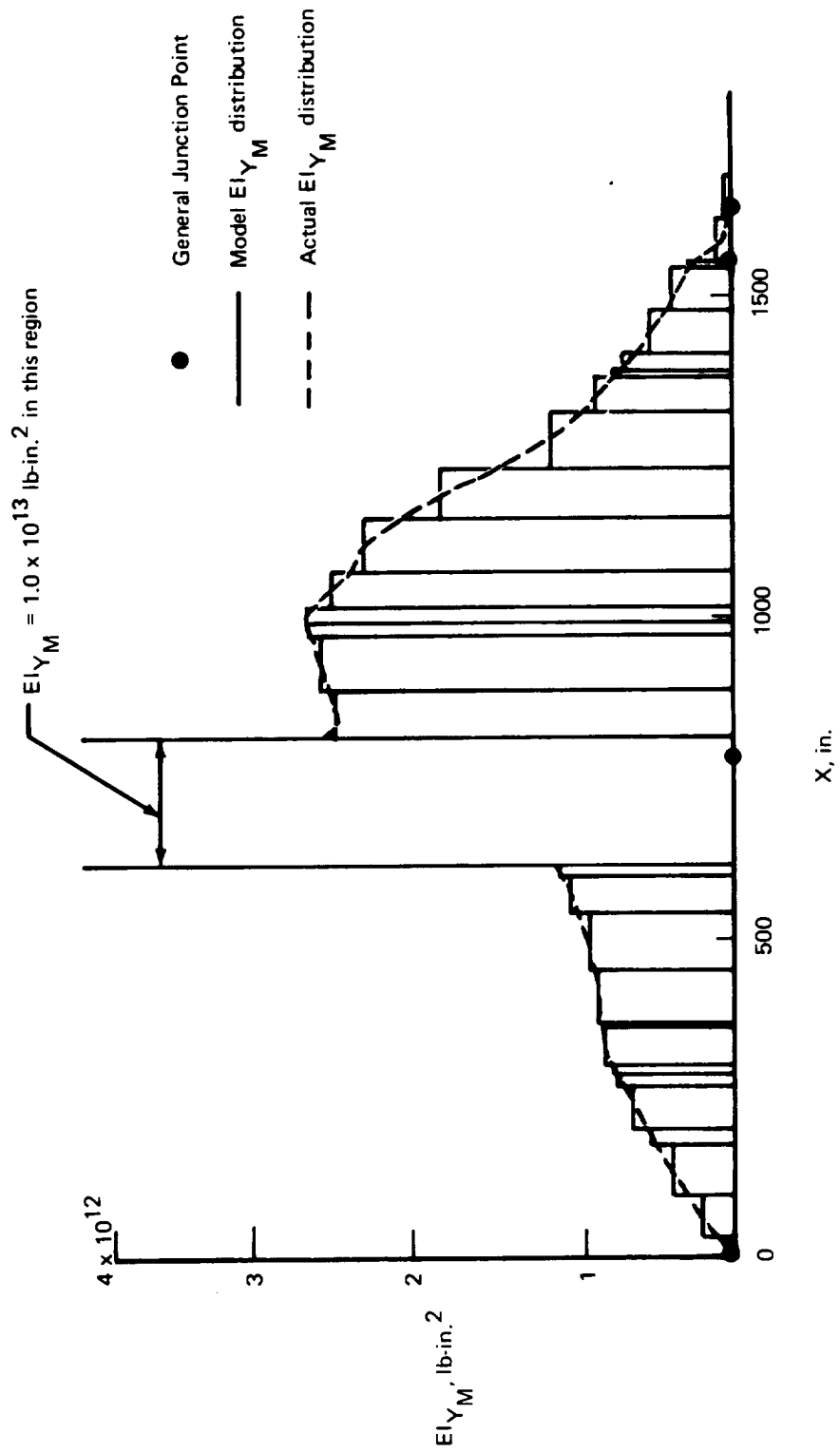


FIGURE 3.4-15. --STIFFNESS MODELING FOR THE 707-320B FUSELAGE

- Associated General Junction Points: From figure 3.4-14 it was noted that junction points II, V, and VI were associated with the wing.
- Number and locations of segments: Step function approximations of the stiffness properties curves similar to the ones made for the fuselage were made so that the stiffness properties of the wing would be well defined. Each step in the approximation defined a constant stiffness elastic segment. A program requirement that all segments which begin or terminate at a General Junction Point have zero sweep was satisfied by inserting short zero-sweep segments (about 10 inches in length) at each of the associated General Junction Points. Allowance for this deviation from the actual elastic axis definition was made in the adjacent segments. At this point the elastic axis model was complete, so the  $x_N$ - and  $y_N$ -locations of the segment ends could be found. This was accomplished by drawing Thin Body Structural Coordinate Systems originating at each of the associated General Junction Points and reading the appropriate  $x_N$ ,  $y_N$ -coordinates. The number of segments per Thin Body was simply counted from the drawing (see fig. 3.4-16).
- Number of interior nodes per segment: Additional structural nodes were required because of the large number of aerodynamic panels on the wing. These were included in the longest segments. (This procedure was designed to minimize the error due to the  $y_{N_i}$ -offset approximation; see fig. 6.2-7, vol II.)
- Segment stiffness properties: The  $EI_{x_{N_i}}$  and GJ values for each elastic segment were taken directly from the stiffness properties drawings.
- Lumped mass distribution and scale factors: The raw data defined the wing as 10 spanwise panels with two mass values and two centers of gravity, one for the wing structure and one for fuel (see fig. 3.4-17). These panels provided a fair spanwise mass distribution, but an unacceptable chordwise distribution. To improve the chordwise mass distribution, a wing planform drawing that included the front and rear spars and the fuel tanks was made. It was decided that the structural masses would be placed on the front and rear spars and the fuel masses at points midway between the edges of the fuel tanks and the elastic axis. Lines indicating these positions were drawn. The program requires that Thin Body masses lie on lines that pass through the associated structural nodes and are perpendicular to the associated segments. Lines meeting these criteria were drawn. The points of intersection of these lines and the set previously described became the model's mass location points. Masses were then distributed to the various points in a manner which preserved each original panel's total mass and center of gravity. The mass distribution obtained was later altered slightly when the airplane's total mass, center of gravity, and moments of inertia were refined. All of the above calculations were made using pounds; therefore, the weights of the lumped masses were input in pounds. As a result, a scale factor of 0.031081 was used to convert the input values into slugs.

*Vertical tail and horizontal stabilizer definitions.*—These bodies were defined in a similar manner. Data required were planform drawings, GD program output, elastic axis definitions, and stiffness and mass properties.

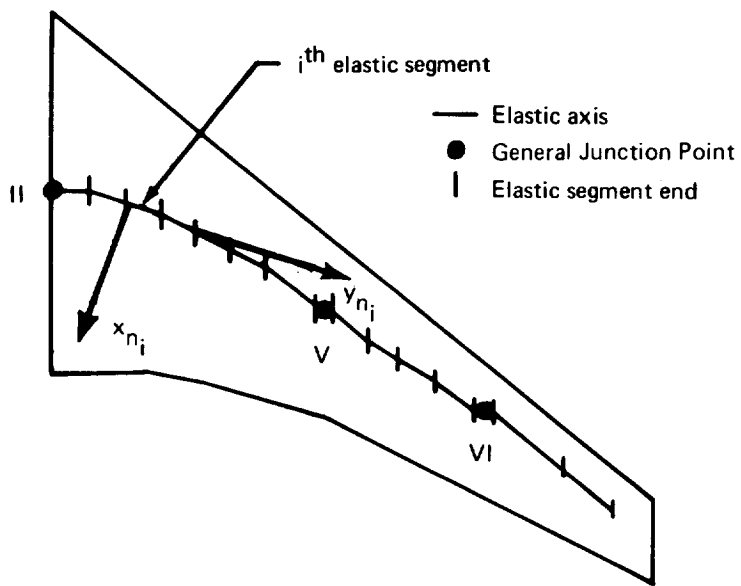
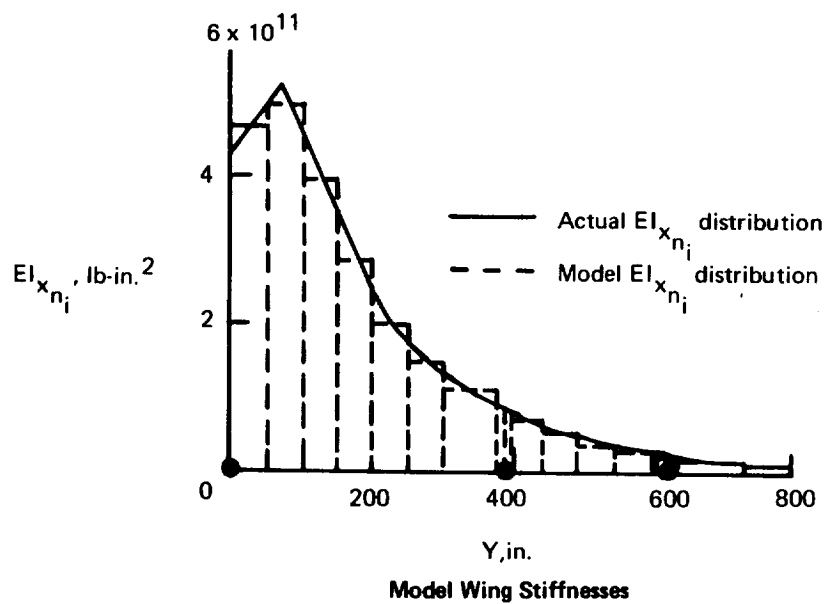


FIGURE 3.4-16.—WING STRUCTURAL MODEL—707-320B

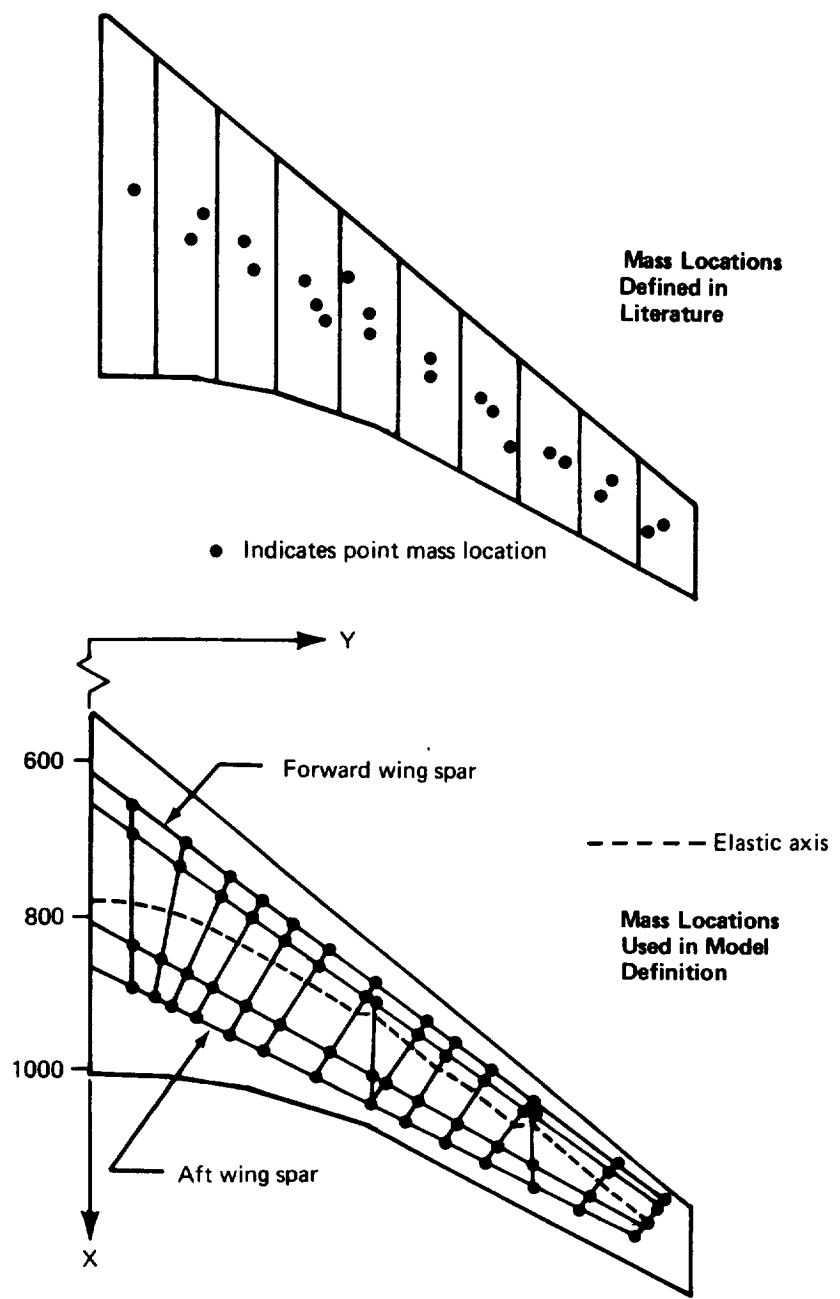


FIGURE 3.4-17.—MODEL MASS DISTRIBUTION—707-320B

- Number of parts: The vertical tail and horizontal stabilizer each had one part.
- Associated General Junction Points: It was noted from figure 3.4-14 that the vertical tail was attached to the fuselage by junction point III and the horizontal stabilizer was attached by junction point IV.
- Number and locations of segments: The segment definitions were made using the same method used for the wing. Initial segment end locations were found by making step approximations of the stiffness properties. These were then modified when the requirement that the first segment of each body have zero sweep was satisfied. The  $x_n$ - $y_n$ -locations of each segment end were measured in terms of Thin Body Structural Coordinate Systems originating at the respective General Junction Points.
- Number of interior structural nodes per segment: A sufficient number of structural nodes (8 nodes for the horizontal stabilizer and 12 nodes for the vertical tail) was defined when forming the segments, so no interior nodes were necessary for either body.
- Segment stiffness properties: These values were found by forming step function approximations to the stiffness property curves based on the revised locations of the segment ends. (Full stiffness values were entered for the vertical tail.)
- Lumped mass distribution and scale factors: Vertical tail and horizontal stabilizer data from company documents divided the bodies into panels and gave the mass and center of gravity for each panel. Model lumped mass locations were situated at the intersections of the front and rear spars, with lines originating from the structural nodes and perpendicular to the respective segments. The masses from the raw data were distributed to these model lumped mass locations in a manner which preserved each defining panel's mass and center of gravity. All of the above calculations were made using pounds and the weights of the lumped masses were input in pounds. As a result, a scale factor of 0.031081 was included to convert the data to slugs. (The vertical tail masses were one-half the actual values.)

*Strut definitions.* – There were no elastic axis or stiffness data available for either strut, so this information was estimated. The data required to prepare the card input were planform drawings, structural drawings, mass data, and the wing input data.

- Number of parts: Each strut had only one part.
- Associated General Junction Points: From figure 3.4-14 it was noted that the inboard strut had structural connections at General Junction Points V and VII, and the outboard strut was connected at junction points VI and VIII.
- Number and locations of segments: The elastic axis chosen for each strut is shown in figure 3.4-18. Each elastic axis consisted of four segments, one of which coincided with the midspar. The  $x_n$ - $y_n$ -coordinates of the segment ends were measured using Thin Body Structural Coordinate Systems originating at junction

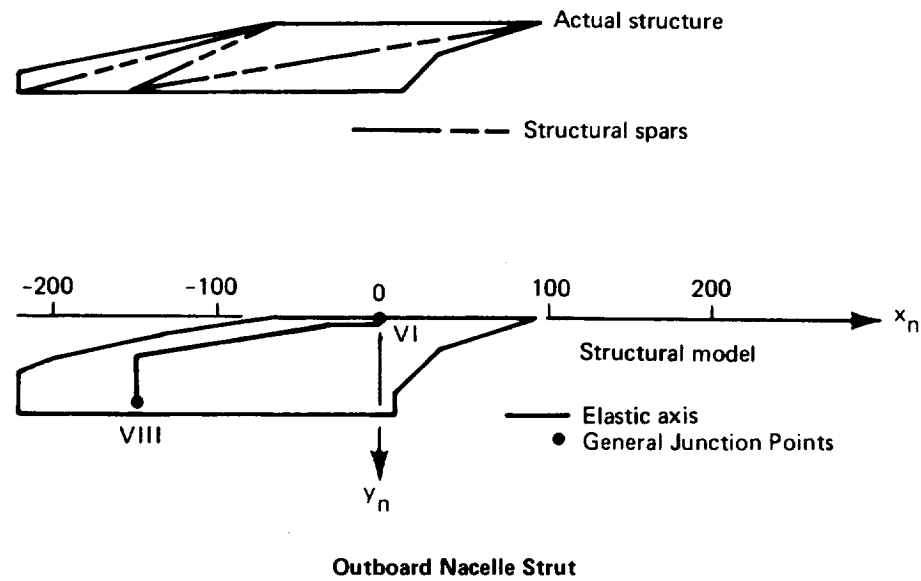
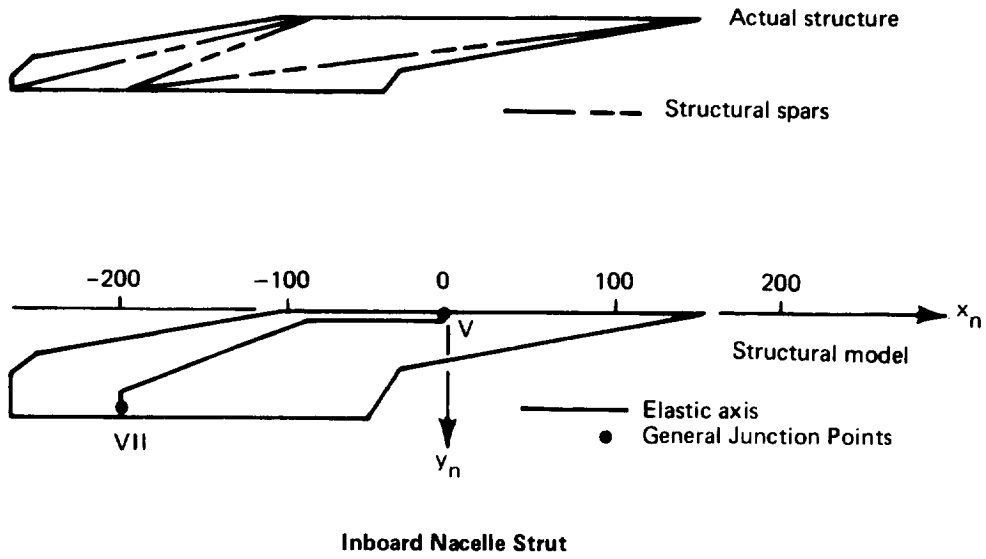


FIGURE 3.4-18.—STRUCTURAL MODELS OF THE 707-320B STRUTS



points V and VI. Note that the first and fourth segments of each elastic axis are perpendicular to the  $x_n$ -axis (and, therefore, the X-axis) as required.

- Number of interior structural nodes per segment: Two interior nodes were placed on the third segment (the longest segment; see fig. 3.4-18) of each body to compensate for the fact that these segments nearly spanned the strut.
- Segment stiffness properties: The struts were assigned stiffnesses that were of the same order of magnitude as those in the wing-fuselage intersection area.
- Lumped mass distribution and scale factors: The mass data available for each strut consisted of a single mass value and location. This mass was divided into four masses which were assigned to the interior nodes mentioned above in a manner which preserved total mass and center of gravity of each strut. The lumped masses were input in slugs; therefore, no scale factors were needed.

*Nacelle definitions.*—The elastic axes and stiffness properties of the nacelles were not available and therefore, were estimated. The information required to generate the input data were the GD program output and the nacelle mass data.

- Number of parts: Each nacelle was divided into two parts by the strut intersection (see fig. 3.4-14). For both bodies, the first part was forward of the intersection and the second part aft.
- Associated General Junction Points: As shown in figure 3.4-14, the inboard nacelle was structurally connected by junction point VII and the outboard nacelle by junction point VIII.
- Number and locations of segments: The elastic axis of each nacelle was assumed to coincide with the  $X_M$ -axis of its Local Slender Body Aerodynamic Coordinate System. Each Slender Body part consisted of one elastic segment.
- Number of interior structural nodes per segment: In order to provide a means of defining an adequate mass distribution, one interior node was placed in the first Slender Body part and two were placed in the second part. This procedure was followed for both nacelles.
- Segment stiffness properties: The  $EI_{Y_M}$ ,  $EI_{Z_M}$ , and GJ for each segment were estimated to be  $1.0 \times 10^{13}$  lb-in. squared. These relatively high stiffness values were specified since it was anticipated that the nacelles would act rigidly. It should be noted that stiffnesses of much higher orders of magnitude were ruled out because of the possibility of introducing errors during inversion of the stiffness matrix to form the flexibility matrix.
- Lumped mass distribution and scale factors: The raw data provided the total mass and center of gravity for each body. Masses were distributed among the five structural nodes of each nacelle such that total masses and centers of gravity were preserved. The masses were input in slugs; therefore, scale factors were not required.

*Refinement of the 707-320B mass data.*—Although the mass definition described provided fairly accurate mass distribution results for each of the bodies, the individual body locations as modeled in the GD program were approximate. Thus, when the total mass, center of gravity, and moments of inertia were calculated, they did not agree with the published figures. To correct this, mass values were changed until the total mass, center of gravity,  $I_{XX}$ ,  $I_{YY}$ , and  $I_{ZZ}$  were within 3 percent of the published figures. All of the changes made involved lumped masses that represented cargo, passengers, and fuel. Therefore, the structural masses were not affected, and the lumped mass representation remained valid.

#### 3.4.5 Elastic Axis Plot Program—EAPLOT-3

The EAPLOT program was used to obtain a graphic display of the structural modeling used in the ISIC program. The results of this program for the 707-320B are given in figure 3.4-19.

#### 3.4.6 Normal Modes Program—NM-3

The NM program input for the 707-320B consisted of the following:

- Structural option: The residual-elastic structural option was chosen for both symmetric and antisymmetric motions since coupled perturbation calculations were to be made in SD&SS.
- Number of modal shapes desired: It was requested that only the first symmetric and first antisymmetric modal shapes be calculated. The second and higher modal shapes were not desired since their frequencies were high enough (greater than 1.9 cycles per second) to be considered inconsistent with the low frequency assumptions made in developing the unsteady aerodynamic theory used in FLEXSTAB.

#### 3.4.7 Normal Modes Plot Program—NMPLOT-3

The NMPLOT program gave a graphic display of the modal shapes calculated in the NM-3 run. Shown in figure 3.4-20 is the participation of each body (with the exception of the vertical tail) in the first symmetric modal shape. (The vertical tail has no degrees of freedom for symmetric boundary conditions and therefore, its displacements are identically zero.)

The participation of Slender Bodies is displayed in terms of aerocentroid displacements in the Y- and Z-directions ( $DY$  and  $DZ$ , respectively). Thin Body aerocentroid displacements are in the  $Z_N$ -direction ( $DZ_N$ ). (Note that the planform locations of the Thin Body aerocentroids are shown in figure 3.4-20 and that the  $Z_N$ -displacements, which are actually normal to the Thin Body plane, are displayed in the  $Y_N$ -direction; the  $Z_N$ -displacement scale is located at the top of each Thin Body modal shape plot.) All displacements are measured from the underformed aerocentroid locations (defined by the GD program) and are normalized with respect to the largest aerocentroid displacement for the entire configuration.

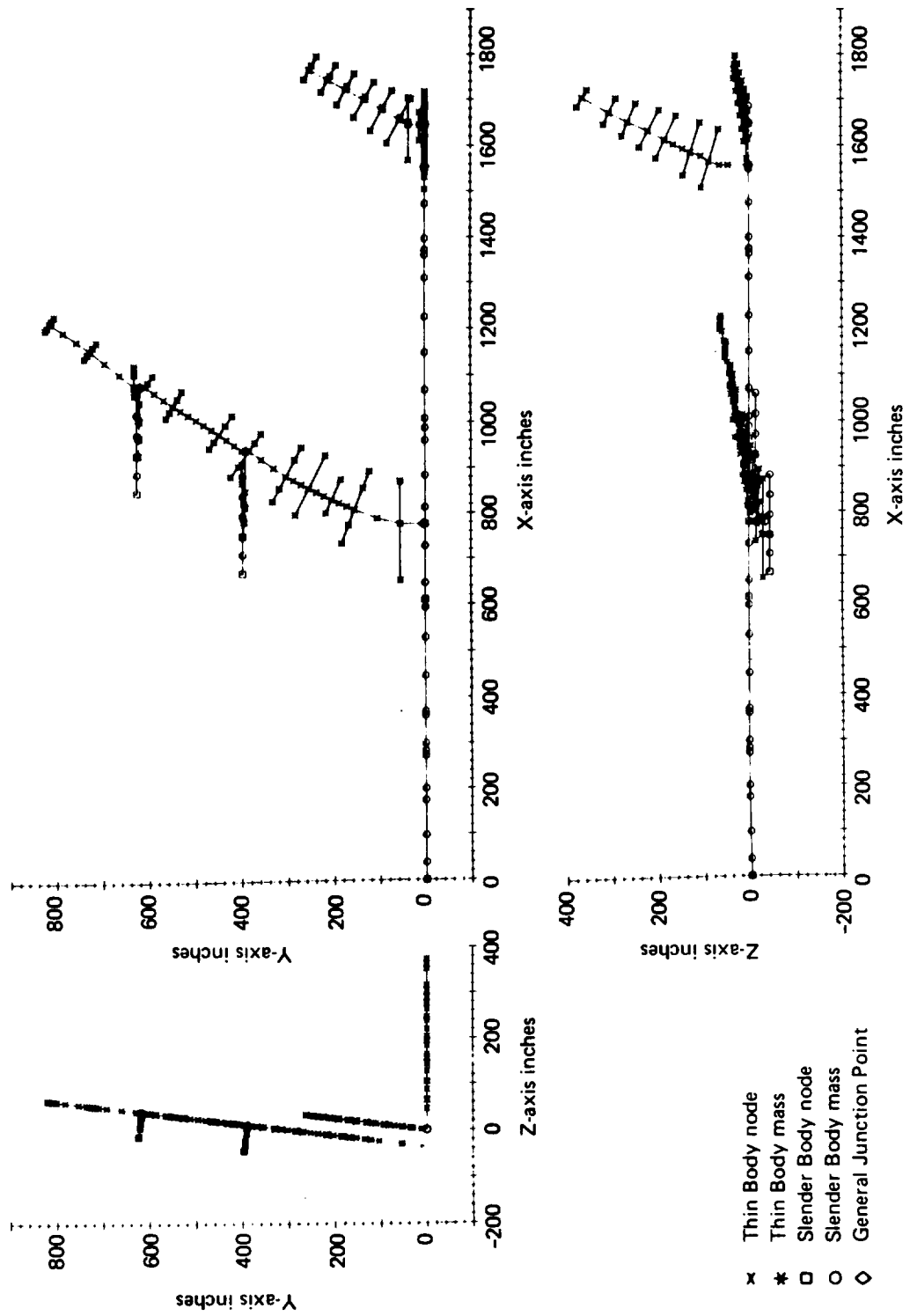
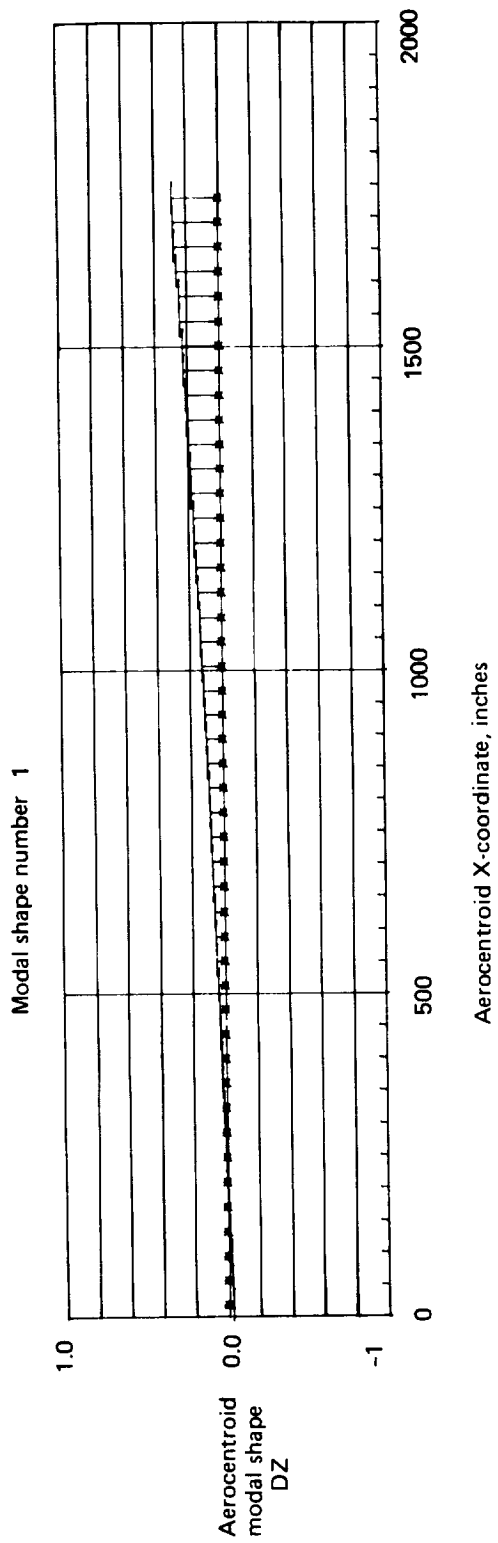


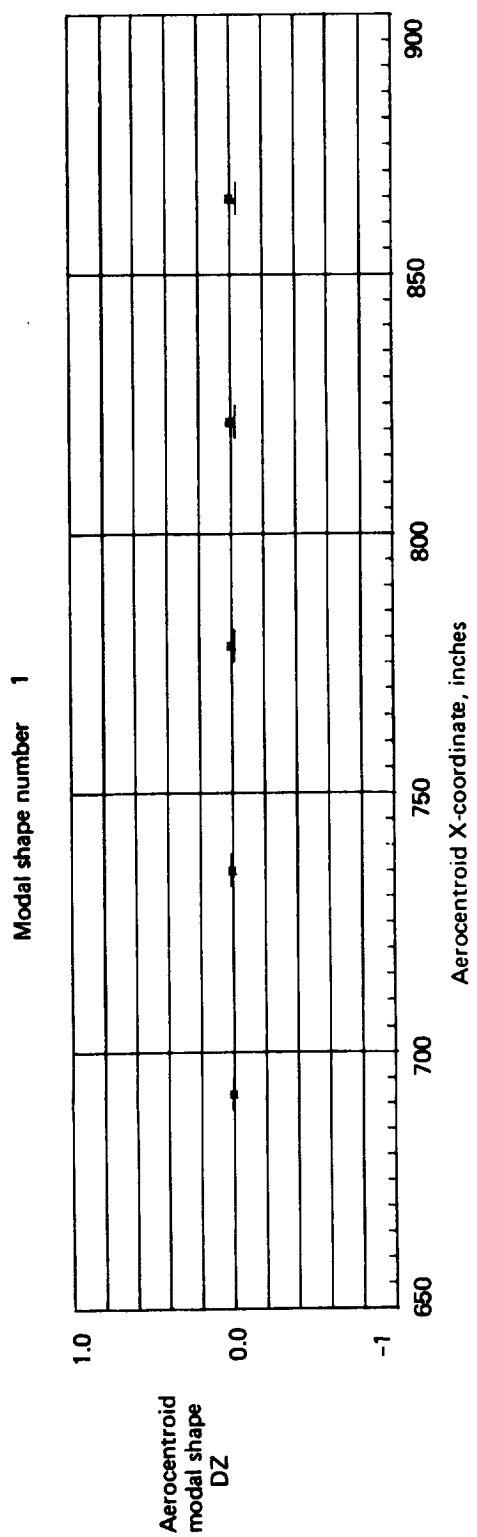
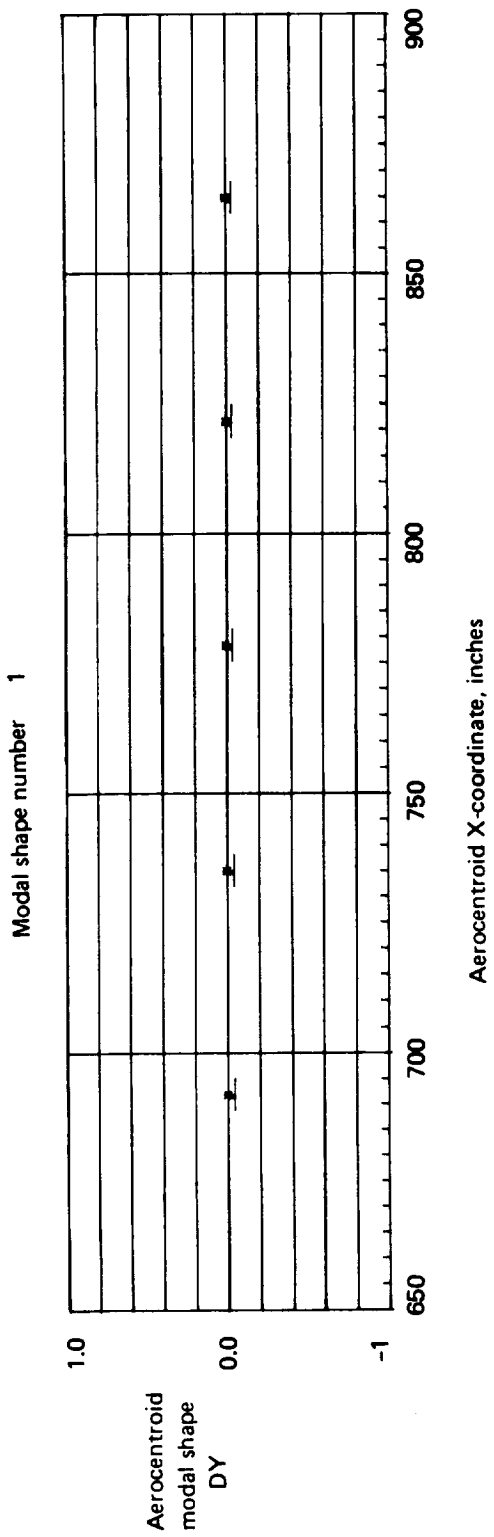
FIGURE 3.4-19.—ELASTIC AXIS PLOT—707-320B



Slender Body 1 (FUSELAGE)  
 $Y_{SB} = 0.000$   $Z_{SB} = 0.000$   
 Symmetric boundary conditions

\* position of aerocentroid in undeformed state  
 — position of aerocentroid in modal shape

FIGURE 3.4-20.—NORMAL MODES PLOT—707-320B



Slender Body 2 (INNAC)  
 $Y_{SB} = 395.993$   $Z_{SB} = -45.708$  \* position of aero-centroid in undeformed state  
 Symmetric boundary conditions - position of aero-centroid in modal shape

FIGURE 3.4-20.—CONTINUED



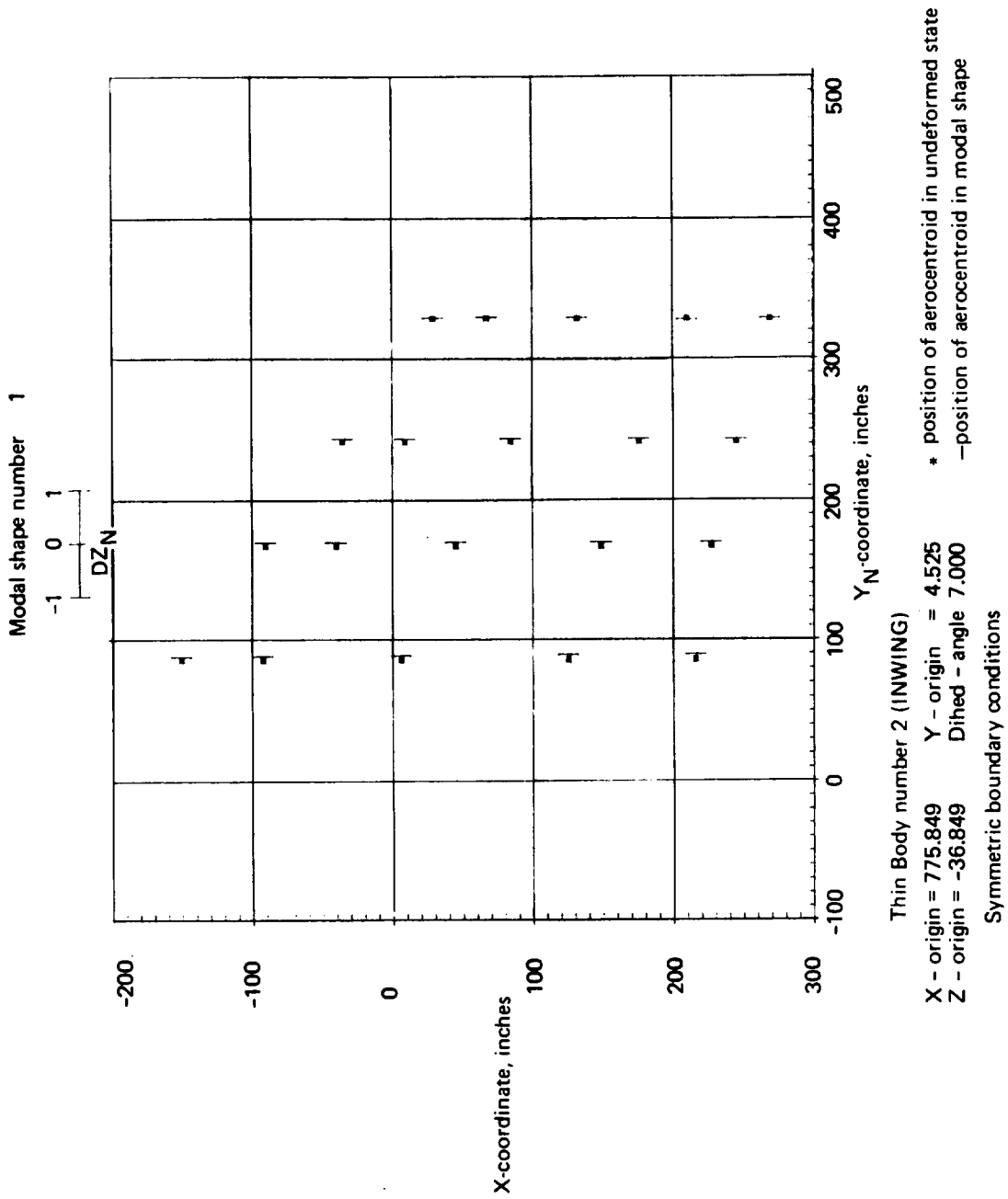
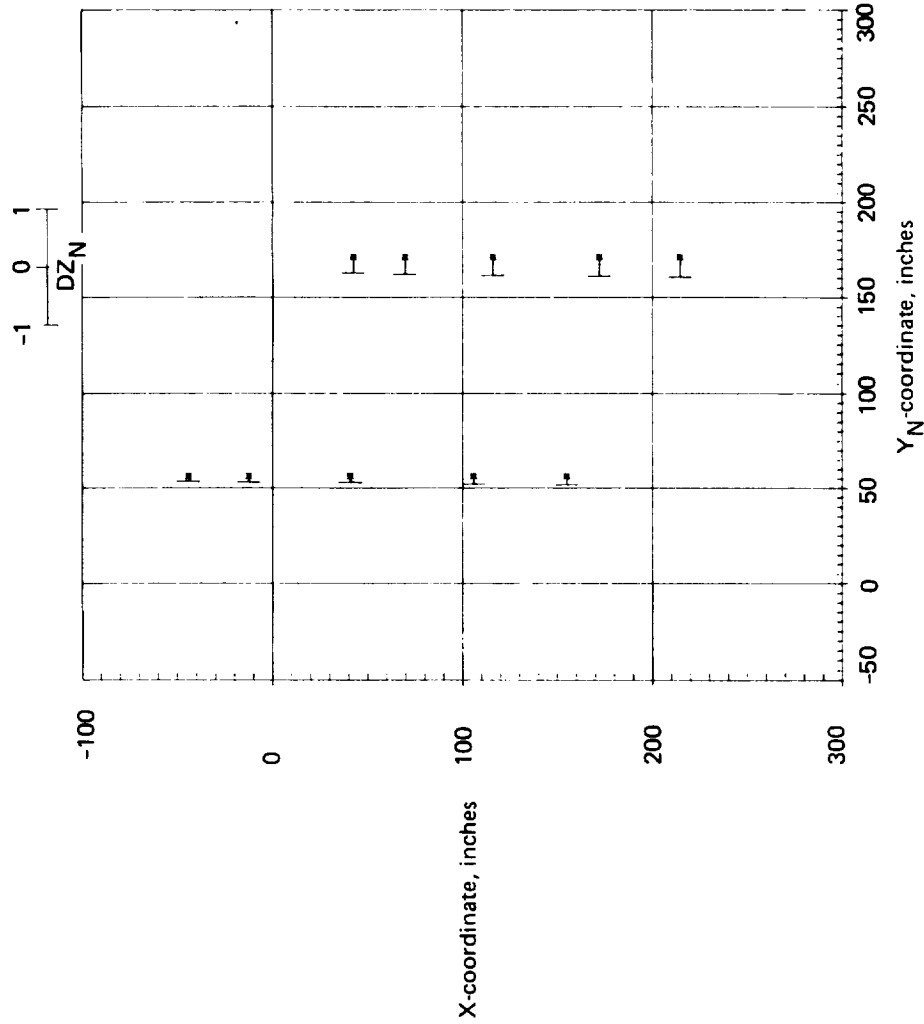


FIGURE 3.4.20.—CONTINUED

Modal shape number 1



Thin Body number 3 (MIDWING)

X - origin = 935.849

Y - origin = 389.107

Z - origin = 10.371

Dihed - angle 7.000

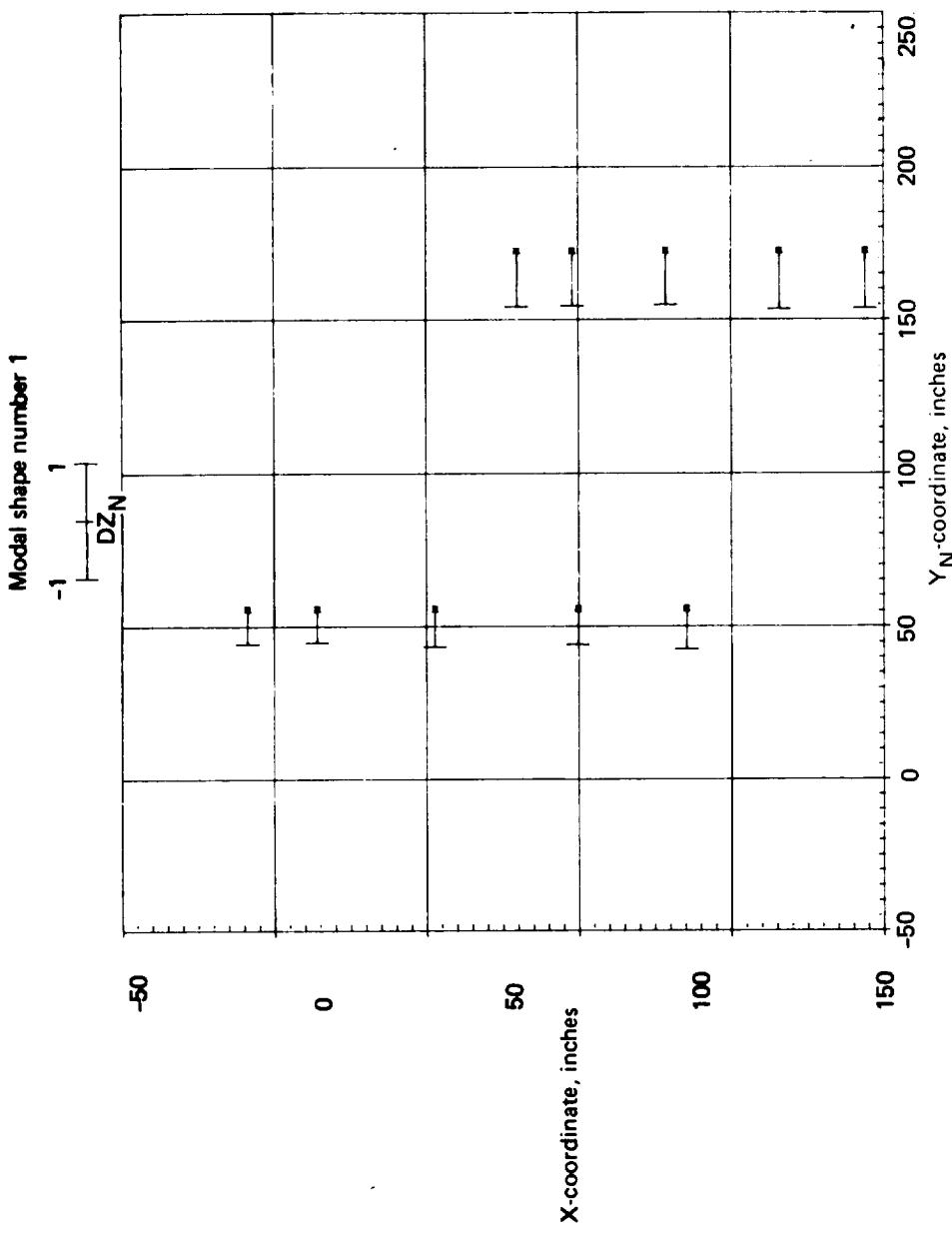
Symmetric boundary conditions

\* position of aerocentroid in undeformed state

- position of aerocentroid in modal shape

FIGURE 3.4-20.—CONTINUED

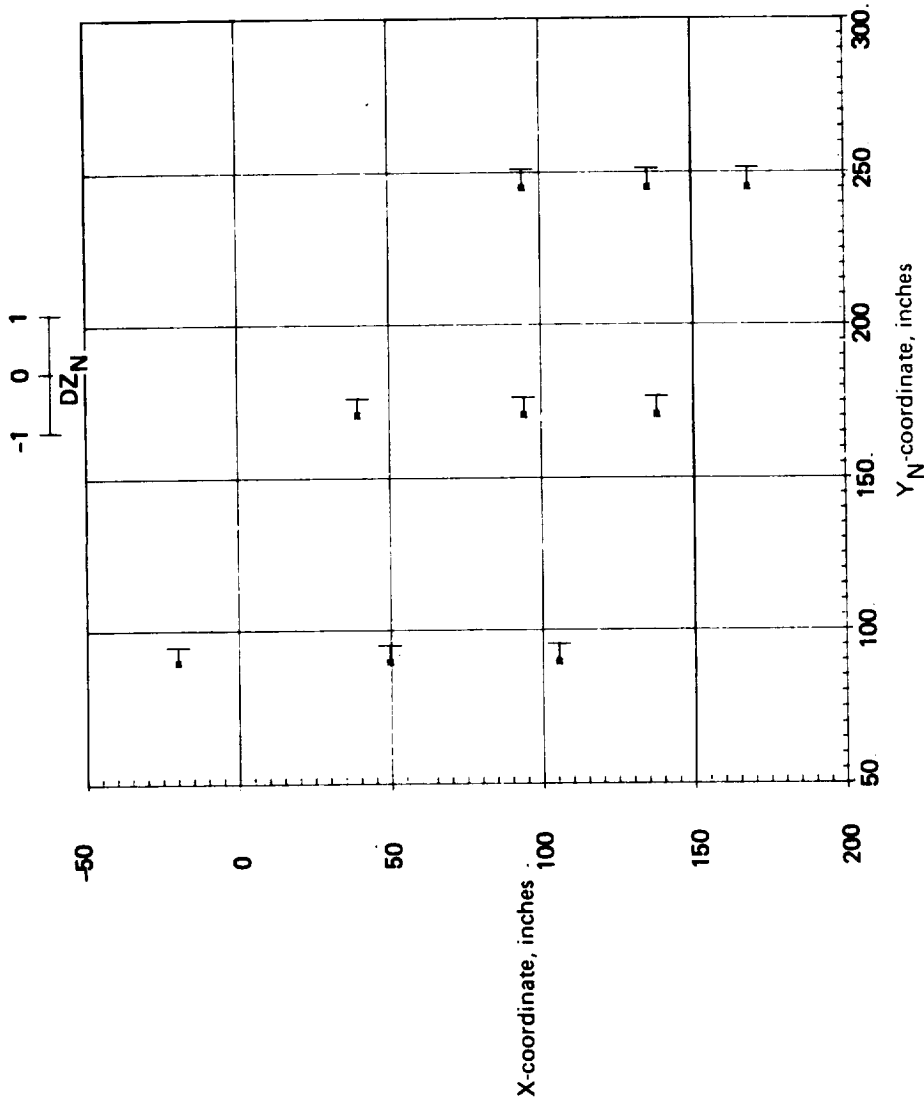




X - origin = 1073.849    Y - origin = 617.393    \* position of aerocentroid in undeformed state  
 Z - origin = 38.401    Dihed - angle 7.000    - position of aerocentroid in modal shape  
 Symmetric boundary conditions

FIGURE 3.4-20.—CONTINUED

Modal shape number 1



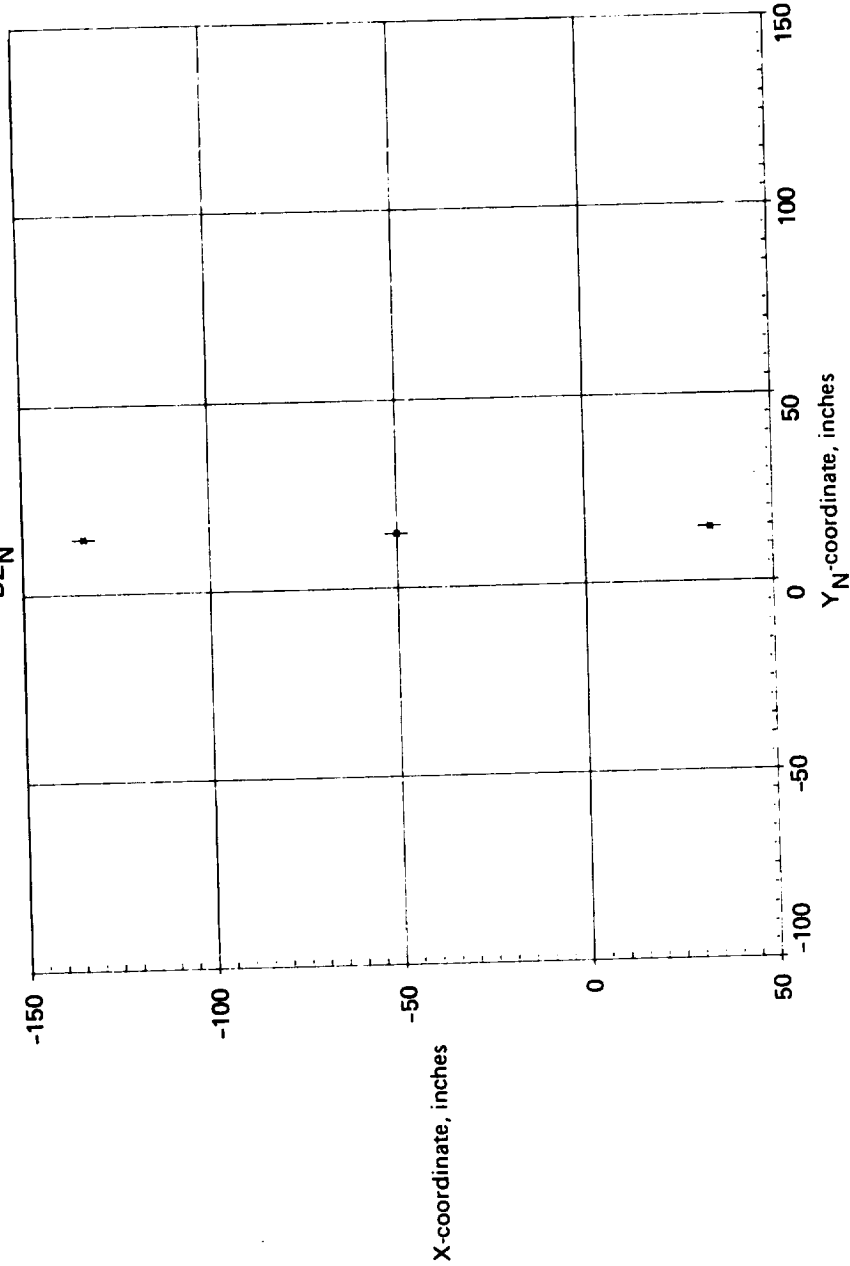
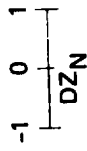
Thin body number 5 (HOR)

X - origin = 1643.446    Y - origin = 0.000    \* position of aerocentroid in undeformed state  
 Z - origin = 0.000    Dihed - angle 7.000    - position of aerocentroid in modal shape

Symmetric boundary conditions

FIGURE 3.4-20.—CONTINUED

Modal shape number 1



Thin Body number 6 (INSTRUT)

X - origin = 935.849

Y - origin = 389.107

• position of aerocentroid in undeformed state

Z - origin = 10.371

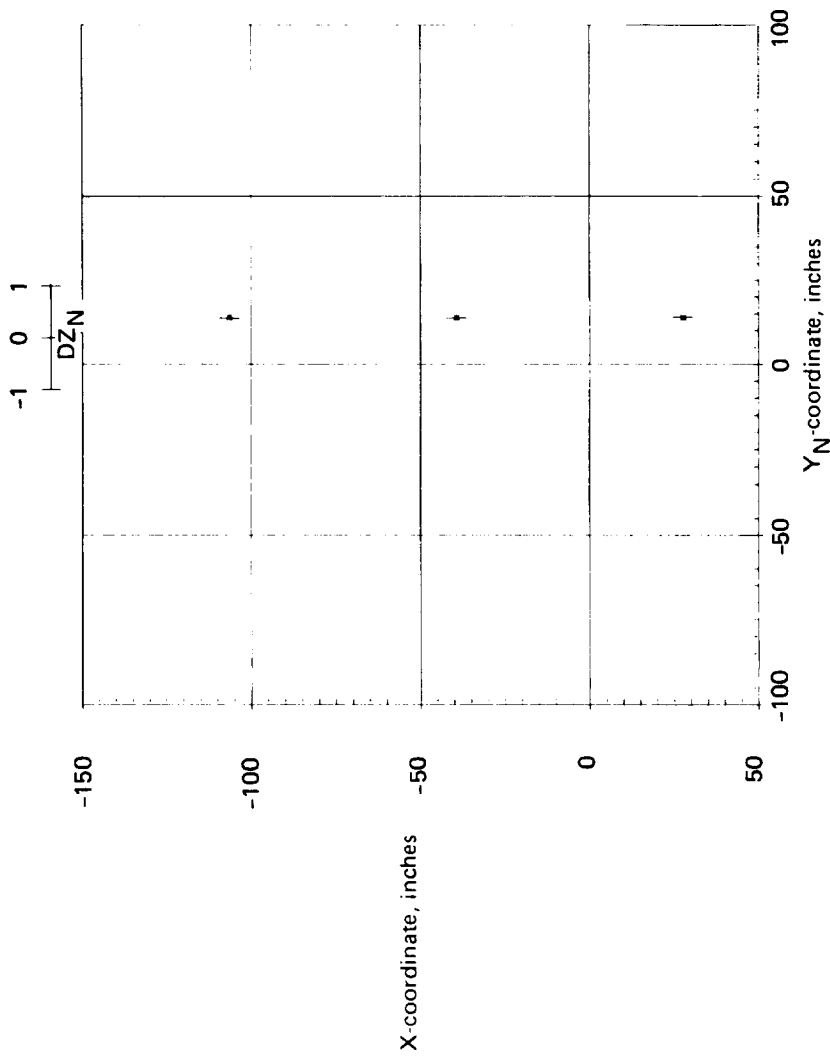
- position of aerocentroid in modal shape

Dihed - angle -83.000

Symmetric boundary conditions

FIGURE 3.4.20. -CONTINUED

Modal shape number 1



Thin Body number 7 (OUTSTRUT)

X - origin = 1073.849    Y - origin = 617.393  
 Z - origin = 38.401    Dihed - angle -83.000

\* position of aerocentroid in undeformed state  
 - position of aerocentroid in modal shape

Symmetric boundary conditions

FIGURE 3.4-20.—CONCLUDED

### 3.5 BOEING 2707-300PT (SST) DEMONSTRATION CASE

The SST was included as a demonstration case to illustrate FLEXSTAB's ability to analyze large supersonic configurations. Empirical corrections were made to the steady aerodynamics with the CAIC program. The structural definition was provided by the ESIC program.

#### 3.5.1 Geometry Definition Program—GD-4

The SST was restricted to symmetric motion, so the vertical tail and the ventral fin were excluded from the geometry definition. The data used to define the geometry were a general configuration drawing and the airfoil ordinates of the wing and horizontal stabilizer. All linear dimensions are in inches.

Fewer illustrations appear in this section since many of the modeling techniques used for the SST are similar to those used in the definition of the 707-320B. The reader may wish to refer to the SST GDPLOT results (see sec. 3.5.2) in order to help visualize the modeling descriptions given below.

*Fuselage definition.*—Before the fuselage could be defined, the location and orientation of the Reference Axis System had to be specified. The Reference Axis System was placed such that its X-axis coincided with the X-axis on the general configuration drawing of the airplane cruise shape and such that the nose of the fuselage was located at  $X = 200.0$ ,  $Y = 0.0$ , and  $Z = -14.0$

- Name of Slender Body: The fuselage Slender Body was named FUSELAGE.
- Slender Body origin: The origin of the fuselage's Local Slender Body Coordinate System was located at  $X = 0.0$ ,  $Y = 0.0$ , and  $Z = -14.0$ .
- Nose and aft end locations: The values  $x_N = 200.0$  and  $x_T = 3639.65$  were taken directly from the drawing.
- Regions influenced by Thin Bodies: In supersonic flow, the effect of a disturbance propagating from a point on the wing can only be felt by those portions of the fuselage that lie in the aft Mach cone emanating from this point. Therefore, the region of the fuselage influenced by the wing was specified to begin at the leading edge of the wing-fuselage intersection line. This region was extended to the aft end of the fuselage due to the large wing root chord and the presence of the horizontal stabilizer (see fig. 3.5-3).
- Number and placement of control points: Fifty control points were evenly distributed along the length of the fuselage by using the automatic option in the GD input.
- Area or radius distribution: The radii of the fuselage (which was nearly circular in cross section) were taken directly from the general configuration drawing. The portion of the fuselage aft of the point of maximum radius was left open; i.e., the

radius was specified to remain a constant value equal to the maximum radius all the way to the end of the Slender Body.

- **Camber line definition:** The camber line was taken to be the mean of the upper and lower fuselage skin lines. The camber measurements were made from the X-axis of the Reference Axis System. It should be noted that it does not matter where the camber line is measured from since the GD program uses the camber definition to calculate camber slopes only.

*Wing definition.*—The wing was modeled with three Thin Bodies. One, named WING1, extended from the plane of symmetry to the inboard nacelle; another, WING2, was defined from the inboard nacelle to the outboard nacelle; and the third, WING3, extended from the outboard nacelle to the wing tip.

- **Name of Thin Body and reference body:** The reference body for WING1 was the fuselage Interference Body, IB1. The reference bodies for WING2 and WING 3 were WING1 and WING 2, respectively.
- **Thin Body origin and dihedral:** The Local Thin Body Coordinate Systems for each of the three Thin Bodies were coincident. Their origins were placed at the point where a linear extrapolation of the wing leading edge intersected the plane of symmetry, that is, at  $X = 1007.0$ ,  $Y = 0.0$ , and  $Z = -37.0$ . The complex dihedral of the wing was ignored since only symmetric motion was under consideration.
- **Planform definition:** The planforms for all three Thin Bodies were measured directly from the top view of the full configuration drawing. The only modification necessary involved the inboard wing, WING1, which was extended inboard to the plane of symmetry (see fig. 3.5-1).
- **Paneling scheme:** The SST wing was defined to have 15 streamwise panel rows with 7 panels in each (see fig. 3.5-3). Eight of the rows were of approximately equal panel span and lay between the inboard edge of WING1 and the outboard edge of WING2. The seven remaining rows, each of which had approximately twice the span of the inboard rows, defined the paneling on WING3. The increased paneling density in the inboard region of the wing was designed to increase the resolution of forces in the areas where interference effects between wing, fuselage, and nacelles are largest.
- **Panel control point locations:** Each panel's control point was placed at the 85% panel chord point on a streamwise line passing through the  $Y_N$ -centroid of each panel row.

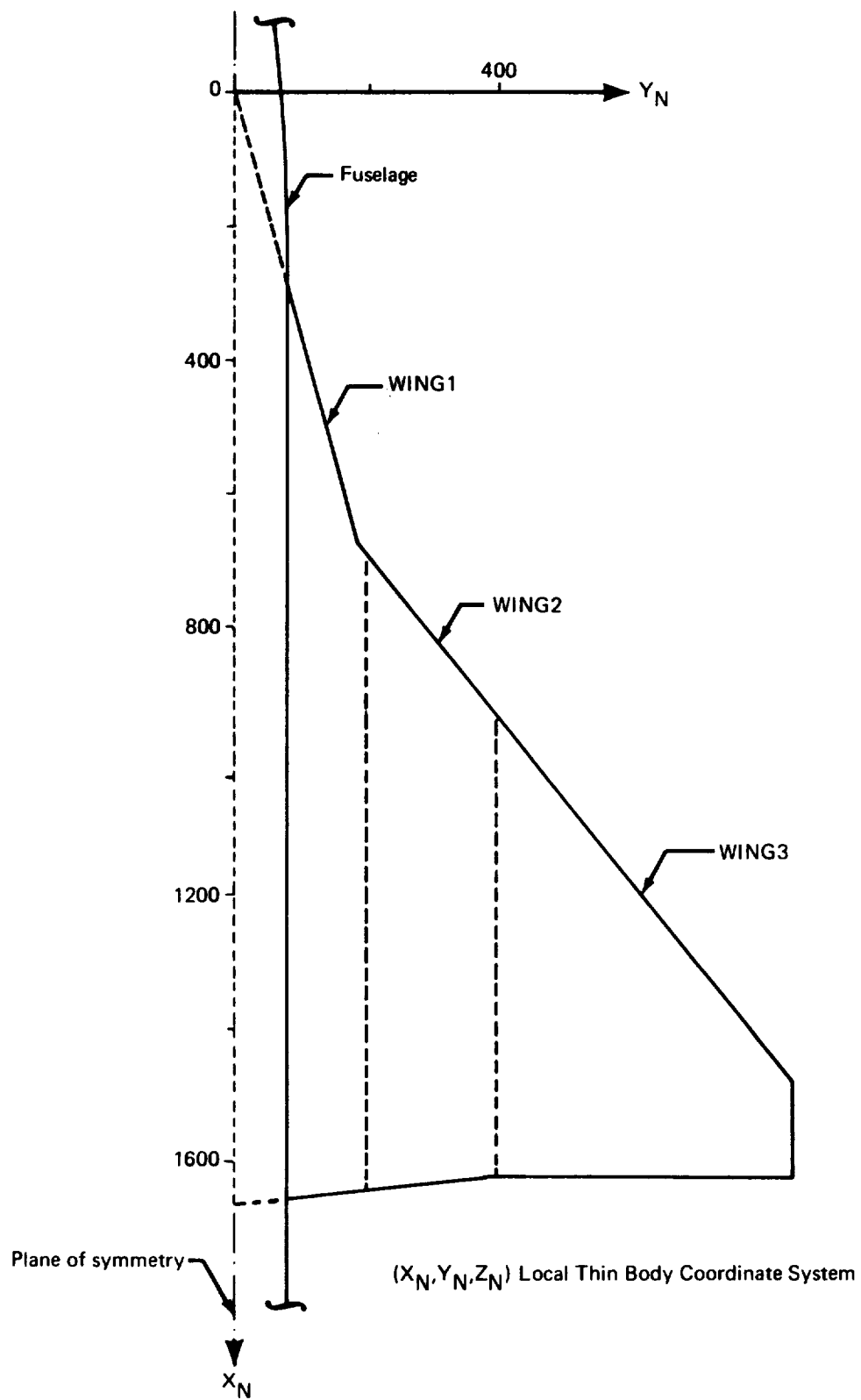


FIGURE 3.5-1.—PLANFORM DEFINITION—SST

- Airfoil definition: The airfoil varies from a biconvex section ( $\approx 3\frac{1}{2}\%$  thick) outboard of the leading-edge break to a modified NACA 65 section at the side of the body. Wing camber and twist were contained in the airfoil definition.
- Twist definition: The incidence of the wing reference plane ( $-1.25^\circ$ ) was input here.

*Fuselage Interference Body definition.* --The fuselage Interference Body was used to model the effects of the wing and horizontal stabilizer on the fuselage.

- Name of Interference Body and reference body: The Interference Body was named IB1; its reference body was FUSELAGE.
- Interference Body origin: The Y- and Z-coordinates of the Local Interference Body Coordinate System origin coincided (as required) with the corresponding coordinates of the Local Slender Body Coordinate System origin. The X-coordinate was set equal to the X-location of the leading edge of the wing-fuselage intersection ( $X = 1268.2676$ ).
- Region where Thin Bodies affect the referenced Slender Body: The leading edge of the Interference Body was placed at the leading edge of the wing-fuselage intersection line (see below) and the trailing edge at the aft end of the fuselage (see fig. 3.5-3).
- Wing-body intersection line: Since the wing was modeled with no dihedral, the Z-location of the wing-body intersection line was the same as that of the origin of the wing's Local Thin Body Coordinate System. The Y-location was taken directly from a cross-sectional view of the wing-body intersection.
- Number and location of cross-sectional panel corner points: Six panels were placed around the defined half of the fuselage. The radius of the interference shell was kept approximately equal to the maximum radius of the fuselage (i.e., 79.4 inches). Because of the high location of the horizontal stabilizer, the Z-location of the Interference Body was shifted upward relative to the fuselage Slender Body in keeping with the modeling techniques described in section 4.2.1 of volume II (see fig. 3.5-2). The top corner point (number 1) was placed at  $Z_{IB} = 94.0$  on the plane of symmetry. Two others (numbers 4 and 7) were placed at  $Y_{IB} = 80.0$ ,  $Z_{IB} = 0.0$ , and  $Y_{IB} = 0.0$ ,  $Z_{IB} = -46.0$ , respectively. The wing-body and horizontal stabilizer intersections defined corner points 5 and 3 at  $Y_{IB} = 70.0$ ,  $Z_{IB} = -23.0$ , and  $Y_{IB} = 70.0$ ,  $Z_{IB} = 51.0$ , respectively. These, with two additional corner points (numbers 2 and 6) located at (40.0, 84.0) and (40.0, -41.0), respectively, defined six panels of approximately equal width -- a recommended procedure.
- Interference Body transverse panel edge locations: The transverse panel edges of the Interference Body were aligned with the wing panel edges at the wing-body intersection (see fig. 3.5-3). Wider panels were used between the wing and the horizontal stabilizer, while a closer spacing was again employed in the region of the horizontal stabilizer.



$(X, Y, Z)$  Reference Axis System  
 $(X_M, Y_M, Z_M)$  Slender Body Coordinate System  
 $(X_{IB}, Y_{IB}, Z_{IB})$  Interference Body Coordinate System

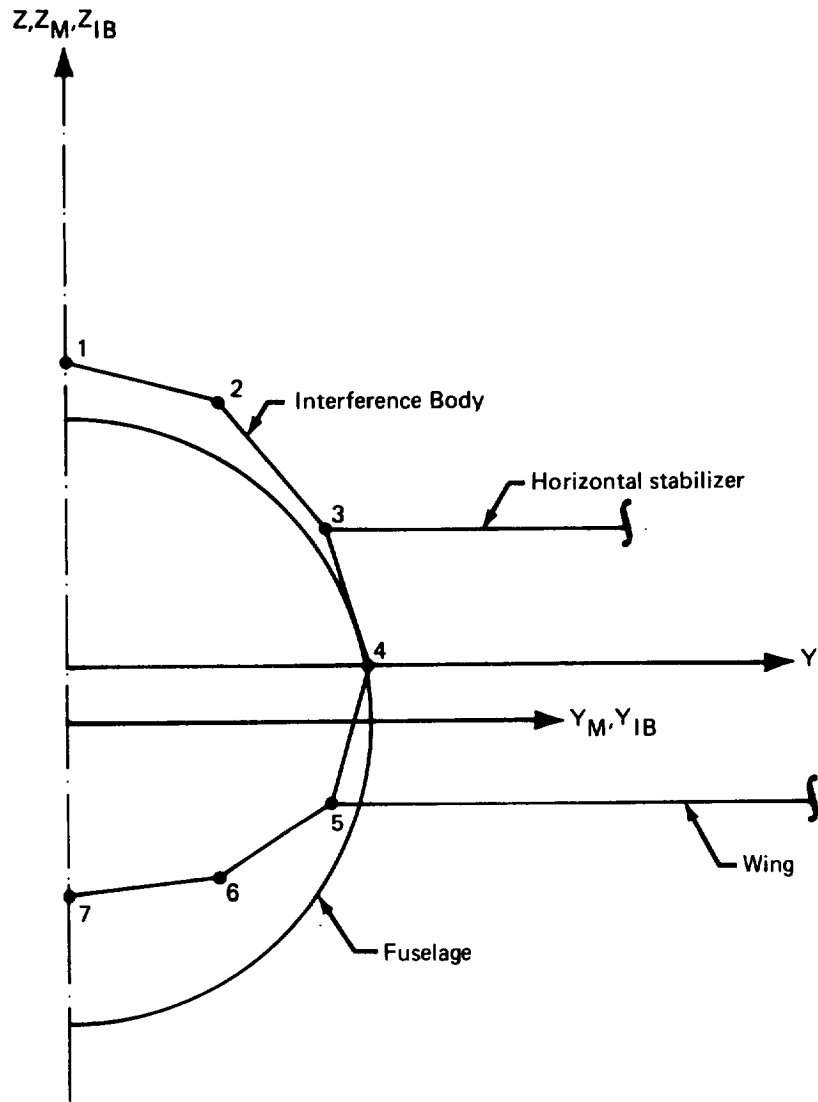


FIGURE 3.5-2.—FUSELAGE INTERFERENCE BODY CROSS SECTION—SST

- Thin Body intersection data: These data were taken directly from the inboard wing and horizontal stabilizer input data.
- Interference Body panel control point locations: The panel control points were placed at 85% of the panel chord.

*Horizontal stabilizer definition.* The data required to define the horizontal stabilizer consisted of the general configuration drawing and the wing and fuselage Interference Body input data.

- Name of Thin Body and reference body: The horizontal stabilizer was given the name HOR; its reference body was IB1.
- Thin Body origin and dihedral: The horizontal stabilizer had no dihedral. The X-location of the Local Thin Body Coordinate System origin was found by linearly extrapolating the leading edge of the actual horizontal stabilizer to the plane of symmetry. The Y-location was found by moving the planform outward until the correct horizontal stabilizer surface area was exposed beyond the fuselage Interference Body. The Z-location was determined by preserving the distance from the top of the fuselage to the horizontal stabilizer.
- Planform definition: The planform was modified by making the root chord streamwise and moving it outboard, as described above.
- Paneling scheme: The planform was divided into five streamwise rows of panels whose edges lined up with the wing panel edges. Each row contained six chordwise divisions (see Fig. 3-5-3). The paneling for this thin body did not follow the recommended paneling rules (cf. Vol. II, page 4-6). The rule states that if wedge-type airfoils are used, care should be taken that panel camber and thickness slopes do not change discontinuously over the chord of a panel. It is recommended that the paneling scheme be such that airfoil discontinuities coincide with panel edges. On the SST horizontal tail the second and third row of spanwise panels span the discontinuous slope at 40.06% and 62.03% chord. The centroid location for the panels of the second and third rows nearly coincides with the slope discontinuity. The algorithm which calculates the slope at the panel centroid computes different values for various streamwise rows of panels. Also, different values of the panel slopes could result at different computer installations due to differing computer accuracy if the paneling scheme, as used in this demonstration case, is followed, rather than the recommended approach.
- Panel control point locations: The panel control points were located at the 85% panel chord points along lines passing through the  $Y_N$ -centroids of the panel rows.
- Airfoil definition: The airfoil section was a 3% thick modified double wedge (see Figure 3.5-3). The airfoil was defined using coordinate  $Y_N = 240$ , which is outboard of the tip ( $Y_N = 200$ ). The procedure caused a warning message

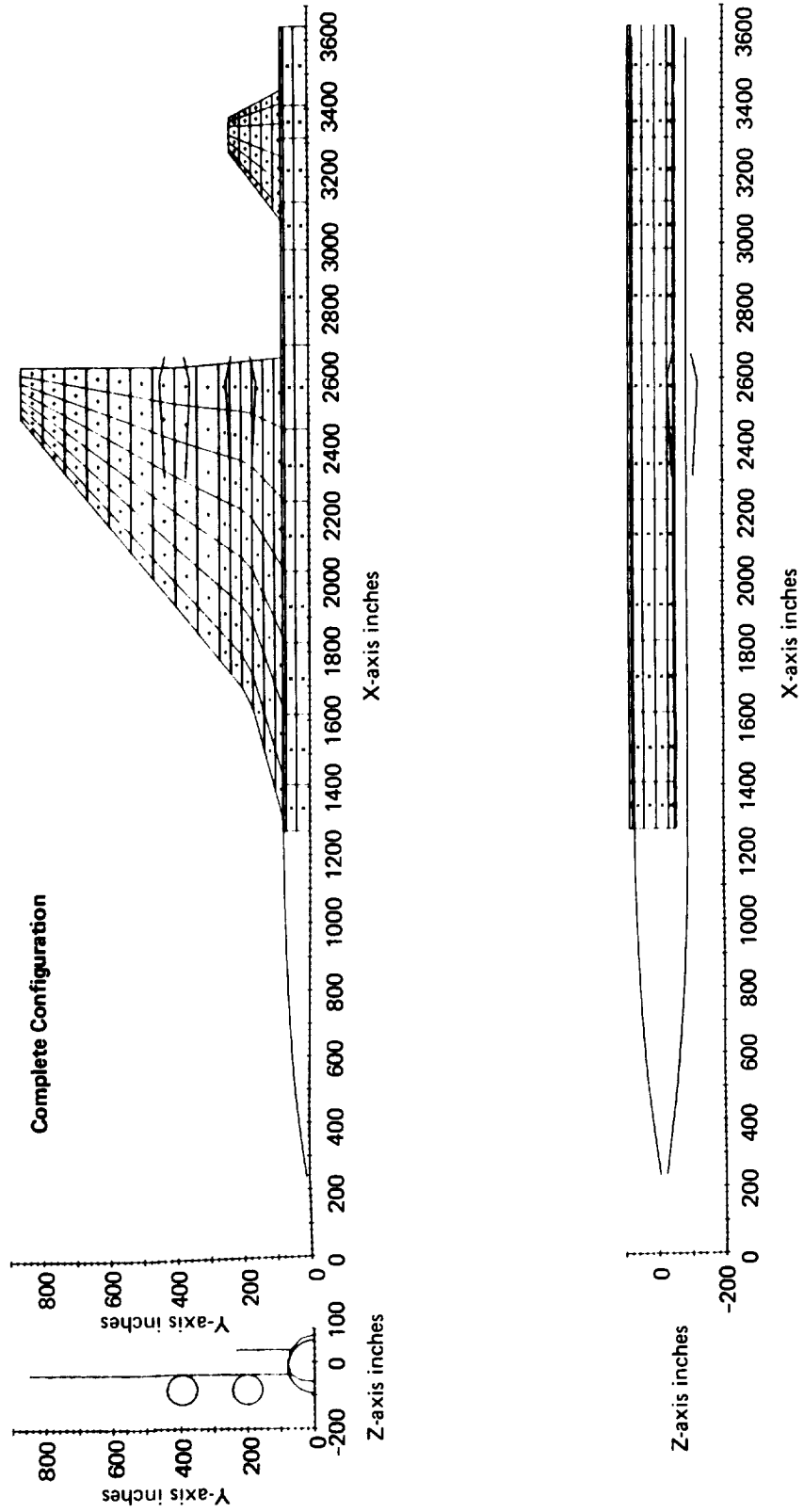


FIGURE 3.5-3.—GEOMETRY DEFINITION PLOT—SST

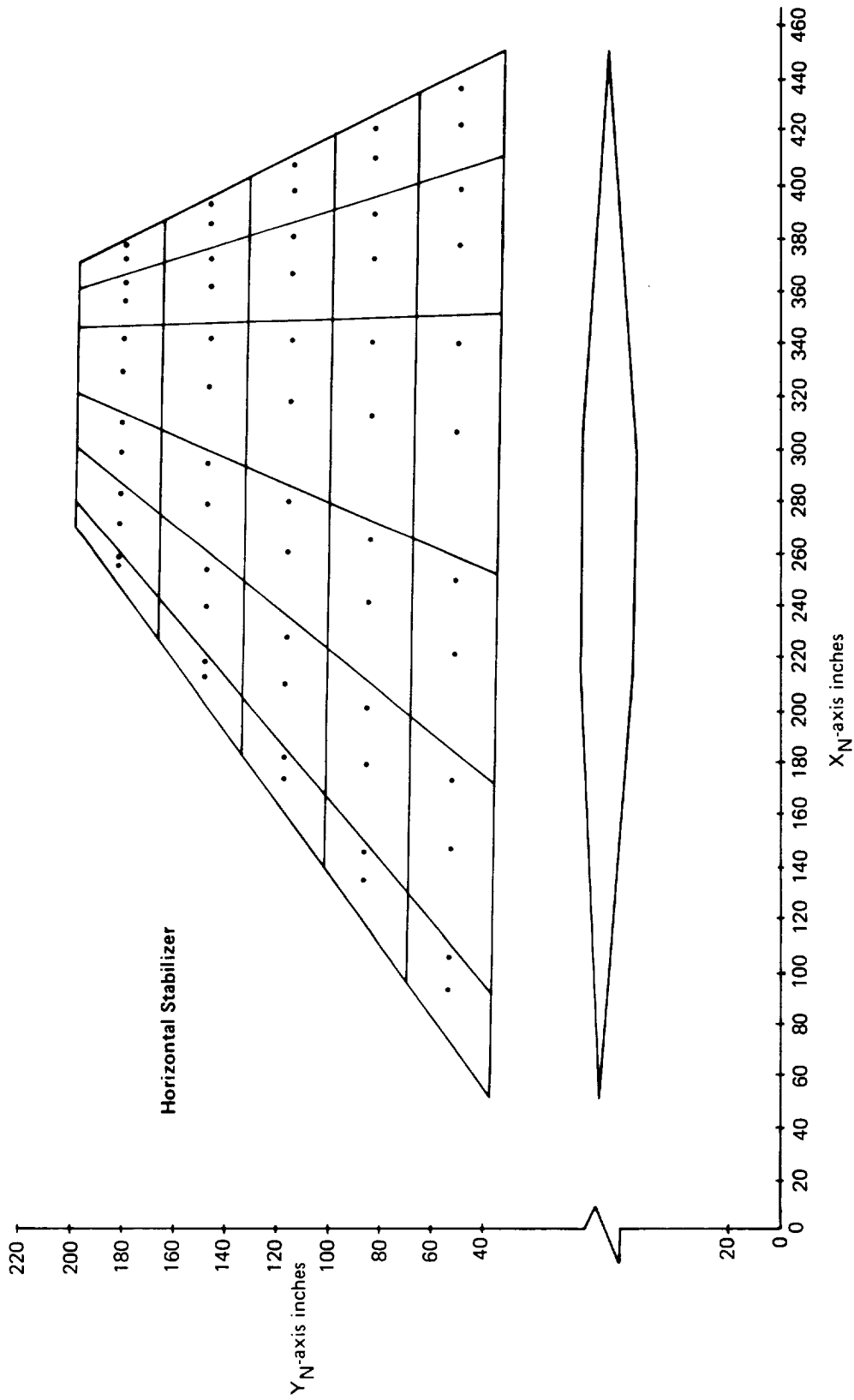


FIGURE 3.5-3.—CONCLUDED

to be printed by the GD program, however, the airfoil definition was computed correctly. This is because the horizontal tail has a constant section and linear interpolation was specified on card 37 of the GD input.

- Twist definition: The horizontal stabilizer had no twist or incidence.

*Nacelle definition.* -- The nacelles on the SST were tailored to the wing's lower surface without struts. Because of their proximity to the wing, the nacelles were modeled without Interference Bodies (see note 12, sec. 4.2.1, vol II). The discussion below applies for each nacelle.

- Name of Slender Body: The inboard and outboard nacelles were given the names INNAC and OUTNAC, respectively.
- Slender Body origin: The Y- and Z-coordinates of the Local Slender Body Coordinate System origin were chosen to coincide with the centerline of the actual nacelle given on the general configuration drawing. The X-coordinate was found by subtracting  $\beta R_i$  from the X-location of the nacelle inlet where  $R_i$  is the nacelle radius at the inlet and  $\beta = \sqrt{M_1^2 - 1}$  is the cotangent of the Mach angle.
- Nose and aft end locations: These nacelles were modeled using the "open-ended Slender Body" technique described in section 4.2.1 of volume II. In accordance with this method, the Slender Body nose location (which defines where the line singularities begin) was placed at the Local Slender Body Coordinate System origin. The aft end location was chosen to coincide with the aft end location of the actual nacelle.
- Regions influenced by Thin Bodies: This information was not required since there were no Interference Bodies associated with the nacelle models.
- Number and placement of control points: 15 control points were evenly distributed along the Slender Body axis between the inlet and tail of the nacelle in keeping with the nacelle modeling techniques given in volume II (see sec. 4.2.1).
- Area or radius distribution: The radius was set equal to the actual nacelle outer surface radius.
- Camber line definition: Although the nacelles had no camber as such, the incidences of their centerlines with respect to the fuselage centerline were input as camber. These data were taken directly from the general configuration drawing.

### 3.5.2 Geometry Definition Plot Program--GD PLOT-4

The GD PLOT program was executed to obtain a graphic display of the results from the GD-4 run. Along with a plot of the complete configuration, an individual plot of the horizontal stabilizer was obtained. The results from this run are given in figure 3.5-3.

### 3.5.3 Aerodynamic Influence Coefficient Program—AIC-4

An output tape from the GD-4 run and an input data deck were required by the AIC program.

*AIC input.*—The following general information was specified in the AIC input data deck.

- Type of reference motion: Only symmetric reference motion was requested since only symmetric structural data were available.
- Mach number: The Mach number was chosen to be 2.7.
- Perturbation delta Mach number: The perturbation delta Mach number was set to 0.25 (as calculated by the equation in volume II). (This parameter must be input if stick speed stability and compressibility correction calculations are to be made in SD&SS.)
- Steady/unsteady option: Unsteady aerodynamics was requested so that unsteady calculations could be made in SD&SS.

### 3.5.4 AIC Matrix Correction Program—CAIC-4

The CAIC program was used to modify the  $[LSC^S]$  matrix produced by AIC-4. The required input consisted of the following information.

- Type of reference motion: The SST was restricted to symmetric reference motion.
- Method of altering the  $[LSC]$  matrix: It was specified that the  $[LSC^S]$  matrix would be corrected by postmultiplication by a diagonal matrix,  $[C_2]$ .
- Values used to alter the  $[LSC]$  matrix: Postmultiplying the original  $[LSC^S]$  matrix by  $[C_2]$  produces a new  $[LSC^S]$  matrix whose columns are different from those of the original matrix by factors equal to the diagonal elements of  $[C_2]$ . The elements of this diagonal matrix were found in the following manner. Wind tunnel pressure data (ref. 3-1) for several angles of attack were integrated over each panel on the wing so that a lift force versus angle-of-attack plot ( $\Delta C_p$  versus  $\alpha$ ) could be made for each panel. The slopes of these curves near  $\Delta C_p = 0.0$  were used to form a column matrix which was set equal to the  $[LSC^S]$  matrix postmultiplied by a column matrix  $\{C_2\}$ :

$$\left\{ \frac{d\Delta C_p}{d\alpha} \right\} = [LSC^S] \{C_2\}$$

This equation was solved to obtain the elements of  $\{C_2\}$ . The diagonal corrector matrix was then formed by placing the elements of  $\{C_2\}$  along the diagonal of  $[C_2]$ .

### 3.5.5 External Structural Influence Coefficient Program—ESIC-4

The low aspect ratio of the SST wing could not be accurately represented by the structural beam theory used in the ISIC program. Therefore, a finite-element structural analysis program, SAMECS (see ref. 3-2), was used to generate most of the structural information. The clamped flexibility matrix,  $[C^S]$ , the free vibration mode shape matrix,  $[\phi \delta_1^S]$ , and the generalized stiffness and mass matrices,  $[k_1^S]$  and  $[m_1^S]$ , were created by the SAMECS program. Before describing the input deck requirements, a discussion of the procedures used to create the flexibility matrix used on NASTAP, the ESIC input tape, will be given.

The basic SST flexibility matrix was originally generated by SAMECS for use in the SST stability and control and static loads project groups. The structural grid used by the SAMECS program is shown in figure 3.5-4. Also shown are the nodes which were to be used by FLEXSTAB (numbered 11-85 on the wing and 93-134 on the horizontal stabilizer). This particular set of nodes was chosen for the SST stability and control analysis. Note that some of these nodes did not correspond to the SAMECS structural nodes (intersections of spar and rib beam elements). For these nodes the elements of the flexibility matrix were based on the characteristics of neighboring SAMECS nodes.

This flexibility matrix was reduced so that only the Z degree of freedom existed for the wing and horizontal stabilizer. All three degrees of freedom were retained for the nacelles while the X and Z degrees were kept for the fuselage.<sup>a</sup> The resulting matrix was multiplied by the scale factor 1.12 in order to simulate the increased flexibility of a hot structure.

After the flexibility matrix was put into the form required by NASTAP, the input data deck was prepared. Table 3.5-1 shows the arrangement of the input flexibility matrix. It was later determined that the flexibility matrix was incorrect; this is elaborated in section 6.2.

*General information.*—This information was taken from the data described above.

- Catalog of input matrices: It was specified that the externally generated matrices,  $[C^S]$ ,  $[\phi \delta_1^S]$ ,  $[k_1^S]$ , and  $[m_1^S]$  occupied files 1, 2, 3, and 4, respectively, of the input tape, NASTAP.
- Reference point location: The origin of the ESIC Reference Coordinate System was placed at the origin of the Reference Axis System.
- Moment data option: It was requested that the moments of inertia, total mass, and center-of-gravity location be calculated from the lumped mass card input.

---

<sup>a</sup>The rows and columns of the flexibility matrix that corresponded to the X degree of freedom for the fuselage contained zeros. Note that the same results would have been obtained if these rows and columns were removed altogether from the input flexibility matrix.

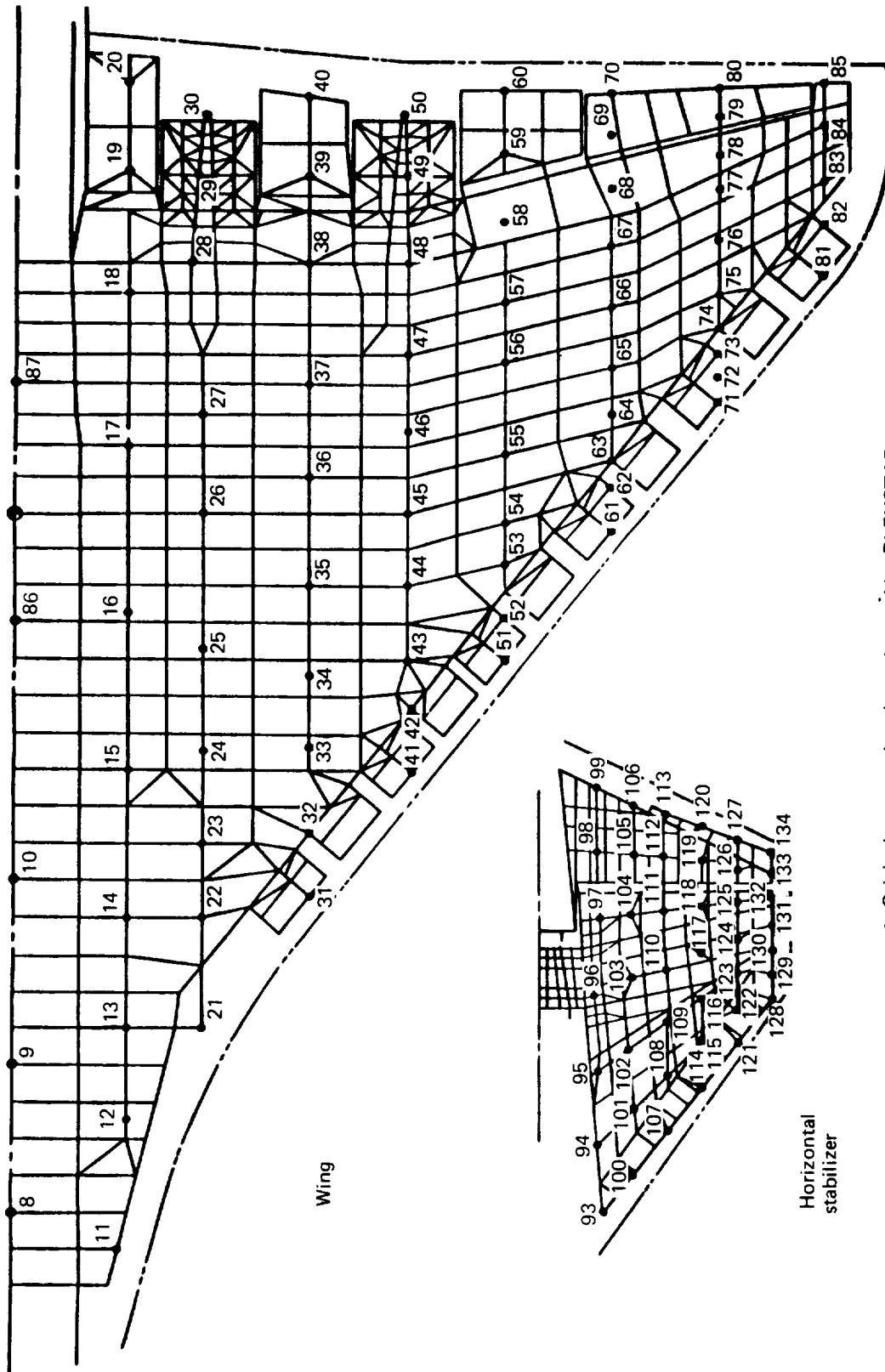


FIGURE 3.5-4. —SAMECS STRUCTURAL GRIDS FOR S8T WING AND HORIZONTAL STABILIZER SHOWING ORIGINAL NODES TO BE USED BY FLEXSTAB



- Structural geometry data input option: The Data Control Card STAPE and the following card were omitted from the input deck since the structural geometry was to be input on cards.
- Degrees of freedom option: Use of this option informed the ESIC program that the fuselage would have X and Z degrees of freedom, the nacelles X, Y, and Z, and all Thin Bodies would have the Z degree of freedom.
- Submatrix position: The flexibility matrix input via NASTAP was set up with the wing submatrix preceding the horizontal stabilizer submatrix. Since this was not the order in which the bodies were input in the GD program, use of the \$POSITION card set was required. This card set was used for each body whose submatrix was positioned differently from the body order used in the GD program. The order of the bodies input to GD was: FUSELAGE, INNAC, OUTNAC, HOR, WING1, WING2, WING3; the flexibility matrix ordering was: FUSELAGE, INNAC, OUTNAC, WING1, WING2, WING3, HOR. Therefore, this card set was required for HOR, WING1, WING2, and WING3.

**TABLE 3.5-1.—ARRANGEMENT OF INPUT FLEXIBILITY MATRIX FOR SST**

Body name (A)	No. of nodes (B)	Degrees of freedom/node (C)	Degrees of freedom/body (D)	Rowwise and columnwise position in flexibility matrix (E)
Fuselage	17	$dX_E, dZ_E$	34	1-34
Inner nacelle	2	$dX_E, dY_E, dZ_E$	6	35-40
Outer nacelle	2	$dX_E, dY_E, dZ_E$	6	41-46
Horizontal	42	$dz_E$	42	132-173
Wing 1	24	$dz_E$	24	47-70
Wing 2	24	$dz_E$	24	71-94
Wing 3	37	$dz_E$	37	95-131

- Note: 1. The body geometry definitions are input in the order of the GD program as listed under (A).
2. The degrees of freedom in the flexibility matrix are arranged according to the positions defined under (E).
3. The ALOADS program calculated displacements will be according to (E) since the identical flexibility matrix is input into the ALOADS program.

*Fuselage definition.*—Fuselage data were taken from the SAMECS structural geometry and mass data and the GD program output.

- Number and location of structural nodes: The SAMECS structural geometry defined 17 structural nodes and their locations.
- Lumped mass distribution and scale factors: The lumped masses assigned to each structural node were specified in the SAMECS data. Some of the mass values were later altered in order to refine the total mass value, center-of-gravity location, and moments of inertia. Scale factors were used to convert pounds to slugs.

*Wing definition.*—The structural geometry of the wing was defined in terms of three Thin Bodies in order to maintain consistency with the geometric definition. This was accomplished by treating the wing first as one body, and then dividing it into three bodies as discussed below.

- Thin Body structural origin and dihedral: The origin of the Thin Body Structural Coordinate System of each of the three Thin Bodies representing the wing was arbitrarily placed at (0.0, 0.0, -37.0). The dihedrals of all three Thin Bodies were set to zero.
- Number of structural nodes and panels: This information was determined by superimposing a drawing of the GD program output on the structural node data shown in figure 3.5-4. The nodes lying within the boundaries of each Thin Body were assigned to that body. The number of structural panels for each body was determined by connecting the structural nodes to form quadrilateral and triangular panels. It was observed during the paneling procedure that the nodes belonging to the flaperons and nacelle support structures could not be satisfactorily paneled. For example, if nodes 39, 40, 49, and 50 were connected to form a panel, a very poor structural representation would result (nodes 39 and 40 belong to the inboard flaperon, a relatively flexible part of the structure, whereas nodes 49 and 50 are a part of the very stiff nacelle support structure). A proper way to alleviate this problem would have been to use more of the SAMECS nodes in these regions. Since these data were no longer available, however, an alternative approach was taken. Each of the nodes in question (nodes 19, 20, 29, 30, 39, 40, 49, 50, 59, and 60 in fig. 3.5-4) was removed and replaced with two nodes which spanned the structural component (see fig. 3.5-5). This was reflected in the flexibility matrix by adding rows and columns (in the appropriate places) whose elements were identical to those corresponding to the original nodes. This amounted to assuming that the regions of the structural components in question had uniform flexibility properties. With the additional nodes, a more representative structural paneling scheme was possible (see fig. 3.5-6<sup>a</sup>). Note that both Thin Body and Slender Body structural nodes were used for the inboard panels. Panels which covered any portion of a Thin Body were assigned to that Thin Body.

---

<sup>a</sup>The node numbers in figures 3.5-4 and 3.5-5 are not the node numbers used in the ESIC-4 input data deck. Figure 3.5-6 uses the ESIC-4 input deck numbering system.

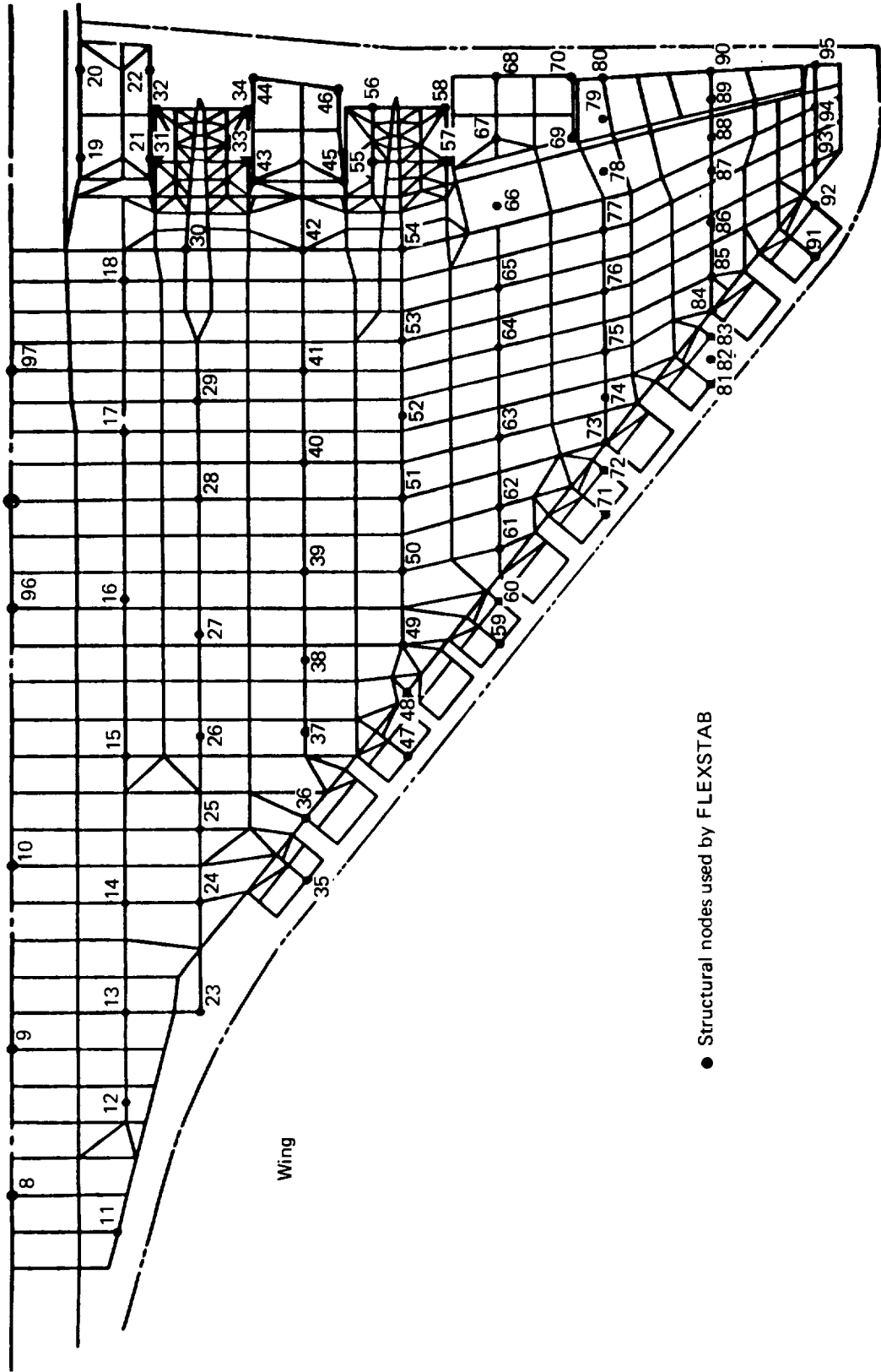


FIGURE 3.5-5.—SAMECS STRUCTURAL GRID FOR SST WING SHOWING NODES USED BY FLEXSTAB

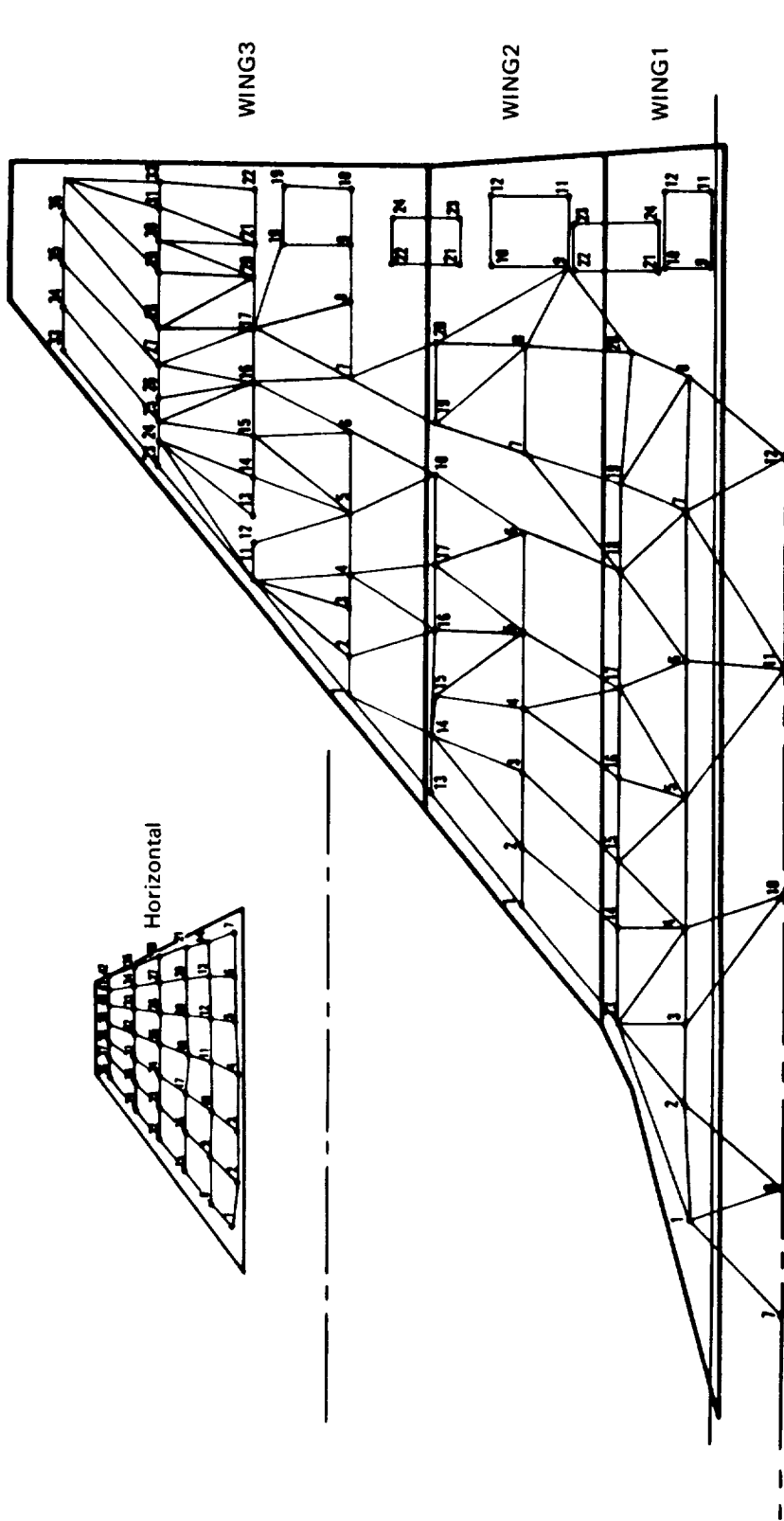


FIGURE 3.5-6.—ESIC STRUCTURAL PANELING FOR SST WING AND HORIZONTAL STABILIZER

- Structural node locations: These locations were found in the SAMECS data.
- Lumped mass distribution and scale factors: The SAMECS data provided lumped mass information for each structural node. For those pairs of nodes which replaced original single nodes (for structural paneling purposes), pairs of lumped masses were defined that preserved the total mass, center-of-gravity locations, and moments of inertia of the original lumped mass data. These values were later altered when the total airplane mass, center of gravity, and moments of inertia were refined. Each of the lumped mass values were multiplied by a scale factor of 0.031081 to convert pounds into slugs.
- Structural panel definitions: The structural panels were defined by listing the node number and body number (from the GD program) of each panel corner point of each structural panel. These were taken from the drawing referred to above (fig. 3.5-6).

*Horizontal stabilizer definition.* – There were no modifications involved in defining the horizontal stabilizer.

- Name of Slender Body: The fuselage Slender Body was named FUSELAGE.
- Thin Body structural origin and dihedral: The origin of the Thin Body Structural Coordinate System was chosen to coincide with the origin of the Thin Body Aerodynamic Coordinate System used in the GD program. The horizontal stabilizer had no dihedral.
- Number of structural nodes and panels: No modifications were made to the original 42 nodes (see fig. 3.5-4). The structural paneling consisted of 30 quadrilateral panels formed by connecting the horizontal stabilizer structural nodes.
- Structural node locations: This information was provided by the SAMECS data.
- Lumped mass distribution and scale factors: The SAMECS output provided lumped mass values for each structural node. These values were later changed in order to refine the total airplane mass, center of gravity, and moments of inertia. The lumped mass values were input in pounds and therefore had to be converted into slugs by use of a scale factor of 0.031081.
- Structural panel definitions: The structural panels (see fig. 3.5-6) were defined by listing the node number of each panel corner point of each structural panel. Body numbers were not needed since only those nodes assigned to the horizontal stabilizer were used.

*Nacelle definitions.*—The SAMECS nacelle data defined one structural node for each nacelle. This node was replaced by two nodes in a manner similar to the node additions made to the wing.

- Number and location of structural nodes: The two nodes were placed arbitrarily between the nose and aft end of the nacelles.
- Lumped mass distribution and scale factors: Lumped masses were specified for each of the two structural nodes which preserved the total mass, center of gravity, and moments of inertia of the original SAMECS data. A scale factor was used to convert the input into slugs.

*Airplane mass data.*—The ESIC program was executed once using the RIGID structural option in order to compare the program-calculated values of total mass, center-of-gravity location, and moments of inertia with the actual values at the given flight condition. Some of the lumped mass values had to be changed in order to obtain better agreement with the actual values.

### 3.6 LOCKHEED YF-12A DEMONSTRATION CASE

The YF-12A was analyzed at two flight Mach numbers—one subsonic and the other supersonic. Two distinct geometric, aerodynamic and structural definitions were created using the GD, AIC, and ESIC programs.

This section describes the formulation of these definitions. A more detailed account may be found in reference 3-3.

#### 3.6.1 Geometry Definition Program—GD-5A and GD-5B

The YF-12A poses some particularly difficult modeling problems because it has a large integrated nacelle at midspan, a large chine blended into the forebody, and another chine blended into the nacelle and outboard portion of the wing (see fig. 3.6-1).

The component bodies used to model the YF-12A are discussed below in the order in which they were input. The subsonic definition, GD-5A, is described first.

##### —Subsonic Model—

*Fuselage definition.*—A Reference Axis System was specified which had its origin located 90 inches forward of the fuselage nose. The definition of the fuselage followed.

- Name of Slender Body: The fuselage Slender Body was named FUSELAGE.
- Slender Body origin: The origin of the Local Slender Body Coordinate System was chosen to coincide with the nose of the fuselage.
- Nose and aft end locations: These data define the beginning and end of the Slender Body line singularities (see CARD 11, sec. 4.2.2, vol. II). They do not necessarily have to agree with the physical nose and tail locations of the body being modeled. For this case, the “nose location” was specified to coincide with the physical nose location of the actual fuselage since the fuselage had a “closed” nose. The aft end of the actual fuselage was also “closed”; however, it was modeled with a Slender Body which did not close (see below). This procedure was designed to more accurately model the actual flow field where a thick boundary layer exists at the rear of the fuselage. To ensure that this procedure would not cause an inaccurate downwash field, the “aft end” was moved well downstream from the physical fuselage end, i.e., on the order of 100 fuselage lengths.
- Regions influenced by Thin Bodies: This region extended from the leading edge of the forebody chine to the aft end of the actual fuselage. Normally, it is recommended that this region extend farther upstream for subsonic flow. In this case,

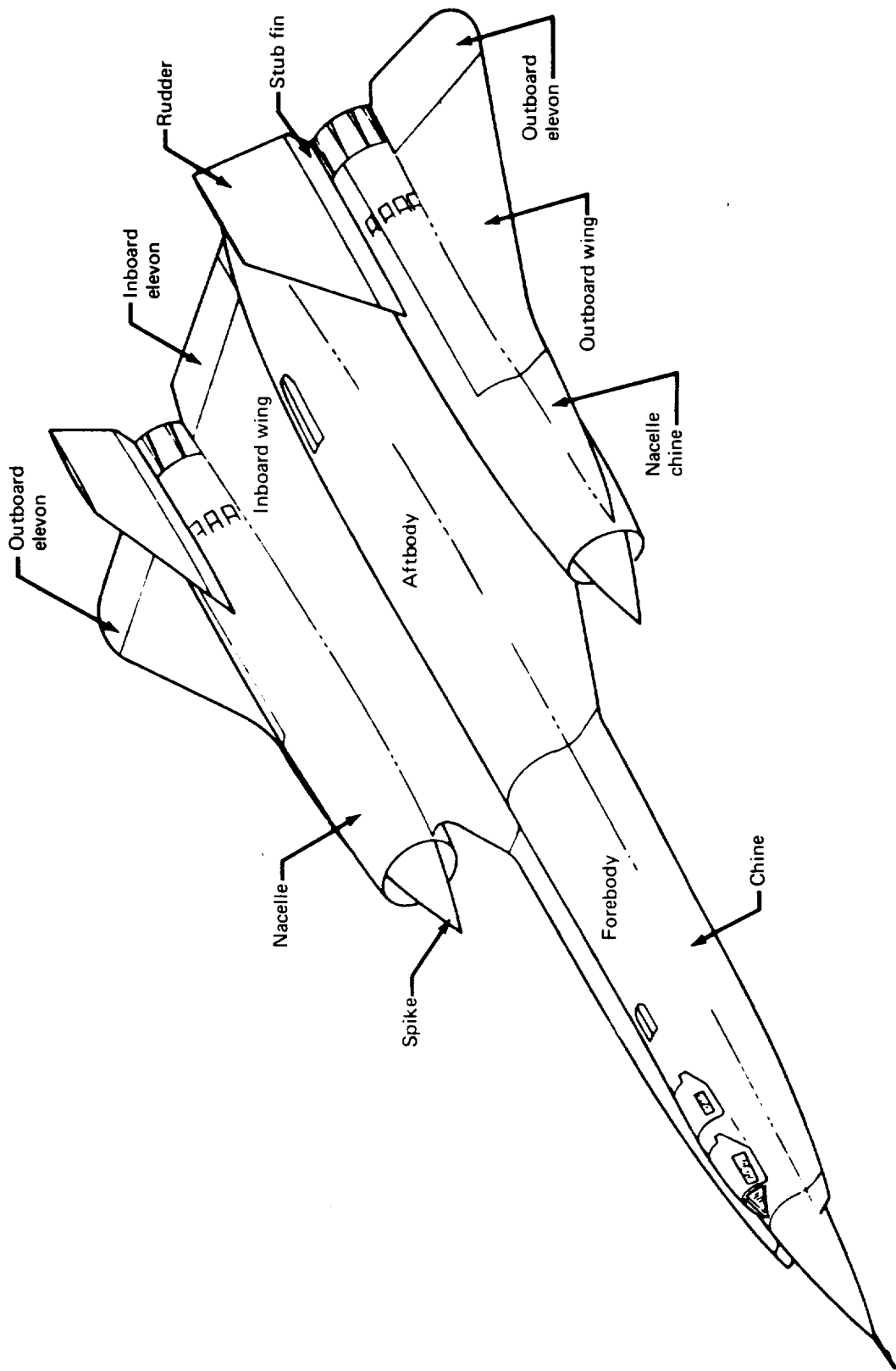


FIGURE 3.6-1.—YF-12A CONFIGURATION



however, little would be gained since the deviation of the geometry of the Slender Body from that of an extended interference shell would increase significantly in this region.

- Number and placement of control points: 50 control points were spaced approximately equally along the length of the fuselage. (Note that the control points had to be placed manually since the automatic placement option distributes the control points between the “nose” and “tail” locations input above. Control points should only be distributed between the actual body nose and tail.
- Area or radius distribution: Radii at 12 body stations were specified to define the Slender Body. From a point approximately one-fourth fuselage length aft of the nose, a constant radius of 32 inches was specified to extend to the aft end of the fuselage.
- Camber line definition: The fuselage camber line was defined by specifying coordinates at 13 body stations.

*Nacelle definition.*—The nacelle was modeled according to the technique described in section 4.2.1 of volume II. An open-ended Slender Body was used to model the isolated thickness and lifting properties of the nacelle with an Interference Body (described below) being used to absorb the interference effects due to other bodies in the configuration. The nacelle Slender Body is discussed here.

- Name of Slender Body: The nacelle was given the name NACT.
- Slender Body origin: The origin of the Local Slender Body Coordinate System was located on the nacelle centerline at the X-location of the nacelle inlet lip.
- Nose and aft end locations: The line singularities were specified to begin at the Slender Body origin. As in the fuselage definition, the “tail” location was located well downstream. The line singularities extended downstream to simulate the nacelle exhaust plume.
- Regions influenced by Thin Bodies: This region was specified to extend from the Slender Body origin to the nozzle of the nacelle. This accounted for the influence of the inboard wing which intersected the nacelle nearly along its entire length.
- Number and placement of control points: 25 control points were used. Again, the control point locations were input manually. They were distributed approximately evenly along the length of the nacelle.
- Area or radius distribution: The nacelle radius distribution was specified by inputting nacelle external radii at four stations.
- Camber line definition: The nacelle camber line was defined at ten body stations.

*Fuselage Interference Body.*—The fuselage Interference Body was defined as follows.

- Name of Interference Body and reference body: The fuselage Interference Body was named FSHELL; its reference body was FUSELAGE.
- Interference Body origin: The origin of the Local Interference Body Coordinate System coincided with that of the Reference Axis System.
- Regions where Thin Bodies affect the referenced Slender Body: These data defined the leading- and trailing-edge locations of the Interference Body and were taken directly from the fuselage Slender Body data.
- Wing-body intersection line: The fuselage Slender Body was intersected by the Thin Body which represented the forebody chine. This Thin Body had no dihedral and was defined in the X-Y plane. Therefore, the wing-body intersection line was located at  $Y_{IB} = 32.0$ ,  $Z_{IB} = 0.0$  (see fig. 3.6-2).
- Number and location of cross-sectional panel corner points: The fuselage Interference Body had five cross-sectional panel corner points on the defined half of the body. These corner points were evenly distributed on the half-shell by using the automatic option in the GD input. The Interference Body “radius” was set to 32.0 inches (see fig. 3.6-2).
- Interference Body transverse panel edge locations: These locations were input manually. The spacing was specified so that the Interference Body transverse panel edges lined up with the spanwise panel edge of the Thin Body which was to represent the forebody chine. There were 21 panels in each streamwise row.
- Thin Body intersection data: Only one Thin Body intersected this Interference Body—the forebody chine. It had no dihedral and its root location was defined to coincide with cross-sectional corner point 3 (see fig. 3.6-2).
- Interference Body panel control point locations: The recommended 85% panel chord location was specified.

*Nacelle Interference Body.*—The nacelle Interference Body was defined in the following manner.

- Name of Interference Body and reference body: NACELLE was the name given to the nacelle Interference Body; its reference body was NACT.
- Interference Body origin: The Local Interference Body Coordinate System origin was placed at the intersection of the nacelle centerline with the Y-Z plane.
- Regions where Thin Bodies affect the referenced Slender Body: This information was taken directly from the nacelle Slender Body data.
- Wing-body intersection line: This criterion did not affect the nacelle Interference Body definition.

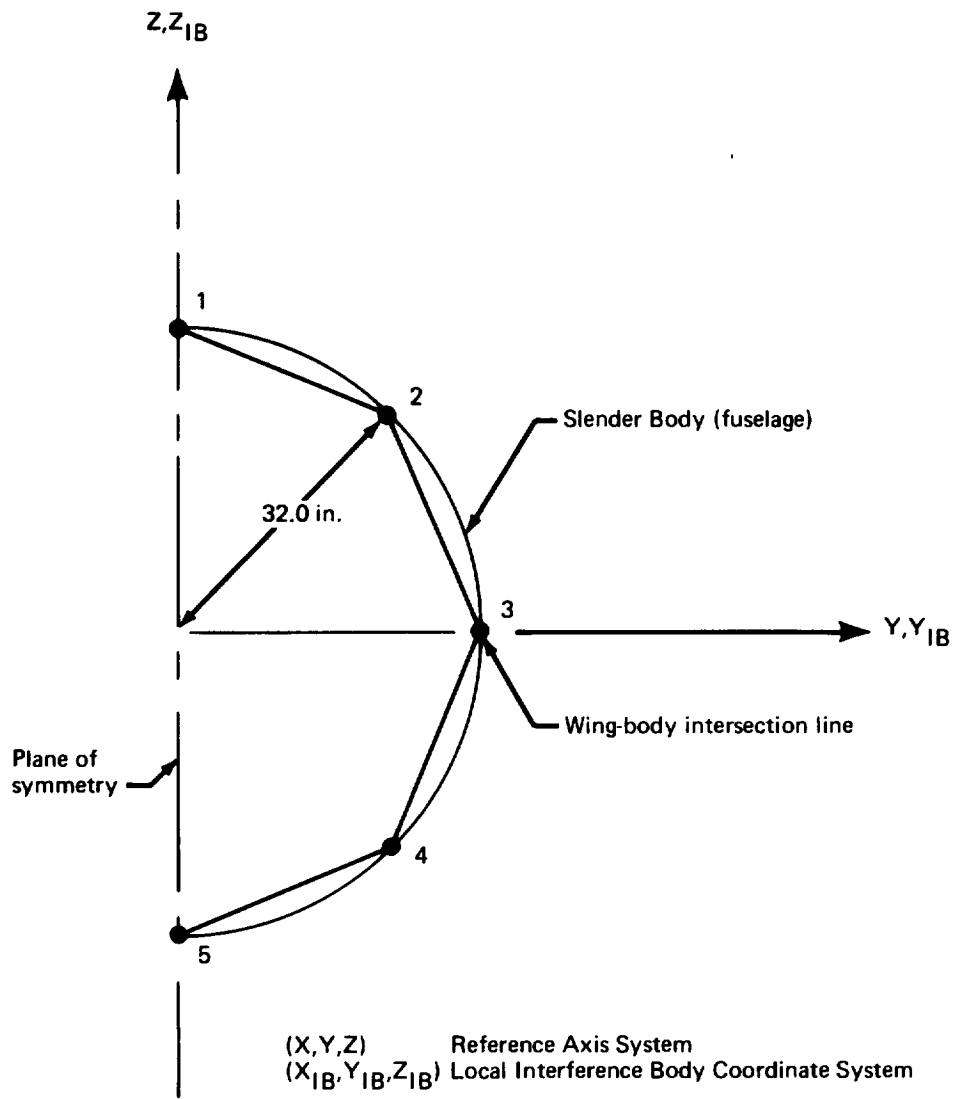


FIGURE 3.6-2.—FUSELAGE INTERFERENCE BODY DEFINITION—YF-12A

- Number and location of cross-sectional panel corner points: Thirteen corner points were spaced equally using the automatic option (radius = 36.0 inches). A relatively dense paneling scheme was used because four Thin Body intersections occurred (see below).
- Interference Body transverse panel edge locations: There were 12 panels in each streamwise row, spaced to match Thin Body panels (where possible).
- Thin Body intersection data: Four Thin Bodies intersected the nacelle Interference Body (see fig. 3.6-3). The Thin Body representing the portion of the wing inboard of the nacelle was defined to lie in the X-Y plane. Its tip coincided with cross-sectional corner point 10. It had a dihedral of  $180^\circ$  with respect to the Local Interference Body Coordinate System. The root of the outer wing Thin Body was defined at corner point 4. It had zero dihedral. The vertical tail Thin Body was translated inboard slightly so that its root was positioned at corner point 1. It had a dihedral of  $105^\circ$ . The ventral fin had its root repositioned to coincide with corner point 7. Its "relative" dihedral was  $-79^\circ$ .
- Interference Body panel control point locations: The recommended location of 85% of the panel chord was specified.

*Chine definition.*—The forebody chine was represented by a Thin Body with a large chord and a very small span. The details of its definition follow.

- Name of Thin Body and reference body: The forebody chine was named CHINE; its reference body was FSHELL.
- Thin Body origin and dihedral: The Local Thin Body Coordinate System origin was chosen to coincide with that of the Reference Axis System. The chine had no dihedral.
- Planform definition: A planform was chosen that modeled as closely as possible the planform of that portion of the actual wing.
- Paneling scheme: Two streamwise rows of panels with 24 panels in each row were used to model the chine. Abrupt changes in panel size or taper between two adjacent panels were avoided (see sec. 3.6.2). The spanwise panel edges which intersected the fuselage Interference Body lined up with its transverse panel edges. This was violated near the trailing edge of the Thin Body, however, where the streamwise paneling density was increased to represent the inboard elevon control surface.
- Panel control point locations: Each panel control point was placed at the recommended location (see CARD SET 36, sec. 4.2.2, vol. II).
- Airfoil definition: Airfoil ordinates at three spanwise stations were input.
- Twist definition: No twist was specified since twist and incidence were included in the airfoil section definition.

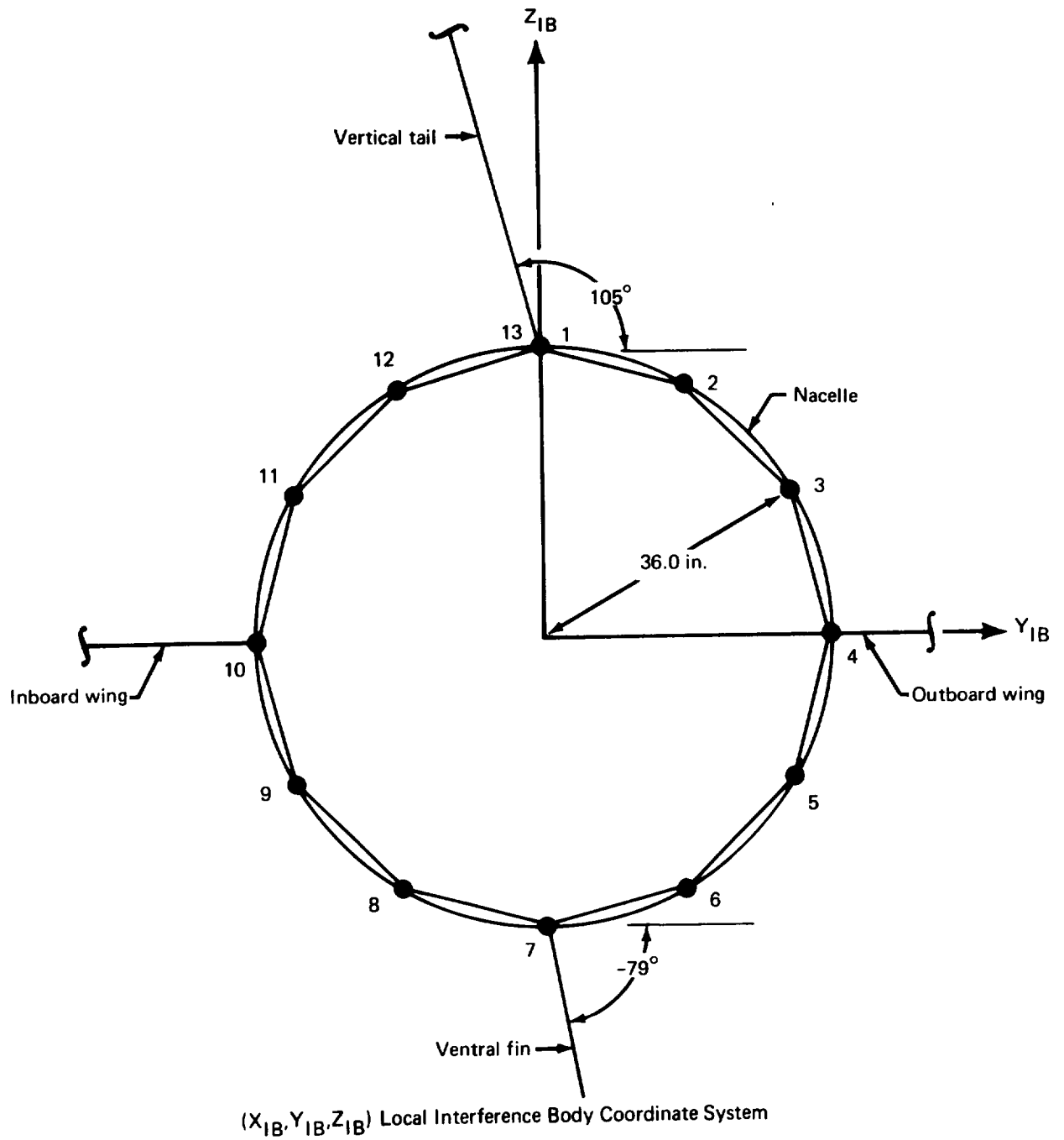


FIGURE 3.6-3.—NACELLE INTERFERENCE BODY DEFINITION—YF-12A

*Inboard wing definition.*—A Thin Body was defined to represent the portion of the wing between the chine and the inboard edge of the nacelle.

- Name of Thin Body and reference body: The inboard wing was named INBOARD and its reference body was CHINE.
- Thin Body origin and dihedral: The origin of this Thin Body's local coordinate system coincided with that of the Reference Axis System. The inboard wing was modeled with no dihedral.
- Planform definition: The actual planform shape was represented without modification.
- Paneling scheme: The inboard wing was modeled with three streamwise rows of panels with 14 panels in each row. The inboard spanwise panel edges matched the outboard spanwise panel edges of the chine Thin Body. The same alignment was made with the transverse edges of the nacelle Interference Body except in the region of the inboard elevon where streamwise paneling density was increased. (Note that the leading edge of the inboard elevon was used as a criterion for paneling the chine and inboard wing; i.e., it defined the leading edge of a spanwise row of panels.)
- Panel control point locations: The control points were placed at 85% chord.
- Airfoil definition: The inboard wing shape was input by specifying airfoil ordinates at five spanwise stations.
- Twist definition: Twist and incidence were included in the airfoil definition.

*Outboard wing definition.*—The portion of the YF-12A wing outboard of the nacelle was represented by one Thin Body.

- Name of Thin Body and reference body: The outboard wing was named OUTBOARD; its reference body was NACELLE.
- Thin Body origin and dihedral: The origin of the Local Thin Body Coordinate System was chosen to coincide with the origin of the Reference Axis System. There was no dihedral.
- Planform definition: The idealized and real planforms were identical except that the rounded wing tip was not represented.
- Paneling scheme: The wing was divided into five streamwise rows with 12 panels in each. The nacelle Interference Body transverse panel edges and the outboard elevon leading-edge line were the primary constraints on the paneling scheme.
- Panel control point locations: The recommended location (85% chord) was specified.
- Airfoil definition: Airfoil section ordinates were specified at six spanwise stations.

- Twist definition: The airfoil section ordinates contained the wing twist and incidence.

*Vertical tail definition.*—The stub fin and rudder (see fig. 3.6-1) comprised the vertical tail and were represented by one Thin Body.

- Name of Thin Body and reference body: The vertical tail was named VERTICAL and its reference body was NACELLE.
- Thin Body origin and dihedral: The origin was placed at the intersection of the extension of the root chord with the Y-Z plane. The dihedral angle was 105°.
- Planform definition: The planform of the vertical tail was represented without modification.
- Paneling scheme: Five streamwise rows with eight panels in each were specified. The span of each row of panels was kept approximately equal; the spanwise panel edges defined lines of constant % chord.
- Panel control point locations: The recommended 85% panel chord location was specified.
- Airfoil definition: The symmetric thickness distribution of the vertical tail was input at three spanwise stations.
- Twist definition: The vertical tail had no twist or incidence.

*Nacelle ventral fin definition.*—The nacelle ventral fin was represented by a Thin Body of very low aspect ratio.

- Name of Thin Body and reference body: VENTRAL was the name given to the ventral fin; its reference body was NACELLE.
- Thin Body origin and dihedral: The origin was placed at the intersection of the extended root chord line with the Y-Z plane. The dihedral angle was -79°.
- Planform definition: The planform was represented without modification.
- Paneling scheme: The nacelle ventral fin was modeled with one streamwise row of eight panels. The internal panel edges were placed at 12.5%, 25.0%, 37.5%, 50.0%, 62.5%, 75.0%, and 87.5% chord.
- Panel control point locations: The recommended location of 85% of the panel chord was specified.
- Airfoil definition: The symmetric thickness distribution was specified at two spanwise stations.
- Twist definition: The nacelle ventral fin had no twist or incidence.

### –Supersonic Model–

The geometry definition for the supersonic case, GD-5B, was different from that of the subsonic case in the Slender Body input data. The definitions of the Interference and Thin Bodies did not change. The revised portions of the Slender Body input data are described below.

*Supersonic fuselage definition.* –The only difference occurred in the line singularity placement (“nose” and “tail” locations) and in the control point placement.

- Nose and aft end locations: As in the subsonic definition, it was specified that the line singularities would begin at the nose of the fuselage. However, the Slender Body “tail” location was chosen to coincide with the actual fuselage tail location. The line singularities were ended here since, in supersonic flow, the effect of any line singularities further downstream cannot be felt by any part of the configuration.
- Number and placement of control points: 50 control points were automatically placed by the GD program.

*Supersonic nacelle definition.* –The changes made to model the nacelles for supersonic flow are described below.

- Slender Body origin: The origin was placed at the intersection of the nacelle centerline with the fore Mach cone emanating from the nacelle inlet. The X-location of this origin is arbitrary; this point was chosen for convenience in placing the line singularities (see below).
- Nose and aft end locations: The “nose” location was chosen to coincide with the origin of the Local Slender Body Coordinate System. This defined the point where the line singularities would begin. The “tail” location was placed at the  $X_M$ -location of the actual nacelle tail. There was no need to extend the line singularities further downstream because the flow was supersonic.
- Number and placement of control points: Twenty-five control points were manually placed between the inlet and exhaust lips of the nacelle.

#### 3.6.2 Geometry Definition Plot Program

The GD PLOT program was used<sup>d</sup> to produce a graphic display of the aerodynamic model provided by the GD program (fig. 3.6-4). Note the overall uniformity of the panel areas and the absence of abrupt changes in panel taper or aspect ratio.

---

<sup>d</sup>Although not a part of the output results on the “FLEXSTAB Source Tape,” the YF-12A GD PLOT results were included in this volume to help illustrate the paneling schemes described in section 3.6.1.



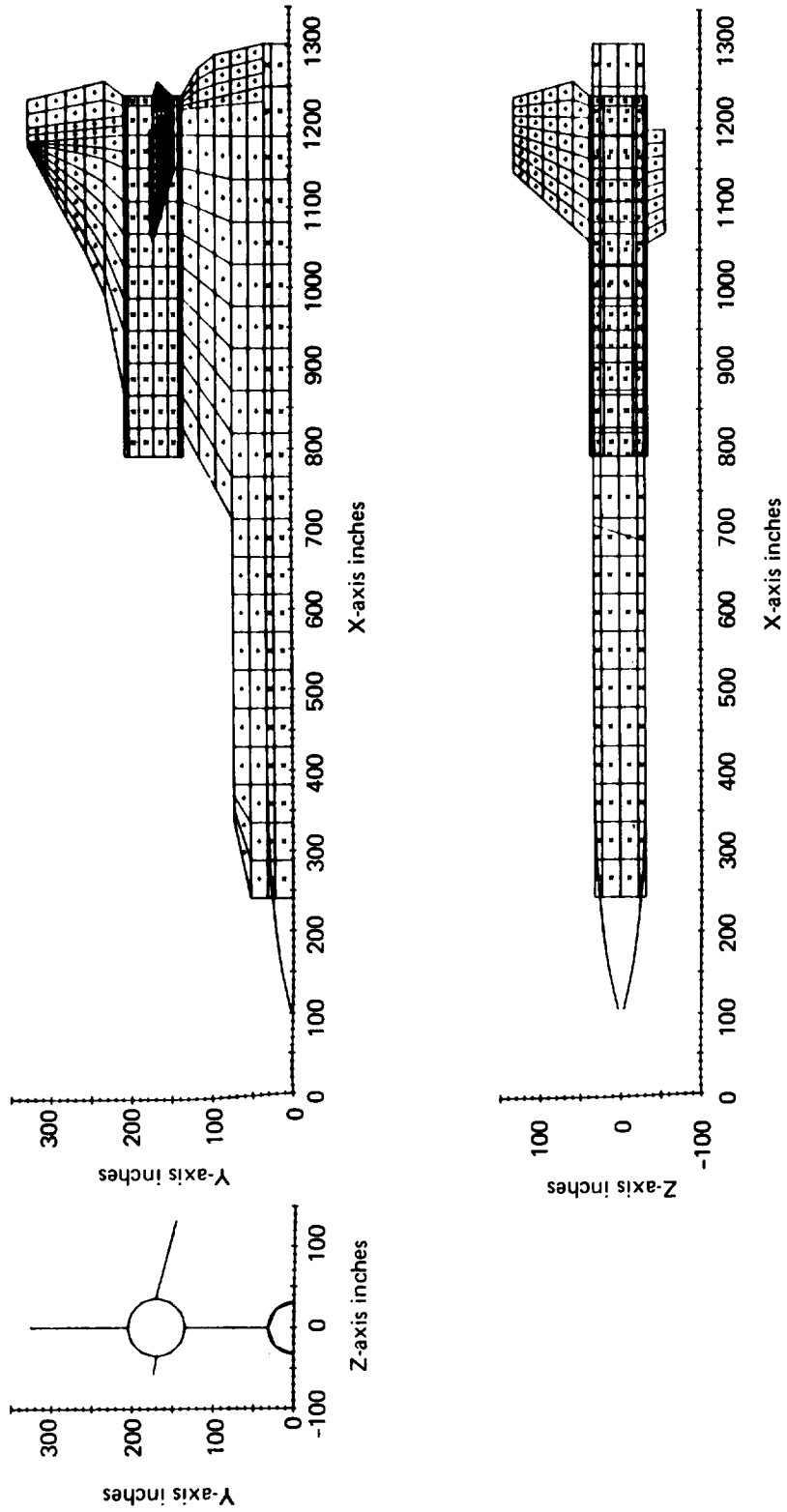


FIGURE 3.6-4.—GEOMETRY DEFINITION PLOT—YF-12A

### 3.6.3 Aerodynamic Influence Coefficient Program—AIC-5A and AIC-5B

The AIC program was executed twice to calculate aerodynamic matrices for the subsonic and supersonic definitions. The input data decks differed only in the value of the Mach number (see below).

*AIC input.* The following general information was input to the AIC program.

- Type of reference motion: The YF-12A was restricted to symmetric reference motion for both runs since only symmetric flight conditions were to be analyzed in SD&SS.
- Mach number: Mach numbers of 0.8 (AIC-5A) and 2.8 (AIC-5B) were specified.
- Perturbation delta Mach number: Speed derivative calculations were not desired; therefore, the perturbation delta Mach number was set to zero.
- Steady/unsteady option: Only steady aerodynamics was desired.

### 3.6.4 External Structural Influence Coefficient Program--ESIC-5A and ESIC-5B

The structural representation of the YF-12A was provided by the ESIC program. The required external structural data was generated by the Lockheed California Company using the NASTRAN structural analysis computer system. Since no dynamic or asymmetric flight conditions were being considered, only the flexibility matrices for symmetric loading for both ambient and hot temperature environments, mass matrices for several weight conditions, and the rigid body mode shapes were provided. The mass and flexibility of the airplane was defined by lumped properties at 346 grid points, containing 396 degrees of freedom. These matrices were selected from a much larger order (1016) NASTRAN study of the airplane (see Ref. 3-4). The fuselage nodes (located on the plane of symmetry) had X and Z degrees of freedom, the nacelle nodes had X, Y and Z degrees of freedom, and the ventral and vertical tail nodes had Z degrees of freedom. All other Thin Body nodes had only the Z degree of freedom. (X, Y, and Z refer to the Local Aerodynamic Coordinate Systems.)

The YF-12A contains a fuselage ventral fin which was not modeled aerodynamically because it is on the plane of symmetry and only symmetric motion is specified. Consequently, there were no elements in the flexibility matrix for the ventral fin. The mass of the fin was redistributed to the fuselage nodes.

Before the NASTRAN generated flexibility matrix could be used in ESIC, however, two additions had to be made. The first addition involved modifying the matrix to properly represent the loading on the nacelle. One of the grid points on the nacelle represented the main nacelle support point. Aerodynamic forces could have no effect on this node since it was located within the nacelle surface. In order to prevent the transfer of aerodynamic forces (at nearby aerocentroids) to this node two mass-less nodes were defined very close to and on either side of this grid point. These nodes would absorb the nearby aerodynamic forces while allowing the node in between to continue representing the correct

nacelle inertia properties. The flexibility characteristics of nearby structural nodes were used to create rows and columns to represent the X, Y and Z degrees of freedom for the two newly defined nodes. Insertion of these six rows and columns in the appropriate places resulted in a  $[C^S]$  matrix, which had a total of 402 degrees of freedom. The second addition to the flexibility matrix involved adding  $Y_N$  degrees of zeros for the 46 nodes on the ventral and vertical fins on the nacelle. These nodes were assigned zero flexibility by entering 46 rows and columns of zeros in the clamped flexibility matrix. Although the fins were considered rigid in the  $Y_N$  direction for the FLEXSTAB analysis, the clamped flexibility matrix had to contain the  $Y_N$  degree of freedom for compatibility with the mass matrix. The final  $[\tilde{C}^S]$  matrix calculated by ESIC then properly represented inertial relief effects for the fin in-plane motions. The resulting final form of the clamped flexibility matrix input,  $[C^S]$ , input to ESIC had a total of 448 degrees of freedom. The arrangement of this matrix is shown in Table 3.6-1.

**TABLE 3.6-1.—ARRANGEMENT OF THE FLEXIBILITY MATRIX INPUT TO THE ESIC PROGRAM FOR YF-12A**

Body name (A)	No. of nodes	Degrees of freedom/node	Degrees of freedom/body	Rowwise and columnwise position in flexibility matrix
Fuselage	22	$dX_E, dZ_E$	44	1-44
Nacelle	16	$dX_E, dY_E, dZ_E$	48	45-92
Chine	106	$dz_E$	106	93-198
Inboard wing	62	$dz_E$	62	199-260
Outboard wing	96	$dz_E$	96	261-356
Vertical	38	$dy_E, dz_E$	76	357-432
Ventral	8	$dy_E, dz_E$	16	433-448

Mass and rigid body mode shape matrices were calculated by ESIC so that only the  $[C^S]$  matrix was input on NASTAP.

Two structural definitions were produced by ESIC. The first, ESIC-5A, represented the subsonic definition and used the "cold" flexibility matrix. The "hot"  $[C^S]$  matrix was used to produce the second definition, ESIC-5B for the supersonic case. The only differences between the two input data decks were in the mass values at certain structural nodes. This occurs because subsonic and supersonic cases represented different weight conditions. The input data deck for the subsonic case was prepared as follows:

*General information.*—The following general information was included in the ESIC input data deck.

- Catalog of input matrices: It was specified that the externally generated flexibility matrix,  $[C^S]$ , occupied file 1 of the input tape, NASTAP.
- Reference point location: The origin of the ESIC Reference Coordinate System was chosen to coincide with that of the Reference Axis System.
- Moment data option: It was requested that the moments of inertia, total mass, and center-of-gravity location be calculated from the lumped mass card input.
- Structural geometry data input option: The \$TAPE INPUT OF STRUCTURAL GEOMETRIC DATA card section was omitted indicating that the structural geometry would be input on cards.
- Degrees of freedom option: This option was used to inform the program of the degrees of freedom associated with each structural node. The X, Y, and Z degrees of freedom were specified for the fuselage and nacelle nodes. (The ESIC program recognizes that the flexibility matrix,  $[C^S]$ , will have only the X and Z degrees of freedom for the fuselage since it is on the plane of symmetry.) The  $Z_N$  degree of freedom was specified for the chine, inboard wing, and outboard wing. The vertical tail and ventral fin had  $Y_N$  and  $Z_N$  degrees of freedom.
- Submatrix position: The \$POSITION card section was not used since the body submatrices were ordered in  $[C^S]$  the same way they were ordered in the GD program.

*Fuselage definition.*—The fuselage structural geometry was defined by using the NASTRAN data and the GD program output.

- Number and location of structural nodes: 22 structural nodes were used to model the fuselage. Their locations were defined in the NASTRAN data.
- Lumped mass distribution and scale factors: The values of the lumped masses assigned to each node were specified in the NASTRAN data. A scale factor of 12.0 was used to convert the input lumped masses from snails to slugs.

*Nacelle definition.*—The NASTRAN data were modified by the addition of two structural nodes.

- Number and location of structural nodes: Originally, 14 nodes were used on the nacelle, their locations being given in the NASTRAN data. The two additional nodes were placed 0.001 inch either side of the node which represented the main nacelle support point.
- Lumped mass distribution and scale factors: The NASTRAN data defined the lumped masses at the original nodes. Zero masses were specified for the two additional nodes. Scale factors were used to convert from snails to slugs.

*Wing definition.*—The structural geometry of the wing was defined in terms of three Thin Bodies. This was accomplished by taking the complete NASTRAN wing definition and dividing into three parts as discussed below.

- Thin Body structural origin and dihedral: The origin of the ESIC Thin Body Structural Coordinate System was chosen to coincide with that of Reference Axis System for each of the three Thin Bodies. The dihedral angles were set to  $0^\circ$ .
- Number of structural nodes and panels: This information was determined by superimposing the structural grid point (node) drawing on a drawing of the wing geometry based on the GD program output. Nodes which were located within the boundaries of a Thin Body (chine, inboard wing, or outboard wing) were assigned to that Thin Body. This process resulted in 106 nodes being assigned to the chine Thin Body, 62 to the inboard wing Thin Body, and 96 to the outboard wing Thin Body. Structural panels were defined by connecting the nodes to form quadrilateral and triangular panels. There were 154 panels defined for the chine, 64 for the inboard wing, and 102 for the outboard wing.
- Structural node locations: This information was taken directly from the NASTRAN data. The  $(x_{E_n}, y_{E_n})$  coordinates of each structural node were input.
- Lumped mass distribution and scale factors: The NASTRAN data provided the lumped mass values, in snails, for each structural node. A scale factor of 12.0 converted these values into slugs.
- Structural paneling definitions: The structural panels were defined by the node number and body number (from the GD program) of each panel corner point of each structural panel.

*Vertical tail and ventral fin definitions.*—Aside from the structural paneling specifications, the NASTRAN data provided most of the information required for these definitions.

- Thin Body structural origin and dihedral: The dihedral angles of the structural coordinate systems were set equal to the values used by the corresponding Thin Body Aerodynamic Coordinate Systems; i.e.,  $105^\circ$  for the vertical tail and  $-79^\circ$  for the ventral fin. The NASTRAN data defined the structural nodes of the vertical tail

with respect to a Thin Body Structural Coordinate System whose origin was located in the plane of the actual vertical tail. The origin of this coordinate system was translated in a direction normal to the vertical tail by an amount that placed it in the plane of the vertical tail Thin Body defined in the GD program. The NASTRAN node data were then used directly with the result that the nodes were now defined in the Thin Body plane. The same modification was necessary for placing the origin of the ventral fin's Thin Body Structural Coordinate System.

- Number of structural nodes and panels: The NASTRAN data defined 38 nodes on the vertical tail and 8 nodes on the ventral fin. Twenty-four structural panels were defined for the vertical tail; three were used on the ventral fin.
- Structural node locations: This information was taken directly from the NASTRAN data.
- Lumped mass distribution and scale factors: The NASTRAN data provided the lumped mass information for each node. Scale factors were used to convert from snails to slugs.
- Structural panel definitions: Structural nodes defined the corner points of quadrilateral and triangular panels. The paneling was specified so that each aerocentroid was contained in a structural panel.

*Supersonic structural definition.*—Certain structural nodes assigned to the fuselage Slender Body and chine Thin Body were designated as portions of the fuel tanks. Slightly smaller lumped masses were input at these locations for the supersonic case. The weight was reduced by about 28,000 pounds and a rearward center-of-gravity shift of about 27 inches occurred. Otherwise, the ESIC-5B input data deck was identical to that of the subsonic case.

## 4.0 AIRPLANE ANALYSIS PROGRAMS

The programs included in FLEXSTAB for the calculation and analysis of airplane stability and structural loading characteristics are the SD&SS, TH, SLOADS, and ALOADS programs. Graphic displays of pressure distributions and time histories can be made with the PDPLOT and THPLOT programs.

This section summarizes the input data required for each of these programs and describes the input data decks used for each demonstration case. Table 4.0-1 gives a list of names used to identify each of the analysis program computer runs, along with the corresponding deck numbers which appear on the first card of each input deck.

### 4.1 SUMMARY OF INPUT REQUIREMENTS

This section describes briefly the input data requirements for the airplane analysis programs in a manner similar to that used in volume II.

#### 4.1.1 Stability Derivatives and Static Stability (SD&SS) Program

The SD&SS program accepts tape and card input data. Tape input includes the GD program output tape, GDTAPE, the AIC program output tape, AICTAP, and either the ISIC or ESIC program output tape, SICTP3. A structures program output tape is not necessary if the configuration is rigid. For static-elastic analysis, either the ISIC or ESIC output tape is required. In order to perform a residual-elastic analysis, either the ISIC and NM program output tapes must be merged or the appropriate matrices must be present on the ESIC program output tape. The data card input is described below. Each card section is identified by its Data Control Card and is discussed individually.

*\$GENERAL SPECIFICATIONS.*—This card section includes some basic option codes describing the case to be run, the flight conditions of the case, and the airplane reference parameters. Specifically, these items include the following:

- Basic option codes (CARD 8): The type of reference motion and elasticity, the optional unsteady, thickness, leading-edge thrust, stick-speed stability, and gust matrix calculations, the load factor/pitch rate input option, the input tape options, and the units, altitude, and alpha options must all be specified in this card set.
- Flight conditions (CARDS 9-11): The flight conditions are input in one of two ways. If the altitude option is turned on, the altitude and deviation from standard temperature must be specified; air density, speed of sound, flight velocity, and dynamic pressure are calculated by the program. If the altitude option is not used, altitude and deviation from standard temperature are not specified; the user must specify flight velocity and either density or dynamic pressure; the program calculates the speed of sound. In addition, the user must specify the reference roll angle and roll rate, the reference pitch rate or load factor (depending on the option mentioned above), and the reference yaw rate.

TABLE 4.0.1.—COMPUTER RUN IDENTIFICATION—AIRPLANE ANALYSIS PROGRAMS

Program	Dart Model I		Dart Model II		707-320B		SST		YF-12A	
	Run name	Deck number	Run name	Deck number	Run name	Deck number	Run name	Deck number	Run name	Deck number
SD&SS	SDSS-1A	01-05	SDSS-2	02-03	SDSS-3A	03-05	SDSS-4A	04-04	SDSS-5A	05-04
	SDSS-1B	01-06			SDSS-3B	03-09	SDSS-4B	04-05	SDSS-5B	05-09
	SDSS-1C	01-10					SDSS-4C	04-08		
	SDSS-1D	01-11								
PDPLOT				PDPLOT-3	03-13					
TH	TH-1	01-07			TH-3	03-06				
THPLOT					THPLOT-3	03-14				
SLOADS	SLOADS-1	01-08			SLOADS-3	03-07				
ALOADS	ALOADS-1	01-12					ALOADS-4	04-06	ALOADS-5A ALOADS-5B	05-05 05-10



- Reference parameters (CARD 12): The reference wing area, chord, and span of the airplane are included in these data.

*\$MATRIX PRINT LIST.*—Use of this optional card section allows the user to select matrices he wishes to have printed.

*\$SDSS MATRIX OUTPUT LIST.*—In this card section, the user can select matrices he wishes to have stored on the SD&SS output tape, SDSSTP.

*\$THRUST DATA.*—This card section must be included whenever thrust is to be used on the model. The input data describe the location and direction of the thrust vectors by indicating the bodies and control points (aerocentroids) from which the thrust originates, and the X-locations, direction cosines, and relative strength of each thrust vector.

*\$GYROSCOPIC DATA.*—This card section is optional and normally is only used if the reference motion is coupled. (It is possible to use this card section with symmetric reference motion, but only if the angular momenta of engines on either side of the plane of symmetry have the opposite sense.) If the model is to be analyzed elastically, the gyroscopic option in the ISIC or ESIC program must have been exercised. In this card section the angular momentum associated with each engine is specified in one of two ways. It can either be specified to be constant, or the partial derivatives of angular momentum with respect to the engine angular velocity may be input for each engine. In the latter case, a table of thrust-versus-engine angular velocity must be input for each engine.

*\$CONTROL SURFACE DATA.*—The control surfaces of the airplanes are defined in this card section. Each control surface is identified as an elevator, an aileron, or a rudder. The program assumes that elevators and ailerons have identical surfaces on the opposite side of the plane of symmetry. For elevators, the surfaces deflect identically, and for ailerons, they deflect oppositely. Rudders are defined on the plane of symmetry and are assumed to act alone. The surfaces are defined by inputting the name of the body on which the control surface lies and the panel numbers that comprise the surface. (Panel numbers are an output of the GD program; the panel numbering scheme is illustrated in fig. 4.2-18, vol. II.)

*\$STABILITY PROBLEM DATA.* In this card section the type of stability problem to be solved and the data necessary for its solution are specified. The different problems and their related data are summarized below.

Problem 1 (CARD 35): Trim using constant coefficients calculated by the program. The input data for problem 1 are:

- Airplane shape (CARD 36)
- Thrust or flightpath angle data (CARD 36)
- X-coordinate of leading edge of reference chord (CARD 36)

- Input/output camber shape and displacement<sup>4</sup> data (CARDS 37-41)
- Pressure and loads output options (CARD 37)
- Maximum and minimum limits for trim parameters (CARDS 43 and 44)

Problem 2 (CARD 35): Trim by iterating over the input data. The required data for problem 2 consist of:

- Airplane shape (CARD 36)
- Thrust or flightpath angle data (CARD 36)
- X-coordinate of leading edge of reference chord (CARD 36)
- Input/output camber shape and displacement data (CARDS 37-41)
- Pressure and loads output options (CARD 37)
- Initial values for trim parameters (CARD 42)
- Maximum and minimum limits for trim parameters (CARDS 43 and 44)
- Convergence tolerances for trim parameters (CARD 45)
- Maximum number of iterations (CARD 46)
- SWIND TUNNEL DATA (see below)

Problem 3 (CARD 35): User-specified trim data. For this problem the data are:

- Airplane shape (CARD 36)
- Thrust or flightpath angle data (CARD 36)
- X-coordinate of leading edge of reference chord (CARD 36)
- Input/output camber shape and displacement data (CARDS 37-41)
- Pressure and loads output options (CARD 37)
- User-specified trim parameters (CARD 42)

*SWIND TUNNEL DATA.* –If stability problem 2 is to be solved, wind tunnel data (or appropriate data from any source) must be input in this card section. Eleven different tables may be input. These include  $C_L$ ,  $C_D$  and  $C_m$  versus  $(\alpha, \delta e)$  and each of  $\Delta C_L$ ,  $\Delta C_D$ , and  $\Delta C_m$

<sup>4</sup>These are the slopes and positions of aerodynamic camber surfaces and lines at the aerocentroids.

versus  $(\alpha, \beta)$ ,  $(\alpha, \delta a)$ , and  $(\alpha, \delta r)$ . The lateral directional tables include  $C_Y$ ,  $C_{\ell}$ , and  $C_n$  versus  $(\alpha, \beta)$ ,  $(\alpha, \delta a)$ ,  $(\alpha, \delta r)$ , and  $(\alpha, \delta e)$ . The last three tables consist of the rate derivatives  $C_{LQ}$ ,  $C_{DQ}$ ,  $C_{mQ}$ ,  $C_{YR}$ ,  $C_{\ell R}$ ,  $C_{nR}$ ,  $C_{YP}$ ,  $C_{\ell P}$ , and  $C_{nP}$  versus  $\alpha$ .

*SPERTURBATION DATA.*—In this card section the user specifies the type of perturbation motion the model will undergo: symmetric, antisymmetric, or both. This instructs the program to calculate the dynamic stability derivatives (symmetric, antisymmetric, or both) used to form the coefficients in the equations of motion for the \$DYNAMIC ANALYSIS option (see below) and the TH program. Additional options can be exercised to calculate control effectivenesses, compressibility corrections for the speed and yaw rate derivatives, unsteady Thin Body pressures, and perturbation load coefficient matrices (see CARD 59, sec. 9.2.2, vol. II). If the user so desires, provisions are included to replace either the steady or unsteady (or both) dynamic stability derivatives with wind tunnel or handbook data.

*\$DYNAMIC ANALYSIS.*—This card section instructs the program to calculate the airplane's dynamic stability characteristics including the frequency, period, and damping information for each mode along with the phase and amplitude of the modal coupling terms. The characteristic motion may include any combination of symmetric and antisymmetric elastic modes (if the model is residual-elastic) as well as the symmetric and antisymmetric rigid-body modes.

*\$EXTERIOR INFLUENCE DATA.*—This card section allows the user to input reference force and moment increments and external downwash matrices from an external source.

*\$STRUCTURAL DATA.*—This card section is used to input total mass, center-of-gravity location, and moments of inertia for rigid analyses.

*\$PRESSURE DATA.*—This card section allows the user to specify an externally generated lifting pressure distribution which is added to the one calculated within the program.

*\$AREA RATIO DATA.*—These cards allow the user to apply a scaling factor to any Thin Body or Interference Body panel. Often a modeling restriction will cause the paneling to differ from the true configuration area (e.g., in the region of curved wing tips). These discrepancies can be alleviated by using this card section.

This completes the input data requirements and options for one SD&SS case. Generally speaking, if another case is to be executed, a new input data deck must be prepared. However, there exists in the SD&SS program a recycle option which enables the user to execute additional cases (for changes in certain parameters and/or options) without having to form the entire SD&SS data deck for each case. This option is exercised by including the card set headed by the following Data Control Card.

*\$RECYCLE DATA.*—In this card section, the user specifies which parameters and/or options are to be different from the previous data case. The SD&SS program then reexecutes with all other parameters and options remaining as they were in the previous case. This option can be used repeatedly to analyze several different flight conditions (see sec. 9.2.3, vol. II).

#### 4.1.2 Pressure Distribution Plot (PDPLOT) Program

The PDPLOT program produces CalComp plots of  $\Delta C_p$  versus  $x/c$  for each row of panels on each Thin Body. Either steady or unsteady lifting pressures may be plotted. The card input for this program is a punched data deck produced by the SD&SS program. The punched output must be requested in the pressure output option mentioned in the \$STABILITY PROBLEM DATA card section description of section 4.1.1.

#### 4.1.3 Time Histories (TH) Program

The TH program accepts input from the SD&SS output tape, SDSSTP, the GD output tape, GDTAPE, and an input data deck and calculates the response of the airplane to large disturbances by integrating the "large perturbation" equations of motion. To form the coefficients of these equations of motion, the TH program uses either the data on the SD&SS output tape or, alternatively, the wind tunnel data supplied by the user in the TH data deck. The required/optional input data are divided into card sections headed by the following Data Control Cards.

*\$INTEGRATION SPECIFICATIONS.*—The information specified in this card section supplies the program with integration and print specifications. These data consist of initial time, final time, print interval, integration interval, and plot-to-print ratio.

*\$INITIAL CONDITIONS.*—The initial values of the perturbation parameters are input in this card section.

*\$ACCURACY CRITERIA.*—This card section allows the user to choose between fixed-step-size and variable-step-size integration. The variable-step sizes are determined by the accuracy constraints supplied by the user.

*\$PRINT SPECIFICATIONS.*—This card section identifies the parameters that the user wishes to have printed.

*\$PLOT SPECIFICATIONS.*— This card section identifies the parameters that the user wishes to have stored on the TH output tape for subsequent plotting by the THPLOT program.

*\$MAXIMUM EULER ANGLES.*—Using this card section allows the user to place upper and lower bounds on the values of the Euler angles.

*\$ELASTIC PERTURBATION DATA.*—The initial values of the generalized coordinates may be specified in this card section. Note that these data only apply if the model is residual-elastic.

*\$TABULAR WIND TUNNEL DATA.*—This optional card section allows the user to input tables of experimental data. The program uses the data in these tables throughout the integration process.

*\$GUST DATA.*—In this card section the user may specify a discrete gust velocity disturbance. The shape, length, and amplitude of the gust is input. In order to use this optional card section, the gust matrix calculations must have been performed in the SD&SS program (see “\$GENERAL SPECIFICATIONS,” sec. 4.1.1).

#### 4.1.4 Time Histories Plot (THPLOT) Program

The THPLOT program accepts as input the output tape from the TH program, THTAPE. From the information stored on this tape it generates CalComp plots of the time histories of the variables listed in the \$PLOT SPECIFICATIONS card section of the TH program.

#### 4.1.5 Structural Loads (SLOADS) Program

The SLOADS program accepts the SD&SS output tape, SDSSTP, an ISIC output tape, EATAPE, and a data deck as input. The information in the data deck specifies which structural load matrices the user wishes to have printed. These matrices are printed in the form of applied forces and moments at each ISIC node location. SLOADS can only be used with an ISIC structural model.

#### 4.1.6 Air Loads (ALOADS) Program

SDSSTP, GDTAPE, a tape (CINTAP) containing the symmetric clamped flexibility matrix,  $[C^S]$ , and a data deck serve as input for the ALOADS program. The ALOADS program performs two basic calculations for symmetric loading conditions. First, it computes the elastic deformation at the ESIC structural nodes, and second, at any specified point, the program calculates the resultant force and couple due to the airload on the aerodynamic surfaces contained in a specified spatial region. ALOADS can only be used with an ESIC structural model.

The calculation of the elastic deformation at the structural nodes requires no card input. This calculation is done automatically if the proper information is available on the input tapes; namely, the load matrices on SDSSTP (placed there by exercising the loads output option in the \$STABILITY PROBLEM DATA card section of the SD&SS program) and a suitable flexibility matrix on CINTAP (this need not be a square matrix—see sec. 18.2.1, vol. II).

In the input data deck the user must specify the following information that is required for the load calculations:

- The number and location of load points (the points at which the forces and moments are evaluated).
- The definition of the regions of space in which the aerodynamic surfaces whose airloads are to be used in the calculation of the forces and moments at each load point are located.
- The reference lengths that are used to normalize the forces and moments and center-of-pressure locations.

## 4.2 DART MODEL I DEMONSTRATION CASE

With the exception of the plotting programs, all of the FLEXSTAB analysis programs were used in the Dart Model I Demonstration Case. The SD&SS program was executed four times (see table 4.2-1): twice using the ISIC structural definition (SDSS-1A and SDSS-1B), and twice using the ESIC definition (SDSS-1C and SDSS-1D). The TH and SLOADS programs were executed using the results from SDSS-1B. Finally, the ALOADS program was executed in conjunction with the results from SDSS-1D.

This section describes the input decks that were used for the Dart Model I Demonstration Case. The format of these descriptions follows that of the previous section. Listings of the input decks for each of the Dart Model I analysis program runs are given in Appendix A.

*TABLE 4.2-1. INPUT DIFFERENCES FOR THE DART MODEL I SD&SS RUNS*

	SD&SS Run			
	SDSS-1A	SDSS-1B	SDSS-1C	SDSS-1D
Structural modeling	ISIC	ISIC	ESIC	ESIC
Reference motion	Coupled	Coupled	Symmetric	Symmetric
Thickness option	Off	On	Off	On
Leading edge thrust option	Off	On	Off	On
Gust option	On	On	Off	Off
Perturbation motion	Coupled	Coupled	Symmetric	Symmetric

### 4.2.1 Stability Derivatives and Static Stability Program--SDSS-1A

GDTAPE from GD-1, AICTAP from AIC-1, and SICTP3, which was formed by merging SICTP2 from ISIC-1 and NMTAP2 from NM-1, were input to SDSS-1A. The description of the input data deck follows. Optional card sections that were not used are omitted from the description.

*\$GENERAL SPECIFICATIONS.--*

- Basic option codes: The reference motion was coupled since an antisymmetric quantity (namely, roll rate) was to be specified. The static-elastic structural option was chosen so that comparisons could be made with the static-elastic ESIC structural model analyzed in SDSS-1C. (If only the static-elastic structural option is to be used in SD&SS, it is not necessary to have selected residual-elastic modeling in ISIC and NM. This was done in ISIC-1 and NM-1 for exemplary purposes only.) Unsteady, stick speed stability, and gust matrix calculations were arbitrarily re-

requested. Thickness effects and the leading edge thrust correction were not desired. It was specified that the pitch rate would be input rather than load factor. The tape options indicated that tape input from the GD, AIC, and ISIC (plus NM) programs was available. The units chosen were meters. The altitude option indicated that the reference altitude would be specified. The alpha option did not apply for Dart Model I since it had no Slender Bodies off the plane of symmetry.

- Flight conditions: The reference altitude,  $h_1$ , was chosen to be sea level. The temperature deviation from standard,  $\Delta T$ , was set to zero. The reference roll angle ( $\phi_1$ ), yaw rate ( $R_1$ ), and pitch rate ( $Q_1$ ) were set to zero. A reference roll rate of  $P_1 = 10$  degrees per second was specified. (Note that the Mach number input on CARD 5 of GD-1 ( $M_1 = 0.5$ ) was used here since  $M_1$  was left blank on CARD 9 of the SDSS-1A data deck.)
- Reference parameters: The reference wing area was set to 2.0, the reference chord was 1.0, and the reference span was set to 4.0.

*\$MATRIX PRINT LIST.* The following matrices were arbitrarily selected for printing: (APT)-S and A, (C DT)-S and A, (C THT)-S and A, (PHI\*M)-S and A, and (L1)-S and A.

*\$CONTROL SURFACE DATA.*—The second (aft) Thin Body panel on the “wing” of Dart Model I was chosen to simultaneously represent the elevator, aileron, and rudder. The relative strength of participation for the rudder was set to zero which, in effect, instructed the program that it was inactive. (Note, however, that the rudder still had to be defined since the reference motion was coupled.)

*\$STABILITY PROBLEM DATA.*—Stability problem 3 was chosen, which meant that user-specified trim parameters would be input. The data input in this card section follows.

- Airplane Shape: The shape input from the GD program was specified to be the jig shape of Dart Model I. Since an elastic analysis was being performed, this meant that the program would calculate the deformed shape of the model. Here, the “deformed shape” refers to the shape that Dart Model I would assume at the input flight condition.
- Thrust data: Since stability problem 3 was specified, it was mandatory that the thrust be constant. In this case, the thrust was set to zero. (Note that specifying a nonzero thrust here would do nothing since the \$THRUST DATA card section, through which the program is informed of where the thrust vector acts, was omitted.)
- X-coordinate of leading edge reference chord: This location was found from the geometry of the configuration, namely,  $X = 1.0$  (see fig. 3.2-2).
- Input/output camber shape and displacement data: The camber shape and aerocentroid position vector of Dart Model I were input via the GD program output tape. It was requested that the output camber shape and aerocentroid position vector be printed.

- Pressure and loads output option: It was requested that the steady, lifting pressures be printed. The load matrices were calculated and stored on the SD&SS output tape.
- User-specified trim parameters: The following trim conditions were specified:  $\alpha_1 = \theta_1 = 0.1$  radian, and  $\delta e_1 = \beta_1 = \delta a_1 = \delta r_1 = 0.0$ .

*SPERTURBATION DATA.* Both symmetric and antisymmetric perturbation motion was requested so that symmetric and antisymmetric dynamic stability derivatives would be calculated. It was requested that the compressibility effects be included in the speed derivative and yaw rate derivative calculations and that the control effectivenesses be calculated. Unsteady pressures were printed. Also, the perturbation load matrices were stored on the SD&SS output tape. No empirical perturbation derivatives were input.

#### 4.2.2 Stability Derivatives and Static Stability Program SDSS-1B

SDSS-1B was compared with SDSS-1A to show the effects of fuselage thickness (the wing has zero thickness) and leading-edge thrust calculations. The same input tapes were used for both runs. The only differences between the two input data decks are given below.

*SGENERAL SPECIFICATIONS.* In addition to the options chosen in SDSS-1A, thickness effects and the leading-edge thrust correction were requested.

#### 4.2.3 Stability Derivatives and Static Stability Program SDSS-1C

GDTAPE from GD-1, AICTAP from AIC-1, and SICTP3 from ESIC-1 were input to SDSS-1C. The results from SDSS-1C were compared with those from SDSS-1A to verify the equivalence of the two structural definitions. With the following exceptions, the input data deck for SDSS-1C was identical to that of SDSS-1A.

*SGENERAL SPECIFICATIONS.* The motion option requested symmetric reference flight since only symmetric structural data was available on SICTP3. Gust matrix calculations were not desired. The tape input option indicated that the structural definition was provided by ESIC.

*SMATRIX PRINT LIST.* Since the reference motion was symmetric, only the symmetric matrices listed in SDSS-1A were specified here. In addition, printout of the (L2)-S and (L12)-S matrices was requested (see app. B, vol. III for a description of these matrices).

*SPERTURBATION DATA.* Only symmetric perturbation motion was requested because the ESIC structural model is only for symmetric motion.

#### 4.2.4 Stability Derivatives and Static Stability Program SDSS-1D

SDSS-1D was compared with SDSS-1C to show the effects that thickness and leading-edge thrust had on the results. The same input tapes were used for each run. The input data deck for SDSS-1D was the same as that for SDSS-1C with the following exceptions.



*\$GENERAL SPECIFICATIONS.*—It was requested that thickness effects and the leading-edge thrust correction be included in the calculations.

#### 4.2.5 Time Histories Program—TH-1

GDTAPE from GD-1 and SDSSTP from SDSS-1B were input to TH-1. The TH-1 input data deck consisted of two analysis cases which requested the response to a modified square wave gust and a sine wave gust. Except where noted, the description below applies for both data cases. Card sections not used are omitted from the description.

*\$INTEGRATION SPECIFICATIONS.*—This card set was included for each case. It called for integration from 0.0 to 0.05 second in 0.005-second intervals. Printout at 0.01-second intervals was requested. The plot-to-print ratio was not input since plotting was not desired.

*\$INITIAL CONDITIONS.*—Each of the components of the initial perturbation vector were set to zero.

*\$PRINT SPECIFICATIONS.*—Printout of all parameters was requested for both cases. (This card section was not needed in the input for the second data case since the TH program automatically uses the print specifications from the previous case.)

*\$GUST DATA.*—A modified square wave gust was specified for the first case. Its wavelength was 30.0 meters and its amplitude (in the  $Z_B$ -direction) was set equal to -0.01 meter/second. In the second case, a sine wave gust with the same wavelength and amplitude was specified.

#### 4.2.6 Structural Loads Program—SLOADS-1

SLOADS-1 made use of EATAPE from ISIC-1 and SDSSTP from SDSS-1B. In the input data deck it was requested that the (L1)-S and (L1)-A matrices be printed.

#### 4.2.7 Air Loads Program—ALoads-1

GDTAPE and SDSSTP from GD-1 and SDSS-1D, respectively, served as input for ALOADS-1. The [CS] matrix used in ESIC-1 was input via CINTAP. The following information was specified in the input data deck:

- One load point was chosen. Its location was specified to be at  $X = 1.5$ ,  $Y = 1.0$ ,  $Z = 0.0$  (the midpoint of the wing root chord).
- The region of forces was chosen to coincide with the wing, i.e., outboard of the load point. (The reference point, R, was located at  $X = 1.5$ ,  $Y = 2.0$ , and  $Z = 0.0$ , i.e., at the midpoint of the wing tip chord; see fig. 18.2-1, vol. II.)
- The following reference lengths were specified: surface area = 4.0, semispan = 2.0, chord = 1.0, vertical span = 1.0. (Note that Dart Model I has no prominent vertical dimension; however, a nonzero vertical span must be input.) The X-coordinate of the leading edge of the reference chord was set to 1.0.

### 4.3 DART MODEL II DEMONSTRATION CASE

SD&SS was the only analysis program used in the Dart Model II Demonstration Case. This section gives a detailed description of the input data deck used for this case.

#### 4.3.1 Stability Derivatives and Static Stability Program—SDSS-2

GDTAPE and AICTAP from GD-2 and AIC-2, respectively, served as tape input for SDSS-2. The input deck description is given below. Card sections not mentioned were not included in the data deck.

*GENERAL SPECIFICATIONS.*—The following general information was specified.

- Basic option codes: Coupled reference motion was specified so that symmetric and antisymmetric static stability derivatives would be calculated. The rigid structural option had to be chosen since no elastic structural definition was created. The calculation options arbitrarily requested unsteady, thickness, leading-edge thrust, and stick-speed stability calculations. No gust matrices were generated. It was specified that pitch rate would be input rather than load factor. The tape options indicated that GD and AIC tapes were being input. The units were chosen to be meters; the altitude option was exercised indicating that the reference altitude would be input; the alpha option was not used.
- Flight conditions: The reference altitude ( $h_1$ ) was sea level. The temperature deviation ( $\Delta T$ ) was set to zero. The reference roll angle ( $\phi_1$ ) and angular velocities ( $P_1, Q_1, R_1$ ) were all set equal to zero.
- Reference parameters: The reference wing area was 12.0 (area of both wings), the reference chord 1.0, and the reference span 6.0.

*CONTROL SURFACE DATA.*—It was specified that the aft Thin Body panels of the upper and lower “wings” of Dart Model II would simultaneously serve as the elevator and aileron. The forwardmost Thin Body panel on the upper wing was defined to be a rudder; its relative strength of participation was arbitrarily set to zero, however.

*STABILITY PROBLEM DATA.*—Stability problem 3 was again chosen (i.e., user-specified trim parameters). The specific input data follows:

- Airplane shape: Since Dart Model II was to be analyzed as a rigid configuration, the shape option input was not important. Dart Model II was arbitrarily specified to be in its jig shape.
- Thrust data: It was specified that the thrust would be constant. Its value was set to zero.

- X-location of leading edge of reference chord: This location is at  $X = 1.0$  (see fig. 3.3-2).
- Input/output camber shape and displacement data: The camber shape was input via the GD program output tape. Since a rigid analysis was being performed, there was no need to input the aerocentroid position vector or calculate the output aerocentroid. Position vector and output camber shape.
- Pressure and loads output option: It was requested that the steady, lifting pressures be printed. The load matrices were not calculated.
- User-specified trim parameters: It was specified that  $\alpha_1 = \theta_1 = 0.1$  radian and that  $\delta e_1 = \beta_1 = \delta a_1 = \delta r_1 = 0.0$ .

*\$PERTURBATION DATA.*—Both symmetric and antisymmetric perturbation flight was arbitrarily requested. Compressibility effects were included in the speed derivative and yaw rate derivative calculations. Control effectiveness calculations were requested, unsteady pressures were printed. Perturbation load matrices were calculated because a rigid analysis was preformed. Empirical perturbation derivatives were not input.

*\$STRUCTURAL DATA.*—Since a structural definition was not input on tape, this card section was required for the SDSS-2 input data deck. The mass of Dart Model II was arbitrarily set to 10.0 kilograms. A center of gravity at  $X = 1.0, Z = 0.0$  was specified. The moments of inertia,  $I_{XX}, I_{YY}, I_{ZZ}$ , and  $I_{XZ}$ , were all set to zero (this was permissible since no angular velocities were specified).

#### 4.4 BOEING 707-320B DEMONSTRATION CASE

With the exception of the ALOADS program, all of the FLEXSTAB analysis programs were used in the 707-320B Demonstration Case. The SD&SS program was executed twice (SDSS-3A and SDSS-3B). SDSS-3A performed an elastic analysis and used the “jig” shape geometry produced by GD-3A. The “cruise” shape geometry of GD-3B was used in the rigid analysis performed by SDSS-3B. The TH and SLOADS programs were executed using the results of SDSS-3A.

This section describes the input data decks that were used in the analysis programs of the 707-320 Demonstration Case. Each of the points brought out in section 4.1 is discussed individually.

##### 4.4.1 Stability Derivatives and Static Stability Program—SDSS-3A

GDTAPE from GD-3A, AICTAP from AIC-3, and SICTP3 (produced by merging SICTP2 from ISIC-3 with NMTAP2 from NM-3 ) were input to SDSS-3A. The description of the input data deck is given below.

###### *GENERAL SPECIFICATIONS.*—

- Basic option codes: Since only a symmetric flight condition was to be analyzed, symmetric reference motion was chosen in the motion option. The residual-elastic structural option was chosen so that the free-vibration modes (calculated in NM-3) would participate in the dynamic analysis. The unsteady option was exercised so that unsteady stability derivatives and unsteady pressures could be calculated. The effects of thickness and leading-edge thrust were included in the analysis, and the calculation of stick speed was requested. Gust matrix calculations were requested since a gust response analysis was to be performed in TH-3. The tape options indicated that tape input was available from the GD, AIC, and ISIC (plus NM) programs. Feet were chosen as the units of length. The altitude option was exercised indicating that the reference altitude would be input. The alpha option was not used.
- Flight conditions: The reference altitude was input as  $h_1 = 35,000$  feet, the cruise altitude of the 707-320B. The temperature deviation from standard ( $\Delta T$ ) was specified to be zero. The reference roll angle ( $\phi_1$ ) and angular velocities ( $P_1, Q_1, R_1$ ) were set to zero.
- Reference parameters: Data from Boeing documents stated that the reference wing area was 2891.7 square feet, the reference wing chord 22.692 feet, and the reference wing span 142.417 feet.

*SMATRIX PRINT LIST.*—The (DFP)-S and (L1)-S matrices were arbitrarily selected for printing.

*STHRUST DATA.*—The thrust vectors were defined to originate along the  $X_M$ -axes of the nacelles (INNAC and OUTNAC). The X-locations of the vectors were chosen to lie half-

way between the nose and aft end of each nacelle. The direction cosines of the thrust vectors were taken from a general configuration drawing of the airplane. The relative strength of each vector was set to 0.25, indicating that all four engines were producing equal thrust.

*\$CONTROL SURFACE DATA.* – Both longitudinal and lateral-directional control surfaces were defined. (Note that the definition of the lateral-directional control surfaces was optional since only symmetric reference motion was being considered.) The Thin Body panels chosen to represent each control surface were found by superimposing a drawing of the paneling scheme on a drawing of the actual wing surface. The panels that most closely represented the actual control surface were identified in this card set. (Note that it is always advisable to consider control surface locations *before* the configuration is paneled in the GD program. A better control surface representation will usually be possible as a result.) The stabilizer, rudder, and ailerons were also defined in this manner.

*\$STABILITY PROBLEM DATA.* – Stability problem 1 was chosen for this case. This meant that the program would trim the airplane using program-calculated, constant coefficients. The data input in this card section is described below.

- Airplane shape: The camber shape of the airplane was to be input via GDTAPE from GD-3A. Since this geometry definition represented the jig shape of the 707-320B (see sec. 3.4.1), the “JIG” shape option was selected here. Consequently, the deformed shape computed by SD&SS will be the shape corresponding to the input flight condition.
- Thrust or flightpath angle data: The program was instructed to solve for thrust. A flightpath angle of  $\gamma_1 = 0.0$  was specified.
- X-coordinate of leading edge of reference chord: This point was found on the general configuration drawing and has the value  $X = 66.007$ .
- Input/output camber shape and displacement data: The camber shape (camber slope vector) and displacements (aerocentroid position vector) were input via GDTAPE from GD-3A. The output values were printed.
- Pressure and loads output option: The steady, lifting pressures were printed and the load matrices were calculated and stored on the SD&SS output tape for future printing by SLOADS-3.
- Maximum and minimum limits for trim parameters: These maximum and minimum values were chosen to allow for a wide variation from the anticipated trim condition also input. The values used were:  $\alpha_{MAX} = 8.0$ ,  $\alpha_{MIN} = -2.0$ ;  $T_{MAX} = 25000$ ,  $T_{MIN} = 0.0$ ;  $\delta e_{pos} = 0.5$ ,  $\delta e_{neg} = -14.0$ ;  $\beta_{MAX} = 4.0$ ,  $\beta_{MIN} = -4.0$ ;  $\delta a_{pos} = 18.5$ ,  $\delta a_{neg} = -18.5$ ;  $\delta r_{pos} = 25.0$ ,  $\delta r_{neg} = -25.0$ .

*\$PERTURBATION DATA.* – Symmetric and antisymmetric perturbation flight was specified since the TH program was to be executed. Compressibility effects and control effectiveness were requested. Unsteady pressures were printed and the perturbation load matrices were stored on the SD&SS output tape. No perturbation derivatives were input.

*\$DYNAMIC ANALYSIS.*—Including this card section in the SDSS-3A input data deck instructed the program to calculate the airplane's dynamic stability characteristics.

In order to make a comparison between aeroelastic results from residual-elastic and static-elastic analyses, another run was made using the static-elastic structural option. This was accomplished by using the recycle option in the SD&SS program. Thus, the SDSS-3A input data deck consisted of two cases: the initial data case using the residual-elastic structural option (described above) and a recycle case (see below), which performed a static-elastic analysis.

*\$RECYCLE DATA.*—The program was instructed to recycle with this data case using the static-elastic structural option. All other input data from the initial data case remained the same.

#### 4.4.2 Stability Derivatives and Static Stability Program--SDSS-3B

SDSS-3B was designed to illustrate the use of wind tunnel data when executing the SD&SS program. The tape input to SDSS-3B consisted of GDTAPE from GD-3B and AICTAP from AIC-3. Since this was a rigid case, a structural definition was unnecessary. Given below is the description of the input data deck.

##### *\$GENERAL SPECIFICATIONS.*—

- Basic option codes: Symmetric reference motion was again chosen since a symmetric flight condition was being analyzed. The “rigid” structural option was used since structural data was not input on tape. The calculation options requested stick-speed stability and gust matrix calculations, but no unsteady, thickness, or leading-edge thrust calculations. (The unsteady option was not used since unsteady stability derivatives were to be input in the \$PERTURBATION DATA card section. The calculation of thickness effects and leading-edge thrust was not requested because the wind tunnel data that was input in the \$WIND TUNNEL DATA card section already included these effects.) The tape options indicated that GD and AIC output tapes were input. The length units were chosen to be feet. The altitude option was not used indicating that flight speed and either density or dynamic pressure would be input. The alpha option was not used.
- Flight conditions: A flight speed of  $U_1 = 773.472$  and a dynamic pressure of  $\bar{q}_1 = 223.99$  were input, which resulted in the same flight conditions of SDSS-3A. Again the reference roll angle ( $\phi_1$ ) and angular velocities ( $P_1, Q_1, R_1$ ) were set to zero.
- Reference parameters: The values used in SDSS-3A were used here.

*\$MATRIX PRINT LIST.*—The (DFP)-S matrix was arbitrarily selected for printing.

*\$THRUST DATA.*—The thrust data used in SDSS-3A was repeated here.

*\$CONTROL SURFACE DATA.*—This card section was identical to the \$CONTROL SURFACE DATA card section of SDSS-3A.

*\$STABILITY PROBLEM DATA.*—Stability problem 2 was specified, which meant that the program would trim the airplane by iterating over the wind tunnel data.

- Airplane shape: The airplane shape was specified as the reference shape since the analysis was rigid. (Specifying the “JIG” shape would also give the same results.)
- Thrust or flightpath angle data: The program was instructed to solve for thrust. A flightpath angle of  $\gamma_1 = 0.0$  was specified.
- X-coordinate of leading edge of reference chord: This location was taken directly from the general configuration drawing and has the value  $X = 66.077$ .
- Input/output camber shape and displacement data: The airplane’s camber shape was input from the GD-3B output tape. The output camber shape and the input and output displacements did not apply since this was a rigid case.
- Pressure and loads output option: It was requested that the steady, lifting pressures be printed and punched by the program. (The punched output would later be used in the PDPLOT program.) Since the model was rigid load vectors were not calculated; therefore, they could not be stored on SDSSTP.
- Initial values for trim parameters: The initial values were arbitrarily set to zero.
- Maximum and minimum limits for trim parameters: The values used in SDSS-3A were used here.
- Convergence tolerances for trim parameters: It was specified that  $\alpha$  and  $\delta e$  converge to within  $\pm 0.01^\circ$  (degrees) and thrust to within  $\pm 1.0$  pound.
- Maximum number of iterations: A maximum of 20 iterations was specified (10 are usually sufficient).

*\$WIND TUNNEL DATA.*—Data from a wind tunnel test BTWT 1246 (ref. 4-1) and the Air Force Datcom (ref. 4-2) were used to produce tables of longitudinal data. Wind tunnel values of  $C_L$ ,  $C_D$  and  $C_m$  were input for  $\alpha$  between  $-4.0^\circ$  and  $+6.0^\circ$  and  $\delta e$  between  $-4.0^\circ$  and  $-2.0^\circ$ . Values of  $C_{LQ}$ ,  $C_{DQ}$ , and  $C_{mQ}$  for  $\alpha$  equal to  $0.0^\circ$  and  $5.0^\circ$  were calculated using the Air Force Datcom and specified in the input.

*\$PERTURBATION DATA.*—Symmetric and antisymmetric perturbation flight was requested since both longitudinal and lateral-directional results were desired in the \$DYNAMIC ANALYSIS card section. Calculation of control surface effectiveness and compressibility effects was requested. Printout of the unsteady pressures was not requested because the unsteady aerodynamics option in the \$GENERAL SPECIFICATIONS card section was not exercised. Perturbation loads were not calculated. Wind tunnel values of  $C_{L\alpha}$ ,  $C_{D\alpha}$ ,  $C_{m\alpha}$ ,  $C_{L_u}$ ,  $C_{D_u}$ , and  $C_{m_u}$  from ref. 4-1; and  $C_{Y\beta}$ ,  $C_{\ell\beta}$  and  $C_{n\beta}$ , from ref. 4-3

were input. The Air Force Datcom was used to calculate  $C_{LQ}$ ,  $C_{DQ}$ ,  $C_{mQ}$ ,  $CL_{\dot{\alpha}}$ ,  $CD_{\dot{\alpha}}$  and  $Cm_{\dot{\alpha}}$ . The yaw rate derivatives,  $C_{YR}$ ,  $C_{lR}$ , and  $C_{nR}$ , were estimated using the methods found in reference 4-3.  $C_{LQ}$ ,  $C_{DQ}$ , and  $C_{mQ}$  were set to zero. The  $\beta$ -derivatives were for a stretched version (not built) of the 707-320 airplane but should be approximately the same for the 707-320 airplane.

*SDYNAMIC ANALYSIS.*—The dynamic stability characteristics of the airplane were calculated as a result of including this card section in the SDSS-3B data deck. In this case, the empirical stability derivatives input in the SPERTURBATION DATA card section were used to form the coefficients of the characteristic equation.

*SSTRUCTURAL DATA.*—Since this was a rigid case and a structural definition was not input via tape, this card section was required. The values of the total mass, center-of-gravity location, and moments of inertia were taken directly from the printout of the ISIC-3 run.

#### 4.4.3 Pressure Distribution Plot Program—PD PLOT-3

The steady, Thin Body, lifting pressure distribution that was punched by SDSS-3B was used to form the input deck for PD PLOT-3. PD PLOT-3 produced CalComp plots of  $\Delta C_p$  versus  $x/c$  for each row of panels on each Thin Body.

#### 4.4.4 Time Histories Program—TH-3

GDTAPE and SDSSTP from GD-3A and SDSS-3A, respectively, served as the tape input for TH-3. (The TH program is only capable of analyzing the output data from the first data case of a multiple-case SD&SS run. Therefore, it was the first case of SDSS-3A—the residual-elastic case—that was analyzed by TH-3). The TH-3 input data deck consisted of five data cases. These are discussed individually.

In the first case, the only nonzero component of the initial perturbation vector was the  $u$ -component. This case was designed to excite the phugoid mode of the airplane.

*SINTEGRATION SPECIFICATIONS.*—Integration was performed between 0.0 and 175.0 seconds at 0.05-second intervals. Printout was requested at 5-second intervals. A plot-to-print ratio of 10 was specified.

*SINITIAL CONDITIONS.*—This card section contained the components of the initial perturbation vector. All components except  $u$  were set to zero. The initial value of  $u$  was set to 600 inches per second.

*SPRINT SPECIFICATIONS.*—It was requested that all parameters be printed.

*S PLOT SPECIFICATIONS.*—Plot data for the  $u$ ,  $\theta_p$ , and  $N_p$  parameters were stored on TH-3 output tape.

The second data case had an initial  $v$ -perturbation designed to excite the Dutch roll mode.



*\$INTEGRATION SPECIFICATIONS.*—Integration between 0.0 and 20.0 seconds was performed at 0.05-second intervals. A plot-to-print ratio of 10 was specified with print steps every 0.5 second.

*\$INITIAL CONDITIONS.*—The v-perturbation was set to 600 inches per second. All other components were set to zero.

*\$PRINT SPECIFICATIONS.*—All parameters were requested for printing.

*\$PLOT SPECIFICATIONS.*—Plot data for  $\beta$ ,  $\phi_p$ , and  $\psi_p$  were stored on tape.

*\$ELASTIC PERTURBATION DATA.*—This card section was not required in the first data case since the generalized coordinates were automatically set to zero. For this and succeeding cases, however, it had to be used to “manually” set these coordinates to zero. (Otherwise, the program would use the values of these coordinates from the last integration step of the previous data case.)

In the third data case a w-perturbation was used to excite the short-period mode.

*\$INTEGRATION SPECIFICATIONS.*—This card section specified integration from 0.0 to 10.0 seconds at 0.05-second intervals. The print interval was set at 0.5 second. A plot-to-print ratio of 10.0 was chosen.

*\$INITIAL CONDITIONS.*—The initial w-perturbation was set to 600 inches per second. All others were zero.

*\$PRINT SPECIFICATIONS.*—All parameters were selected for printing.

*\$PLOT SPECIFICATIONS.*—Plot data was stored on tape for  $\alpha$ ,  $\theta_p$ , and  $N_p$ .

*\$ELASTIC PERTURBATION DATA.*—The initial values of the generalized coordinates were set to zero.

The fourth data case included a p-perturbation. This was designed to demonstrate rolling convergence.

*\$INTEGRATION SPECIFICATIONS.*—Integration was performed from 0.0 to 10.0 seconds at 0.05-second intervals. Printout was requested at 0.25-second intervals; the plot-to-print ratio was specified to be 5.0.

*\$INITIAL CONDITIONS.*—With the exception of the p-perturbation, all components of the initial perturbation vector were set to zero. The value of  $p$  was specified to be 0.50 radian per second.

*\$PRINT SPECIFICATIONS.*—It was requested that all parameters be printed.

*\$PLOT SPECIFICATIONS.*—Plot data for  $\phi_p$  and  $p$  were stored on tape.

*\$ELASTIC PERTURBATION DATA.*—The initial generalized coordinates were set to zero.

The fifth and final data case was designed to show the airplane response to a “one-minus-cosine” gust disturbance.

*\$INTEGRATION SPECIFICATIONS.*—The program was instructed to integrate from 0.0 to 5.0 seconds at 0.0125-second intervals. The plot-to-print ratio was set to 20.0; the print interval was specified to be 0.25 second.

*\$INITIAL CONDITIONS.*—All components of the initial perturbation vector were set to zero.

*\$PRINT SPECIFICATIONS.*—Only  $\theta_P$  and  $N_P$  were selected for printing.

*\$PLOT SPECIFICATIONS.*—The plot data for  $\theta_P$  and  $N_P$  were stored on the TH-3 output tape.

*\$ELASTIC PERTURBATION DATA.*—Again, the values of generalized coordinates were set to zero.

*\$GUST DATA.*—It was specified that the shape of the gust disturbance was that of a “one-minus-cosine” wave (see fig. 10.2-3, vol. II). The gust wavelength was specified to be 8169.12 inches, i.e., 30 reference chord lengths. The gust amplitude was set to -12.0 inches per second in the  $Z_B$ -direction. The antisymmetric gust component ( $Y_B$ -direction) was set to zero.

#### 4.4.5 Time Histories Plot Program—THPLOT-3

THPLOT-3 produced graphic displays of the results calculated in TH-3. Only those variables specified in the *\$PLOT SPECIFICATIONS* card section of TH-3 were plotted. THPLOT-3 produced a total of 13 plots.

#### 4.4.6 Structural Loads Program—SLOADS-3

The input tapes used for SLOADS-3 consisted of EATAPE and SDSSTP from ISIC-3 and SDSS-3A, respectively. As was the case for TH-3, SLOADS-3 was only capable of handling the output data from the residual-elastic data case in SDSS-3A.

In the SLOADS-3 input data deck it was specified that (L1)-S, the symmetric, aerodynamic plus inertia load matrix, and (LUE)-S, the symmetric, dynamic load matrix due to modal deflection, were to be printed. The engineering symbols for the load matrices are given in table 17.2-1, Volume II. Equation 5.7-16 of Volume I presents the equation for (L1)-S and (LUE)-S is shown on the top of page 6-43 of Volume I without an equation number.

#### 4.5 BOEING 2707-300PT (SST) DEMONSTRATION CASE

The SST was analyzed using the SD&SS and ALOADS programs. The SD&SS program was executed three times (see table 4.0-1). SDSS-4A was used to calculate the "JIG" shape for the SDSS-4B and SDSS-4C runs. SDSS-4C used the results from CAIC-4, whereas SDSS-4B used the uncorrected AIC-4 data. The ALOADS program was executed using the results from SDSS-4B.

The input data decks are described below. These descriptions follow the format introduced in section 4.1.

##### 4.5.1 Stability Derivatives and Static Stability Program -SDSS-4A

The output tapes from GD-4, AIC-4, and ESIC-4 (GDTAPE, AICTAP, and SICTP3, respectively) were used to execute SDSS-4A. The input data deck description follows.

###### *\$GENERAL SPECIFICATIONS.* -

- Basic option codes: Symmetric reference motion was requested (a requirement when exercising the "DESIGN" shape option). The static-elastic structural option was selected since this is all that is required for the "DESIGN" option. Thickness and leading-edge thrust calculations were requested, but unsteady, stick-speed stability, and gust matrix calculations were not. (Since the sole purpose of this run was to generate a "jig" shape for SDSS-4B and SDSS-4C, those options which did not directly affect the shape calculation were not exercised.) It was specified that pitch rate rather than load factor would be input. The tape options indicated that tape input was available from the GD, AIC, and ESIC programs. The units were chosen to be feet and the altitude option was exercised. The alpha option was exercised indicating that all Slender Bodies off the plane of symmetry (the nacelles) would not be affected by angle of attack (see sec. 9.2.1, vol. II).
- Flight conditions: The reference altitude ( $h_1$ ) was set to 60,000 feet, the cruise altitude of the SST. The temperature deviation from standard ( $\Delta T$ ) was zero. Reference roll angle ( $\phi_1$ ) and angular velocities ( $P_1, Q_1, R_1$ ) were all specified to be zero.
- Reference parameters: These data were obtained from Boeing documents. The wing area was 7700 square feet, the reference wing chord 101.5 feet, and the wing span 141.667 feet.

*\$MATRIX PRINT LIST.* - The (DFP)-S matrix was selected for printing.

*\$THRUST DATA.* - Thrust vectors were assigned to Slender Bodies INNAC and OUTNAC. These bodies represented the inboard and outboard engine nacelles, respectively. The thrust vectors were assumed to originate midway between the ends of the nacelles on the nacelle centerlines. The direction cosines were taken from the general configuration drawing. The relative participation parameter for each was set equal to 0.25 indicating that each engine produced equal thrust.

*\$CONTROL SURFACE DATA.*—The entire horizontal stabilizer serves as the longitudinal control surface for the SST. In addition, the aft portion of this horizontal stabilizer acts as a geared elevator. In order to model this control surface, the whole horizontal stabilizer was defined as the elevator in this card section. To account for the presence of the actual geared elevator, the relative strength of participation parameter was set equal to 1.75 for those panels representing the geared elevator and 1.0 for the remaining horizontal stabilizer panels. Thus, for each degree of horizontal stabilizer deflection, the geared elevator deflected 1.75°.

*\$STABILITY PROBLEM DATA.*—Stability problem 1 was specified indicating that the program would trim the airplane using constant, program-calculated coefficients.

- Airplane shape: The airplane shape was specified to be the design shape. This meant that the airplane would be trimmed rigidly, loads would be calculated, and the jig shape determined.
- Thrust or flightpath angle data: The program was requested to solve for thrust. The flightpath angle ( $\gamma_1$ ) was set to zero.
- X-coordinate of leading edge of reference chord: This location ( $X = 120.83$ ) was determined from the general configuration drawing.
- Input/output camber shape and displacement data: The input camber shape and displacements were read from the GD tape. The output camber shape and displacements were printed and punched on cards. The punched output was used in runs SDSS-4B and SDSS-4C.
- Pressure and loads output option: The pressures were not printed. Load calculations were not stored on the SD&SS output tape.
- Maximum and minimum limits for trim parameters: Reasonable limits for angle of attack and thrust were estimated from available wind tunnel data. Structural limitations given on the general configuration drawing determined the elevator angle limits.

#### 4.5.2 Stability Derivatives and Static Stability Program--SDSS-4B

SDSS-4B analyzed the jig shape calculated by SDSS-4A. Tape input consisted of the output tapes from GD-4, AIC-4, and ESIC-4. The input data deck description follows.

*\$GENERAL SPECIFICATIONS.*—In the SDSS-4B input data deck, unsteady and stick-speed stability calculations were requested. Otherwise, this card section was identical to the one used in SDSS-4A (see sec. 4.5.1). The ESIC-4 output tape contained matrices sufficient for the residual-elastic structural option, however, a change of plans subsequent to the ESIC run resulted in only the static-elastic option being selected for SDSS-4B.

*\$MATRIX PRINT LIST.*—It was requested that the (DFP)-S matrix be printed.

*\$THRUST DATA.*—This card section was identical to the \$THRUST DATA card section of SDSS-4A (see sec. 4.5.1).

*§CONTROL SURFACE DATA.*—The control surface data were identical to those defined in SDSS-4A (see sec. 4.5.1).

*§STABILITY PROBLEM DATA.*—Stability problem 1 was specified. This meant that the airplane was trimmed using constant, program-calculated coefficients.

- Airplane shape: The airplane shape was defined as the jig shape. This implied that the loads would be calculated and applied to the structure, and that the camber shape and displacements of the trimmed airplane would be calculated.
- Thrust or flightpath angle data: The program was instructed to solve for thrust. The flightpath angle ( $\gamma_1$ ) was set at zero degrees.
- X-coordinate of leading edge of reference chord: This location ( $X = 120.83$ ) was found on the general configuration drawing.
- Input/output camber shape and displacement data: The camber shape and displacements were input on cards which were punched by SDSS-4A. Printout of the output camber shape and displacements was requested.
- Pressure and loads output options: Printout of the pressures was requested. It was also specified that the load matrices be stored on the SD&SS output tape (for use in the ALOADS program).
- Maximum and minimum limits for the trim parameters: These limits were identical to those used in SDSS-4A.

*§PERTURBATION DATA.*—It was requested that the symmetric perturbation derivatives be calculated. Compressibility effects were included in the speed derivative calculations. Unsteady pressures were not requested. The program was instructed to calculate control effectivenesses and to store the perturbation load matrices on the SD&SS output tape. (Note that storing the perturbation load matrices on SDSSTP is actually only useful for ISIC modeled structures since it is only in conjunction with ISIC that the SLOADS program can be used to print these matrices.) No perturbation derivatives were input.

*§DYNAMIC ANALYSIS.*—The stability characteristics of the SST were calculated by solving its characteristic equation. Since only symmetric reference and perturbation flight was being considered, only the longitudinal stability characteristics were calculated.

#### 4.5.3 Stability Derivatives and Static Stability Program --SDSS-4C

The only difference between SDSS-4C and SDSS-4B occurred in the tape input data. SDSS-4C used the empirically corrected aerodynamic data stored on the CAIC-4 output tape, whereas SDSS-4B used the AIC-4 output tape. The input data deck for SDSS-4C was identical to that of SDSS-4B (see sec. 4.5.2).

#### 4.5.4 Air Loads Program—ALOADS-4

The output tapes from GD-4 and SDSS-4B, and a tape containing the constrained flexibility matrix,  $[C^S]$ , served as the input tapes for ALOADS-4. The input data deck description is given below.

- Only one load point was specified. It was located at  $X = 3300.0$ ,  $Y = 70.0$ , and  $Z = 37.0$  inches. This location corresponded to a point on the root chord of the horizontal stabilizer.
- The region of forces extended outboard, above and below, and fore and aft of the load point.
- The reference lengths used to normalize the force and moment coefficients were taken from the general configuration drawing.

## 4.6 YF-12A DEMONSTRATION CASE

The analysis portion of the YF-12A demonstration case consisted of executing the SD&SS and ALOADS programs for both the subsonic and supersonic definitions. The subsonic runs are designated as SDSS-5A and ALOADS-5A; the supersonic analyses as SDSS-5B and ALOADS-5B. A description of the input data deck used for each is given below.

### 4.6.1 Stability Derivatives and Static Stability Program—SDSS-5A

Tape input to SDSS-5A consisted of the output tapes from GD-5A, AIC-5A, and ESIC-5A (GDTAPE, AICTAP, and SICTP3, respectively). The input data deck consisted of six data cases which encompassed three flight conditions and two elasticity options. The detailed description follows.

#### *\$GENERAL SPECIFICATIONS.—*

- Basic option codes: Only symmetric reference motion was requested since the structural modeling was only for symmetric loading. The static-elastic structural option was chosen to be consistent with the ESIC-5A modeling. Thickness effects were included in the calculations; unsteady, leading-edge thrust, stick speed stability, and gust matrix calculations were not requested since the objective of this run was simply to calculate static loads. It was specified that load factor (rather than pitch rate) would be input. The tape options indicated that tape input was available from the GD, AIC, and ESIC programs. The inch/feet units option was selected. The altitude option was not used; this indicated that flight speed and density or dynamic pressure would be input. The alpha option was not used.
- Flight conditions: The flight speed ( $U_1$ ) was set to 869.7 feet per second. The dynamic pressure ( $\bar{q}_1$ ) was input as 667.0 pounds per square foot. Initial roll angle ( $\phi_1$ ) was set to zero. A normal load factor (NZ) of 1.5 was specified.  $P_1$  and  $R_1$  were set to zero.
- Reference parameters: The following reference parameters were specified: wing area, 258,480 square inches; reference chord, 486.667 inches; wing span, 652 inches.

*\$MATRIX PRINT LIST.—*The (L1)-S, (FA)-S, (L2)-S, and (L12)-S matrices were arbitrarily selected for printing.

*\$THRUST DATA.—*A thrust vector was assigned to the Slender Body representing the nacelle. It was assumed to originate midway between the nose and aft end of the nacelle and its direction was parallel to that of the X-axis. The relative strength of this thrust vector was set to 0.5 (see CARD 22, sec. 9.2.2, vol II).

*\$CONTROL SURFACE DATA.*—Since only symmetric motion was being considered, it was only necessary to define a longitudinal control surface. Longitudinal control for the YF-12A is supplied by the symmetric deflection of the inboard and outboard elevons. The Thin Body panels that were within the boundaries of these control surfaces were specified in this card section. The relative strength of participation parameter for each panel was set equal to the cosine of its control surface hinge line sweep angle. This ensured that a 1° deflection on the actual configuration would be correctly represented on the FLEXSTAB model (see sec. 3.5.2.1, vol. I).

*\$STABILITY PROBLEM DATA.*—Stability problem 1 was specified, which meant that the program would trim the airplane using constant coefficients.

- Airplane shape: The shape option indicated that the airplane was in its jig shape. This implied that the loads and airplane shape at the input flight condition would be calculated.
- Thrust data: The program was instructed to solve for thrust. The flightpath angle was specified to be 7.19°.
- X-coordinate of leading edge of reference chord: This value was taken from the general configuration drawing.
- Input/output camber shape and displacement data: The camber shape (obtained from Lockheed) was input on cards and the displacements were read from the GD tape. Printout of the output camber shape and displacements was requested.
- Pressure and loads output options: The pressures were printed and the load matrices were saved on the SD&SS output tape.
- Maximum and minimum limits for trim parameters: Very large limits were placed on angle of attack, elevator angle, and thrust since several flight conditions were to be analyzed (see below).

*\$AREA RATIO DATA.*—The areas of certain Thin Body and Interference Body panels were altered so that they would more accurately represent the actual configuration surfaces. In particular, several fuselage Interference Body panels near the nose and aft end of the fuselage had their areas reduced so that they would more closely represent the adjacent fuselage surface segments with which they were associated. Similarly, the areas of certain Thin Body panels in the region of curved edges (wing tips, leading and trailing edges, etc.) were altered accordingly.

This completed the input data for the first data case. Five additional data cases were included in the SDSS-5A data deck by using the \$RECYCLE DATA card section five times. The new flight conditions for each case are given below.

*\$RECYCLE DATA.*—The normal load factor was reset to 1.0; the flightpath angle was 3.82°.



*\$RECYCLE DATA.*—The load factor was 0.51; the flightpath angle 11.04°.

*\$RECYCLE DATA.*—The load factor and flightpath angle were reset to their initial values of 1.5 and 7.19°, respectively; in addition, the elastic option was changed so that a rigid analysis was performed.

*\$RECYCLE DATA.*—The load factor was set to 1.0; the flightpath angle 3.82°.

*\$RECYCLE DATA.*—The values of the load factor and flightpath angle were set to 0.51 and 11.04°, respectively.

#### 4.6.2 Stability Derivatives and Static Stability Program—SDSS-5B

SDSS-5B, the supersonic analysis, used data stored on the GD-5B, AIC-5B, and ESIC-5B output tapes. The input data deck included six data cases representing three different flight conditions and two different structural options.

*\$GENERAL SPECIFICATIONS.*—This card section was identical to the one used in SDSS-5A except for the flight speed and dynamic pressure. These values were set equal to 2690.0 feet per second and 628.0 pounds per square foot, respectively.

*\$MATRIX PRINT LIST.*—The (L1)-S, (FA)-S, (L2)-S, and (L12)-S matrices were selected for printing.

*\$THRUST DATA.*—This card section had the same content as the one used for SDSS-5A (see sec. 4.6.1).

*\$CONTROL SURFACE DATA.*—The control surfaces defined here were identical to the ones defined in SDSS-5A.

*\$STABILITY PROBLEM DATA.*—Except for the flightpath angle and the input camber shape, this card section was identical to that of SDSS-5A. In this case, the flightpath angle was specified to be 6.29°. The input camber shape (jig shape) was again input on cards; however, this “jig shape” was different from the one input to SDSS-5A. This was because the supersonic case was modeled with a “hot” structure, which meant that thermal deflections were included in the camber shape definition.

*\$AREA RATIO DATA.*—This card section had the same content as the one used in SDSS-5A (see sec. 4.6.1).

As in the subsonic analysis, five additional data cases were included in the SDSS-5B data deck through use of the SD&SS recycle capability. The flight conditions for each recycle data case are given below.

*\$RECYCLE DATA.* The normal load factor was reset to 0.98. The respecified value of the flightpath angle was 4.09°.

*\$RECYCLE DATA.*—The load factor was input as 0.46; the flightpath angle was 2.44°.

*\$RECYCLE DATA.*—In the fourth data case, the initial values of the load factor and flightpath angle were used (1.50 and 6.29°, respectively); in addition, the rigid structural option was specified.

*\$RECYCLE DATA.*—The load factor and flightpath angle were reset to 0.98 and 4.09°, respectively.

*\$RECYCLE DATA.*—In the final data case, the normal load factor was set equal to 0.46 and the flightpath angle was input as 2.44°.

#### 4.6.3 Air Loads Program—ALOADS-5A

Tape input to ALOADS-5A consisted of the GDTAPE from GD-5A, the SDSSTP from SDSS-5A, and CINTAP, which contained a suitable constrained flexibility matrix,  $[CS]$ . In this case, the input flexibility matrix had dimensions  $N1 \times N2$ , where  $N1$  corresponded to the number of degrees of freedom in the modified NASTRAN matrix, 1022, and  $N2$  corresponds to the number of degrees of freedom associated with the flexibility matrix input to ESIC-5A, 448 (see sec. 3.6.4). By postmultiplying this 1022 x 448 matrix by the load vectors calculated in SDSS-5A (of dimensions 448 x 1), ALOADS-5A was able to calculate the displacements associated with the 1022 structural degrees of freedom (see sec. 18.3, vol. II, for a description of these displacements). This correspondence is defined in table 4.6-1.

**TABLE 4.6-1—ARRANGEMENT OF THE FLEXIBILITY MATRIX INPUT TO THE ALOADS PROGRAM FOR YF-12A**

Body name (A)	No. of nodes (B)	Degrees of freedom for displacements (C)	Degrees of freedom for forces (D)	Position in flexibility matrix	
				Rowwise (E)	columnwise (F)
Fuselage	22	$dx_E, dz_E$	$dx_E, dz_E$	1-44	1-44
Nacelle	16	$dx_E, dy_E, dz_E$	$dx_E, dy_E, dz_E$	45-92	45-92
Chine	106	$dx_E, dy_E, dz_E$	$dz_E$	93-410	93-198
Inboard wing	62	$dx_E, dy_E, dz_E$	$dz_E$	411-596	199-260
Outboard wing	96	$dx_E, dy_E, dz_E$	$dz_E$	597-884	261-356
Vertical	38	$dx_E, dy_E, dz_E$	$dy_E, dz_E$	885-998	357-432
Ventral	8	$dx_E, dy_E, dz_E$	$dy_E, dz_E$	999-1022	433-448

- Note: 1. The rowwise positions (E) define the arrangement of displacement vectors output in the ALOADS program.
2. The columnwise positions (F) define the arrangement of the nodal force vectors:  $\{L1\}$ ,  $\{L2\}$ ,  $\{L12\}$ , calculated in the SD&SS program.

It is possible to include more than one data case in the ALOADS input data deck. If the SD&SS output tape input to ALOADS contains the results from a multiple data case SD&SS run, then including the same number of data cases in the ALOADS input deck will result in a one-to-one correspondence between the data cases of the two programs. That is, the first ALOADS data case will use the output data from the first SD&SS data case, the second ALOADS case uses output from the second SD&SS case, and so on. The ALOADS-5A input data deck was composed of six identical data cases; therefore, the same ALOADS calculations were made for each of the six data cases of SDSS-5A. "Elastic displacements" are calculated for both the elastic and rigid models. In the recycle SD&SS run the first three cases are flexible and the last three cases rigid. The rigid SD&SS cases result in the ALOADS program applying the rigid loads to the constrained flexibility matrix. The description given below applies for all six ALOADS-5A data cases.

- Six load points were specified. The first three were located along the centerline of the forward part of the fuselage. The remaining three were placed on the wing at approximately the midchord locations of three spanwise stations.
- The force and moment calculations at the first three load points were based only on the airloads which existed forward of their respective locations. The load points located on the wing were affected only by those airloads which occurred outboard of their locations.
- The reference lengths were different for each load point. The values used were based on the geometry of the airplane and the load point locations.

#### 4.6.4 Air Loads Program--ALOADS-5B

ALOADS-5B used the output tapes from GD-5B and SDSS-5B, and a tape containing a "hot" constrained flexibility matrix (of dimensions 1016x448) as tape input. The input data deck included six identical data cases, which were also exactly the same as those used in ALOADS-5A. Thus, the same airload calculations were performed for the supersonic case.



## 5.0 TIMING FOR THE DEMONSTRATION CASES

In this section the approximate computing times for each of the demonstration case runs are presented. Tables 5.0-1 through 5.0-5 give the times for the Dart Model I, Dart Model II, Boeing 707-320B, Boeing 2707-300PT (SST), and YF-12A Demonstration Cases, respectively. All of the demonstration case runs were executed on both the Boeing Computer Service's CDC 6600 and the NASA Ames Research Center CDC 7600 computer, except the plotting programs, GDPLOT, PDPLOT, EAPLOT, NMPLOT and THPLOT, which could not be exercised at the NASA ARC facility due to a lack of CALCOMP equipment. Where available, the central processor times and the "wall-clock" times at each installation are given.

It should be pointed out that the "wall-clock" execution times listed in the tables are highly system-dependent. Even using the same operating system on the same computer, they are generally nonrepeatable. Nevertheless, these times have been included in order to give the user a rough idea of the total processing time required by each run.

The Boeing Computer Service's CDC 6600 operates under the KRONOS 2.1 operating system using the FORTRAN EXTENDED (with option No. 1) compiler. The NASA Ames Research Center CDC 7600 computer system operates under the SCOPE 2.1 operating system using the FORTRAN EXTENDED (with option No. 1) compiler.

**TABLE 5.0-1.—TIMING FOR THE DART MODEL I DEMONSTRATION CASE**

Program name	Run name	Deck number	BCS 6600		LBL 7600	
			CPSECS	WCSECS	CPSECS	WCSECS
GD	GD-1	01-01	0.7	5	0.2	7
AIC	AIC-1	01-02	4.8	123	1.6	9
ISIC	ISIC-1	01-03	11.6	156	4.7	102
NM	NM-1	01-04	1.8	22	0.8	64
ESIC	ESIC-1	01-09	1.5	21	0.7	15
SD&SS	SDSS-1A	01-05	19.1	329	6.8	114
	SDSS-1B	01-06	28.8	381	10.8	127
	SDSS-1C	01-10	6.2	190	2.1	7
	SDSS-1D	01-11	18.8	525	3.7	20
TH	TH-1	01-07	1.6	73	0.5	3
SLOADS	SLOADS-1	01-08	0.4	3	0.1	1
ALOADS	ALOADS-1	01-12	0.5	7	0.1	3

CPSECS – Central processing seconds  
 WCSECS – "Wall clock" execution time (seconds)

**TABLE 5.0-2.—TIMING FOR THE DART MODEL II DEMONSTRATION CASE**

Program name	Run name	Deck number	BCS 6600		LBL 7600	
			CPSECS	WCSECS	CPSECS	WCSECS
GD	GD-2	02-01	1.2	5	0.3	3
AIC	AIC-2	02-02	18.8	740	5.0	51
SD&SS	SDSS-2	02-03	17.7	1210	7.5	62

CPSECS – Central processing seconds  
 WCSECS – "Wall clock" execution time (seconds)

TABLE 5.0-3.—TIMING FOR THE BOEING 707-320B DEMONSTRATION CASE

Program name	Run name	Deck number	BCS 6600		LBL 7600	
			CPSECS	WCSECS	CPSECS	WCSECS
GD	GD-3A	03-01	5.4	20	1.1	4
	GD-3B	03-08	5.9	20	1.1	3
GD PLOT	GD PLOT-3	03-10	17	89	—	—
AIC	AIC-3	03-02	806	3160	173	1281
ISIC	ISIC-3	03-03	1943	7010	551	2186
EAPLOT	EAPLOT-3	03-11	18	24	—	—
NM	NM-3	03-04	123	532	37	244
NM PLOT	NM PLOT-3	03-12	77	230	—	—
SD&SS	SDSS-3A	03-05	1717	6220	624	3628
	SDSS-3B	03-09	40	487	14	53
PD PLOT	PD PLOT-3	03-13	16	21	—	—
TH	TH-3	03-06	123	866	25	90
TH PLOT	TH PLOT-3	03-14	4	8	—	—
SLOADS	SLOADS-3	03-07	1.4	11	0.4	3

CPSECS — Central processing seconds

WCSECS — "Wall clock" execution time (seconds)

TABLE 5.0-4.—TIMING FOR THE BOEING 2707-300PT(SST) DEMONSTRATION CASE

Program name	Run name	Deck number	BCS 6600		LBL 7600	
			CPSECS	WCSECS	CPSECS	WCSECS
GD	GD-4	04-01	6.3	26	1.1	3
GD PLOT	GD PLOT-4	04-09	43	136	—	—
AIC	AIC-4	04-02	1639	25020	307	2440
CAIC	CAIC-4	04-07	6.2	431	1.4	11
ESIC	ESIC-4	04-03	367	2580	149	1113
SD&SS	SDSS-4A	04-04	644	4570	151	813
	SDSS-4B	04-05	1985	24860	440	2623
	SDSS-4C	04-08	2048	10410	440	3023
ALOADS	ALOADS-4	04-06	2.3	18	0.7	4

CPSECS — Central processing seconds  
 WCSECS — "Wall clock" execution time (seconds)

TABLE 5.0-5.—TIMING FOR THE LOCKHEED YF-12A DEMONSTRATION CASE

Program name	Run name	Deck number	BCS 6600		LBL 7600	
			CPSECS	WCSECS	CPSECS	WCSECS
GD	GD-5A	05-01	9.8	26	1.8	3
	GD-5B	05-06	8.9	N.A.	1.8	3
AIC	AIC-5A	05-02	3424	11600	596	3631
	AIC-5B	05-07	2355	N.A.	447	2928
ESIC	ESIC-5A	05-03	2157	31010	475	2900
	ESIC-5B	05-08	2106	N.A.	473	1110
SD&SS	SDSS-5A	05-04	1609	19350	365	1934
	SDSS-5B	05-09	1437	N.A.	364	1987
ALOADS	ALOADS-5A	05-05	82	N.A.	23	187
	ALOADS-5B	05-10	98	N.A.	23	187

CPSECS — Central processing seconds  
 WCSECS — "Wall clock" execution time (seconds)  
 N.A. — Not available



## 6.0 DEMONSTRATION CASE RESULTS, OTHER FLEXSTAB RESULTS AND COMPARISONS

This section presents a summary of the analysis program results for the 707-320B, SST and YF-12A Demonstration cases. For the 707 and SST cases, some of the results are compared with the similar results obtained from wind tunnel, flight test or project data. In addition, selected FLXSTAB results from a wing-body model of the SST airplane, and an arrow wing configuration (Reference 6-11) are compared with the wind tunnel results. The purpose of these comparisons is to provide a frame of reference for interpretation of the FLEXSTAB results for similar, future applications. Most of the data presented, and all of the data compared are output from the SD&SS program. The only other data presented are the dynamic characteristics derived from the TH program, and the structural deflections from the ALOADS program.

As mentioned previously, the Dart Model I and Dart Model II Demonstration cases were designed primarily to illustrate the preparation of input data, particularly for the airplane definition programs. Results from the analysis programs therefore have no engineering significance and are not listed here.\* However, they do provide some validation of the engineering formulation and associated assumptions. The SD&SS results confirmed the equivalence of the two Dart Model I structural definitions (see Sect. 3.2.5) for the symmetric reference motion. The ISIC structural model results from SDSS-1A and SDSS-1B were identical in all respects to the ESIC model results obtained from SDSS-1C and SDSS-1D, respectively. In addition, the symmetry properties of Dart Model II were reflected in the aerodynamic results of the SDSS-2 run results as anticipated in Section 3.3. From the stability derivatives output in the static stability section, the following relations were seen to be approximately true (approximate due to the coordinate transformation through  $\alpha$ ):

$$C_{L_a} = -C_{Y_\beta} ; C_{m_a} = -\frac{b}{\bar{c}} C_{n_\beta}$$
$$C_{L_Q} = \frac{b}{\bar{c}} C_{Y_R} ; C_{m_Q} = \left(\frac{b}{\bar{c}}\right)^2 C_{n_R}$$

In the dynamic stability section of the SD&SS program, the compressibility effects are added to the yaw rate derivatives. It is assumed that the compressibility effects are significant in the Y-direction (spanwise) but not in the Z-direction (vertical) due to the generally larger spanwise dimension relative to the vertical dimension. This assumption is obviously not true for the Dart II model. The Q- and R-derivatives printed in the dynamic stability section were therefore not equal.

---

\*The output listings for the Dart Models I and II are included on the tape which contains the FLEXSTAB source code.

In the following subsections, the FLEXSTAB results are presented and compared, or simply presented in a tabular format. The accompanying text makes no attempt to discuss all of the data; however, comments are made concerning those comparative data from which useful conclusions can be drawn.

## 6.1 RESULTS AND COMPARISONS OF THE BOEING 707-320B DEMONSTRATION CASE

Results obtained from both rigid and elastic models of the 707-320B aircraft are presented. The aerodynamic stability and control data calculated by the FLEXSTAB program are compared with wind tunnel, handbook and project data. The FLEXSTAB data discussed are identified by the Run name and Deck number (see Table 4.0-1). These Run numbers and some pertinent information relating to each are tabulated below:

Run Name, Deck Number	Shape	Structural Model	Source of Coefficients
SDSS-3X (not a demonstration case)*	Cruise	Rigid	FLEXSTAB
SDSS-3A, 03-05 (residual elastic)	Cruise	Residual elastic	FLEXSTAB
SDSS-3A, 03-05 (static elastic)	Cruise	Static elastic (Recycle case)	FLEXSTAB
SDSS-3B, 03-09	Cruise	Rigid	External

Tables 6.1.1, 6.1.2 and 6.1.3 present a comparison of the results of SDSS-3X calculations with results obtained from handbook methods as calculated in Reference 6-1,\*\* demonstration case SDSS-3B, and with wind tunnel data.\*\*\* The aerodynamic coefficients  $C_{L_0}$ ,  $C_{D_0}$ , and  $C_{m_0}$  are calculated in FLEXSTAB at  $\alpha = 0$  and  $\delta_e = 0$ . From the tabulated data it is apparent that the FLEXSTAB value of the lift coefficient is substantially higher than that for the wind tunnel (0.317 vs. 0.216) data, but that the pitching moment coefficient  $C_{m_0}$  agrees very well. To obtain comparable drag coefficients (the value of  $C_{D_0}$  computed by FLEXSTAB does not include viscous effects) the skin friction, calculated in Reference 6-2 as .0132, was deducted from the wind tunnel value of .0209. The result, .0077, is 10% lower than the FLEXSTAB value of .0086. However, since it is not possible to estimate the accuracy of the skin friction computation, or to appraise the effect of Reynolds number on the wind tunnel drag data, definitive conclusions cannot be drawn.

---

\*The cruise shape geometry from the demonstration case GD-3B and the aerodynamics from the demonstration case AIC-3 were used to obtain the computed data for SDSS-3X.

\*\*The handbook data in Reference 6-1 were derived from the 1960 edition of the USAF DATCOM.

\*\*\*The SDSS-3B results are equivalent to the wind tunnel data, since the wind tunnel data were input as tabular series in the demonstration case SDSS-3B.

TABLE 6.1-1.—COMPARISON OF METHODS FOR CALCULATING  
AERODYNAMIC STABILITY AND CONTROL DATA—  
BOEING 707-320B(RIGID)

$M_1 = 0.8$ ,  $h_1 = 35,000$  ft,  $\gamma_1 = 0.0$ ,  $cg = 0.25\bar{c}$ ,  $wt = 268,000$  lb

Parameter	Unit	FLEXSTAB <sup>a</sup> (balanced solution) SDSS-3X	HANDBOOK METHODS (reference 6-1)		WIND TUNNEL	
			NACA TR 1098	USAF DATCOM	Data	Origin
$\alpha_1$	deg	1.156	NA	NA	2.218	SDSS-3B
$T_1$	lb	16424	NA	NA	18113	SDSS-3B
$\delta e_1$	deg	-2.374	NA	NA	-3.03	SDSS-3B
$C_{L_o}$	—	0.317	NA	NA	0.216	SDSS-3B
$C_{D_o}$	—	0.00863 <sup>b</sup>	NA	NA	0.0209 0.0077 <sup>c</sup>	SDSS-3B
$C_{m_o}$	—	-0.0750	NA	NA	-0.076	SDSS-3B
$C_{L_\alpha}$	deg <sup>-1</sup>	0.110	NA	0.1065	0.1057	ref. 4-1
$C_{D_\alpha}$	deg <sup>-1</sup>	0.00359	NA	0.00425	0.00442	ref. 4-1
$C_{m_\alpha}$	deg <sup>-1</sup>	-0.0195	NA	-0.0361	-0.0180	ref. 4-1
$C_{L_Q}$	rad <sup>-1</sup>	12.789	NA	10.3	NA	
$C_{D_Q}$	rad <sup>-1</sup>	0.315	NA	NA	NA	
$C_{m_Q}$	rad <sup>-1</sup>	-18.527	NA	-17.8	NA	
$C_{L_{\delta e}}$	deg <sup>-1</sup>	0.0136	NA	0.0144	0.0147	ref. 4-1
$C_{D_{\delta e}}$	deg <sup>-1</sup>	0.000320	NA	NA	NA	
$C_{m_{\delta e}}$	deg <sup>-1</sup>	-0.0393	NA	-0.0419	-0.0419	ref. 4-1
$C_{L_u}$	—	0.383 <sup>d</sup>	NA	NA	0.444 <sup>d</sup>	ref. 4-1
$C_{D_u}$	—	0.0169 <sup>d</sup>	NA	NA	0.0304 <sup>d</sup>	ref. 4-1
$C_{m_u}$	—	-0.0564 <sup>d</sup>	NA	NA	-0.0154 <sup>d</sup>	ref. 4-1

TABLE 6.1-1.—CONTINUED

$M_1 = 0.8, h_1 = 35,000 \text{ ft}, \gamma_1 = 0.0, c_g = 0.25\bar{c}, wt = 268,000 \text{ lb}$

Parameter	Unit	FLEXSTAB <sup>a</sup> (balanced solution) SDSS-3X	HANDBOOK METHODS (reference 6-1)		WIND TUNNEL	
			NACA TR 1098	USAF DATCOM	Data	Origin
$C_{Y_P}$	rad <sup>-1</sup>	-0.131	-0.115	-0.0850	NA	
$C_{\ell_P}$	rad <sup>-1</sup>	-0.517	-0.412	-0.437	NA	
$C_{n_P}$	rad <sup>-1</sup>	-0.0289	-0.0123	-0.0290	NA	
$C_{Y_R}$	rad <sup>-1</sup>	0.661	0.349	NA	NA	
$C_{\ell_R}$	rad <sup>-1</sup>	0.255	0.245	0.222	NA	
$C_{n_R}$	rad <sup>-1</sup>	-0.261	-0.200	NA	NA	
$C_{L\dot{a}}$	rad <sup>-1</sup>	-7.311	NA	-1.350	NA	
$C_{D\dot{a}}$	rad <sup>-1</sup>	-0.298	NA	NA	NA	
$C_{m\dot{a}}$	rad <sup>-1</sup>	-12.490	NA	-21.000	NA	
$C_{Y_\beta}$	deg <sup>-1</sup>	-0.0115	NA	-0.00876	-0.0158	ref. 4-3
$C_{\ell_\beta}$	deg <sup>-1</sup>	-0.00228	NA	-0.00305	-0.00323	ref. 4-3
$C_{n_\beta}$	deg <sup>-1</sup>	0.00302	NA	0.00162	0.00297	ref. 4-3
$C_{L\dot{Q}}$	rad <sup>-1</sup>	-26.441	NA	NA	NA	
$C_{D\dot{Q}}$	rad <sup>-1</sup>	-0.983	NA	NA	NA	
$C_{m\dot{Q}}$	rad <sup>-1</sup>	-8.691	NA	NA	NA	
$C_{Y_{\dot{\beta}}}$	rad <sup>-1</sup>	-0.148	NA	0.0250 <sup>e</sup>	NA	
$C_{\ell_{\dot{\beta}}}$	rad <sup>-1</sup>	0.00603	NA	0.00244 <sup>e</sup>	NA	
$C_{n_{\dot{\beta}}}$	rad <sup>-1</sup>	-0.00525	NA	-0.0107 <sup>e</sup>	NA	
$C_{Y_{\dot{P}}}$	rad <sup>-1</sup>	-0.129	NA	NA	NA	
$C_{\ell_{\dot{P}}}$	rad <sup>-1</sup>	0.0139	NA	NA	NA	
$C_{n_{\dot{P}}}$	rad <sup>-1</sup>	0.0639	NA	NA	NA	

TABLE 6.1-1.—CONCLUDED

$M_1 = 0.8, h_1 = 35,000 \text{ ft}, \gamma_1 = 0.0, c_g = 0.25\bar{c}, wt = 268,000 \text{ lb}$

Parameter	Unit	FLEXSTAB <sup>a</sup> (balanced solution) SDSS-3X	HANDBOOK METHODS (reference 6-1)		WIND TUNNEL	
			NACA TR 1098	USAF DATCOM	Data	Origin
$C_{Y\dot{R}}$	rad <sup>-1</sup>	-0.0421	NA	NA	NA	
$C_{\ell\dot{R}}$	rad <sup>-1</sup>	-0.00126	NA	NA	NA	
$C_{n\dot{R}}$	rad <sup>-1</sup>	-0.0109	NA	NA	NA	
$C_{Y\delta_a}$	deg <sup>-1</sup>	-0.000107	NA	NA	NA	
$C_{\ell\delta_a}$	deg <sup>-1</sup>	-0.00144	NA	NA	-0.000605	ref. 6-2
$C_{n\delta_a}$	deg <sup>-1</sup>	-0.000069	NA	NA	NA	
$C_{Y\delta_r}$	deg <sup>-1</sup>	0.00701	NA	NA	NA	
$C_{\ell\delta_r}$	deg <sup>-1</sup>	0.000439	NA	NA	0.000234	ref. 6-2
$C_{n\delta_r}$	deg <sup>-1</sup>	-0.00324	NA	NA	-0.00138	ref. 6-2
$h_n$ <sup>-h</sup>	% $\bar{c}$	17.64	NA	33.8	17.06	SDSS-3B
$h_n$	% $\bar{c}$	42.64	NA	58.8	42.1	SDSS-3B
$h_m$ <sup>-h</sup>	% $\bar{c}$	20.38	NA	36.5	19.7	SDSS-3B
$h_m$	% $\bar{c}$	45.38	NA	61.5	44.7	SDSS-3B
$\Delta\delta e/n-1$	deg/g	-2.243	NA	-4.20	-2.565	SDSS-3B
$d\delta e/dV$	deg/(ft/sec)	0.0050	NA	0.0135	0.0064	SDSS-3B

<sup>a</sup>Not a Demonstration case

<sup>b</sup>FLEXSTAB does not include viscous drag

<sup>c</sup>Wind tunnel measured drag less calculated skin friction drag (see text)

$$d \quad C_{L_u} = M_1 \frac{\partial C_L}{\partial M}, \quad C_{D_u} = M_1 \frac{\partial C_D}{\partial M}, \quad C_{m_u} = M_1 \frac{\partial C_m}{\partial M}$$

<sup>e</sup>Calculated by considering only the vertical tail

**TABLE 6.1-2.—COMPARISON OF METHODS FOR CALCULATING LONGITUDINAL DYNAMIC CHARACTERISTICS—BOEING 707-320B (RIGID)**

$M_1 = 0.8, h_1 = 35,000 \text{ ft}, \gamma_1 = 0.0, c_g = 0.25\bar{c}, wt = 268,000 \text{ lb.}$

Results from		FLEXSTAB <sup>a</sup> with all program calculated derivatives (SDSS-3X)	FLEXSTAB with empirical data input (SDSS-3B)	Reference 6-1	
				USAF DATCOM	WIND TUNNEL
SHORT PERIOD	Period sec	3.76	4.26	2.75	3.53
	$T_{1/2}$ or $T_2^*$ sec	0.705	0.607	0.612	0.592
	$C_{1/2}$ or $C_2^*$ cycles	0.188	0.142	0.222	0.167
PHUGOID	Period sec	112	171	148	247
	$T_{1/2}$ or $T_2^*$ sec	297	283	590	500†
	$C_{1/2}$ or $C_2^*$ cycles	2.64	1.65	4.0	2.0†

\*Time or cycles to half or twice the amplitude.

†Indicates it is for twice the amplitude.

<sup>a</sup>Not a demonstration case

**TABLE 6.1-3.—COMPARISON OF METHODS FOR CALCULATING LATERAL-DIRECTIONAL DYNAMIC CHARACTERISTICS—BOEING 707-320B (RIGID)**

Results from		FLEXSTAB <sup>a</sup> with all program calculated derivatives (SDSS-3X)	FLEXSTAB with empirical data input (SDSS-3B)	Reference 6-1		
				NACA TR1098	USAF DATCOM	WIND TUNNEL
DUTCH ROLL	Period sec	4.87	5.01	5.19	6.38	5.18
	$T_{1/2}$ or $T_2^*$ sec	7.25	12.6	15.2	23.7	12.2
	$C_{1/2}$ or $C_2^*$ cycles	1.48	2.52	2.95	3.70	2.30
ROLL CONVER- GENCE	$T_{1/2}$ or $T_2^*$ sec	0.714	0.774	0.839	0.779	0.565
SPIRAL MODE	$T_{1/2}$ or $T_2$ sec	141.7	310	125	62	270

\*Time or cycles to half or twice the amplitude

† Indicates it is for twice the amplitude

<sup>a</sup> Not a demonstration case



Inspection of the  $\alpha$  derivatives ( $C_{L\alpha}$ ,  $CD_{\alpha}$ ,  $C_{m\alpha}$ , Table 6.1.1) shows that for the SDSS-3X case, DATCOM predicts a slightly more accurate value for  $C_{L\alpha}$  than FLEXSTAB, and a substantially more accurate  $CD_{\alpha}$ . However, it is known that  $CD_{\alpha}$  is a strong function of  $\alpha$  and the difference in  $CD_{\alpha}$  from FLEXSTAB and DATCOM may be largely due to the difference in trim  $\alpha$ . The wind tunnel value of  $C_{m\alpha}$  is more closely predicted by FLEXSTAB than by DATCOM. For the  $\delta_e$  derivatives DATCOM predicts better values for both  $CL_{\delta_e}$  and  $C_{m\delta_e}$ . In the case of the  $\beta$ -derivatives ( $C_{Y\beta}$ ,  $C_{\ell\beta}$ ,  $C_{n\beta}$ ) FLEXSTAB produced distinctly better results than those obtained from handbook methods with the exception of  $C_{\ell\beta}$ . The longitudinal control and maneuvering parameters (static margin, maneuver point, elevator angle per g, etc.) computed by FLEXSTAB are all distinctly more accurate than those derived by use of DATCOM, and in general agree very well with the experimental results.

The speed derivatives calculated by the program may be compared with the simulator data after making adjustments to account for the differences in the definition of speed derivatives in FLEXSTAB and simulator data. In FLEXSTAB, the speed derivatives are calculated as illustrated for  $C_{L\hat{u}}$ :

$$\begin{aligned} C_{L_u} &= \frac{1}{\bar{q}_1 S_w} \frac{\partial}{\partial(u/U_1)} (q_1 S_w C_L) \\ &= 2C_{L_1} + \frac{\partial C_L}{\partial(u/U_1)} \end{aligned}$$

as opposed to the apparently similar definition of

$$C_{L_u} = \frac{\partial C_L}{\partial(u/U_1)}$$

The calculation of speed derivatives is influenced by the user input of  $\Delta M$ , in Card 4 of the AIC program. The recommended value of  $\Delta M = 0.1\beta$  was based on an empirical evaluation in 1971. It appears that the program changes since 1971 may have invalidated the 1971 recommendation. Until the recommendation of  $\Delta M = 0.1\beta$  is reviewed, it is suggested that the user execute the program at more than one Mach number to evaluate speed derivatives since:

$$C_{L_u} = 2C_{L_1} + \frac{\partial C_L}{\partial(u/U_1)} = 2C_{L_1} + M_1 \frac{\partial C_L}{\partial M} + 2q_1 \frac{\partial C_L}{\partial \bar{q}}$$

The  $\bar{q}$ -derivative is zero for a rigid model and  $\partial C_L / \partial M$  can be calculated from finite-difference approximation.

In summary, based upon the relatively few comparisons available for this case, it is seen that the DATCOM results for some of the derivatives are more accurate than those computed by FLEXSTAB, whereas the reverse is true for other derivatives and for the longitudinal control and maneuvering parameters.

Tables 6.1.2 and 6.1.3 contain the comparative results for the longitudinal- and lateral-directional dynamic characteristics, respectively. For the longitudinal results, the short period frequency result from SDSS-3X agrees better with the wind tunnel results than the handbook results. All methods predict a positively damped phugoid mode, whereas the wind tunnel results give negative damping. The picture for the lateral results is mixed – but each method produces results which generally leave much to be desired.

Table 6.1.4 presents comparative data from the static-elastic and residual-elastic cases (both from SDSS-3A run), and simulator document. The simulator document from which the comparison data were reduced have been replaced with a more up-to-date document. The comparison with the previous simulator documents has been retained since the comparison data had been derived earlier and was readily available. For subsonic transport airplanes, the base derivatives for the simulator document are usually calculated with respect to a kinematically constrained axis system. These derivatives are modified based on pilot evaluation to obtain satisfactory correlation between the simulator response and the airplane response. Therefore, comparison with the simulator data is valuable if comparing airplane response but comparison of individual derivatives has obvious limitations.

In the output for a residual-elastic model, the stability derivatives printed under “Static Stability Derivatives” have different values than those printed under “Dynamic Stability Derivatives.” In Table 6.1.4, the values of derivatives listed under residual-elastic column are from the dynamic section of the program. For example, the following values of  $CL_{\alpha}$  are output in the two sections of the program for SDSS-3A:

$CL_{\alpha}$ Printed Under	Rigid	Elastic Increment	Total
Static Stability Derivatives	.110149	-.014775	.095374
Dynamic Stability Derivatives	.110149	-.009151	.100999

The difference noted in the elastic increment arises from the fact that the residual-elastic formulation is applicable in the dynamic section of the program. The incremental aeroelastic operator in the two cases is defined in Volume 1 as:

*Static Section*

$$[G_{\theta E}] = [G_T] [T_{TF}] [\Delta \tilde{D}^{-1}]_1 [A_{F\theta}], \quad (5.3-32)$$

Vol. I

where

$$[\Delta \tilde{D}^{-1}]_1 = [\tilde{D}]_1^{-1} - [I],$$

and

$$[\tilde{D}]_1 = [I] - \bar{q}_1 [A_{F\theta}] [\tilde{C}_{\theta T}]_1 [T_{TF}] \quad (5.3-5)$$

Vol. I

**TABLE 6.1-4.—COMPARISON OF METHODS FOR CALCULATING  
AERODYNAMIC STABILITY AND CONTROL DATA—  
BOEING 707-320B (FLEXIBLE)**

$M_1 = 0.8, h_1 = 35,000 \text{ ft}, \gamma_1 = 0.0, c_g = 0.25\bar{c}, wt = 268,000 \text{ lb}$

Parameter	Unit	FLEXSTAB (balanced solution) SDSS-3A (STATIC- ELASTIC)	FLEXSTAB  SDSS-3A (RESIDUAL ELASTIC)	HANDBOOK RESULTS (reference 6-1) USAF DATCOM	FLIGHT SIMULATOR DOCUMENT (references 6-3, 6-4)
$a_1$	deg	1.624	1.624	NA	2.28
$T_1$	lb	19548	19548	NA	13700
$\delta e_1$	deg	-1.960	-1.960	NA	-3.7 <sup>a</sup>
$C_{L_o}$	—	0.277	0.277	NA	0.247
$C_{D_o}$	—	0.00659 <sup>b</sup>	0.00659 <sup>b</sup>	NA	0.0154
$C_{m_o}$	—	-0.0520	-0.0520	NA	-0.0736
$C_{L_a}$	deg <sup>-1</sup>	0.0954	0.1010	0.0933	0.0897
$C_{D_a}$	deg <sup>-1</sup>	0.00408	0.00448	NA	0.00379
$C_{m_a}$	deg <sup>-1</sup>	-0.00855	-0.01188	-0.0203	-0.0190
$C_{L_Q}$	rad <sup>-1</sup>	10.687	10.872	5.12	NA
$C_{D_Q}$	rad <sup>-1</sup>	0.428	0.441	NA	NA
$C_{m_Q}$	rad <sup>-1</sup>	-15.056	-15.162	-12.25	-15.07
$CL_{\delta_e}$	deg <sup>-1</sup>	0.0136	0.0123	0.00907	0.0100
$CD_{\delta_e}$	deg <sup>-1</sup>	0.00689 <sup>b</sup>	0.00060	NA	0.00042
$C_{m_{\delta_e}}$	deg <sup>-1</sup>	-0.0331	-0.0323	-0.0263	-0.0294
$C_{L_u}$	—	0.03904 <sup>c</sup>	0.2410 <sup>c</sup>	NA	0.122 <sup>c</sup>
$C_{D_u}$	—	0.0267 <sup>c</sup>	0.0167 <sup>c</sup>	NA	0.0288 <sup>c</sup>
$C_{m_u}$	—	-0.0529 <sup>c</sup>	-0.0187 <sup>c</sup>	NA	-0.0835 <sup>c</sup>

TABLE 6.1-4.—CONTINUED.

$M_1 = 0.8, h_1 = 35,000 \text{ ft}, \gamma_1 = 0.0, c_g = 0.25\bar{c}, wt = 268,000 \text{ lb}$

Parameter	Unit	FLEXSTAB (balanced solution) SDSS-3A (STATIC- ELASTIC)	FLEXSTAB  SDSS-3A (RESIDUAL ELASTIC)	HANDBOOK RESULTS (reference 6-1) USAF DATCOM	FLIGHT SIMULATOR DOCUMENT (references 6-3, 6-4)
$C_{Y_P}$	rad <sup>-1</sup>	-0.121	-0.116	-0.0943	-0.190
$C_{\ell_P}$	rad <sup>-1</sup>	-0.363	-0.457	-0.243	-0.393
$C_{n_P}$	rad <sup>-1</sup>	-0.0111	-0.0180	-0.0211	-0.0140
$C_{Y_R}$	rad <sup>-1</sup>	0.595	0.594	0.259	0.373
$C_{\ell_R}$	rad <sup>-1</sup>	0.183	0.184	0.231	0.1405
$C_{n_R}$	rad <sup>-1</sup>	-0.242	-0.241	-0.119	-0.1665
$C_{L\dot{\alpha}}$	rad <sup>-1</sup>	-6.078	-7.661	NA	NA
$C_{D\dot{\alpha}}$	rad <sup>-1</sup>	-0.292	-0.404	NA	NA
$C_{m\dot{\alpha}}$	rad <sup>-1</sup>	-11.338	-10.394	NA	-6.102
$C_{Y_\beta}$	deg <sup>-1</sup>	-0.0106	-0.0106	-0.00677	-0.0140
$C_{\ell_\beta}$	deg <sup>-1</sup>	-0.00203	-0.00170	-0.00488	-0.00296
$C_{n_\beta}$	deg <sup>-1</sup>	0.00268	0.00270	0.00076	0.00208
$C_{L\dot{Q}}$	rad <sup>-1</sup>	-24.209	-26.159	NA	NA
$C_{D\dot{Q}}$	rad <sup>-1</sup>	-1.131	-1.269	NA	NA
$C_{m\dot{Q}}$	rad <sup>-1</sup>	-8.113	-6.951	NA	NA
$C_{Y\dot{\beta}}$	rad <sup>-1</sup>	-0.131	-0.131	NA	NA
$C_{\ell\dot{\beta}}$	rad <sup>-1</sup>	0.00788	0.00961	NA	NA
$C_{n\dot{\beta}}$	rad <sup>-1</sup>	-0.0124	-0.0124	NA	0.0172

TABLE 6.1.4.—CONTINUED

$M_1 = 0.8, h_1 = 35,000 \text{ ft}, \gamma_1 = 0.0, c_g = 0.25\bar{c}, wt = 268,000 \text{ lb}$

Parameter	Unit	FLEXSTAB (balanced solution) SDSS-3A (STATIC- ELASTIC)	FLEXSTAB  SDSS-3A (RESIDUAL ELASTIC)	HANDBOOK RESULTS (reference 6-1) USAF DATCOM	FLIGHT SIMULATOR DOCUMENT (references 6-3, 6-4)
$C_{Y\dot{p}}$	rad <sup>-1</sup>	-0.117	-0.118	NA	NA
$C_{l\dot{p}}$	rad <sup>-1</sup>	0.013	0.032	NA	NA
$C_{n\dot{p}}$	rad <sup>-1</sup>	0.0585	0.0598	NA	NA
$C_{Y\dot{R}}$	rad <sup>-1</sup>	-0.0515	-0.0516	NA	NA
$C_{l\dot{R}}$	rad <sup>-1</sup>	-0.00186	-0.00303	NA	NA
$C_{n\dot{R}}$	rad <sup>-1</sup>	-0.00668	-0.00668	NA	NA
$C_{Y\delta_a}$	deg <sup>-1</sup>	-0.000165	-0.000160	NA	nil
$C_{l\delta_a}$	deg <sup>-1</sup>	-0.000891	-0.000991	NA	-0.000324
$C_{n\delta_a}$	deg <sup>-1</sup>	0.000008	0.000002	NA	nil
$C_{Y\delta_r}$	deg <sup>-1</sup>	0.00469	0.00466	NA	0.00395
$C_{l\delta_r}$	deg <sup>-1</sup>	0.000472	0.000108	NA	0.00040
$C_{n\delta_r}$	deg <sup>-1</sup>	-0.00223	-0.00223	NA	-0.00170
$h_n$ -h	% $\bar{c}$	8.97	8.97	21.7	21.3
$h_n$	% $\bar{c}$	33.97	33.97	46.7	46.3
$\Delta h_n$ (E-R)	% $\bar{c}$	-8.54	-8.54	NA	NA
$h_m$	% $\bar{c}$	36.19	36.19	48.7	48.49
$h_m$ -h	% $\bar{c}$	11.19	11.19	23.7	23.49
$\Delta\delta e/n-1$	deg/g	-1.431	-1.431	-3.70	-3.499

TABLE 6.1-4.—CONCLUDED

$$M_1 = 0.8, h_1 = 35,000 \text{ ft}, \gamma_1 = 0.0, c_g = 0.25\bar{c}, wt = 268,000 \text{ lb}$$

Parameter	Unit	FLEXSTAB (balanced solution) SDSS-3A (STATIC- ELASTIC)	FLEXSTAB  SDSS-3A (RESIDUAL ELASTIC)	HANDBOOK RESULTS (reference 6-1) USAF DATCOM	FLIGHT SIMULATOR DOCUMENTS (references 6-3, 6-4)
$d\delta e/dV$	deg/ ft/sec	0.0027	0.0027	0.0053	NA

<sup>a</sup>From reference 6-2

<sup>b</sup>FLEXSTAB does not include viscous drag

<sup>c</sup>

$$C_{L_u} = \frac{\partial C_L}{\partial u} = M_1 \frac{\partial C_L}{\partial M} + 2\bar{q}_1 \frac{\partial C_L}{\partial \bar{q}}; \text{ similarly for } C_{D_u} \text{ and } C_{m_u}$$

Dynamic Section

$$[G_{R\theta E}] = [G_T] [T_{TF}] [\Delta \tilde{D}_R^{-1}] [A_{F\theta}] \quad (6.3-28)$$

Vol. I

where

$$[\Delta \tilde{D}_R^{-1}] = [\tilde{D}_R]^{-1} - [N], \quad (6.3-26)$$

Vol. I

$$[\tilde{D}_R]_1 = [N] - \bar{q}_1 [A_{F\theta}] [\tilde{C}_{R\theta T}]_1 [T_{TF}], \quad (6.3-27)$$

Vol. I

and

$$[\tilde{C}_{R\theta T}] = [\tilde{C}_{\theta T}]_1 - [P_\theta] [\phi_{\delta_1}] [K_1]^{-1} [\phi_{\delta_1}]^T [P_T]^T$$

The last equation is obtained by combining equations (4.2-83) and (6.3-2) of Volume I. To understand the above equations in detail, reference should be made to Volume I. The differences in the derivatives can be explained by the differences in the  $[G_{\theta E}]$  and  $[G_{R\theta E}]$ . These aeroelastic increments to the rigid forces and hence the derivatives are calculated in the static section from  $[G_{\theta E}]$ , and in the dynamic section from  $[G_{R\theta E}]$ . Since the contribution of the modal degrees of freedom is deleted from the static-elastic, free-free flexibility matrix,  $[\tilde{C}_{\theta T}]$ , to obtain  $[\tilde{C}_{R\theta T}]$ , the aeroelastic increments in the dynamic

section are different than those in the static section. The modal degrees of freedom appear in the perturbation equations of motion and contribute to perturbation forces as illustrated by the perturbation aerodynamic forces

$$\begin{aligned} \{F_B^A\}_P &= [A_1^A] \{V\}_P + [A_2^A] \{\dot{V}\}_P + [A_3^A] \{u_1\}_P + \\ & [A_4^A] \{\dot{u}_1\}_P + [A_5^A] \{\ddot{u}_1\}_P \end{aligned} \quad (6.2-4)$$

Vol. I

where  $\{V\}_P$  contains perturbations to the components of the rigid body translation and angular velocities, and  $\{u_1\}$  are the amplitudes of the free vibration modes. For static-elastic model there are only the  $\{V\}_P$  and  $\{\dot{V}\}_P$  terms, and the total flexibility contribution due to  $[\tilde{C}_{\theta T}]$  is via  $[A_1^A]$  and  $[A_2^A]$  whose coefficients are the force derivatives. In case of the residual-elastic model, the total flexibility contribution is introduced through the force derivatives determined from the residual flexibility matrix,  $[\tilde{C}_{R\theta T}]$ , and the modal degrees of freedom,  $\{u_1\}$ . These differences affect the results from the linear dynamic analysis performed in the SD&SS program, and the nonlinear dynamic analysis performed in the TH program.

The comments about the speed derivatives made with reference to Table 6.1-1 are also applicable to the speed derivatives for the flexible airplane. However, for a flexible model,  $\partial C_L / \partial \bar{q}$  is not zero and can be calculated by recycling on  $\bar{q}$  in the SD&SS program and using the finite-difference approximation for a derivative.

The dynamic stability characteristics calculated by the SD&SS program for flexible models. SDSS-3A (static-elastic) and SDSS-3A (residual-elastic), are compared in Tables 6.1-5 and 6.1-6. The results labeled semi-empirical were calculated using stability derivatives determined as illustrated below for  $C_{m\alpha}$ :

$$C_{m\alpha} = \left( C_{m\alpha \text{Wind Tunnel}} \right) \left( \frac{C_{m\alpha \text{Elastic}}}{C_{m\alpha \text{Rigid}}} \right)_{\text{Computed}}$$

where the elastic-rigid ratio was computed from a lifting-surface theory computer program. This program used a "flat-airplane" representation and was limited to a maximum of 80 panels. For the Dutch roll, Table 6.1-6, the semi-empirical results from Reference 6-1 do not agree well with the flight test results. The FLEXSTAB results for the static-elastic and residual-elastic models are not significantly different indicating that the 707-320B responds in an essentially static-elastic manner. There is no significant coupling between the rigid body and elastic degrees of freedom since the frequencies of the elastic degrees of freedom were much higher than those of the rigid body motions (see Table 6.1-7).

The TH-3 demonstration run, based on SDSS-3A (residual-elastic) data, calculated the nonlinear dynamic motion of the 707-320B in response to given initial perturbation velocities. The results of this run are presented in the form of graphic displays produced

**TABLE 6.1-5.—COMPARISON OF METHODS FOR CALCULATING LONGITUDINAL DYNAMIC CHARACTERISTICS—BOEING 707-320B (FLEXIBLE)**

$$M_1 = 0.8, h_1 = 35,000 \text{ ft}, \gamma_1 = 0.0, cg = 0.25\bar{c}, wt = 268,000 \text{ lb}$$

Results from		FLEXSTAB Static-Elastic model	FLEXSTAB Residual-Elastic model	Semi-empirical Static-Elastic Model (reference 6-1)
SHORT PERIOD	Period sec	6.038	6.086	3.66
	$T_{1/2}$ or $T_2^*$	0.825	0.836	0.662
	$C_{1/2}$ or $C_2^*$ cycles	0.137	0.137	0.180
PHUGOID	Period sec	96.90	96.478	123
	$T_{1/2}$ or $T_2^*$ sec	300.39	263.251	730
	$C_{1/2}$ or $C_2^*$ cycles	3.100	2.729	6.1

\*Time or cycles to half or twice the amplitude

† Indicates it is for twice the amplitude

by THPLOT-3, Figures 6.1-1 through 6.1-12, give the results for the five TH-3 data cases (see Sect. 4.4.4). The first data case corresponds to a u-perturbation of 600 inches per second chosen to excite the phugoid mode. In order to excite the Dutch-roll-mode, a v-perturbation of 600 inches per second was specified in the second case. Comparisons of the results from these two data cases (as read from the corresponding THPLOT traces) with the linear dynamic characteristics calculated by the first data case of SDSS-3A are given in Tables 6.1-8 and 6.1-9. The agreement shown in these comparisons indicates that the response of the 707-320B to these perturbation velocities is essentially linear. Note the participation of the first symmetric free-vibration mode in the w-perturbation results (Figures 6.1-7 through 6.1-9 and in the gust response (Figures 6.1-12 and 6.1-13).

The computer run PDPLOT-3 produced a graphic display of the lifting Thin Body pressure distribution calculated in SDSS-3B. A portion of these results are shown in Figure 6.1.14. There is one plot for each inboard streamwise panel row of each Thin Body (with the exception of the vertical tail which carries no load in symmetric reference flight). Each plot is identified by body name as well as the Y- and Z-coordinates of the line passing through the  $Y_N$ -centroid of the panel row.

It is noted that the FLEXSTAB model was fairly sparsely paneled (see Figure 3.4-13). The effect of denser paneling on the results was not evaluated. Therefore, it is not known if a greater paneling density would have given substantially improved results for this case.



**TABLE 6.1-6.—COMPARISON OF METHODS OF CALCULATING LATERAL-DIRECTIONAL DYNAMICS CHARACTERISTICS—BOEING 707-320B (FLEXIBLE)**

$M_1 = 0.8, h_1 = 35,000 \text{ ft}, \gamma_1 = 0.0, c_g = 0.25\bar{c}, \text{wt} = 268,000 \text{ lb}$

Results from		FLEXSTAB Static-Elastic model	FLEXSTAB Residual-Elastic model	Flight Test (ref. 6-5)	Semi-Empirical Static-Elastic model (ref. 6-1)
DUTCH ROLL	Period sec	5.213	5.254	5.8	7.95
	$T_{1/2}$ or $T_2^*$ sec	8.029	7.664	12.8	6.1†
	$C_{1/2}$ or $C_2^*$ cycles	1.540	1.459	2.21	0.73†
	$ \theta/\beta $	0.735	0.723	0.448	—
	Phase angle degrees	-29.477	-29.016	-40	—
Roll convergence $T_{1/2}$ - sec		0.996	1.007	—	0.939
Spiral mode $T_{1/2}$ or $T_2^*$ sec		682.134†	1026.09†	—	22.0

\*Time or cycles to half or twice the amplitude

† Indicates it is for twice the amplitude

**TABLE 6.1-7.—COMPARISON OF BOEING 707-320B RIGID BODY AND NORMAL MODES FREQUENCIES—SDSS-3A (RESIDUAL ELASTIC)**

Longitudinal		Lateral-directional	
Mode	Freq., cps	Mode	Freq., cps
Short-period	0.164	Dutch Roll	0.190
1st symmetric free vibration	1.194	1st antisymmetric free vibration	1.883

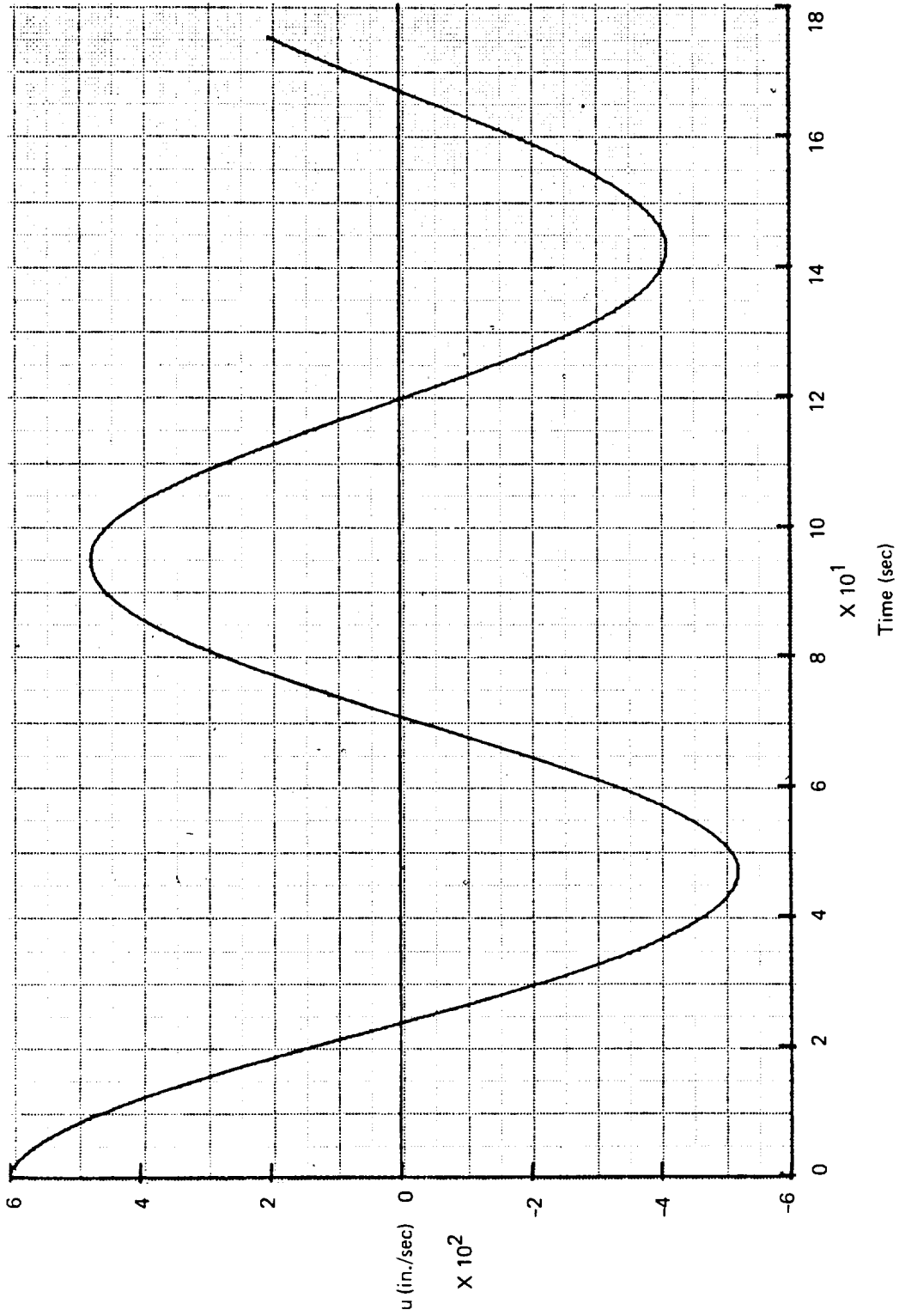


FIGURE 6.1-1.—707-320B, THPLOT-3,  $u$ -PERTURBATION = 600 IPS,  $u$  VS TIME;  
 BASED ON SDSS-3A (RESIDUAL ELASTIC) DATA

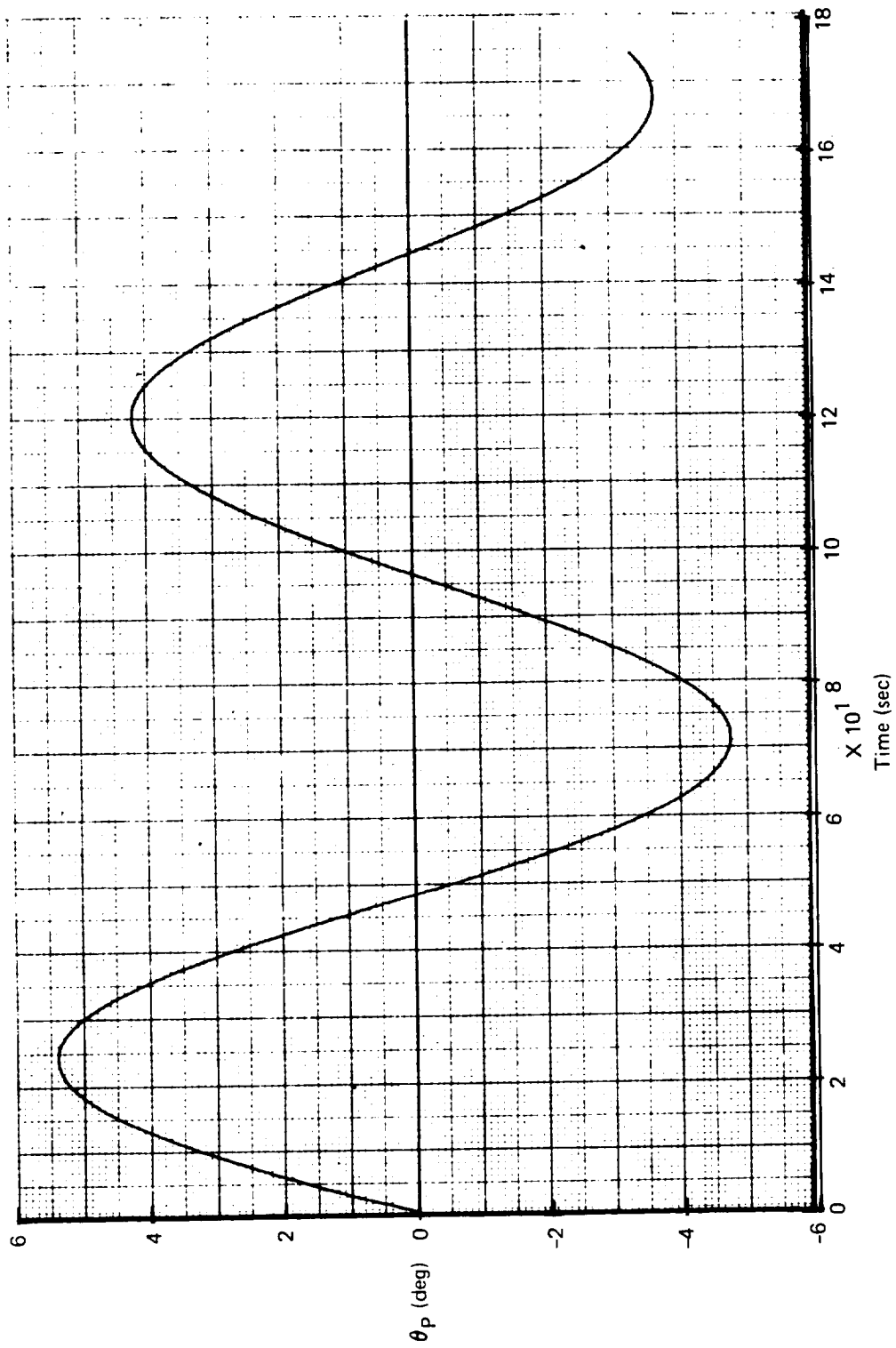


FIGURE 6.1-2.—707-320B, THPLOT-3,  $u$ -PERTURBATION = 600 IPS,  $\theta_p$  VS TIME;  
 BASED ON SDSS-3A (RESIDUAL ELASTIC) DATA

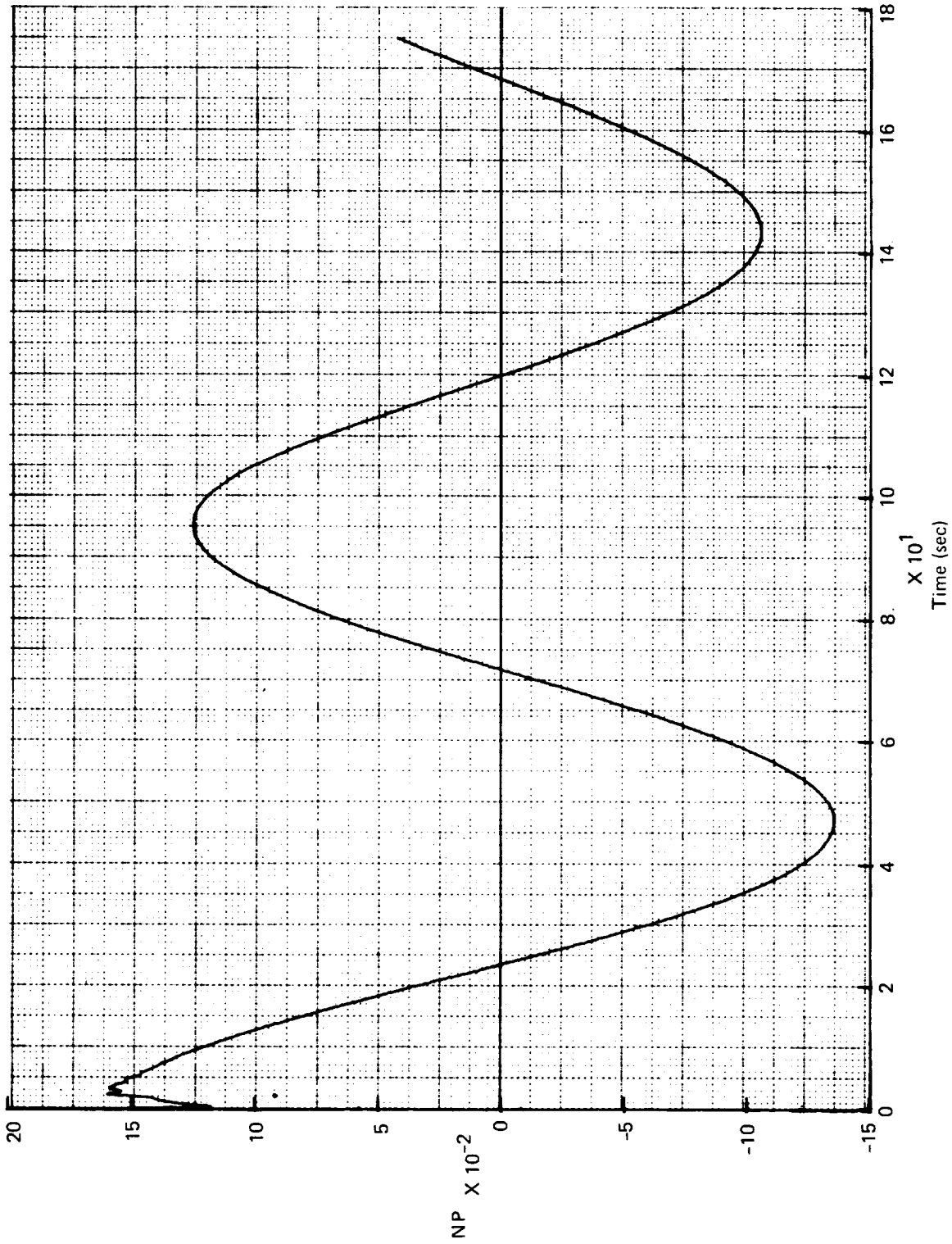


FIGURE 6.1-3.—707-320B, THPLOT-3,  $u$ -PERTURBATION = 600 IPS,  $N_P$  VS TIME;  
 BASED ON SDSS-3A (RESIDUAL ELASTIC) DATA

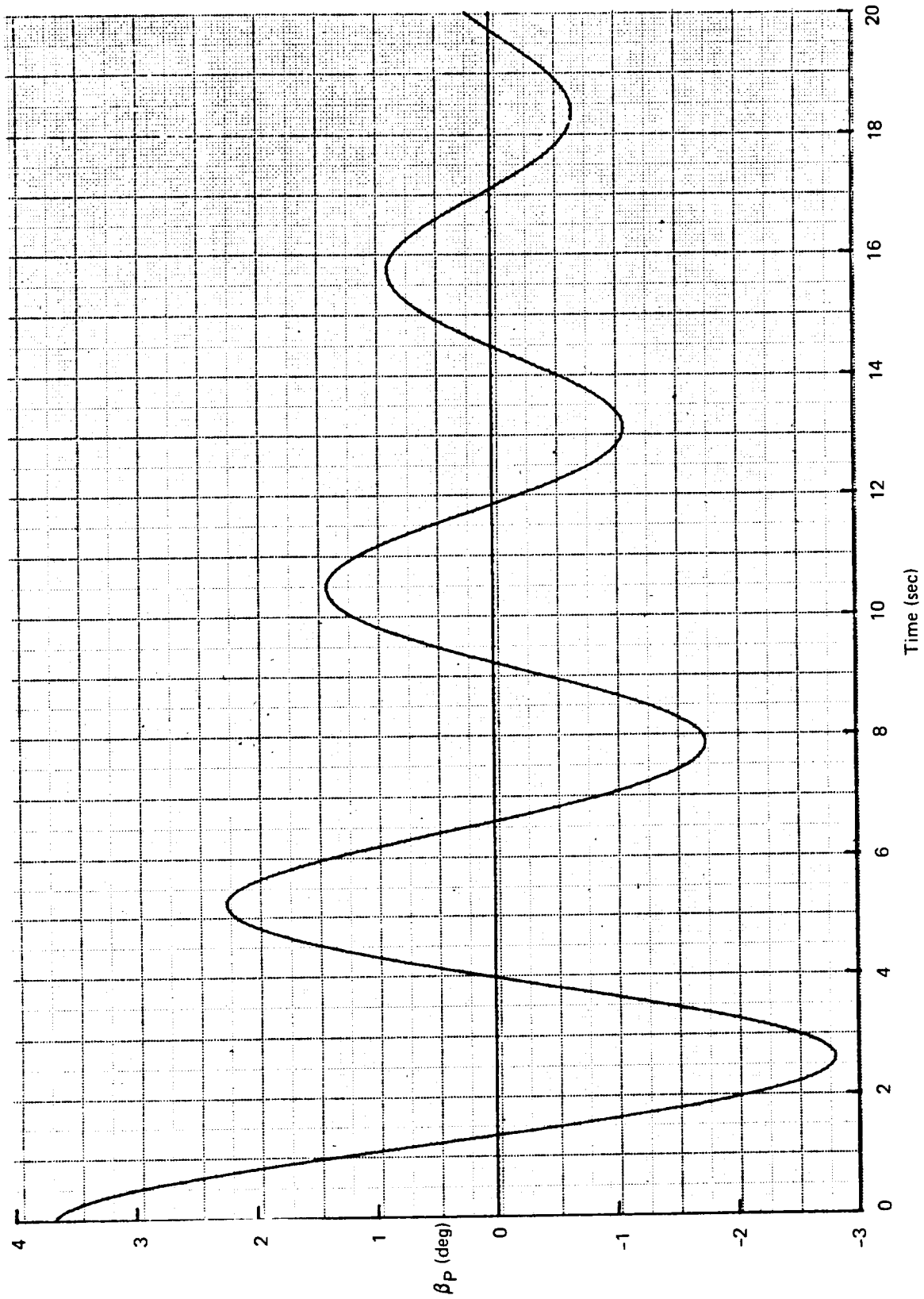


FIGURE 6.1-4. -707-320B, THPLOT-3,  $v$ -PERTURBATION = 600 IPS,  $\beta_p$  VS TIME;  
 BASED ON SDSS-3A (RESIDUAL ELASTIC) DATA

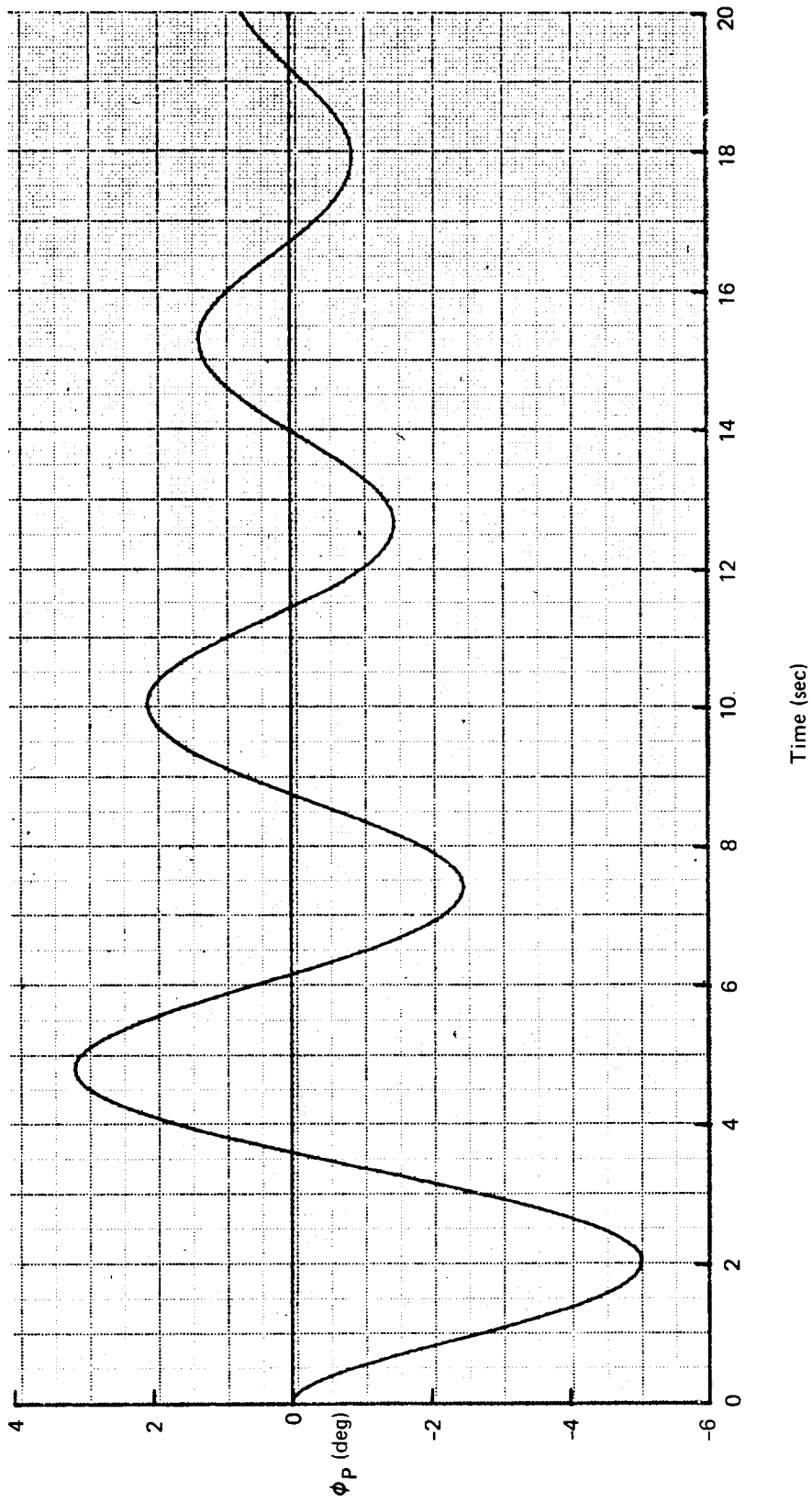


FIGURE 6.1-5.—707-320B, THPLOT-3,  $\nu$ -PERTURBATION = 600 IPS,  $\phi_p$  VS TIME;  
 BASED ON SDSS-3A (RESIDUAL ELASTIC) DATA

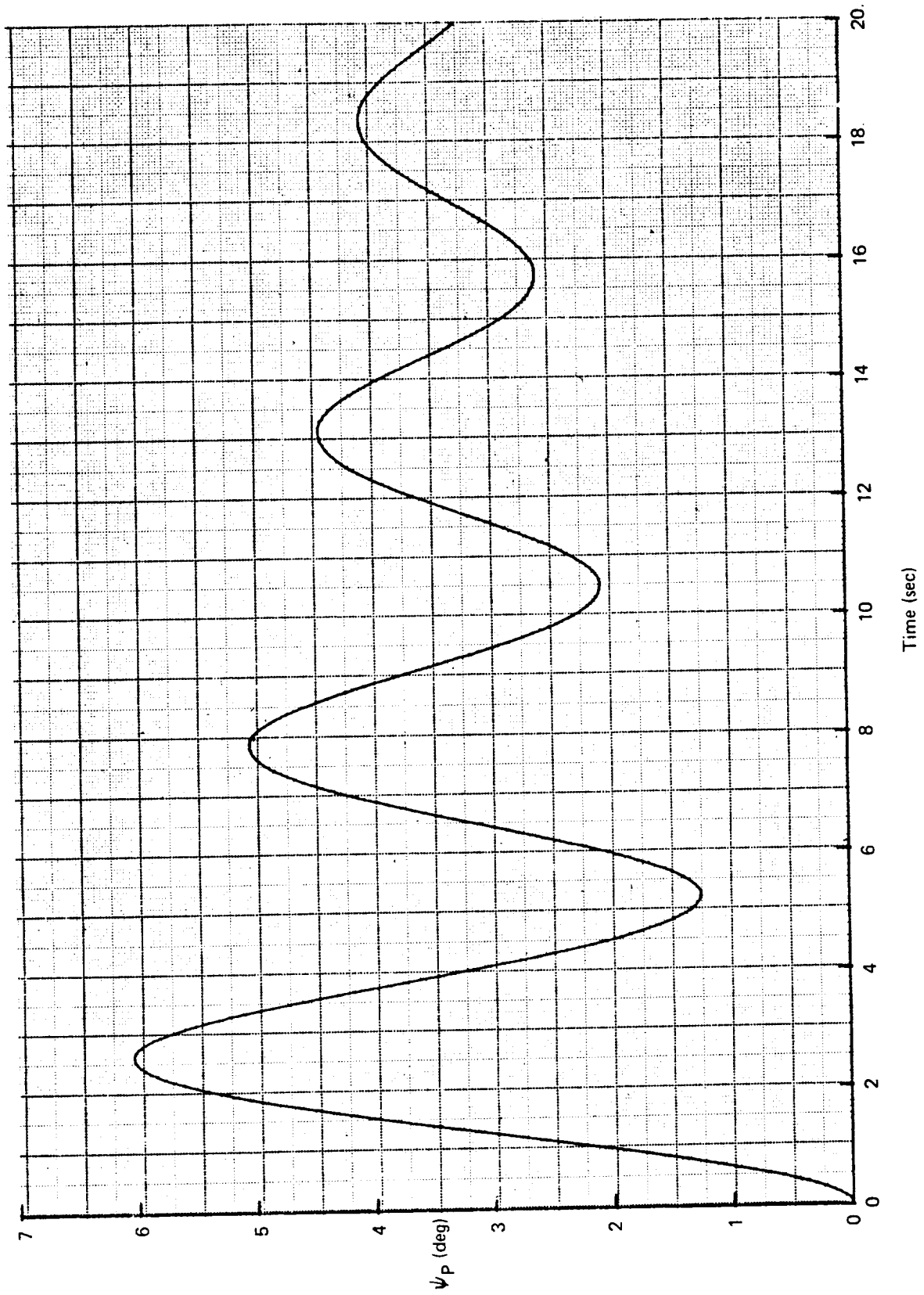


FIGURE 6.1-6.—707-320B, THPLOT-3, v-PERTURBATION = 600 IPS,  $\psi_p$  VS TIME;  
 BASED ON SDSS-3A (RESIDUAL ELASTIC) DATA

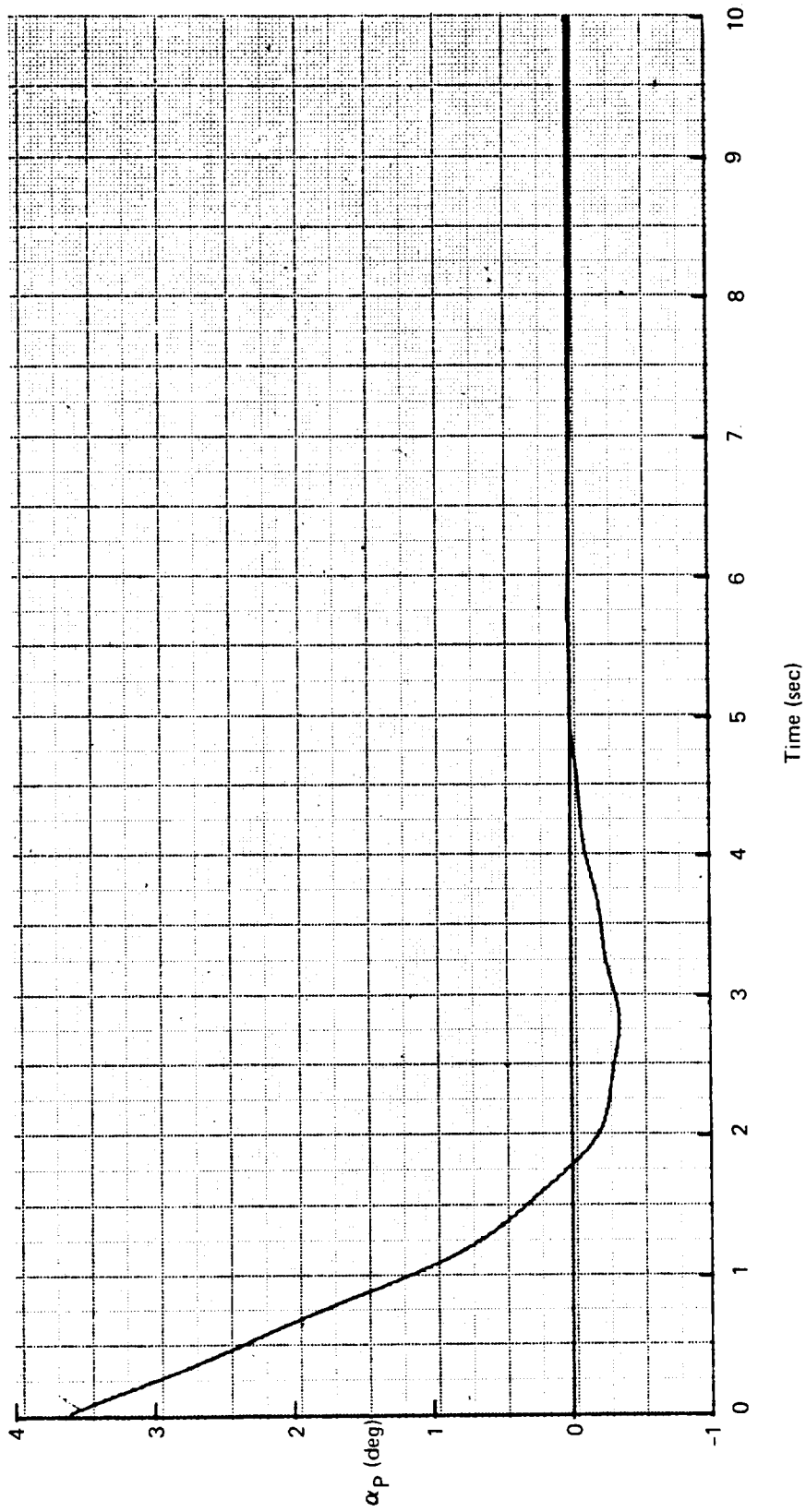


FIGURE 6.1-7. -707-320B, THPLOT-3, w-PERTURBATION = 600 IPS,  $\alpha_p$  VS TIME;  
 BASED ON SDSS-3A (RESIDUAL ELASTIC) DATA



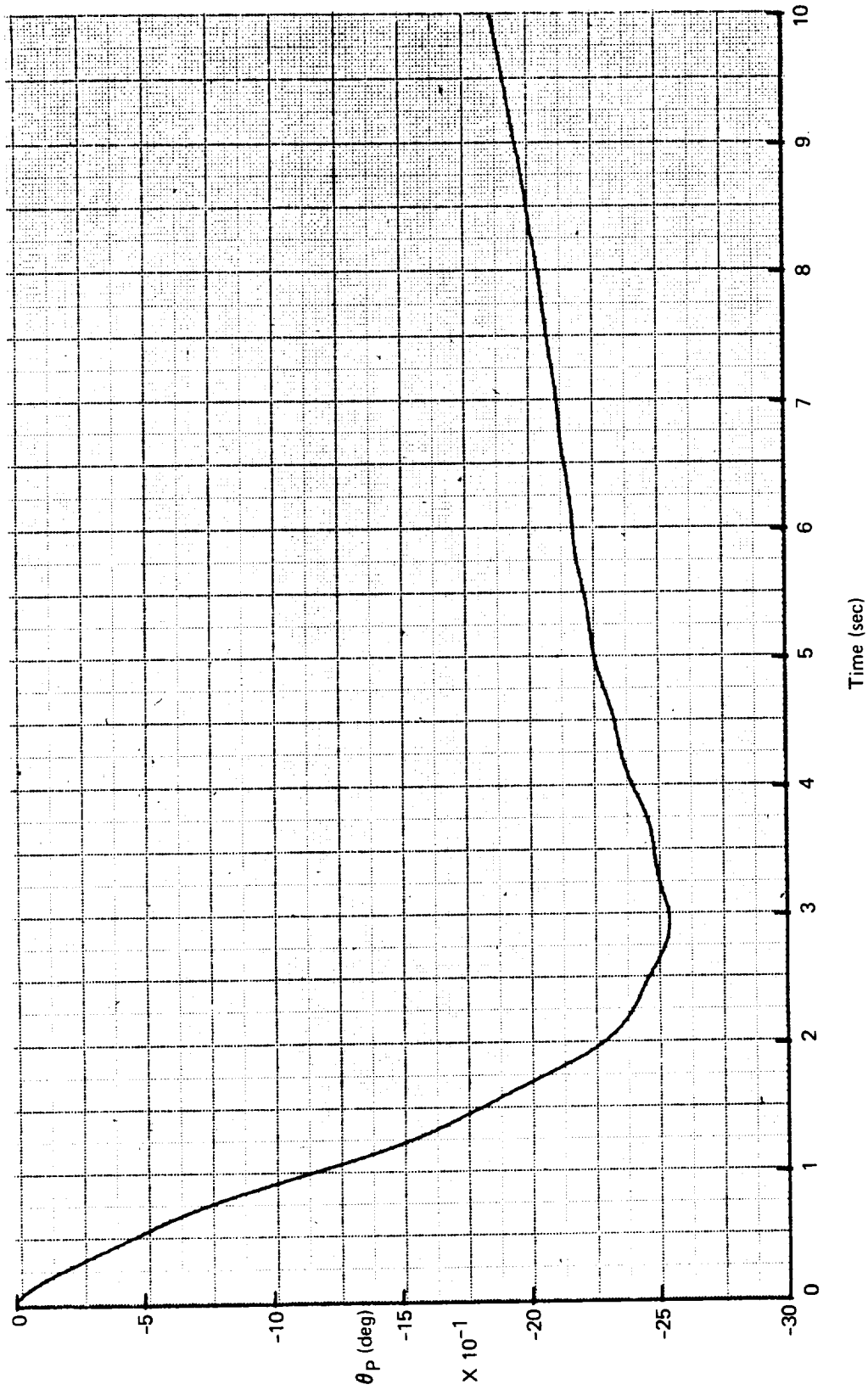


FIGURE 6.1-8. -707-320B, THPLOT-3, w-PERTURBATION = 600 IPS,  $\theta_p$  VS TIME;  
 BASED ON SDSS-3A (RESIDUAL ELASTIC) DATA

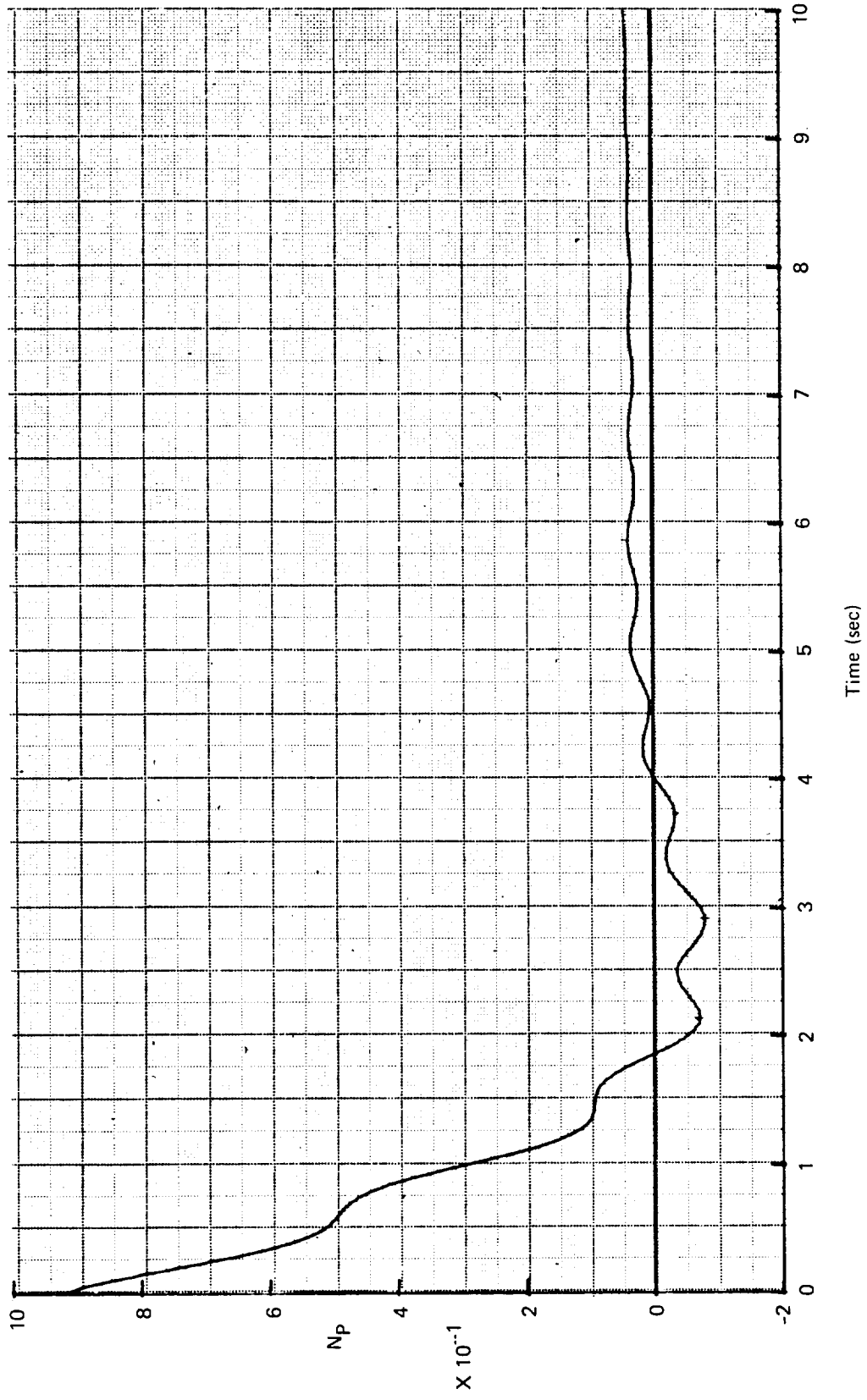


FIGURE 6.1-9.—707-320B, THPLOT-3, w-PERTURBATION = 600 IPS,  $N_p$  VS TIME;  
 BASED ON SDSS-3A (RESIDUAL ELASTIC) DATA

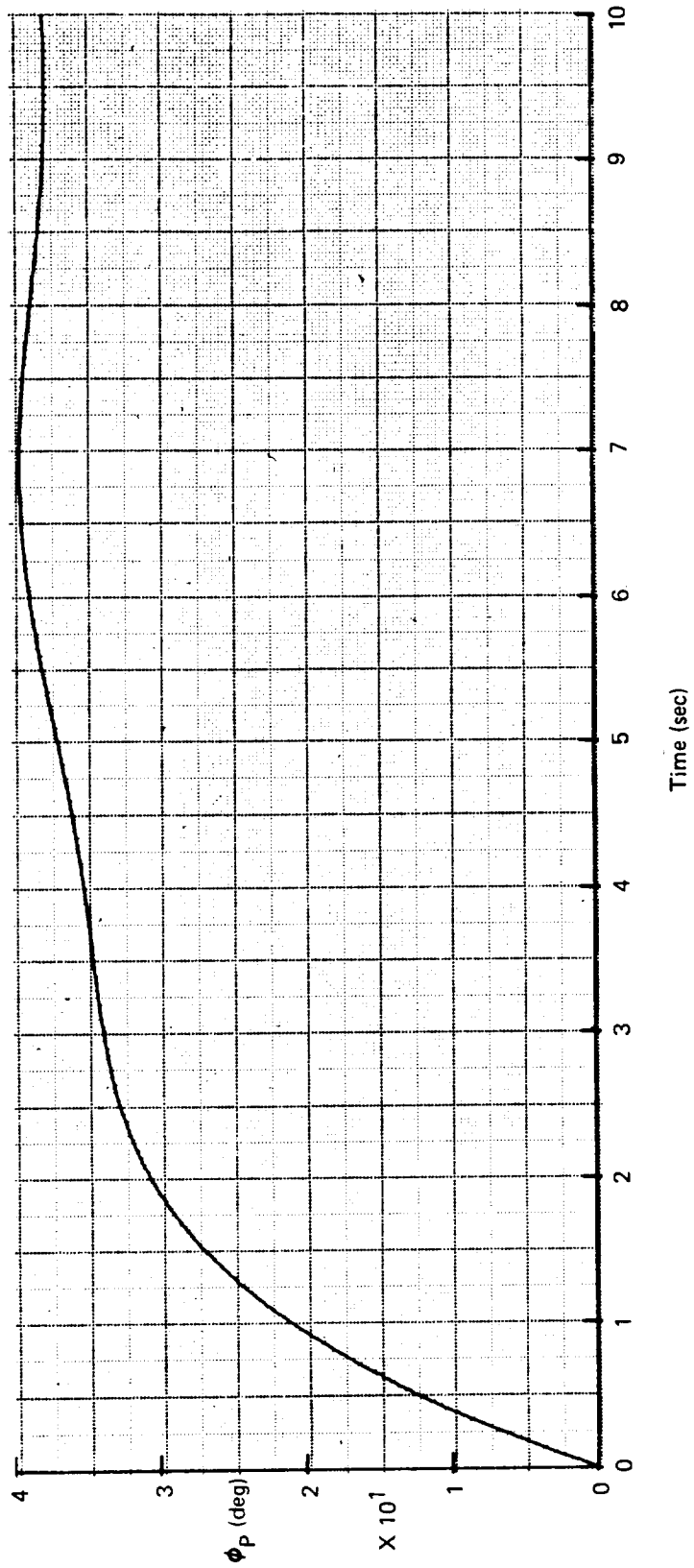


FIGURE 6.1-10. — 707-320B, THPLOT-3,  $\rho$ -PERTURBATION = 0.50 RAD/SEC,  $\phi_p$  VS TIME;  
 BASED ON SDSS-3A (RESIDUAL ELASTIC) DATA

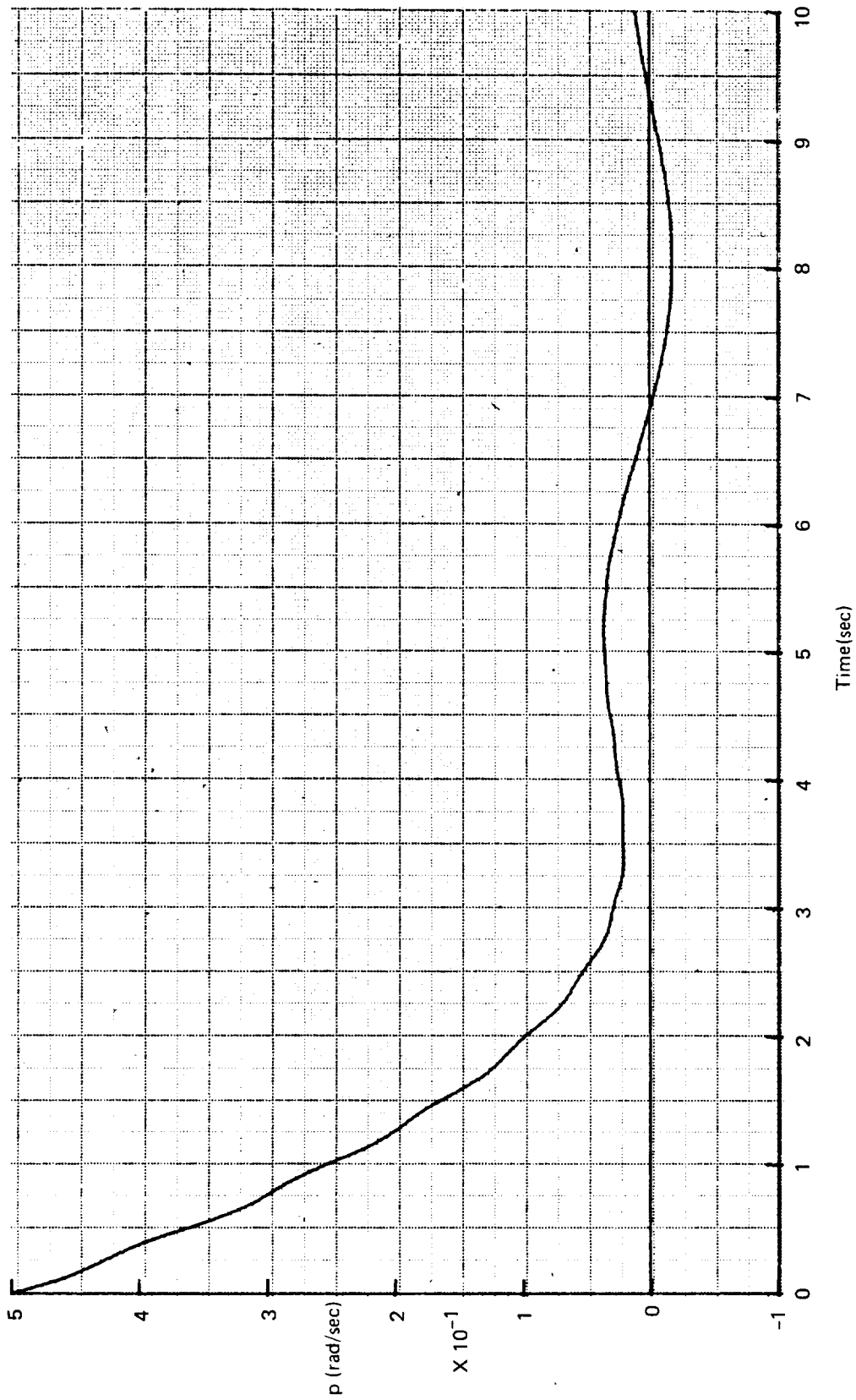


FIGURE 6.1-11.—707-320B, THPLOT-3,  $p$ -PERTURBATION = 0.50 RAD/SEC,  $p$  VS TIME;  
 BASED ON SDSS-3A (RESIDUAL ELASTIC) DATA

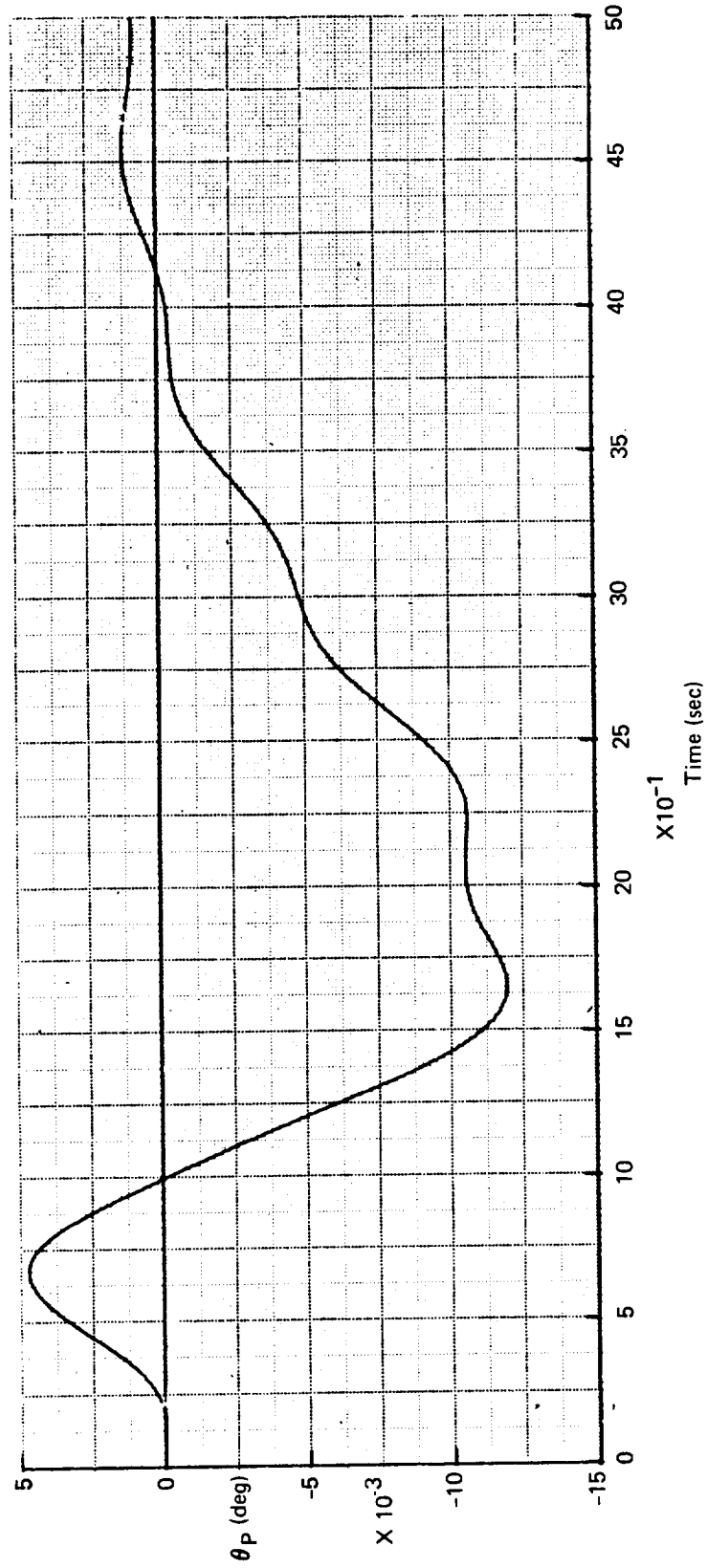


FIGURE 6.1-12. -707-320B, THPLOT-3, ONE MINUS COSINE GUST,  $w = -12.0$  IPS,  
 LENGTH =  $30.0 \bar{c}$ ,  $\theta_P$  VS TIME; BASED ON SDSS-3A  
 (RESIDUAL ELASTIC) DATA

**TABLE 6.1-8.—COMPARISON OF BOEING 707-320B PHUGOID CHARACTERISTICS FROM THE TH-3 AND SDSS-3A (RESIDUAL ELASTIC)**

Type of trace	TH Program		SD&SS Program
	Initial disturbance $u_0 = 600$ ips		
	$u$	$\theta_p$	
Logarithmic decrement, $\delta$	0.237	0.251	0.254
Period, sec	96.0	96.5	96.5

**TABLE 6.1-9.—COMPARISON OF BOEING 707-320B LATERAL-DIRECTIONAL DYNAMIC CHARACTERISTICS FROM THE TH-3 AND SDSS-3A (RESIDUAL ELASTIC)**

TH Results			SD&SS Dutch-roll characteristics
Initial disturbance, $v_0 = 600$ ips			
Type of trace	$\beta$	$\psi$	
Period, sec	5.24	5.26	5.25
Logarithmic decrement,	0.488	0.47	0.475
$ \phi / \beta $	1.41		1.38
$ \phi / \psi $		1.68	1.45

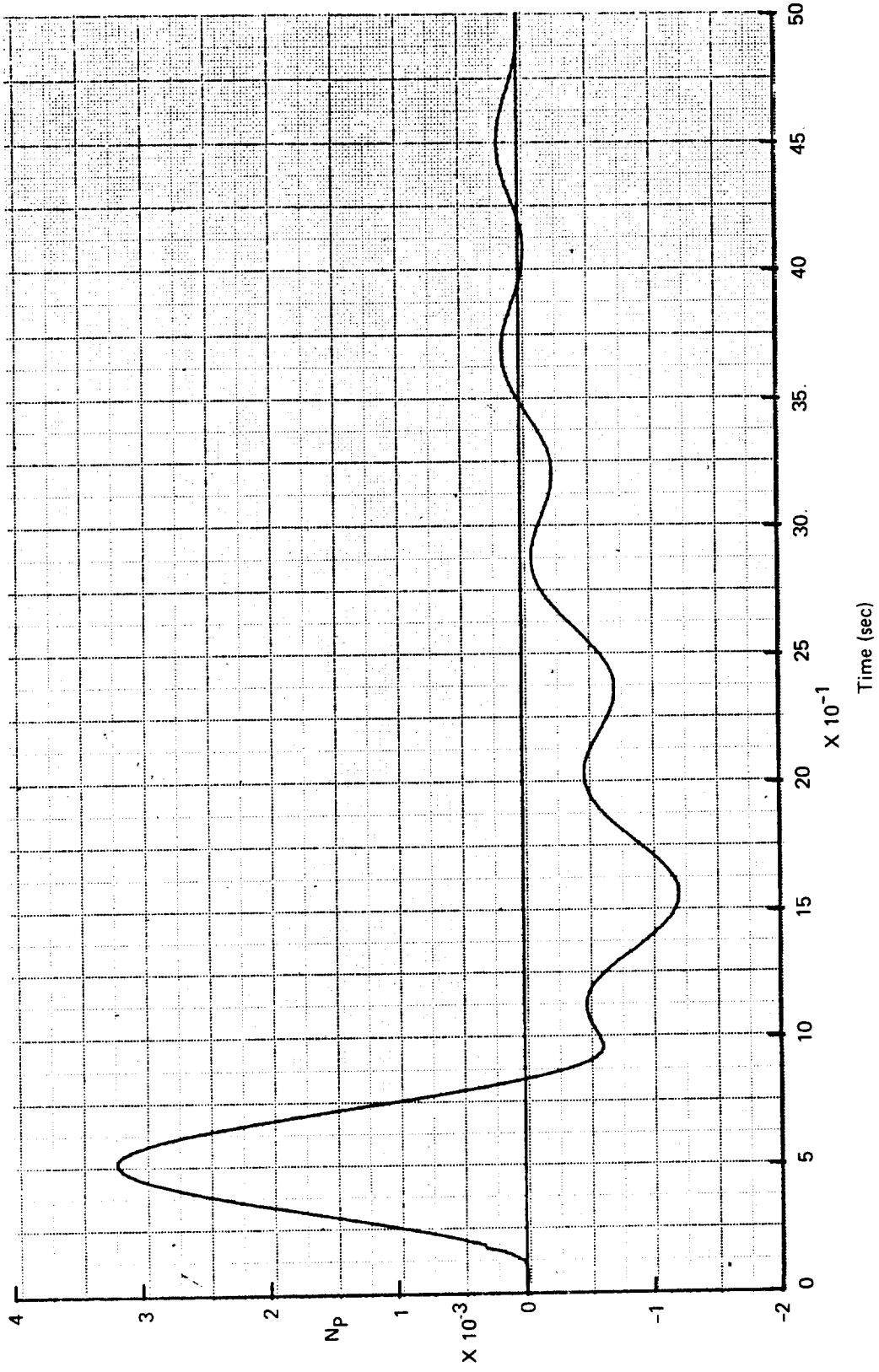


FIGURE 6.1-13. -707-320B, THPLOT-3, ONE MINUS COSINE GUST,  $w = -12.0$  IPS,  
 LENGTH =  $30.0 \bar{c}$ ,  $N_p$  VS TIME; BASED ON SDSS-3A  
 (RESIDUAL ELASTIC) DATA

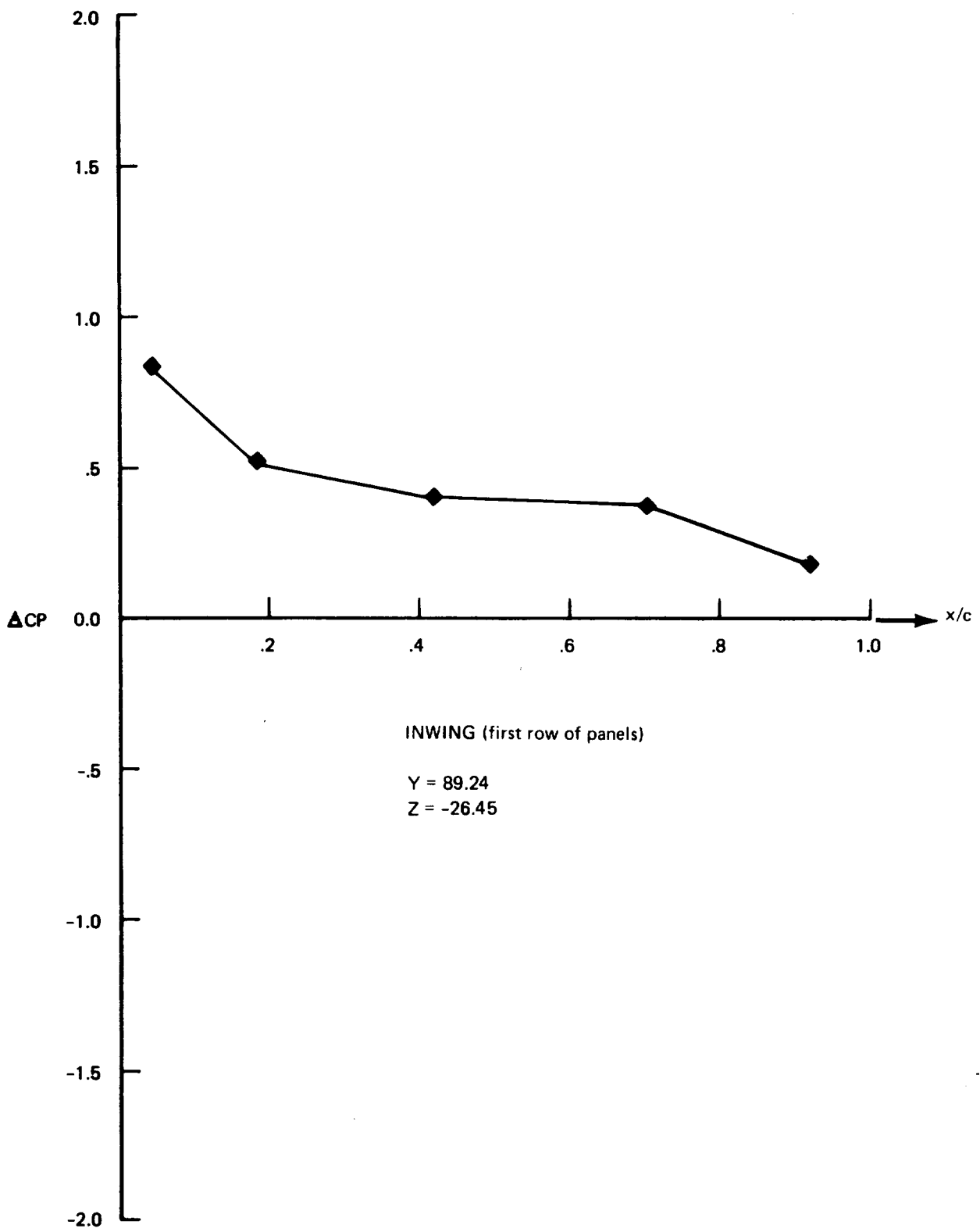


FIGURE 6.1-14.—PRESSURE DISTRIBUTION PLOT—707-320B



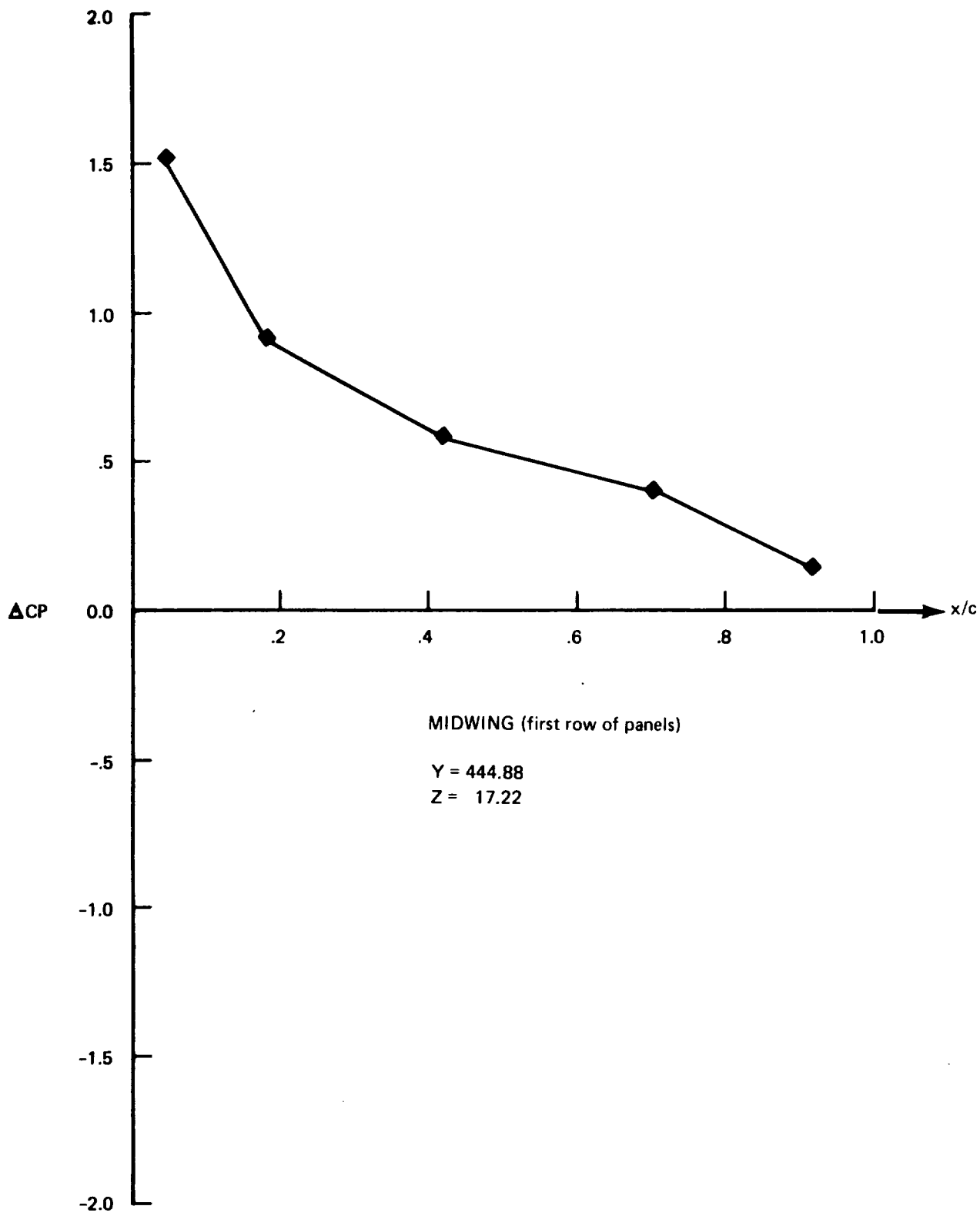


FIGURE 6.1-14.—CONTINUED

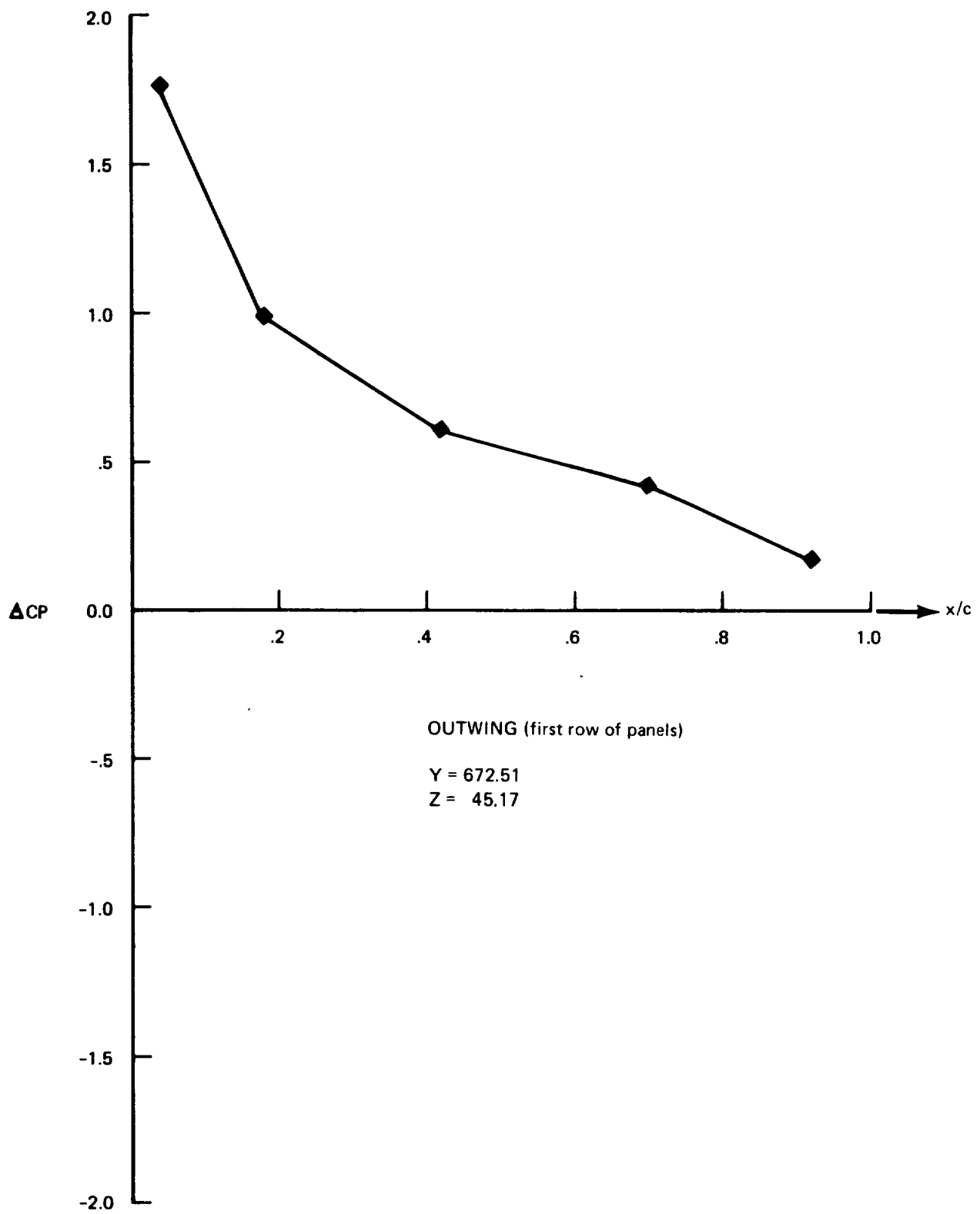


FIGURE 6.1-14.—CONTINUED

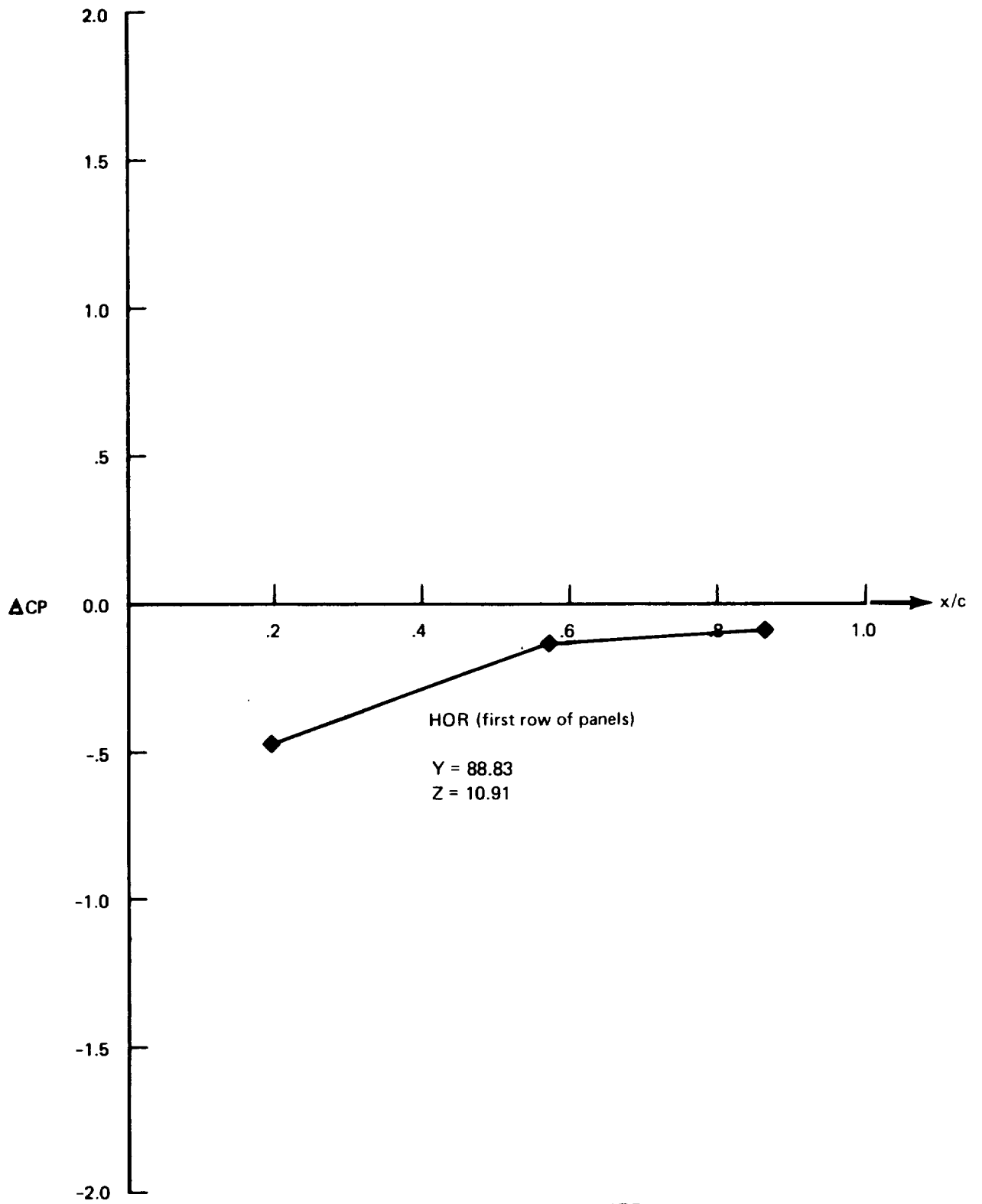


FIGURE 6.1-14.—CONTINUED

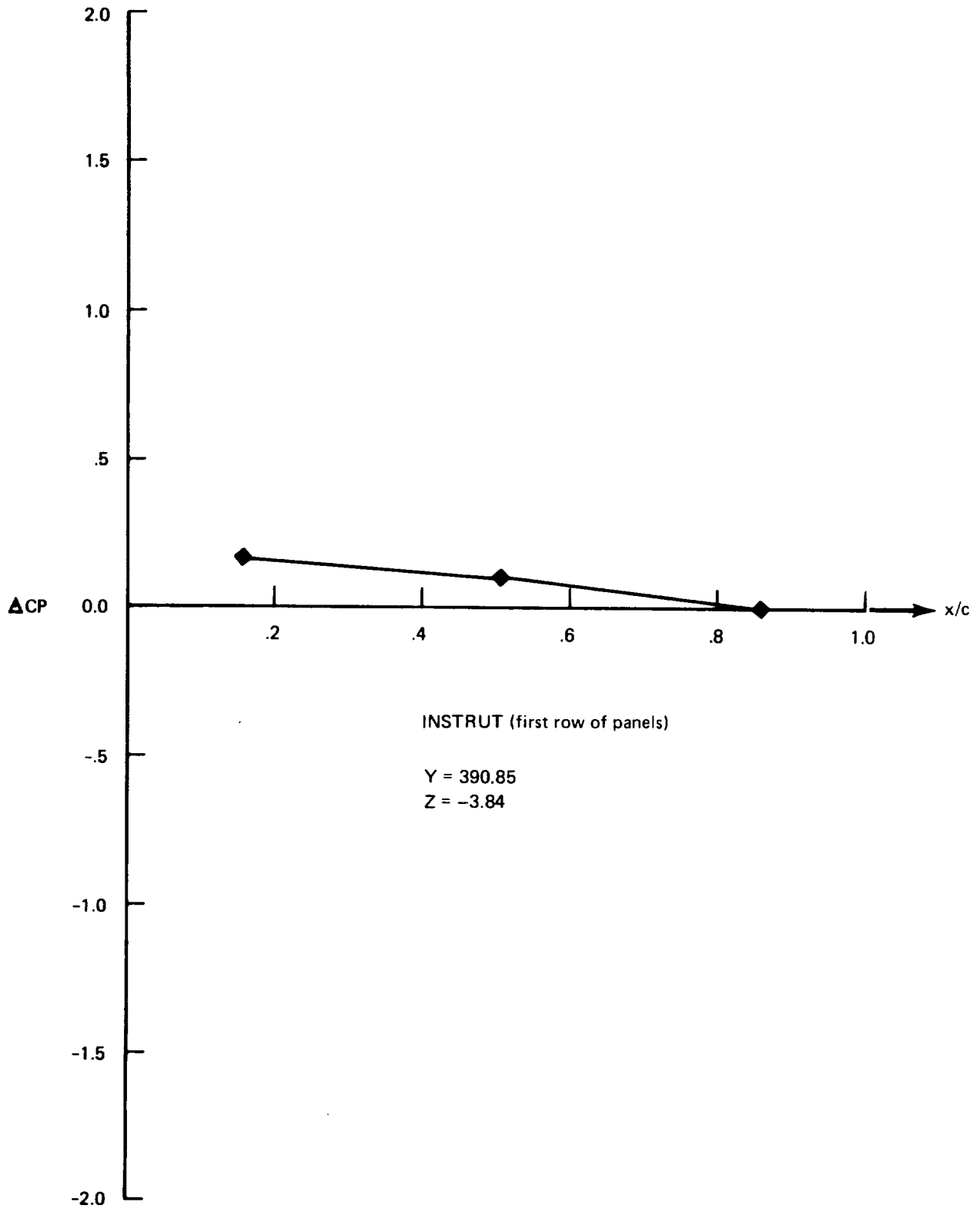


FIGURE 6.1-14.—CONTINUED

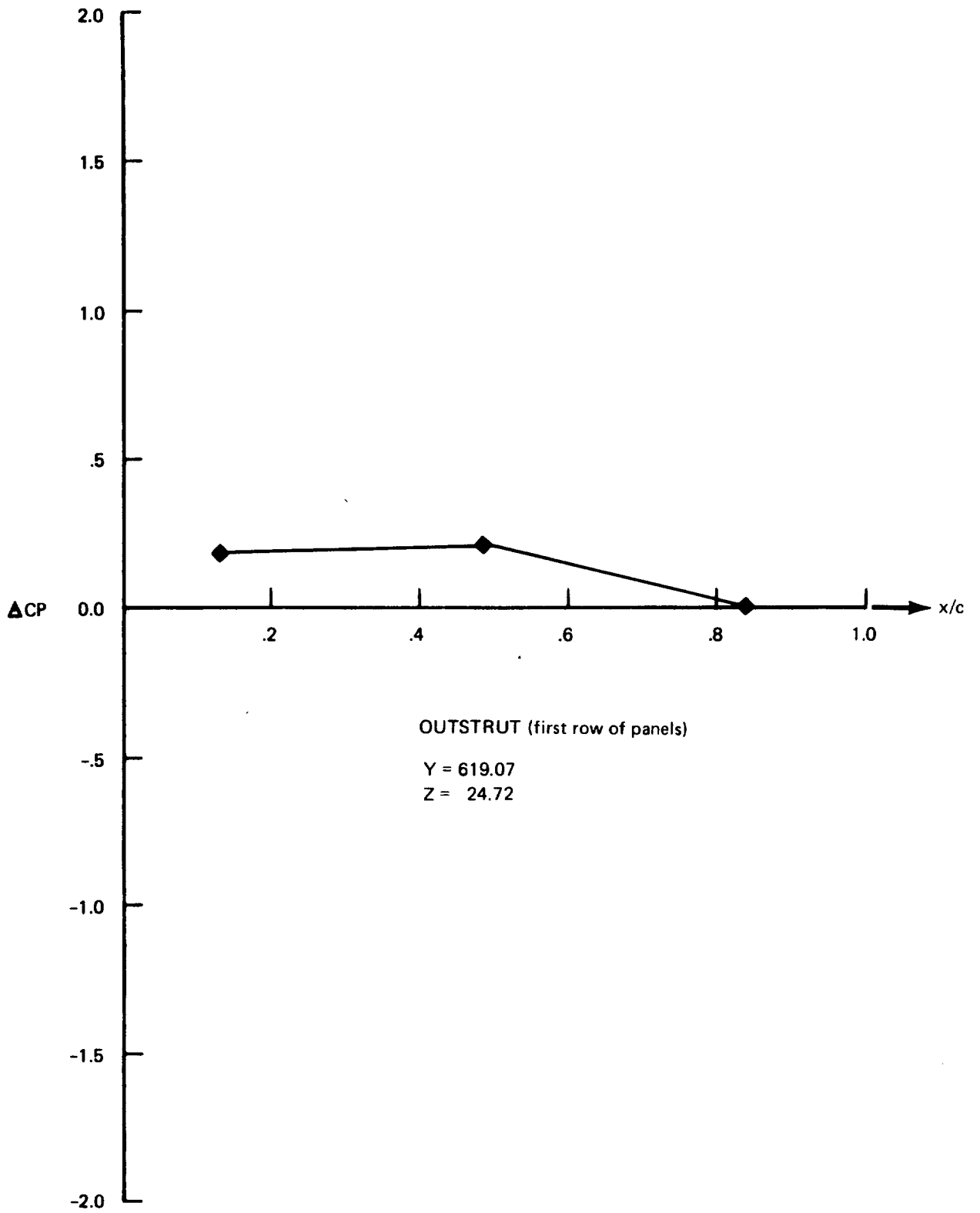


FIGURE 6-1-14.—CONCLUDED

## 6.2 RESULTS AND COMPARISONS OF BOEING 2707-300 (SST) DEMONSTRATION CASE

The results for a rigid SST model are compared with the wind tunnel results in Table 6.2-1. This model is hereafter referred to as SDSS-4X, and is not a demonstration case. The relationship to SDSS-4X, to other SD&SS cases is discussed later in this section. The viscous drag (not accounted for in FLEXSTAB) was separately calculated from a Boeing computer program. Reference 6-8, as 0.0081. This value was deducted from the wind tunnel drag 0.0105 to obtain 0.0025, as compared to  $CD_O = 0.00779$  obtained from FLEXSTAB. The drag calculated by the FLEXSTAB program for the supersonic flow includes the wave drag due to thickness and the wave drag due to lift. The strake leading-edge is subsonic at  $M = 2.7$ , but the rest of the wing leading edge is supersonic. For a fully supersonic leading edge, the leading-edge correction is not required. The available information, however, does not provide an explanation for the poor agreement of the  $CD_O$  values. It is evident from the results in Table 6.2.1 that in this case the leading-edge thrust correction has only a slight effect on the results.

The values calculated for  $CL_\alpha$  and  $CD_\alpha$  agree quite well with the wind tunnel results. However, the difference for  $C_{m\alpha}$  at trim angle of  $4.9^\circ$ , between the FLEXSTAB (-0.00209) and the wind tunnel value (-0.00015) is large. In order to understand the reasons for this difference, the calculated and experimental values of  $C_m$  vs.  $\alpha$  were plotted (Figure 6.2.1) for both the tail-on and tail-off configurations. At  $\alpha = 4.9^\circ$  (FLEXSTAB trim value), the wind tunnel results for tail-on show a nonlinear  $C_m$  vs.  $\alpha$  variation. In the range of  $\alpha = 0^\circ$ , the variation is approximately linear. The agreement for  $C_{m\alpha}$ , though better than at  $\alpha = 4.9^\circ$ , still appears unsatisfactory at  $\alpha = 0$  (-0.00209 vs. -0.00015). For the tail-off configuration, the wind tunnel data for  $C_m$  vs.  $\alpha$  are close to being linear. However, the FLEXSTAB results of  $C_{m\alpha}$  do not show any better agreement (-0.000053 vs. 0.00069 at  $\alpha = 0$ ). Since  $C_{m\alpha}$  is a function of the c.g. location, it is usually more informative to compare the vehicle aerodynamic center (neutral point,  $h_n$ , in FLEXSTAB). Thus the following comparisons are made:

	$\alpha$ deg	Wind Tunnel $h_n, \% \bar{c}$	FLEXSTAB $h_n, \% \bar{c}$
Tail-off Configuration	0	59.68	62.16
	4.9	57.97	62.16
Tail-on Configuration	0	65.02	68.31
	4.9	62.44	68.31
Increment in $h_n$ due to	0	5.34	6.15
tail	4.9	4.47	6.15

TABLE 6.2-1.—COMPARISON OF METHODS FOR CALCULATING AERODYNAMIC STABILITY AND CONTROL DATA—BOEING 2707-300PT (SST)

$$M_1 = 2.7, h_1 = 60,000 \text{ ft}, \gamma_1 = 0, c_g = 0.62\bar{c}, wt = 553,910$$

Parameter	Unit	FLEXSTAB <sup>a</sup> (balanced solution) SDSS-4X		WIND TUNNEL	
		With L.E. thrust	Without L.E. thrust	Value	Origin
		$\alpha_1$	deg		
$T_1$	lb	60396	57137	NA	
$\delta e_1$	deg	1.157	1.212	NA	
$C_{L_o}$		-0.0718	-0.0715	-0.05	ref. 6-6
$C_{D_o}$		0.00779 <sup>b</sup>	.00783 <sup>b</sup>	0.0105 0.0025 <sup>c</sup>	ref. 6-7
$C_{m_o}$		0.0127	0.0128	0.0065	ref. 6-6
$C_{L_\alpha}$	deg <sup>-1</sup>	0.0331	0.0331	0.034	ref. 6-6
$C_{D_\alpha}$	deg <sup>-1</sup>	0.00330	0.00320	0.0033	ref. 6-6
$C_{m_\alpha}$	deg <sup>-1</sup>	-0.00209	-0.00209	-0.00015 (-0.00103 at $\alpha = 0$ )	ref 6-6
$C_{L_Q}$	rad <sup>-1</sup>	0.549	0.548	NA	
$C_{D_Q}$	rad <sup>-1</sup>	0.0309	0.0349	NA	
$C_{m_Q}$	rad <sup>-1</sup>	-0.676	-0.676	NA	
$C_{L_{\delta e}}$	deg <sup>-1</sup>	0.00280	0.00280	0.00240	ref. 6-6
$C_{D_{\delta e}}$	deg <sup>-1</sup>	0.000253 <sup>b</sup>	0.00213 <sup>b</sup>	0.00050	ref. 6-6
$C_{m_{\delta e}}$	deg <sup>-1</sup>	-0.00259	-0.00260	-0.00239	ref. 6-6
$C_{L_u}^\dagger$		0.0154	0.0159	-0.216	ref. 6-6
$C_{D_u}^\dagger$		-0.00483	-0.00349	-0.0231	ref. 6-6
$C_{m_u}^\dagger$		-0.0890	-0.0890	0.0222	ref. 6-6

TABLE 6.2-1.—CONCLUDED

$M_1 = 2.7, h_1 = 60,000 \text{ ft}, \gamma_1 = 0, c_g = 0.62\bar{c}, wt = 553,910$

Parameter	Unit	FLEXSTAB <sup>a</sup> (balanced solution) SDSS-4X		WIND TUNNEL	
		With L.E. thrust	Without L.E. thrust	Value	Origin
		$C_{L\dot{\alpha}}$	rad <sup>-1</sup>		
$C_{D\dot{\alpha}}$	rad <sup>-1</sup>	0.00169	0.00356	NA	
$C_{m\dot{\alpha}}$	rad <sup>-1</sup>	0.00915	0.00914	NA	
$C_{L\dot{Q}}$	rad <sup>-1</sup>	-0.221	-0.220	NA	
$C_{D\dot{Q}}$	rad <sup>-1</sup>	-0.011	-0.014	NA	
$C_{m\dot{Q}}$	rad <sup>-1</sup>	0.0396	0.0396	NA	
$h_n \cdot h$	% $\bar{c}$	6.31	6.31	0.44 (3.03 at $\alpha = 0$ )	Calculated from wind tunnel values of $C_{m\alpha}$ and $C_{L\alpha}$
$h_n$	% $\bar{c}$	68.3	68.3	62.44 (65.02 at $\alpha = 0$ )	
$h_m$	% $\bar{c}$	68.47	68.47	NA	
$h_m \cdot h_n$	% $\bar{c}$	64.8	64.8	NA	
$\Delta\delta e/n \cdot 1$	deg/g	-2.497	-2.494	NA	
$d\delta e/dV$	deg/ (ft/sec)	-0.0120	-0.0120	NA	

<sup>a</sup> Not a demonstration case; cruise shape - design shape

<sup>b</sup> FLEXSTAB does not include viscous drag

<sup>c</sup> WT drag less calculated skin friction drag (see text)

$$t \ C_{L_u} = M \frac{\partial C_L}{\partial u} ; C_{D_u} = M \frac{\partial C_D}{\partial u} , C_{m_u} = M \frac{\partial C_m}{\partial u}$$



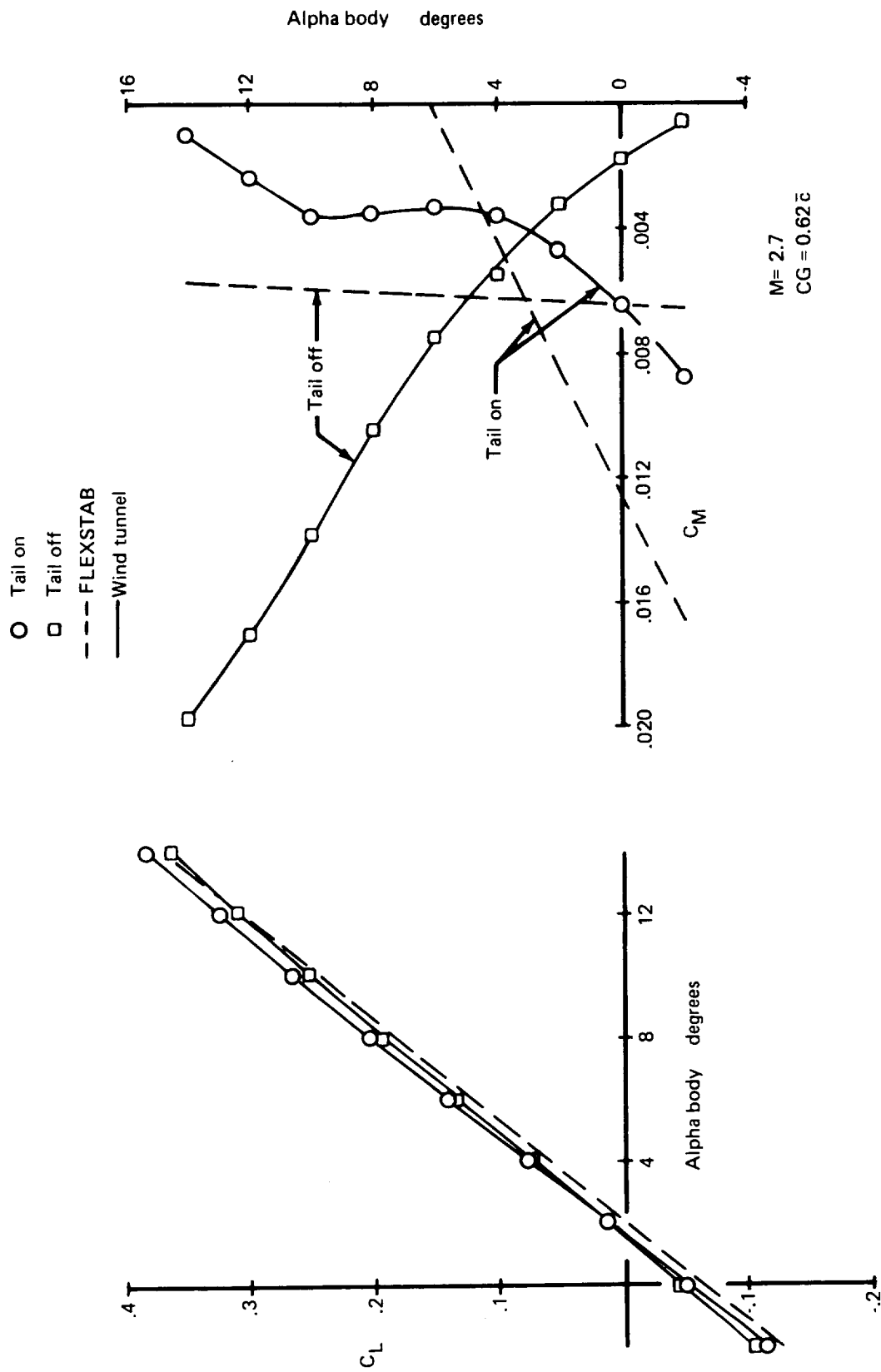


FIGURE 6.2.1.—VARIATIONS OF LIFT AND PITCHING MOMENT WITH ANGLE OF ATTACK FOR SST

The following points can be made from the comparison of  $h_n$  values:

- a. The comparison is better at  $\alpha = 0^\circ$  than at  $\alpha = 4.9^\circ$
- b. The difference of about 3% at  $\alpha = 0^\circ$  would usually be considered satisfactory for preliminary design
- c. The difference of about 6% at  $\alpha = 4.9^\circ$  is not satisfactory
- d. The shift in vehicle aerodynamic center is predicted satisfactorily by FLEXSTAB; the prediction is quite good for  $\alpha = 0^\circ$

Figure 6.2.2 is taken from Reference 3-3 and shows the effect of Mach number on  $CL_\alpha$  and aerodynamic center ( $h_n$ ); it also shows the value of  $h_n$  at  $M = 2.7$  obtained for the tail-off model derived from the current SST demonstration model. (The ordinate values corresponding to  $CL_\alpha$ , per radian, shown in Ref. 3-3 should read 1.0 instead of .01, 2.0 instead of .02, etc.) The FLEXSTAB predictions of Reference 3-3 agree well with the wind tunnel data. The value of  $h_n$  ( $62.16\% \bar{c}$ ) for the current model is significantly different than the earlier result shown in Figure 6.2.2. A rerun of the FLEXSTAB model used to obtain the results of Reference 3-3, produced a value of  $59.89\% \bar{c}$  -- about the same as obtained earlier. Thus the FLEXSTAB model used for Reference 3-3 predicted a value of  $h_n$  which is closer to the wind tunnel result ( $h_n = 59.68\% \bar{c}$  at  $\alpha = 0$ ) than the current FLEXSTAB model. The two models were developed independently, and are different even though they represent the same airplane geometry.

Figure 6.2.4 shows comparison between the FLEXSTAB and wind tunnel pressure distribution for the tail-off configuration at angles of attack of  $5.25^\circ$  and  $9.25^\circ$ . At  $\alpha = 5.25^\circ$ , the FLEXSTAB results (except at the 56% semi-span station) agree reasonably well with the wind tunnel measurements. At  $\alpha = 9.25^\circ$ , however, particularly outboard of the 50% semi-span position, the FLEXSTAB lifting pressures vary significantly from the wind tunnel measurements. The FLEXSTAB center of pressure is shifted aft resulting in a greater negative  $C_m$  relative to the wind tunnel results. It is also observed that at subsonic leading edge (at 12.7% semi-span), FLEXSTAB predicts higher than wind tunnel pressure. At the supersonic leading edges at other spanwise stations, the calculated pressures are lower than the measured pressures. The effect of this has not been evaluated.

In summary, it is concluded that (a)  $C_{m\alpha}$  results for this configuration are not satisfactory for the FLEXSTAB model described in Section 3.5, (b)  $C_{m\alpha}$  results for the tail-off configuration derived from the FLEXSTAB model used in an earlier study (Reference 3-3) result in an excellent correlation for the aerodynamic center location, (c) the difficulty for poor correlation (from the current FLEXSTAB model) in the linear range appears to be due to modeling, and (d) a significant part of the problem can reasonably be attributed to the nonlinear character of the experimental  $C_m$  vs  $\alpha$  variation.

The speed derivatives do not compare very well. The  $CL_u$  derivative is seen to differ even in sign. The positive sign of the  $CL_u$  calculated by FLEXSTAB is determined by the relatively large positive value of  $\partial CL_0 / \partial M$  ( $= .05261$ ). The cause(s) for this is (are) not known. However, it is suggested that until the reason(s) can be determined, the speed derivatives should be evaluated as suggested in Section 6.1.

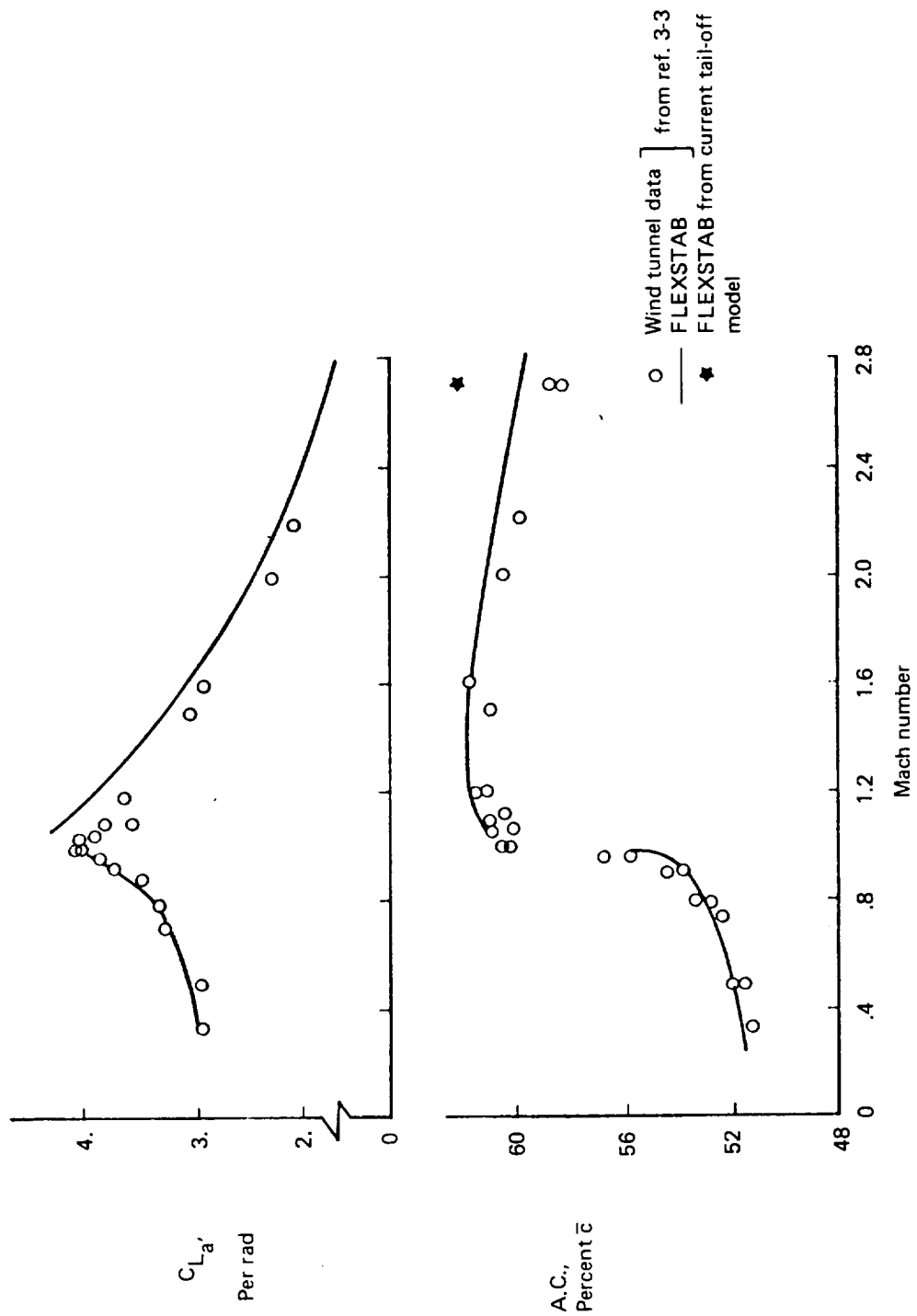
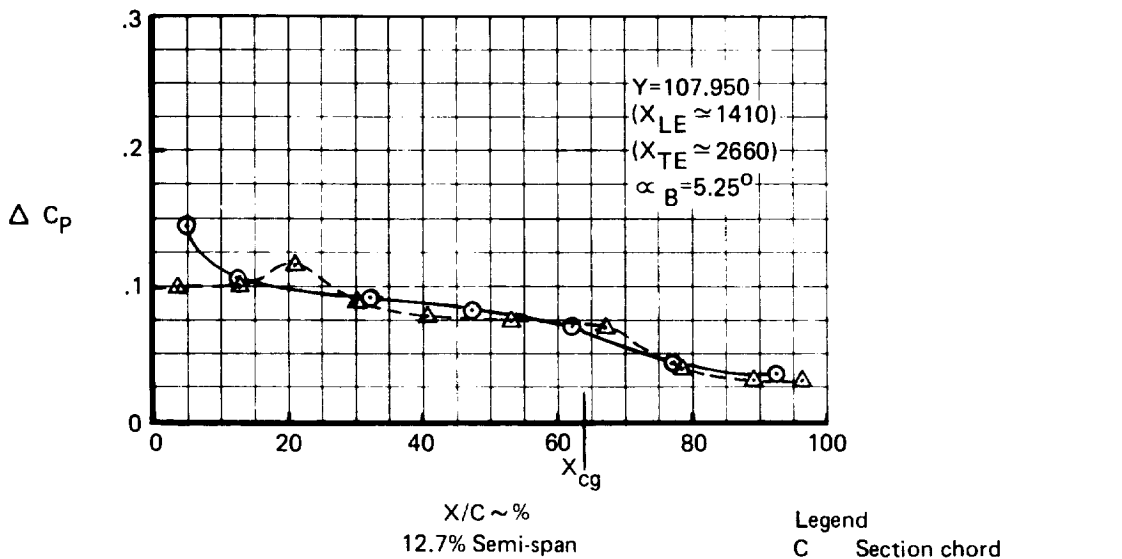


FIGURE 6.2.2.—EFFECT OF MACH NUMBER ON LIFT SLOPE AND AERODYNAMIC CENTER FOR SST, TAIL-OFF



- Legend
- C Section chord
  - X<sub>LE</sub> X-coordinate of the section leading edge
  - X<sub>TE</sub> X-coordinate of the section trailing edge
  - X<sub>cg</sub> Relative location of the airplane center of gravity
  - △-- Experiment
  - FLEXSTAB

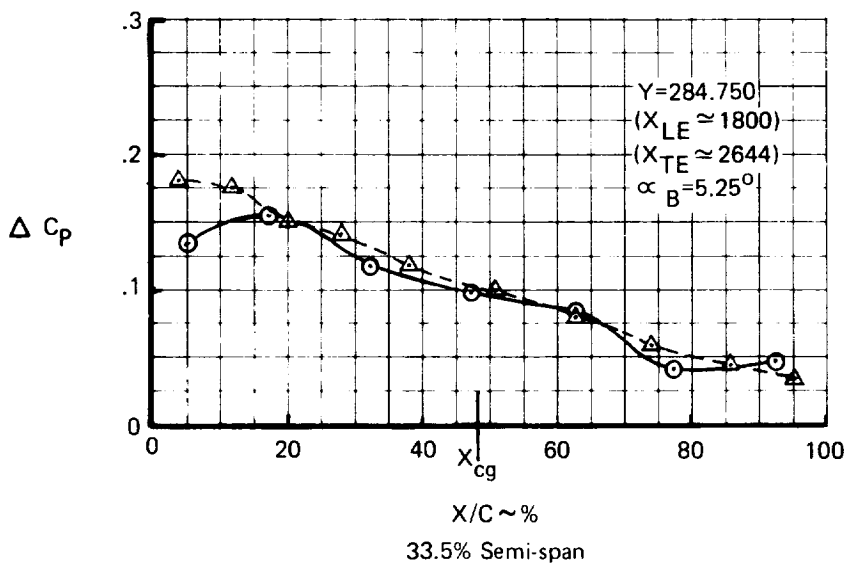
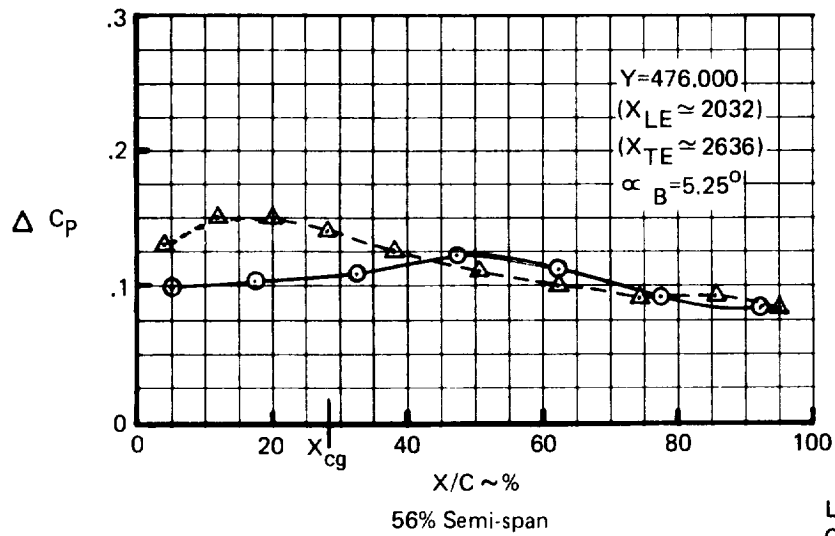


FIGURE 6.2-3.—WING PRESSURE COMPARISONS FOR SST, TAIL-OFF



- Legend
- C Section chord
  - $X_{LE}$  X-coordinate of the section leading edge
  - $X_{TE}$  X-coordinate of the section trailing edge
  - $X_{cg}$  Relative location of the airplane center of gravity
  - $\Delta$ -- Experiment
  - $\circ$ — FLEXSTAB

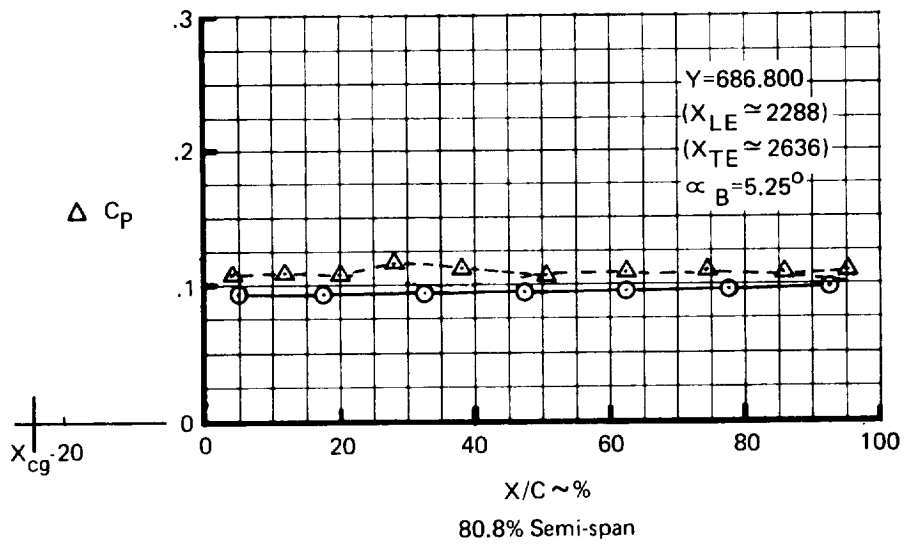


FIGURE 6.2-3.—CONTINUED

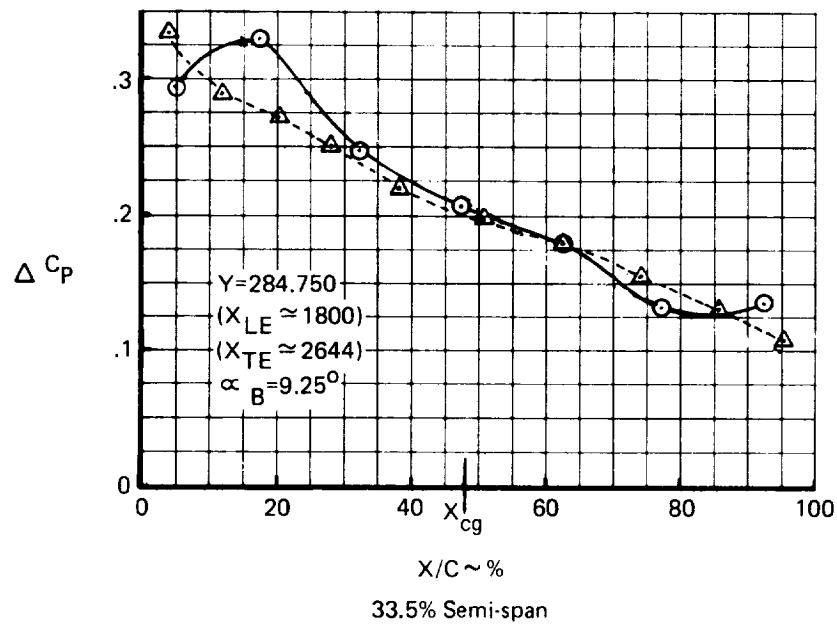
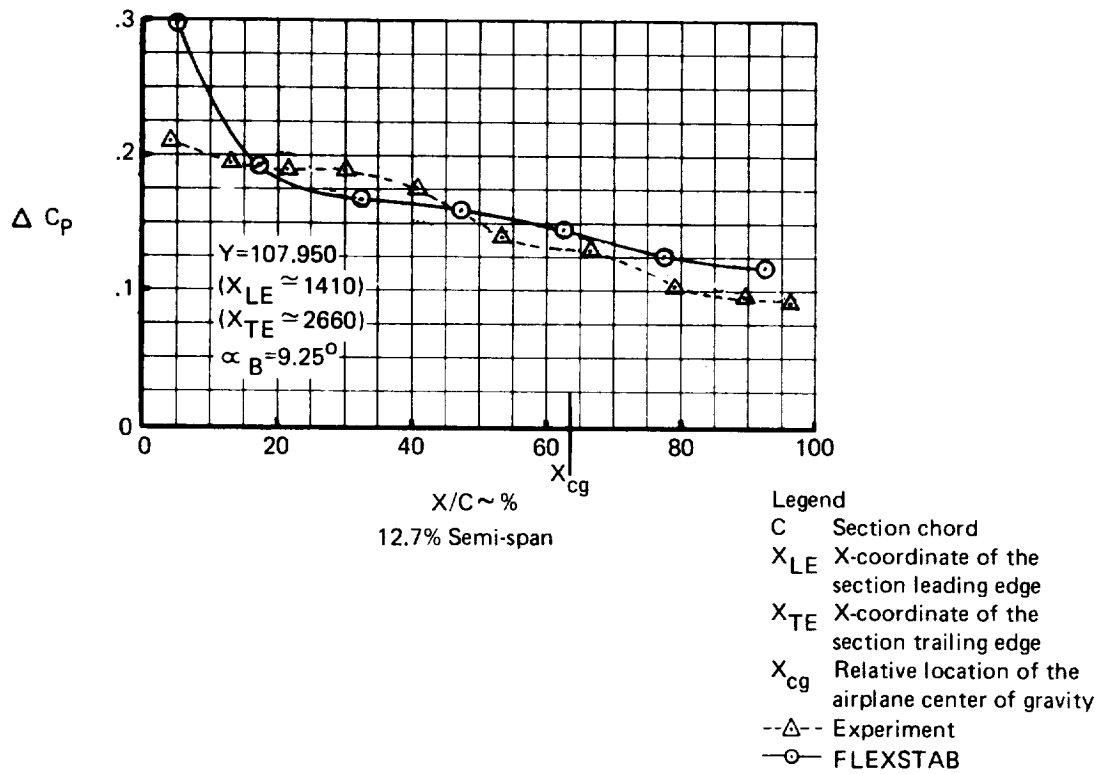
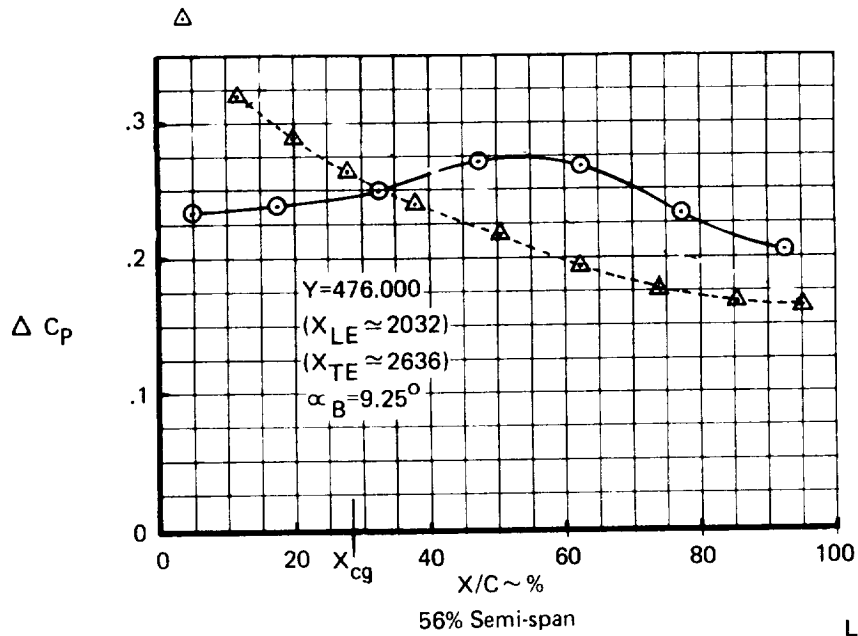


FIGURE 6.2-3.—CONTINUED



- Legend
- C Section chord
  - $X_{LE}$  X-coordinate of the section leading edge
  - $X_{TE}$  X-coordinate of the section trailing edge
  - $X_{cg}$  Relative location of the airplane center of gravity
  - $\Delta$ --- Experiment
  - $\circ$ — FLEXSTAB

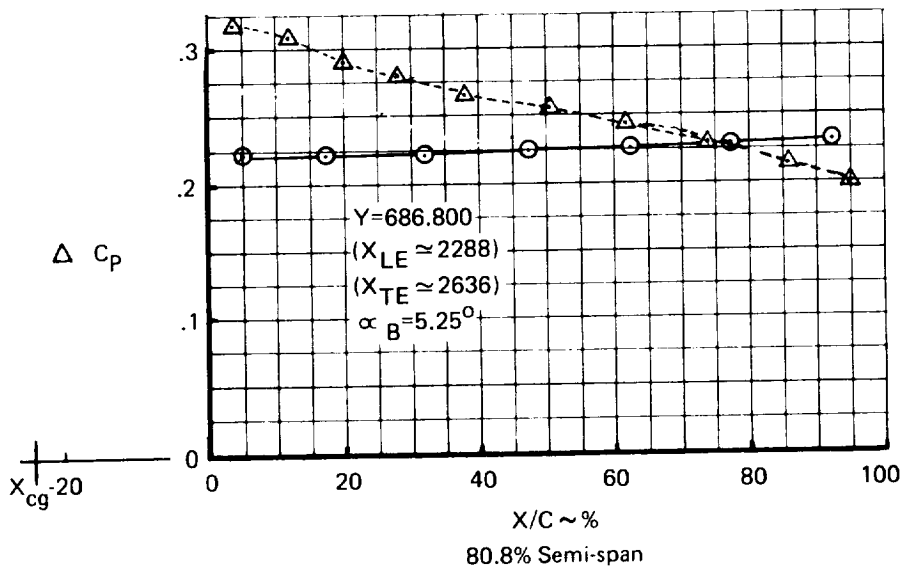


FIGURE 6.2-3.—CONCLUDED

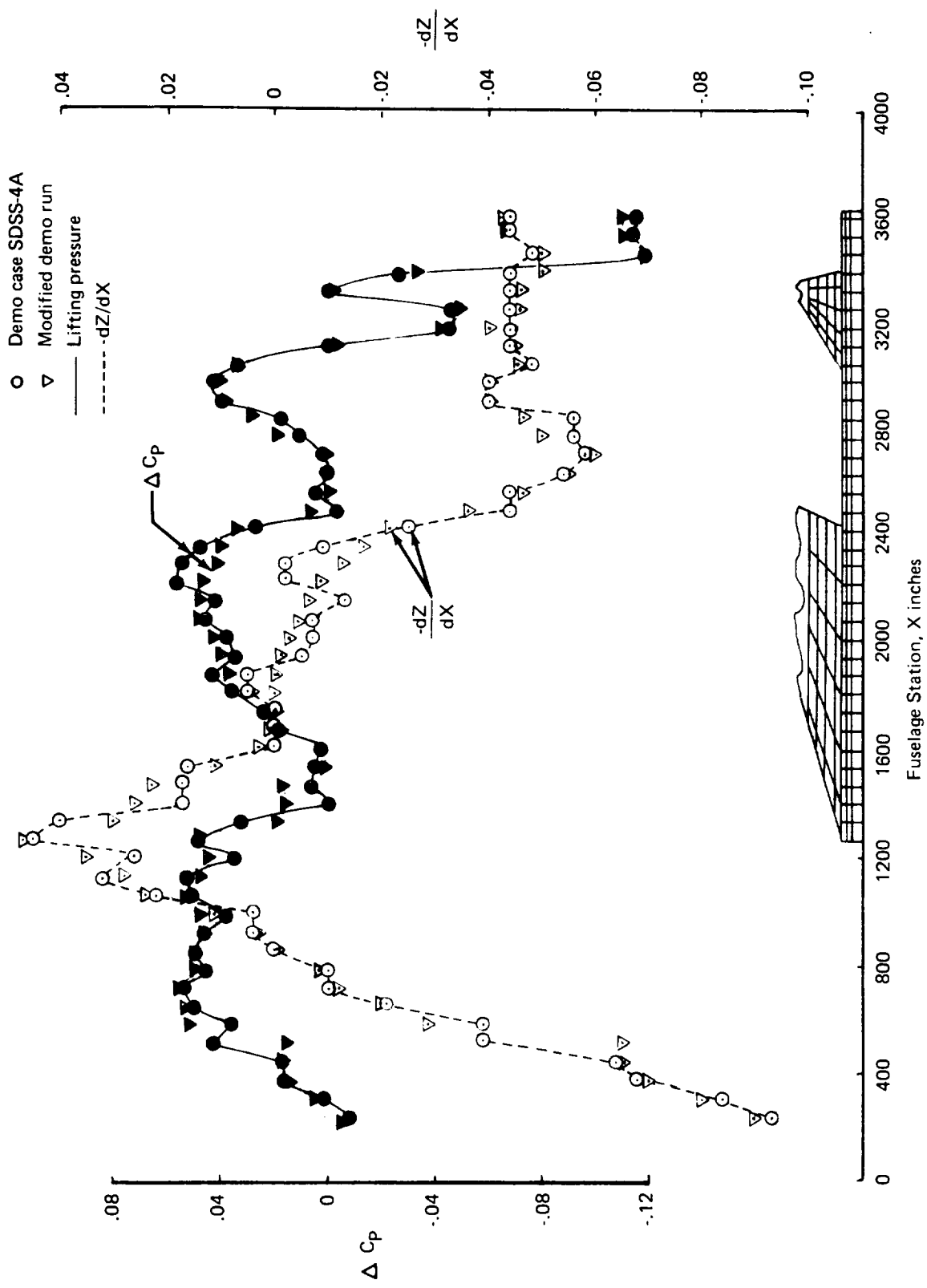


FIGURE 6.2.4.—FUSELAGE PRESSURE DISTRIBUTIONS FOR SST



The fuselage pressure distribution for the SST demonstration cases is oscillatory. It was determined that the pressure oscillations are due to the oscillations in the camber slope variation along the fuselage. Figure 6.2-5 shows the camber slopes,  $-dZ/dX$ , and the lifting pressure coefficients calculated by the FLEXSTAB program from the GD input of GD-4 and the modified GD input. The modification affected only the fuselage camber shape input. The camber shape input in run GD-4 has a reasonably smooth curvature. However, due to the relative locations of the camber definition points and the aerocentroids, the camber slope calculated by the GD program does not have a smooth variation. In the modified GD input, the camber shape was defined at a point on either side of each aerocentroid to ensure that linear interpolation will result in a "correct" camber slope corresponding to the camber shape. Thus the camber shape was defined at 100 points to get the "correct" camber slope at 50 aerocentroids on the fuselage. This technique is not described in the Volume II usage guidelines. The resulting pressure distribution calculated by the FLEXSTAB program is seen to be less oscillatory than the original. In fact, a definite relation can be observed between variations in  $\Delta C_p$  and  $-dZ/dX$ . However, the oscillatory pressure distribution does not appear to significantly affect the overall force and moment coefficients for this configuration.

The results discussed thus far were obtained from runs which are not a part of demonstration cases. Three SD&SS demonstration cases were executed as described in Section 4.5. The SDSS-4A run was executed with a "static-elastic" structural model and "Design" shape option. It calculated trim parameters, total forces and moments, and rigid static stability derivatives corresponding to the cruise shape in addition to determining the jig shape. The input to the SDSS-4X run was identical to the input for SDSS-4A except for the following inputs which were different for SDSS-4X: (a) "RIGID" structural model, (b) "REFERENCE" shape option, (c) "PERTURBATION DATA," and (d) "DYNAMIC ANALYSIS."

The trim parameters, total forces and moments, and static stability derivatives obtained from SDSS-4X and SDSS-4A were identical except for round-off differences. The jig shape calculated from SDSS-4A was input into SDSS-4B which recalculated the same cruise shape (except for differences due to round-off) as input to SDSS-4A (and SDSS-4X). The trim parameters, and the total forces and moments are the same between SDSS-4A and SDSS-4B. The aerodynamic coefficients  $CL_0$ ,  $CD_0$  and  $CM_0$ , and stability derivatives are different due to different input shapes and elasticity. However, the rigid portion of the stability derivatives from SDSS-4B is same as the corresponding derivatives from SDSS-4A since the reference shape is the same in both the cases. None of the results from SDSS-4C would be expected to be identical to those from the other runs, since a corrected AIC matrix was input to SDSS-4C (see Section 4.5.3). No comparisons between the FLEXSTAB results and the SST project data for the static-elastic model are included since an error (discussed later in this section) in the flexibility matrix input into the FLEXSTAB program was discovered from the calculated elastic displacements output from the SD&SS and ALOADS program. In addition, the project flexible airplane data were determined by theoretically calculating the elastic increments to the rigid wind tunnel data using a "flat-airplane" representation. Also, the total derivatives thus determined were with respect to a kinematically constrained axis system rather than a mean-axis system as used in FLEXSTAB. The differences in the calculated derivatives with respect to these two axis

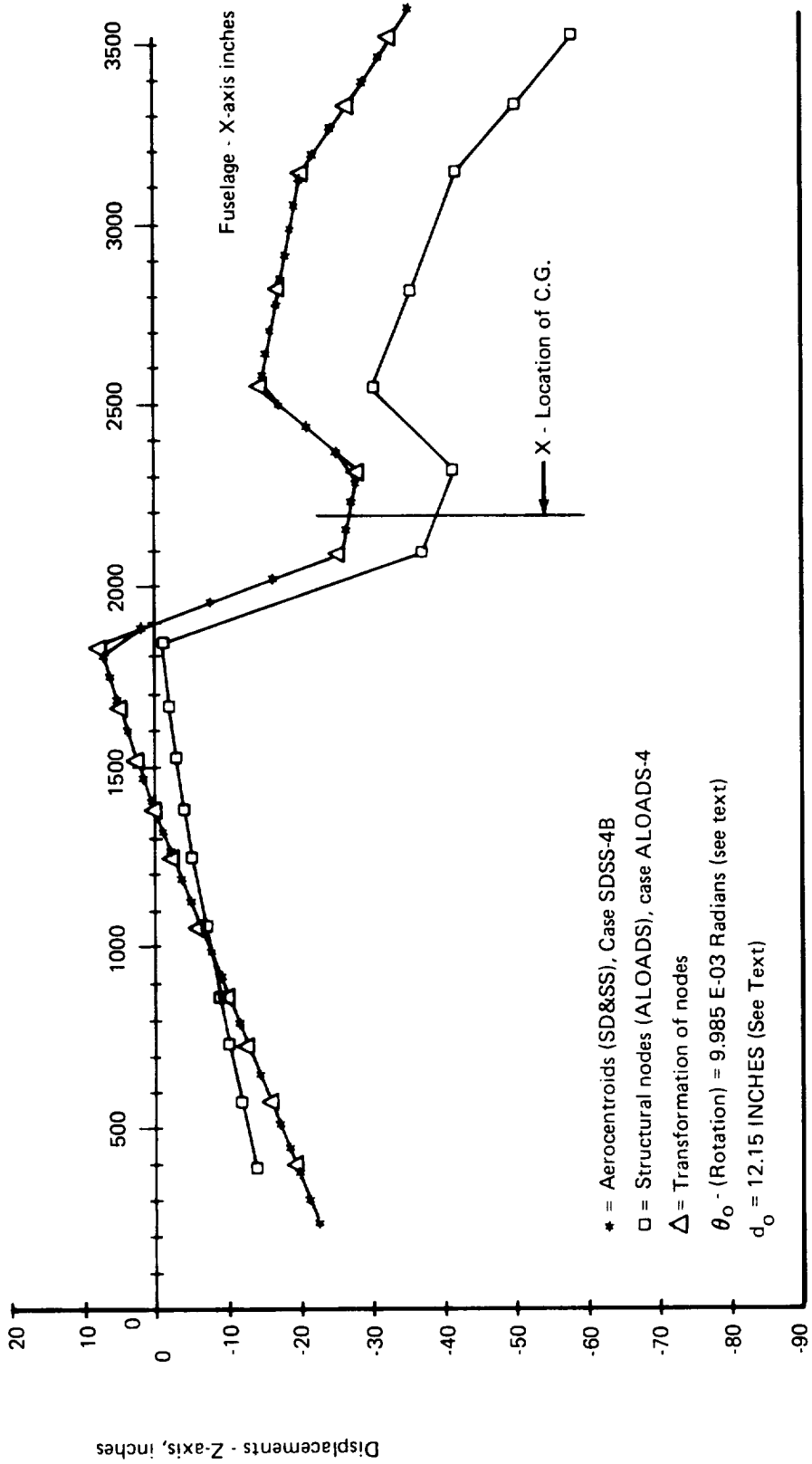


FIGURE 6.2-5. -2707-300PT (SST) SD&SS AND ALOADS PROGRAMS DISPLACEMENT  
OUTPUT AND RECONCILIATION OF THE TWO

systems are presented in reference 6-11 for a FLEXSTAB model of the arrow-wing supersonic transport.

Table 6.2-2 lists the longitudinal dynamic characteristics obtained from the SD&SS program and the project document. The SD&SS results are for a rigid model whereas the project data contain the elastic increments determined as described with reference to Tables 6.1-5 and 6.1-6. The project data for the rigid airplane is not available. The results, although not directly comparable, indicate that the FLEXSTAB results and the project data for the rigid airplane would also be considerably different.

**TABLE 6.2-2.—COMPARISON OF METHODS FOR CALCULATING LONGITUDINAL DYNAMIC CHARACTERISTICS—BOEING 2707-300PT (SST)**

$$M_1 = 2.7, h_1 = 60,000 \text{ ft}, \gamma_1 = 0.0, c_g = 0.62\bar{c}, wt = 553,910 \text{ lb}$$

Results from		FLEXSTAB RIGID MODEL (Not a demonstration case) SDSS-4X		SST project data, <sup>1</sup> Elastic model (ref. 6-10)
		With L.E. thrust	Without L.E. thrust	
SHORT PERIOD	Period sec	4.835	4.834	9.97
	$T_{1/2}$ or $T_2^*$ sec	2.990	2.993	4.12
	$C_{1/2}$ or $C_2^*$ cycles	0.618	0.619	0.413
A PERIODIC ROOTS	$T_{1/2}$ or $T_2^*$ sec	18.516	18.404	—
	$T_{1/2}$ or $T_2^*$ sec	12.551†	12.641	—

\*Time or cycles to half or twice the amplitude

† Indicates it is for twice the amplitude

1 Project data has a Phugoid of period = 131.2 sec.

The error in the flexibility matrix mentioned above is illustrated by Figure 6.2.4, which shows the elastic deformations along the fuselage as calculated by the SD&SS (case SDSS-4B) and ALOADS (case ALOADS-4) programs.\* The deformations appear to be abnormally large near the center of gravity of the airplane ( $1850 \leq X < 2550$ ). To explain this anomaly the clamped flexibility matrix input to the case ESIC-4 (and ALOADS-4) was examined. The deflections due to a unit load at each node, obtained by multiplying the input flexibility matrix by a unit vector, showed deformation characteristics similar to the program output. It was concluded that the input flexibility matrix was in error.

\*The SD&SS program computes the elastic displacements at the aerocentroids with respect to the mean axis while the ALOADS program calculates the elastic displacements at structural nodes with respect to the structural reference or clamped axis.

The curves in Figure 6.2.4 labeled (SDSS) and (ALOADS) represent the same deformed shape, but as measured from the two different reference frames. The X-axes of both these frames are plotted as a single axis in the figure, thus the two measures of the deformed shape appear as two separate curves. These two curves are directly related to each other by the relative rotation and translation (in the z direction only) of the two axis systems in which they are measured (See Section 4.2.2 of Volume IV). The equation relating these curves is:

where:

$\delta_i$  -- displacement obtained from SDSS-4B (measured with respect to the X-axis of the mean axis system)

$\delta'_i$  -- displacement obtained from ALOADS-4 (measured with respect to the X-axis of the structural reference axes).

$d_o = (\delta_i - \delta'_i)$  at  $x_i = x_{cg}$  ( $x_{cg}$  is the axial location of the center of gravity, equal to 2250 in. for this configuration)

$x_i = \bar{x}_i - x_{cg}$

$\theta_o$  -- rotational displacement of the ALOADS-4 curve with respect to that of the SDSS-4B curve, positive in the clockwise direction.

$x_i$  -- abscissa of the point in question

Evaluating the above equation at  $x_i = 0$  and at  $x_i = 990$  (or at any other two points) gives the numerical values of  $\theta_o$  and  $d_o$  noted in Figure 6.2.4. Observe also the excellent agreement obtained when this transformation is used to shift the ALOADS-4 curve with respect to the SDSS-4B curve. In making these calculations it was assumed, since the rotation,  $\theta_o$ , is small, that the  $x_i$  coordinates of the two curves are identical.

### 6.3 RESULTS OF THE LOCKHEED YF-12A DEMONSTRATION CASE

Tables 6.3-1 through 6.3-6 present the stability and controls results calculated by the SDSS-5A and SDSS-5B demonstration case runs. Each table gives a rigid versus flexible comparison for each different flight condition. These results are compared with flight test data in Reference 3-3 (confidential).

TABLE 6.3-1.—AERODYNAMIC STABILITY AND CONTROL DATA—  
LOCKHEED YF-12A

$$M_1 = 0.80, NZ = 1.5, \bar{q}_1 = 667 \text{ lb/ft}^2, \gamma_1 = 7.19^\circ, c_g = 0.195\bar{c}$$

Parameter	Unit	Static-elastic model	Rigid model
576 singularities, symmetric reference flight			
$a_1$	deg	4.0656	4.7520
$\delta e_1$	deg	-2.4803	-1.2606
$C_{L_o}$	—	-0.006816	-0.019492
$C_{D_o}$	—	0.000338	0.000487
$C_{m_o}$	—	0.008862	0.013419
$C_{L_a}$	deg <sup>-1</sup>	0.042881	0.039586
$C_{D_a}$	deg <sup>-1</sup>	0.005135	0.005334
$C_{m_a}$	deg <sup>-1</sup>	-0.005815	-0.005241
$C_{L_Q}$	rad <sup>-1</sup>	3.094026	3.400769
$C_{D_Q}$	rad <sup>-1</sup>	0.195024	0.254623
$C_{m_Q}$	rad <sup>-1</sup>	-1.234435	-1.372276
$C_{L_{\delta e}}$	deg <sup>-1</sup>	0.005485	0.016312
$C_{D_{\delta e}}$	deg <sup>-1</sup>	0.000414	0.001246
$C_{m_{\delta e}}$	deg <sup>-1</sup>	-0.005511	-0.009423
static stability parameters			
$h_n$ -h	% $\bar{c}$	13.56	13.24
$h_n$	% $\bar{c}$	29.56	29.24
$h_m$ -h	% $\bar{c}$	14.65	14.45
$h_m$	% $\bar{c}$	30.65	30.46
$\Delta\delta e/n-1$	deg/g	-3.0013	-1.9383

TABLE 6.3-2.—AERODYNAMIC STABILITY AND CONTROL DATA—  
LOCKHEED YF-12A

$$M_1 = 0.80, NZ = 1.0, \bar{q}_1 = 667 \text{ lb/ft}^2, \gamma_1 = 3.82^\circ, c_g = 0.195\bar{c}$$

Parameter	Unit	Static-elastic model	Rigid model
576 singularities, symmetric reference flight			
$a_1$	deg	2.6934	3.1472
$\delta e_1$	deg	-1.0873	-0.3129
$C_{L_o}$	—	-0.006816	-0.019492
$C_{D_o}$	—	0.000338	0.000487
$C_{m_o}$	—	0.008862	0.013419
$C_{L_a}$	deg <sup>-1</sup>	0.042897	0.039600
$C_{D_a}$	deg <sup>-1</sup>	0.003186	0.003354
$C_{m_a}$	deg <sup>-1</sup>	-0.005798	-0.005221
$C_{L_Q}$	rad <sup>-1</sup>	3.097809	3.406566
$C_{D_Q}$	rad <sup>-1</sup>	0.120875	0.159281
$C_{m_Q}$	rad <sup>-1</sup>	-1.234435	-1.372276
$C_{L_{\delta e}}$	deg <sup>-1</sup>	0.005493	0.016341
$C_{D_{\delta e}}$	deg <sup>-1</sup>	0.000283	0.000789
$C_{m_{\delta e}}$	deg <sup>-1</sup>	-0.005511	-0.009423
static stability parameters			
$h_n \cdot h$	% $\bar{c}$	13.52	13.18
$h_n$	% $\bar{c}$	29.52	29.19
$h_m \cdot h$	% $\bar{c}$	14.61	14.40
$h_m$	% $\bar{c}$	30.61	30.40
$\Delta \delta e/n-1$	deg/g	-2.9915	-1.9293

TABLE 6.3-3.—AERODYNAMIC STABILITY AND CONTROL DATA—  
LOCKHEED YF-12A

$$M_1 = 0.80, N_Z = 0.51, \bar{q}_1 = 667 \text{ lb/ft}^2, \gamma_1 = 11.04^\circ, c_g = 0.195\bar{c}$$

Parameter	Unit	Static-elastic model	Rigid model
576 singularities, symmetric reference flight			
$a_1$	deg	1.4376	1.5464
$\delta e_1$	deg	0.4567	0.6341
$C_{L_o}$	—	-0.006816	-0.019492
$C_{D_o}$	—	0.000338	0.000487
$C_{m_o}$	—	0.008862	0.013419
$C_{L_a}$	deg <sup>-1</sup>	0.042895	0.039596
$C_{D_a}$	deg <sup>-1</sup>	0.001430	0.001385
$C_{m_a}$	deg <sup>-1</sup>	-0.005789	-0.005209
$C_{L_Q}$	rad <sup>-1</sup>	3.099714	3.409687
$C_{D_Q}$	rad <sup>-1</sup>	0.052953	0.064055
$C_{m_Q}$	rad <sup>-1</sup>	-1.234435	-1.372276
$C_{L_{\delta e}}$	deg <sup>-1</sup>	0.005498	0.016356
$C_{D_{\delta e}}$	deg <sup>-1</sup>	0.000162	0.000332
$C_{m_{\delta e}}$	deg <sup>-1</sup>	-0.005511	-0.009423
static stability parameters			
$h_n \cdot h$	% $\bar{c}$	13.50	13.15
$h_n$	% $\bar{c}$	29.50	29.16
$h_m \cdot h$	% $\bar{c}$	14.59	14.37
$h_m$	% $\bar{c}$	30.59	30.37
$\Delta \delta e/n-1$	deg/g	-2.9870	-1.9247



TABLE 6.3-4.—AERODYNAMIC STABILITY AND CONTROL DATA—  
LOCKHEED YF-12A

$$M_1 = 2.80, NZ = 1.5, \bar{q}_1 = 628 \text{ lb/ft}^2, \gamma_1 = 6.29^\circ, c_g = 0.250\bar{c}$$

Parameter	Unit	Static-elastic model	Rigid model
576 singularities, symmetric reference flight			
$a_1$	deg	5.7933	5.8950
$\delta e_1$	deg	-12.0367	-9.4788
$C_{L_0}$	—	0.004090	0.000306
$C_{D_0}$	—	0.002180	0.002205
$C_{m_0}$	—	0.001864	0.003883
$C_{L_a}$	deg <sup>-1</sup>	0.023794	0.025369
$C_{D_a}$	deg <sup>-1</sup>	0.004454	0.004607
$C_{m_a}$	deg <sup>-1</sup>	-0.003023	-0.004005
$C_{L_Q}$	rad <sup>-1</sup>	0.799013	0.913059
$C_{D_Q}$	rad <sup>-1</sup>	0.080358	0.092321
$C_{m_Q}$	rad <sup>-1</sup>	-0.716992	-0.783782
$C_{L_{\delta e}}$	deg <sup>-1</sup>	0.001519	0.002976
$C_{D_{\delta e}}$	deg <sup>-1</sup>	0.000161	0.000302
$C_{m_{\delta e}}$	deg <sup>-1</sup>	-0.001196	-0.002055
static stability parameters			
$h_n^{-h}$	% $\bar{c}$	12.71	15.79
$h_n$	% $\bar{c}$	34.33	37.41
$h_m^{-h}$	% $\bar{c}$	12.78	15.87
$h_m$	% $\bar{c}$	34.40	37.49
$\Delta\delta e/n-1$	deg/g	-10.4420	-8.2052

TABLE 6.3-5.—AERODYNAMIC STABILITY AND CONTROL DATA—  
LOCKHEED YF-12A

$$M_1 = 2.80, N_Z = 0.98, \bar{q}_1 = 628 \text{ lb/ft}^2, \gamma_1 = 4.09^\circ, c_g = 0.250\bar{c}$$

Parameter	Unit	Static-elastic model	Rigid model
576 singularities, symmetric reference flight			
$a_1$	deg	3.6806	3.7575
$\delta e_1$	deg	-7.1340	-5.3464
$C_{L_o}$	—	0.004090	0.000306
$C_{D_o}$	—	0.002180	0.002205
$C_{m_o}$	—	0.001864	0.003883
$C_{L_a}$	deg <sup>-1</sup>	0.023837	0.025405
$C_{D_a}$	deg <sup>-1</sup>	0.002815	0.002915
$C_{m_a}$	deg <sup>-1</sup>	-0.003005	-0.003980
$C_{L_Q}$	rad <sup>-1</sup>	0.801432	0.915867
$C_{D_Q}$	rad <sup>-1</sup>	0.050848	0.058203
$C_{m_Q}$	rad <sup>-1</sup>	-0.716992	-0.783782
$C_{L_{\delta e}}$	deg <sup>-1</sup>	0.001524	0.002985
$C_{D_{\delta e}}$	deg <sup>-1</sup>	0.000105	0.000191
$C_{m_{\delta e}}$	deg <sup>-1</sup>	-0.001196	-0.002055
static stability parameters			
$h_n$ -h	% $\bar{c}$	12.60	15.66
$h_n$	% $\bar{c}$	34.22	37.28
$h_m$ -h	% $\bar{c}$	12.68	15.75
$h_m$	% $\bar{c}$	34.30	37.37
$\Delta\delta e/n-1$	deg/g	-10.3505	-8.1314

TABLE 6.3-6.—AERODYNAMIC STABILITY AND CONTROL DATA—  
LOCKHEED YF-12A

$$M_1 = 2.80, NZ = 0.46, \bar{q}_1 = 628 \text{ lb/ft}^2, \gamma_1 = 2.44^\circ, c_g = 0.250\bar{c}$$

Parameter	Unit	Static-elastic model	Rigid model
576 singularities, symmetric reference flight			
$a_1$	deg	1.5612	1.6067
$\delta e_1$	deg	-2.0549	-1.1850
$C_{L_o}$	—	0.004090	0.000306
$C_{D_o}$	—	0.002180	0.002205
$C_{m_o}$	—	0.001864	0.003883
$C_{L_a}$	deg <sup>-1</sup>	0.023859	0.025422
$C_{D_a}$	deg <sup>-1</sup>	0.001181	0.001218
$C_{m_a}$	deg <sup>-1</sup>	-0.002995	-0.003966
$C_{L_Q}$	rad <sup>-1</sup>	0.802765	0.917406
$C_{D_Q}$	rad <sup>-1</sup>	0.021175	0.023789
$C_{m_Q}$	rad <sup>-1</sup>	-0.716992	-0.783782
$C_{L_{\delta e}}$	deg <sup>-1</sup>	0.001527	0.002990
$C_{D_{\delta e}}$	deg <sup>-1</sup>	0.000049	0.000079
$C_{m_{\delta e}}$	deg <sup>-1</sup>	-0.001196	-0.002055
static stability parameters			
$h_n$ -h	% $\bar{c}$	12.55	15.60
$h_n$	% $\bar{c}$	34.17	37.22
$h_m$ -h	% $\bar{c}$	12.63	15.69
$h_m$	% $\bar{c}$	34.25	37.31
$\Delta\delta e/n-1$	deg/g	-10.3017	-8.0917

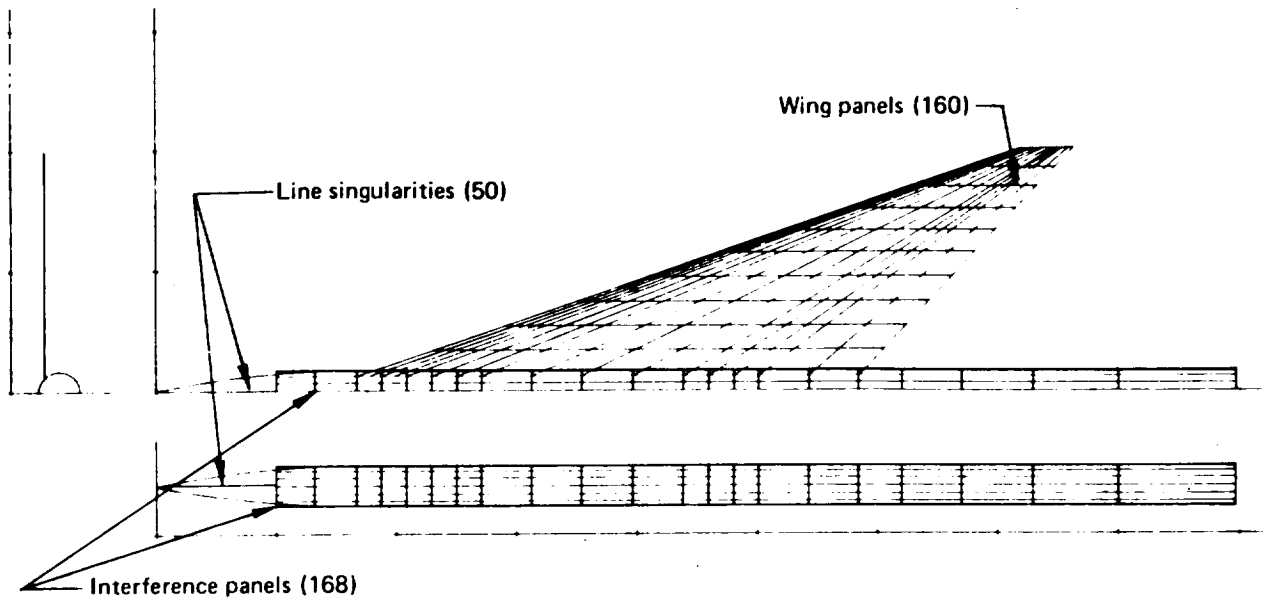
## 6.4 RESULTS AND COMPARISONS OF THE ARROW-WING CONFIGURATION

Selected results from an extensive study documented in References 6-12 and 6-13, are presented in this section. In the referenced study, a wind tunnel test of an arrow-wing configuration (Figure 6.4.1) employing both a twisted and flat wing was conducted to provide experimental data useful in indicating the range of validity of linear theoretical methods applied to configurations of this general type. The basic aerodynamic geometry (arrangement "a" in Figure 6.4.1) caused oscillatory pressure on the wing at low supersonic Mach numbers of 1.05 and 1.1. The aerodynamic geometry of arrangement "b" resulted in satisfactory pressure distribution at these two Mach numbers.

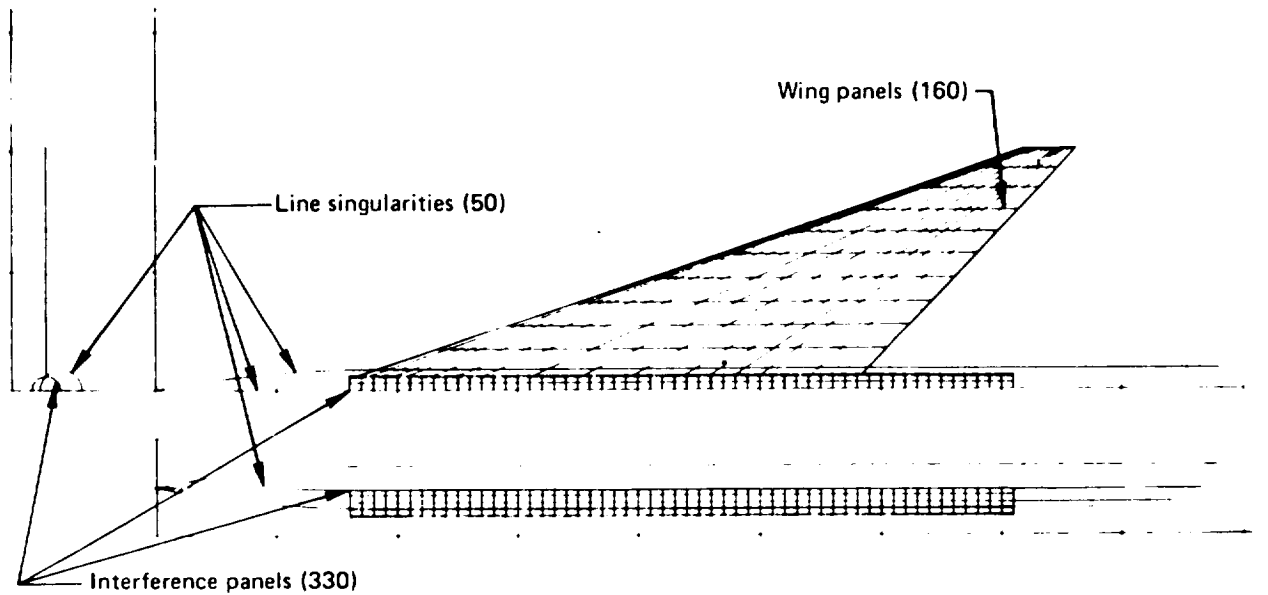
The comparison data included here is for the flat wing. The FLEXSTAB results for the twisted wing show the same degree of capability. However, the range of angle of attack  $\alpha$ , showing good FLEXSTAB experiment agreement is slightly shifted (to higher  $\alpha$ ) for the twisted wing due to the washout at the wing tip.

For subsonic Mach numbers, surface pressure data calculated using a modified version of FLEXSTAB are compared with the results from the TEA-230 program and the wind tunnel results (The 1.02.00 Version of FLEXSTAB does not have the capability to calculate upper and lower surface pressures separately, but rather computes the pressure difference  $\Delta C_p = C_{p_l} - C_{p_u}$ ). The TEA-230 program is a Boeing subsonic, potential flow aerodynamics program (Reference 6-14), that can treat an arbitrary three-dimensional configuration with lift. It solves Laplace's equation and approximates the compressibility effects by the G6thert rule. In contrast with the FLEXSTAB mean surface model, the aerodynamic singularities are distributed on planar panels approximating the actual configuration surface, and the boundary conditions are satisfied on these panels. In addition, there are two other important differences between FLEXSTAB and TEA-230. First, in FLEXSTAB, the linearized potential flow equations are solved at zero angle of attack, and the solution at any other angle of attack is obtained by considering small perturbation about the zero angle of attack. In TEA-230, the linearized potential flow equation is solved for the specified flow direction. Secondly, a linear pressure velocity relation is used in FLEXSTAB whereas a nonlinear pressure velocity relation is available in the TEA-230. As a result, it will be seen later in this section that (a) TEA-230 solution predicts more accurate (relative to FLEXSTAB) pressure distribution closer to the wing leading edge, and (b) TEA-230 results in a nonlinear (normal force)  $C_n$  vs.  $\alpha$  variation, in contrast with a linear variation from FLEXSTAB, obtained from solving the linearized potential flow equation.

Figures 6.4.2 and 6.4.3 show comparisons of the results from FLEXSTAB, TEA-230 and experiment at  $M = 0.40$  and  $0.85$  for  $\alpha = 2.1^\circ$ . The FLEXSTAB and TEA-230 results compare well with the experiment results except at the leading edge. The TEA-230 results agree with the experiment results closer to the leading edge than the FLEXSTAB results. The comparisons for  $\alpha = 2.0^\circ$  at  $M = 1.05$  and  $2.5$  between FLEXSTAB and experiment are shown in Figure 6.4.4 and 6.4.5. The agreement for the supersonic flow is not as good as for the subsonic flow, but is reasonably good except at the leading edge. The leading edge remains subsonic at both Mach numbers and the FLEXSTAB solution shows the subsonic characteristics at the leading edge.



(a) Basic Arrangement of Panels Used for all but Low Supersonic Mach Numbers



(b) Arrangement of Panels Used for Low Supersonic Mach Numbers ( $M=1.05, 1.1$ )

FIGURE 6.4.1.—FLEXSTAB AERODYNAMIC GEOMETRY OF THE ARROW-WING CONFIGURATION

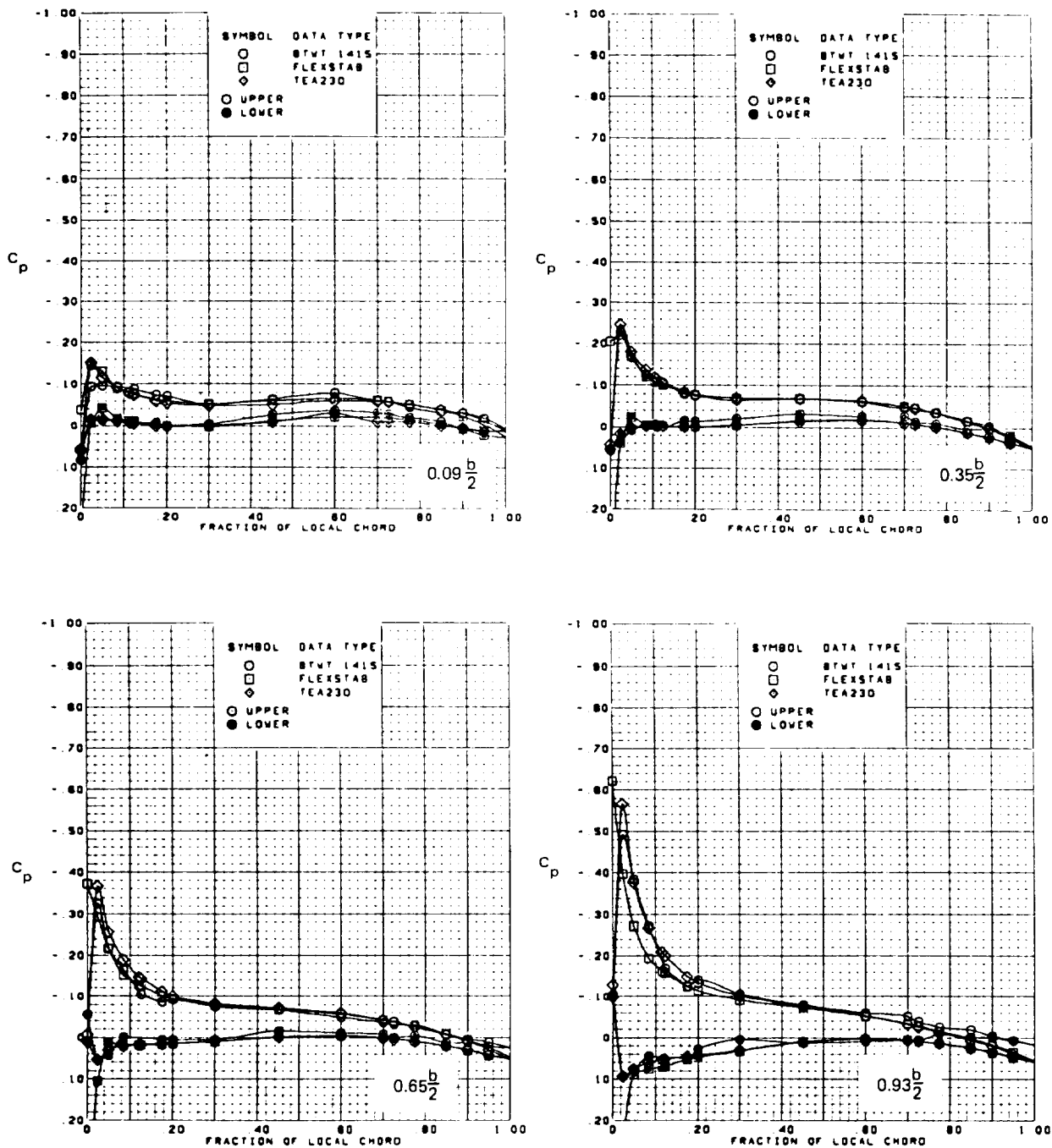


FIGURE 6.4-2.—ANALYSIS-TO-EXPERIMENT PRESSURE COMPARISON FOR ARROW-WING CONFIGURATION, TRAILING EDGE FLAP UNDEFLECTED  
 $M=0.40, \alpha=2.1^\circ$

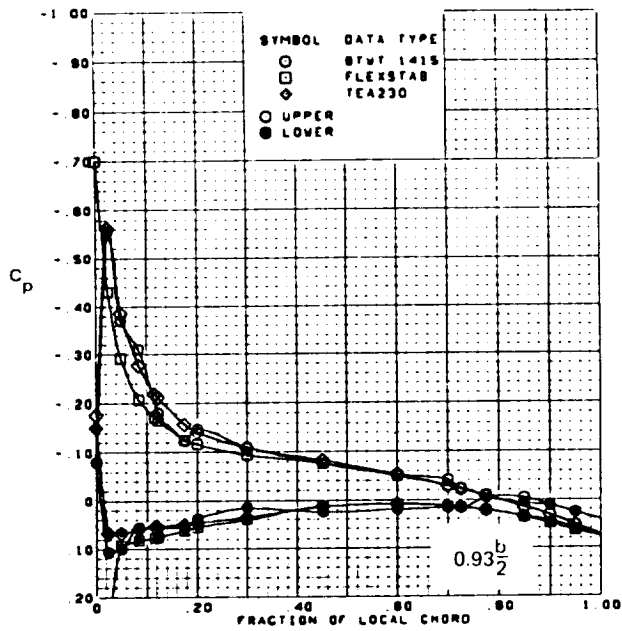
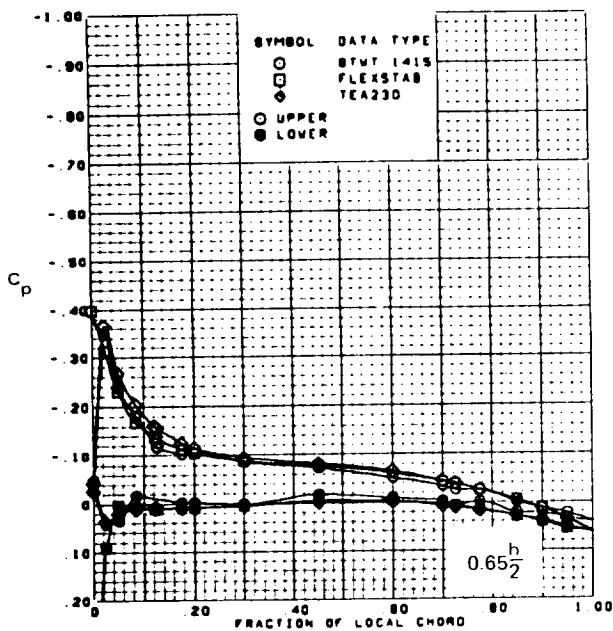
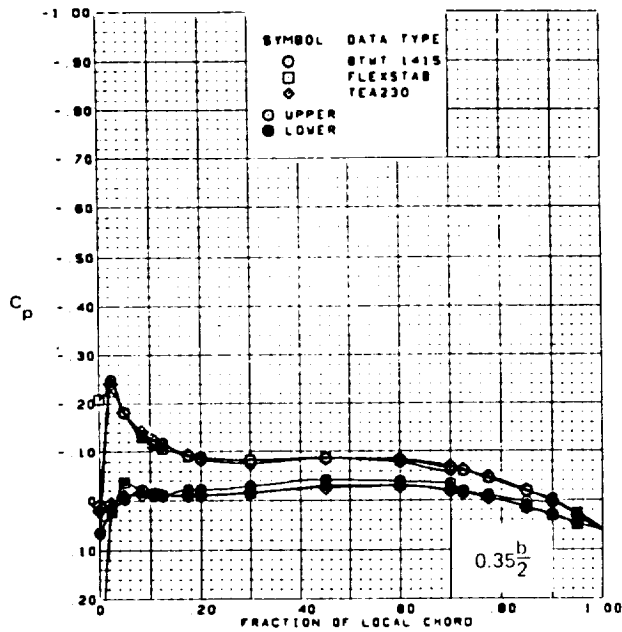
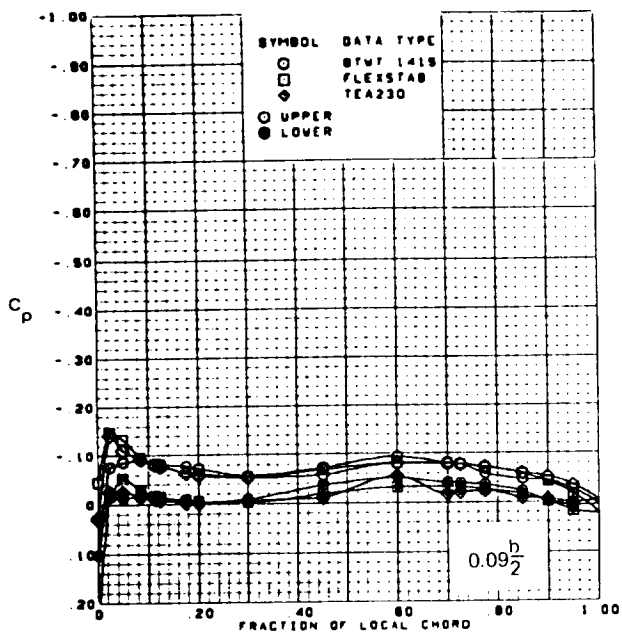


FIGURE 6.4-3.—ANALYSIS-TO-EXPERIMENT PRESSURE COMPARISON FOR ARROW-WING CONFIGURATION; TRAILING EDGE FLAP UNDEFLECTED  
 $M=0.85, \alpha=2.1^\circ$

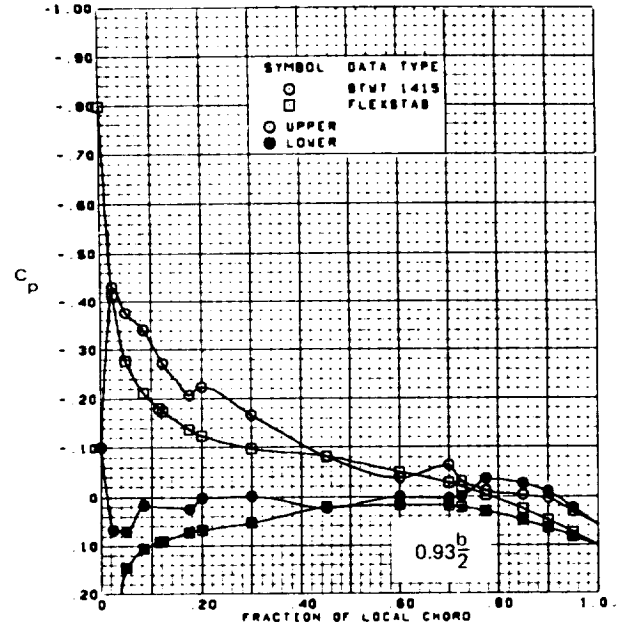
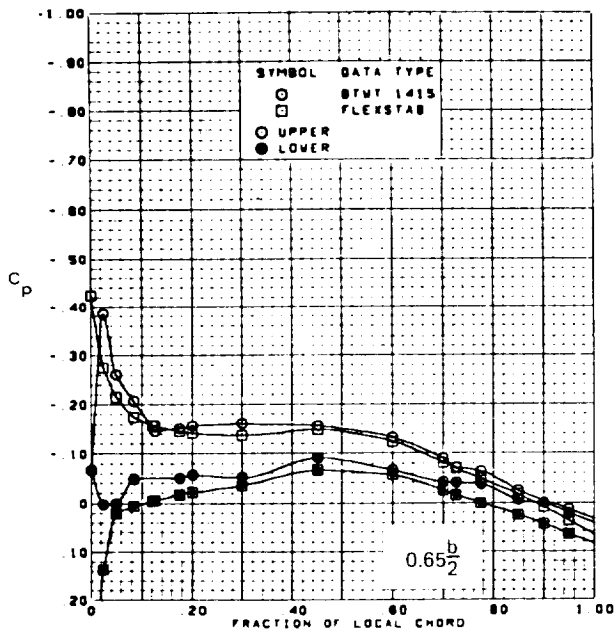
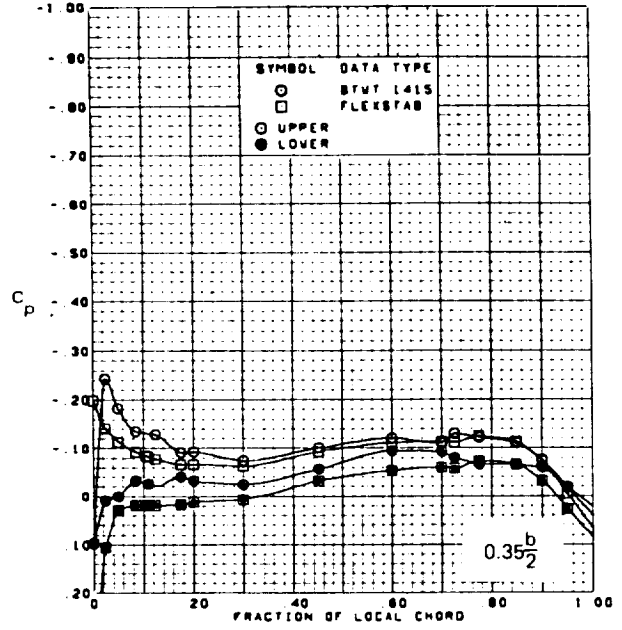
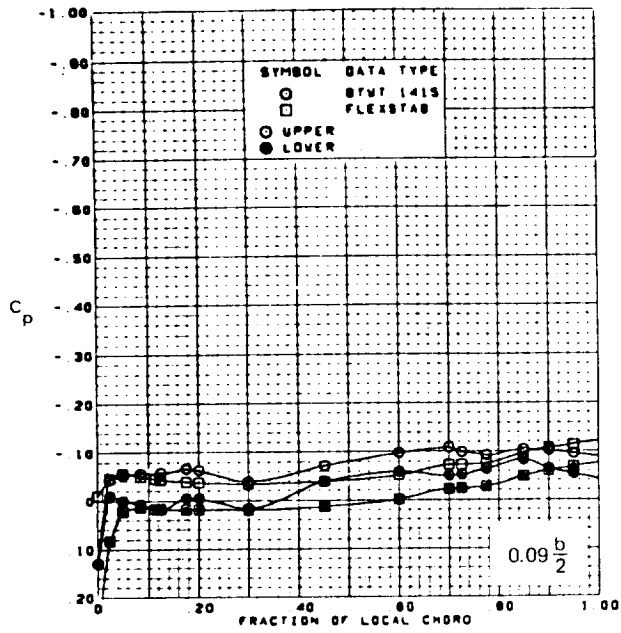


FIGURE 6.4.4.—ANALYSIS-TO-EXPERIMENT PRESSURE COMPARISON FOR ARROW-WING CONFIGURATION; TRAILING EDGE FLAP UNDEFLECTED  
 $M=1.05, \alpha=2.0^\circ$



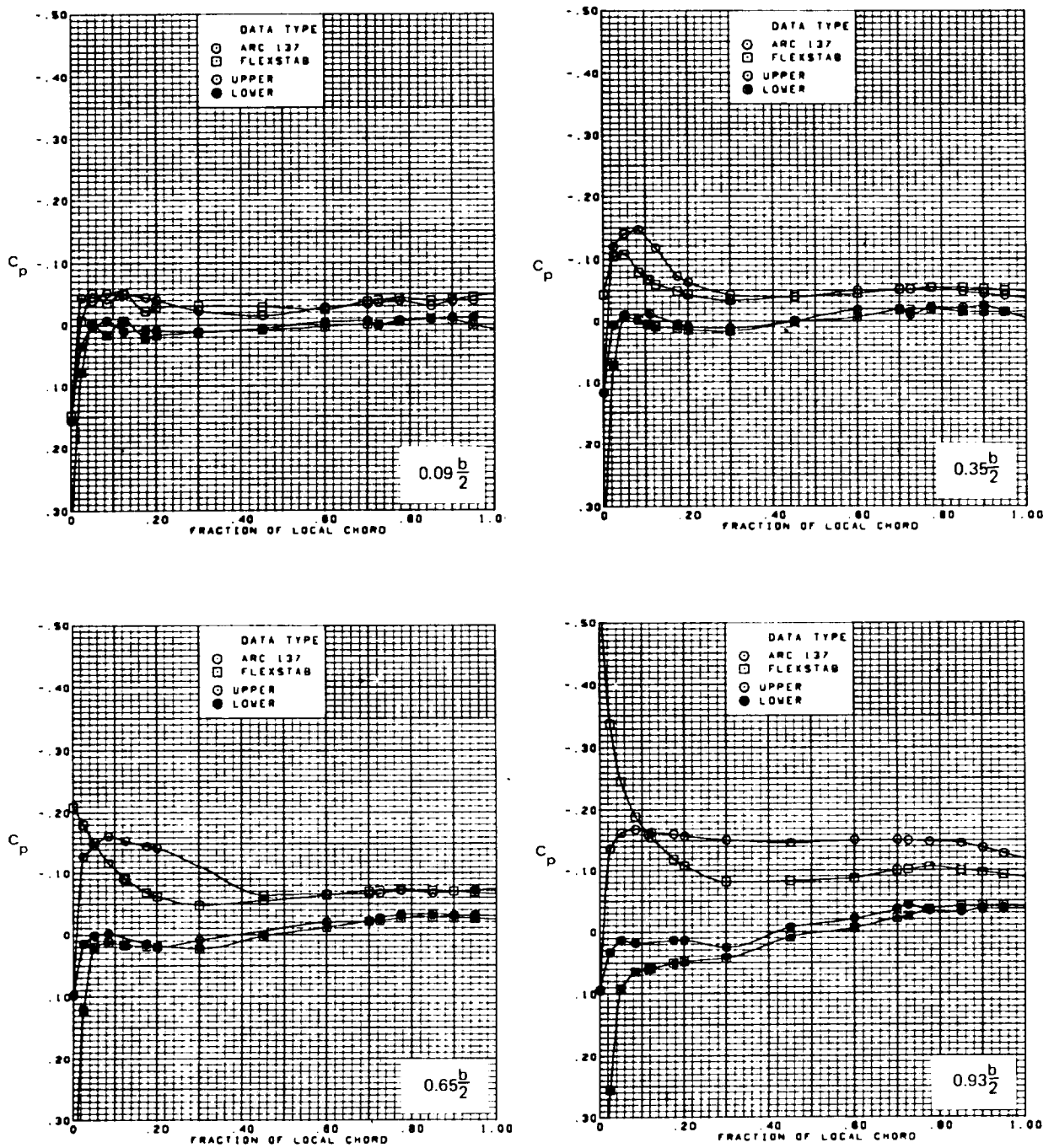


FIGURE 6.4.5.—ANALYSIS-TO-EXPERIMENT PRESSURE COMPARISON FOR ARROW-WING CONFIGURATION; TRAILING EDGE FLAP UNDEFLECTED

$$M=2.5, \alpha=2.0^\circ$$

Figures 6.4.6, 6.4.7, 6.4.8 and 6.4.9 show pressure distributions at  $\alpha = 8^\circ$  for  $M = 0.40, 0.85, 1.05$  and  $2.5$ , respectively. The comparisons of the potential flow results with the wind tunnel results get worse proceeding outboard. The formation of the leading edge vortex has changed the nature of the flow over most of the wing such that it is no longer amenable to the potential flow aerodynamics (see Reference 6-11). Figure 6.4.10 shows spanwise load distribution for  $M = 0.4, 0.85, 1.05$  and  $2.5$  at the two angles of attack. For the larger angle of attack, the presence of the leading edge vortex is seen to cause a higher than predicted load on the outboard sections.

A comparison of calculated vs. wind tunnel results when the flaps are deflected is shown in Figure 6.4.11, 6.4.12 and 6.4.13. At  $M = 0.40$ , the TEA-230 results show a better agreement with the experimental results than the FLEXSTAB results except at  $2y/b = 0.09$ . This is believed to be due to the linearized surface boundary conditions in FLEXSTAB which typically overpredicts the pressures on the control surfaces. This trend is also evident at  $M = 1.05$ . The spanload distribution due to the trailing edge flap deflection is also overpredicted. The results for the leading edge flap deflections are not included here. The theory-to-experiment comparisons were better because the vortex formation is delayed due to the leading edge droop (Reference 6-11).

Figures 6.4-14 and 6.4-15 show the variation of normal force and pitching moment coefficients with angle of attack for  $M = 0.4, 0.85, 1.05$  and  $2.5$ , respectively. These indicate generally good agreement between the FLEXSTAB and wind tunnel results in the linear range. As might be expected, the agreement for the integrated results (coefficients) is qualitatively better than that for the surface pressure distributions. Note the nonlinear variation of the normal force calculated from TEA-230.

In the other results (not included here) from the arrow-wing study it was seen that at lower angles of attack, the twisted wing results were generally in better agreement with the experimental results compared to the flat wing results. The wing twist delays the formation of the leading edge vortex to a higher angle of attack. At higher angles of attack, the twisted wing results show the same characteristics as the flat wing. Reference 6-11 also discusses the failure of the aerodynamic matrix correction schemes (including those available in the CAIC program) in predicting the aeroelastic loads in the presence of separated flow.

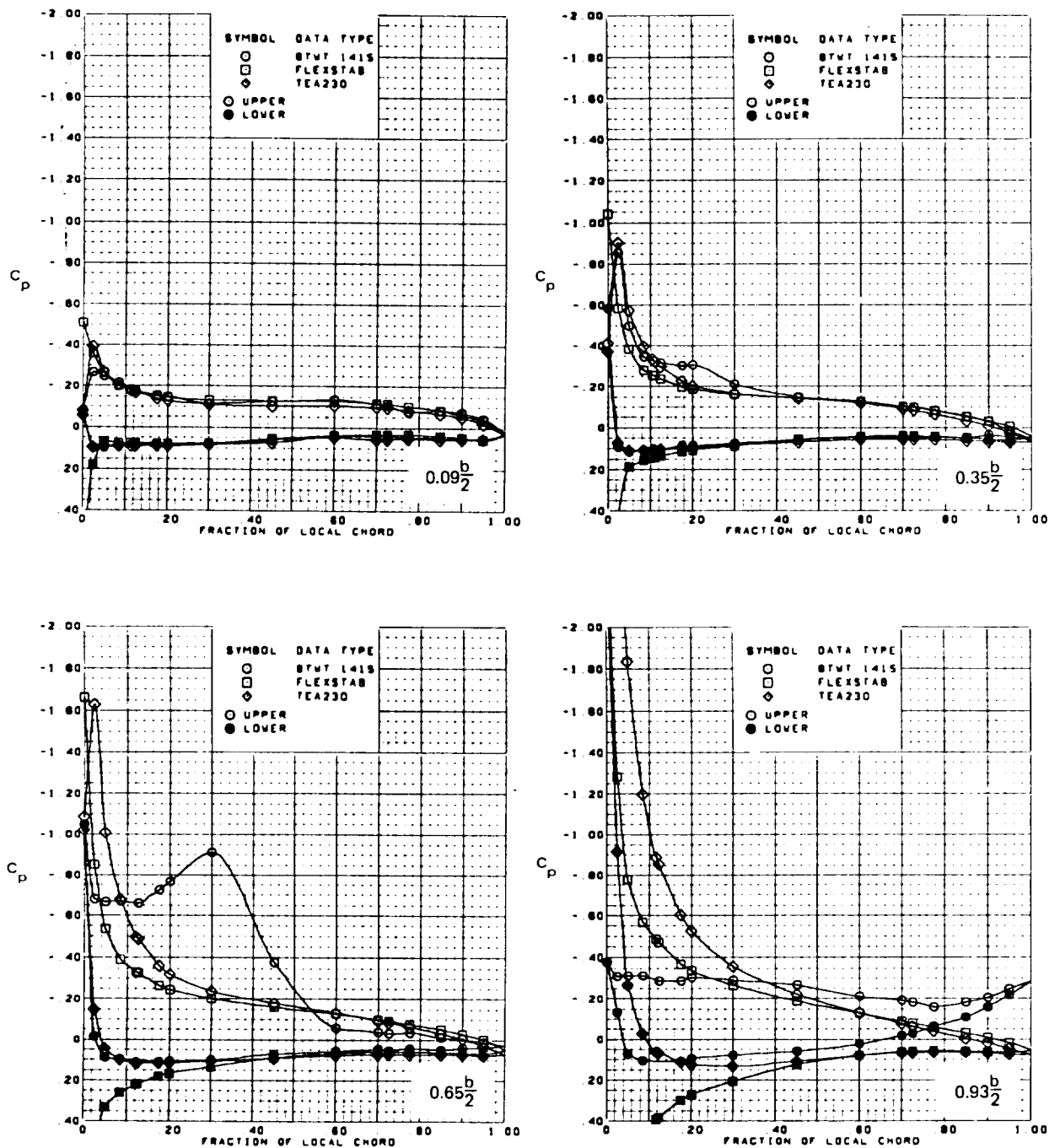


FIGURE 6.4-6.—ANALYSIS-TO-EXPERIMENT PRESSURE COMPARISON FOR ARROW-WING CONFIGURATION; TRAILING EDGE FLAP UNDEFLECTED  
 $M=0.40, \alpha=8.0^\circ$

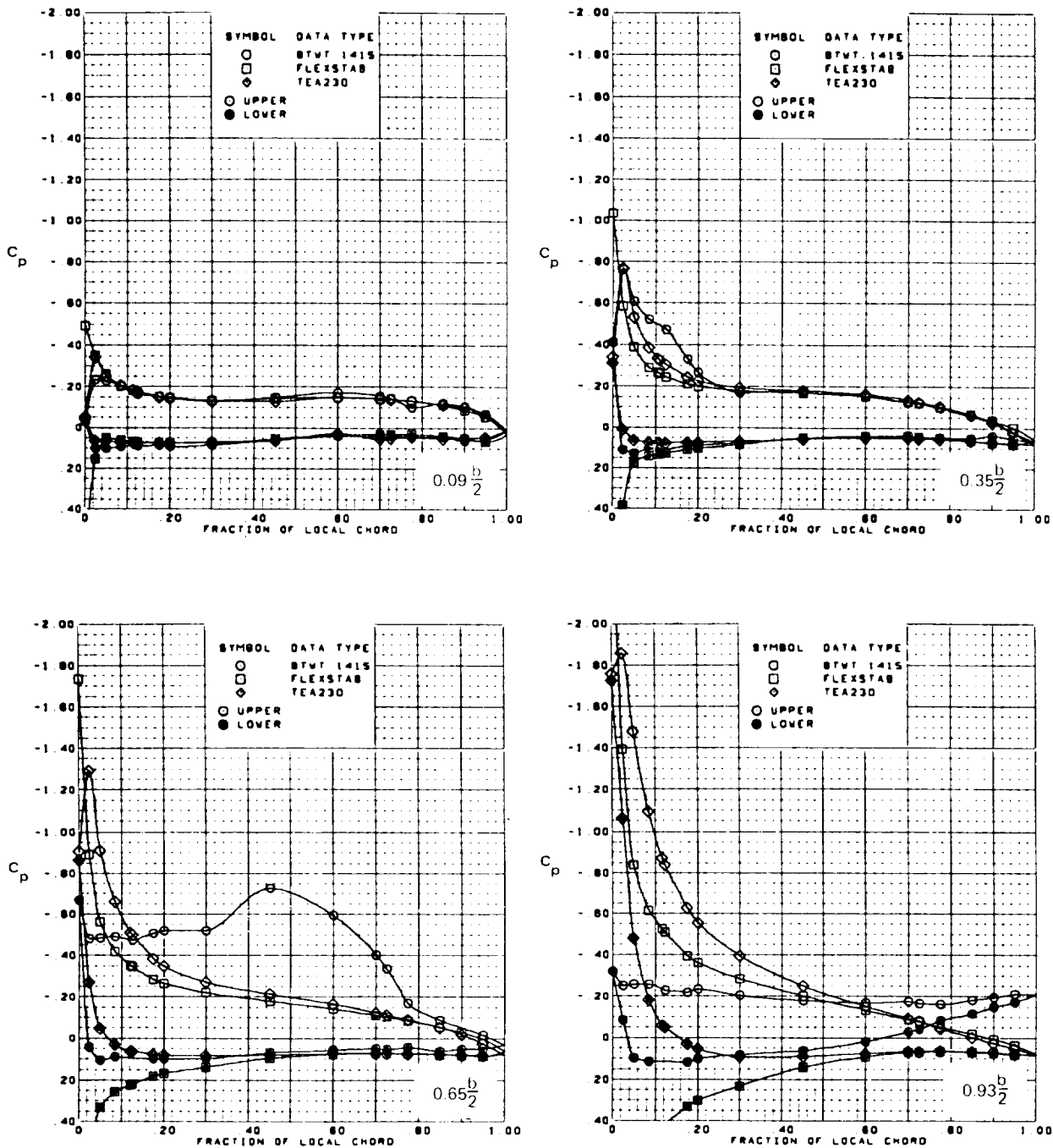


FIGURE 6.4-7.—ANALYSIS-TO-EXPERIMENT PRESSURE COMPARISON FOR ARROW-WING CONFIGURATION; TRAILING EDGE FLAP UNDEFLECTED  
 $M=0.85, \alpha=7.9^\circ$

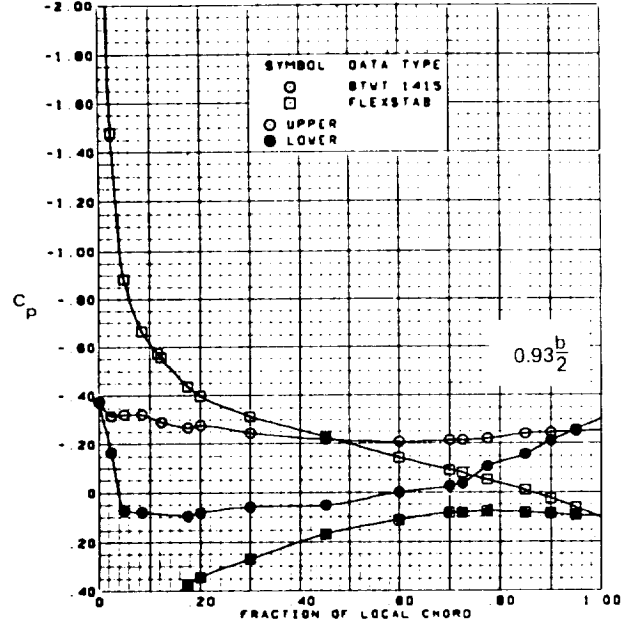
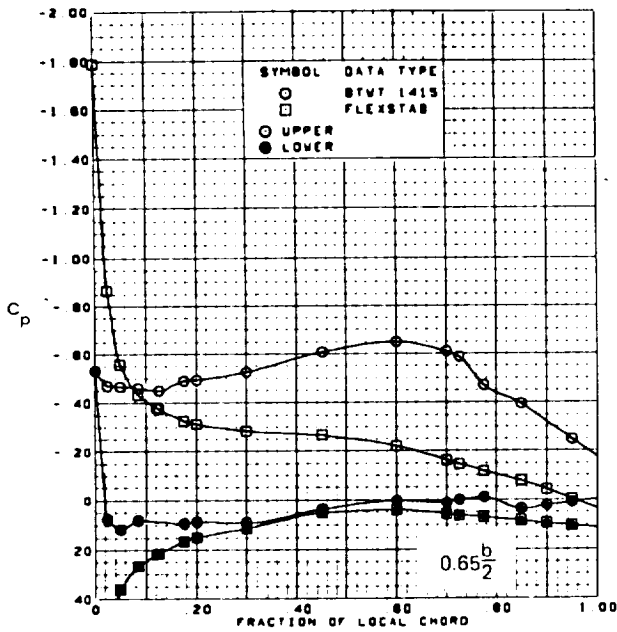
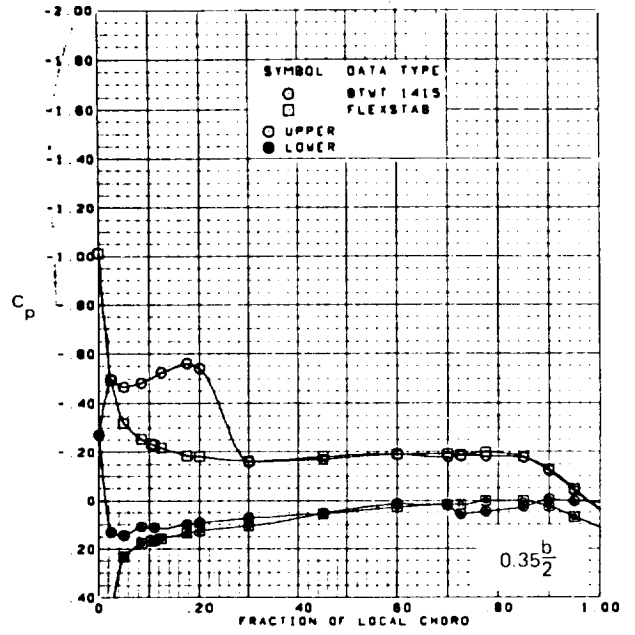
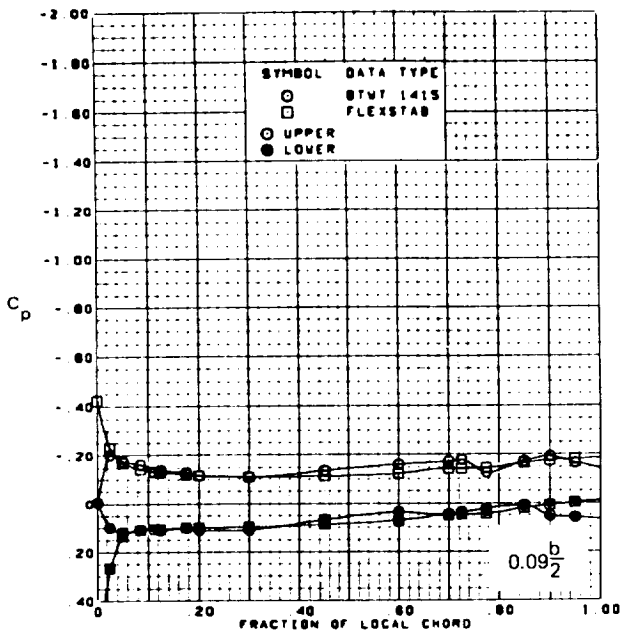


FIGURE 6.4-8.—ANALYSIS TO EXPERIMENT PRESSURE COMPARISON FOR ARROW-WING CONFIGURATION; TRAILING EDGE FLAP UNDEFLECTED  
 $M=1.05, \alpha=7.9^\circ$

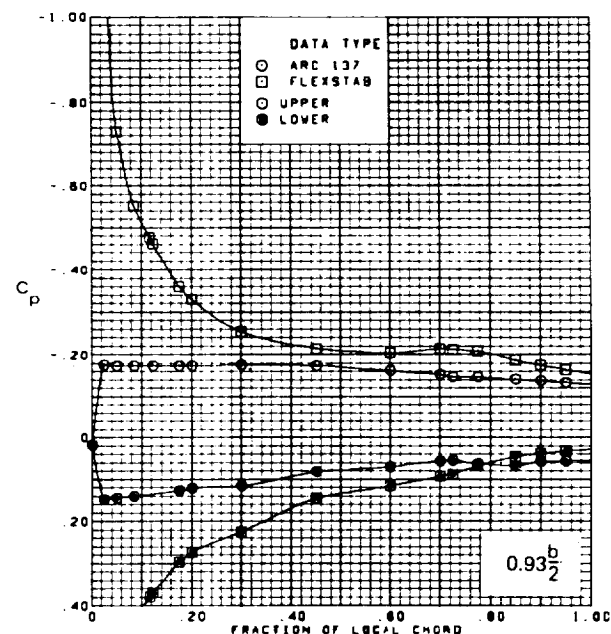
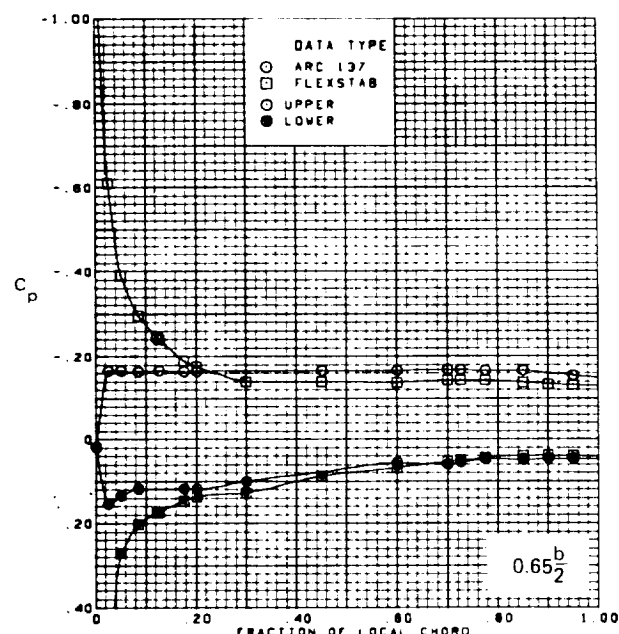
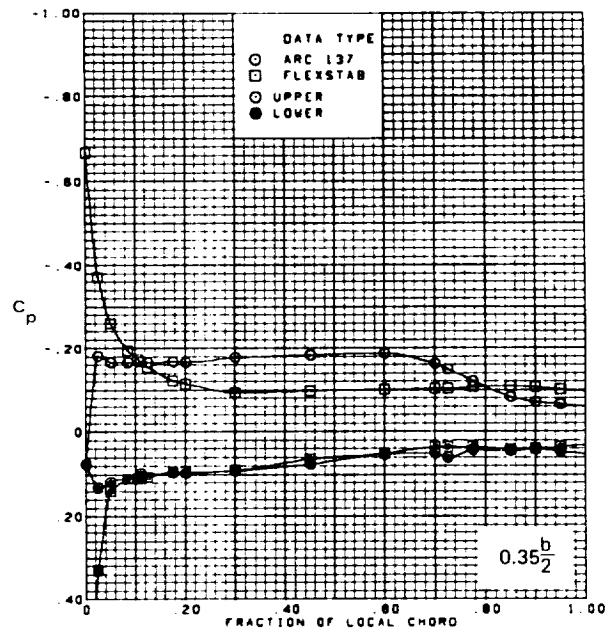
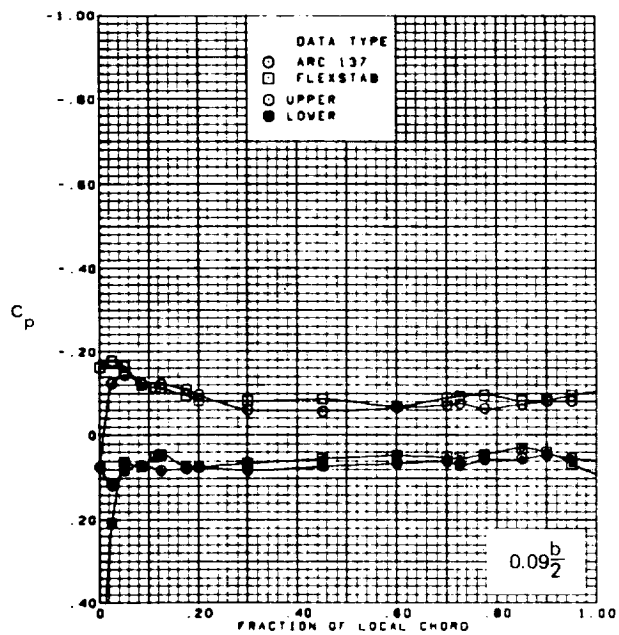


FIGURE 6.4-9.—ANALYSIS-TO-EXPERIMENT PRESSURE COMPARISON FOR ARROW-WING CONFIGURATION; TRAILING EDGE FLAP UNDEFLECTED  
 $M=2.5, \alpha=7.9^\circ$

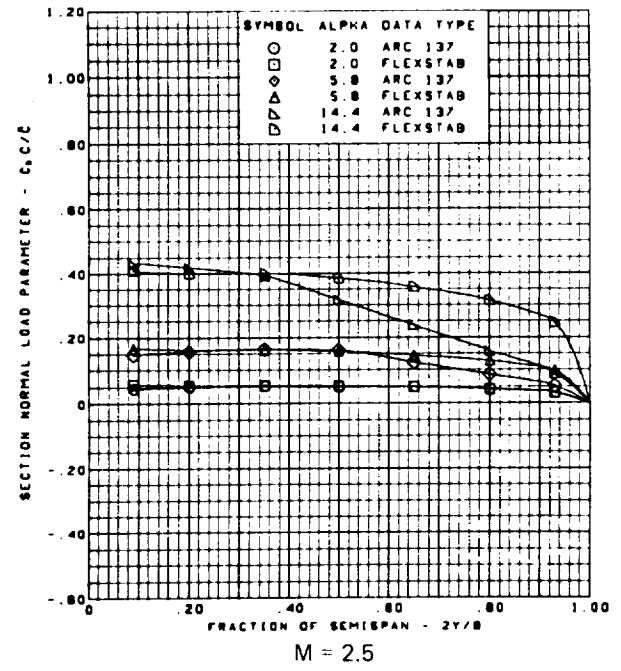
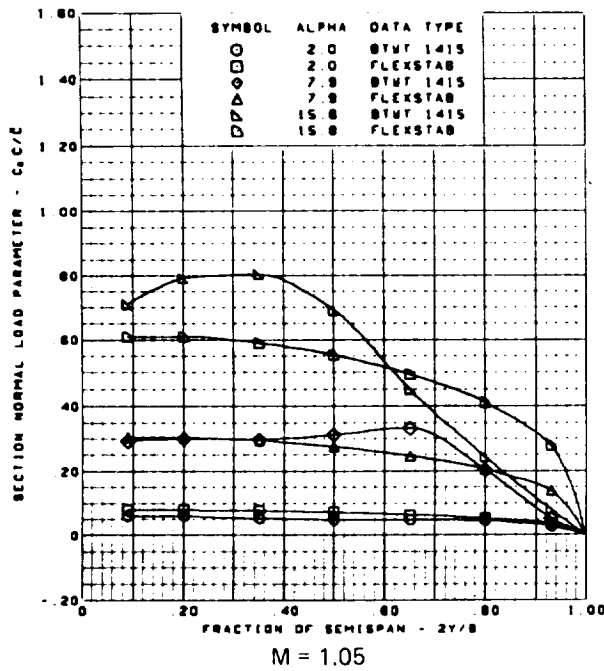
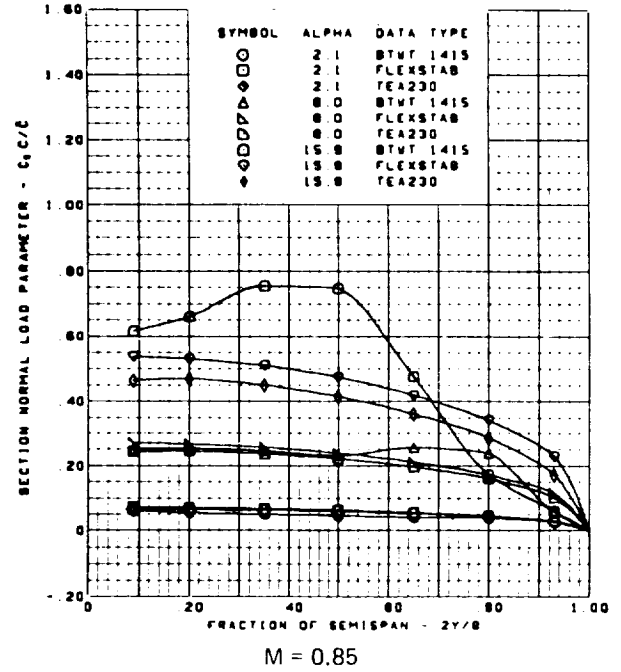
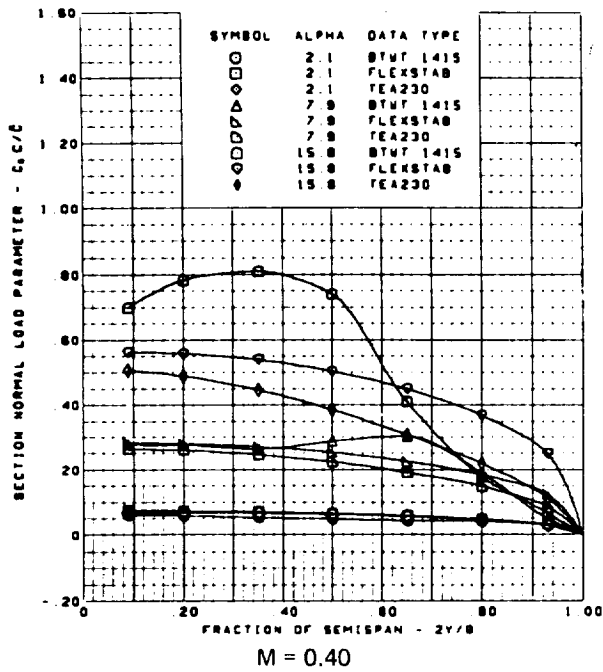


FIGURE 6.4-10.—ANALYSIS-TO-EXPERIMENT SPANLOAD COMPARISON FOR ARROW-WING CONFIGURATION; TRAILING EDGE FLAP=0.0°

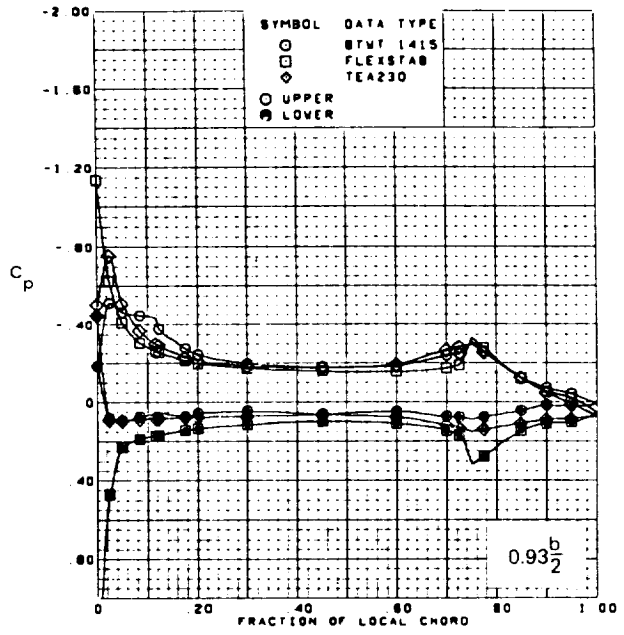
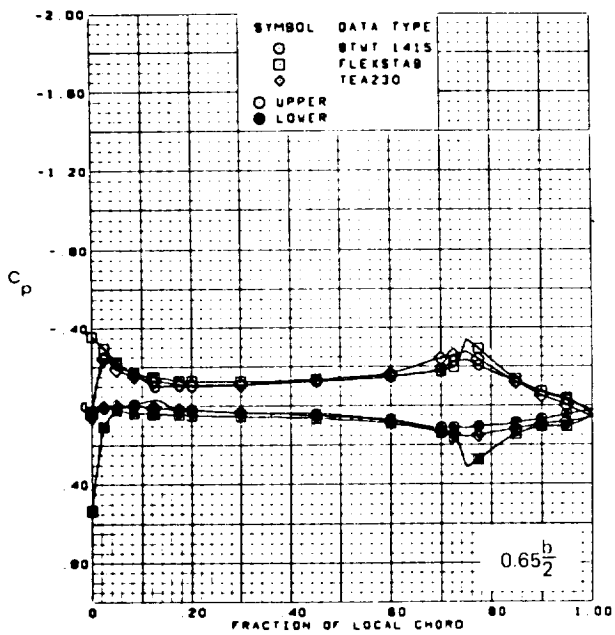
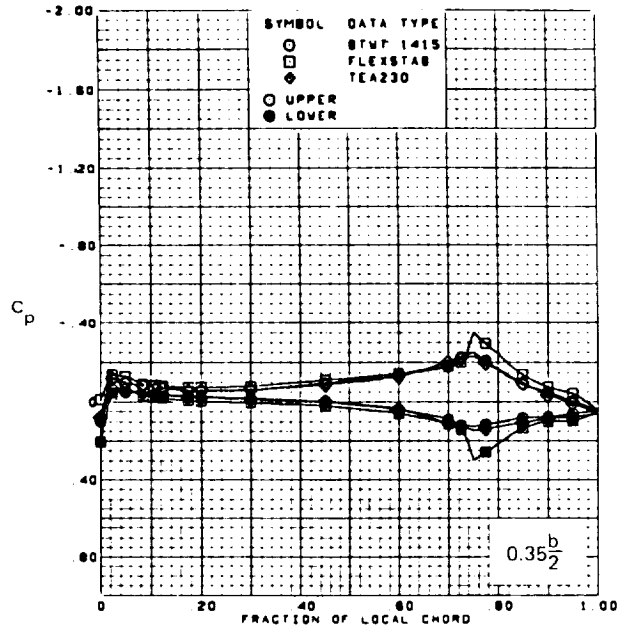
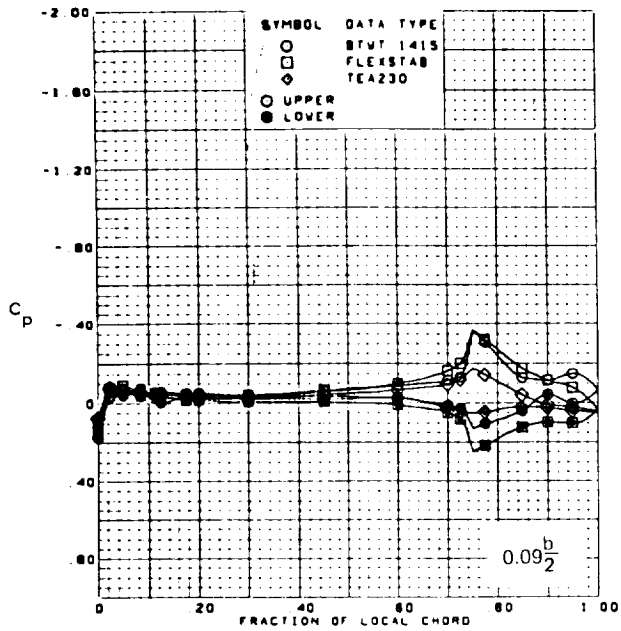


FIGURE 6.4-11.—ANALYSIS-TO-EXPERIMENT PRESSURE COMPARISON FOR  
 ARROW-WING CONFIGURATION; TRAILING EDGE FLAP= $8.3^\circ$   
 $M=0.40, \alpha=0.1^\circ$



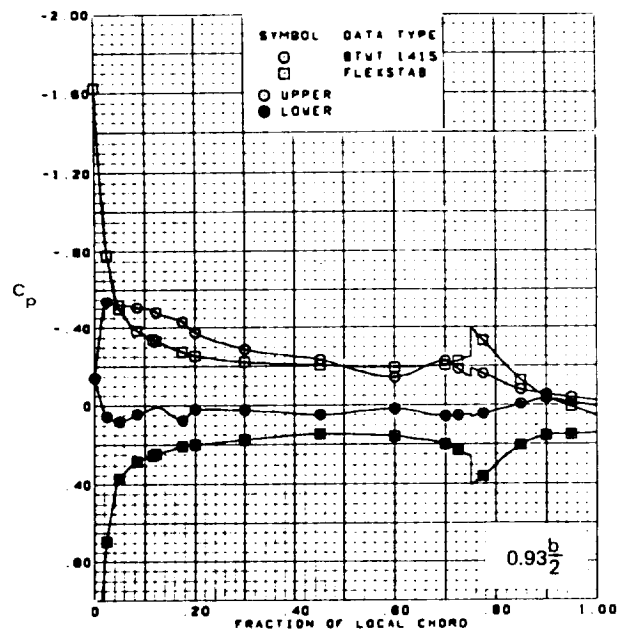
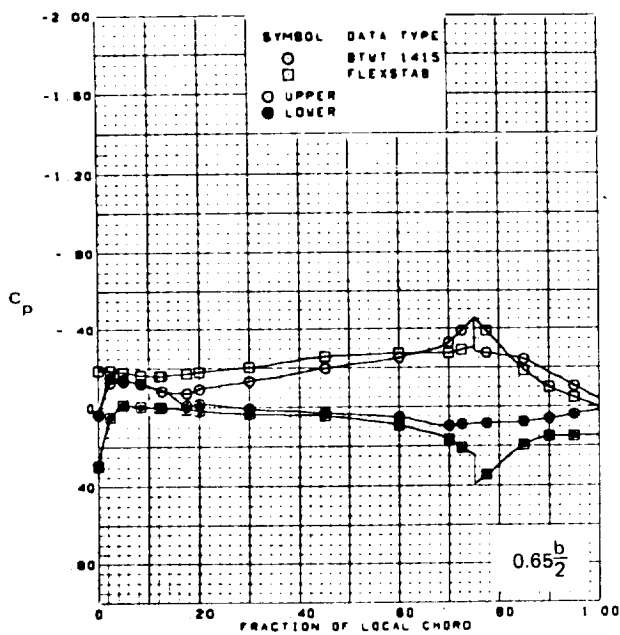
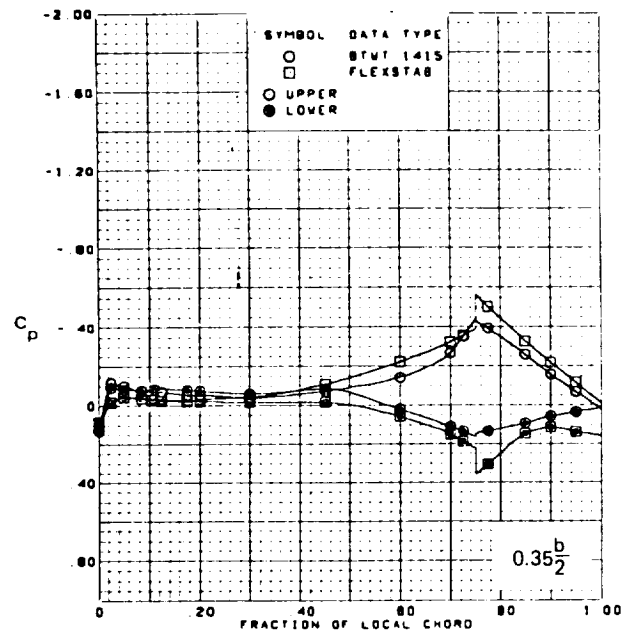
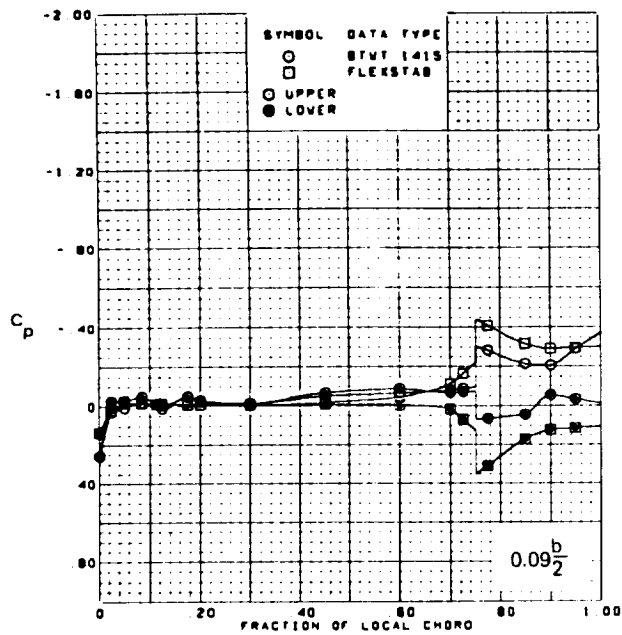


FIGURE 6.4-12.—ANALYSIS-TO-EXPERIMENT PRESSURE COMPARISON FOR  
 ARROW-WING CONFIGURATION; TRAILING EDGE FLAP=8.3°  
 M=1.05,  $\alpha=0.0^\circ$

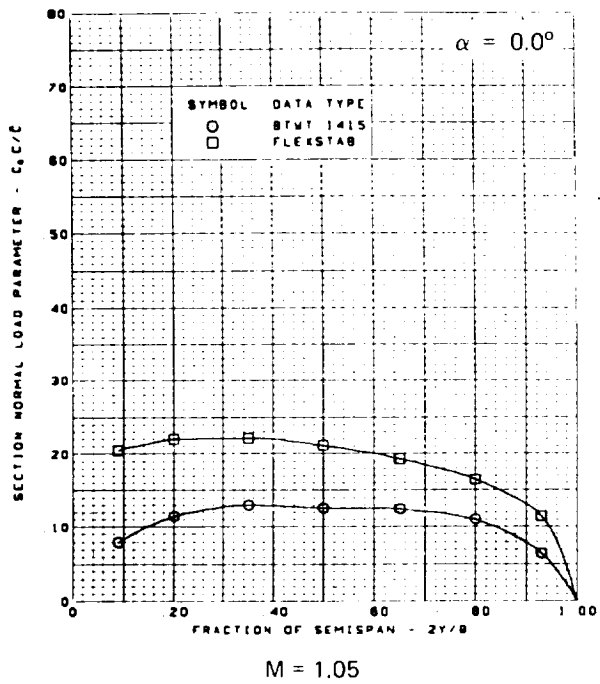
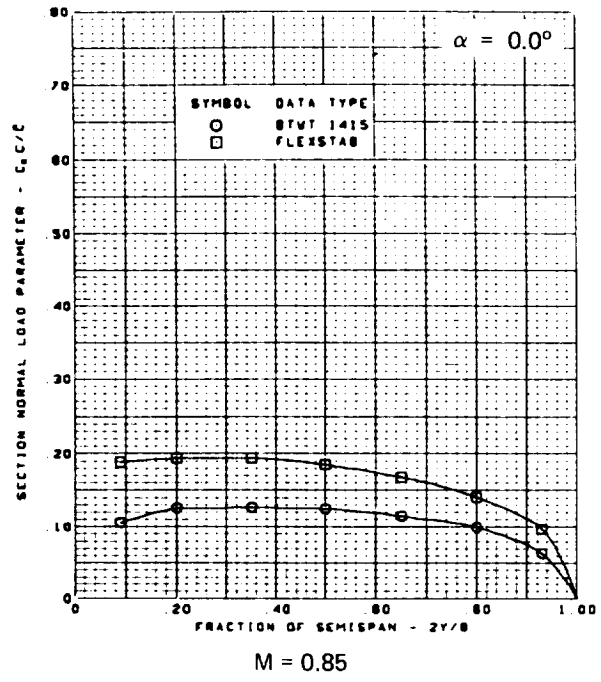
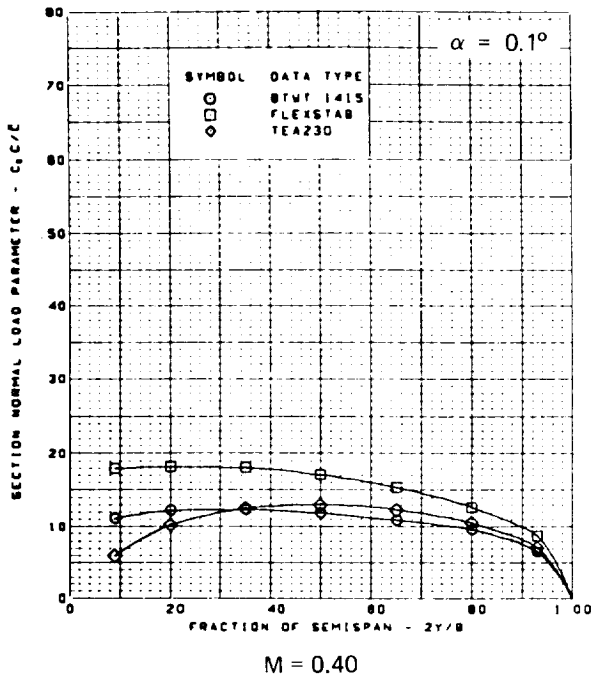


FIGURE 6.4-13.—ANALYSIS-TO-EXPERIMENT SPANLOAD COMPARISON FOR ARROW-WING CONFIGURATION; TRAILING EDGE FLAP= $8.3^\circ$

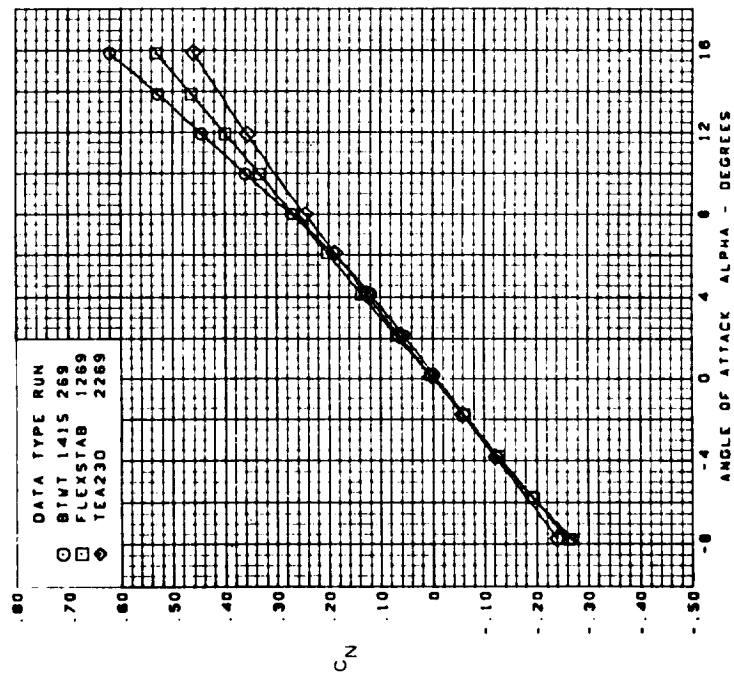
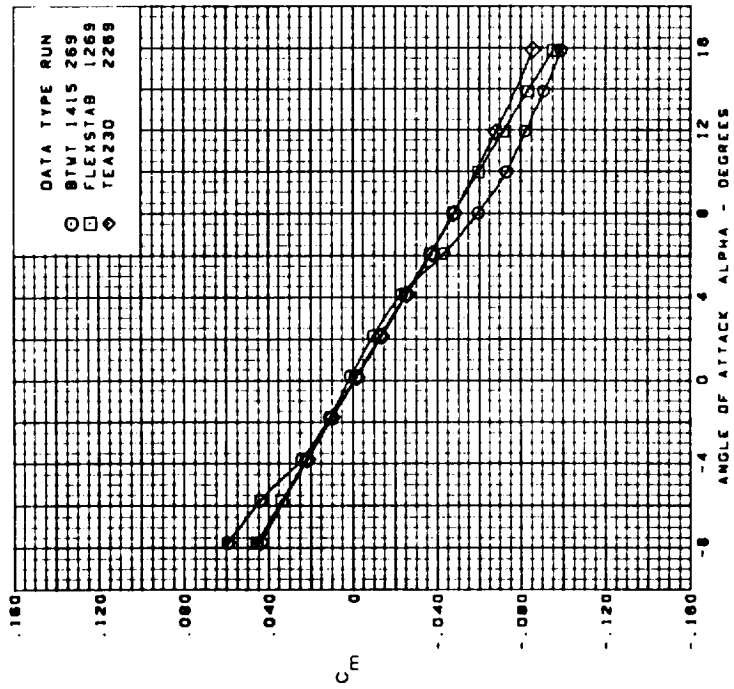


FIGURE 6.4-14.—ANALYSIS-TO-EXPERIMENT NORMAL FORCE AND PITCHING MOMENT  
 COMPARISON FOR ARROW-WING CONFIGURATION  
 $M = .40$

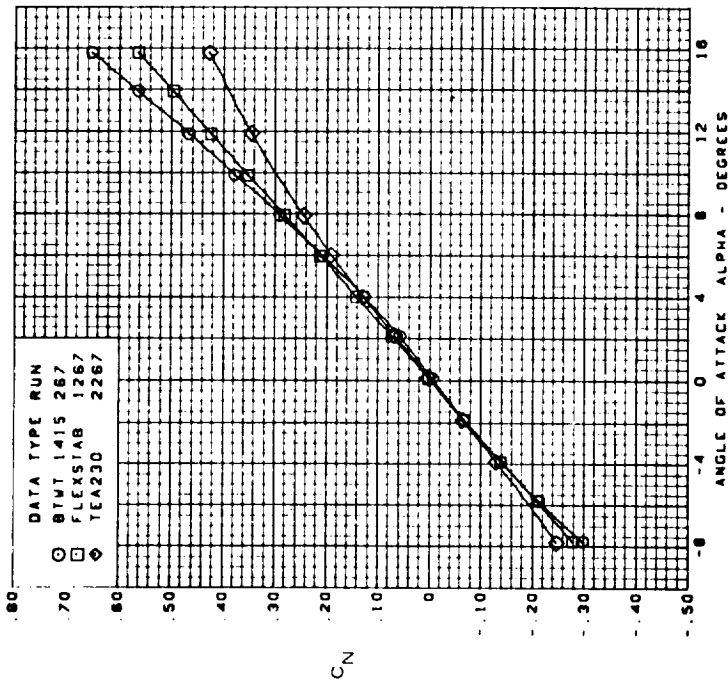
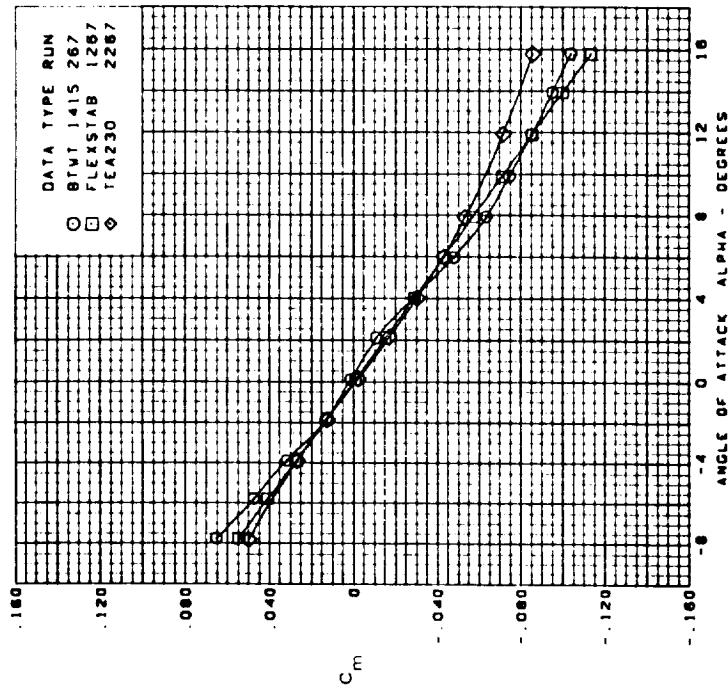


FIGURE 6.4-15. -- ANALYSIS-TO-EXPERIMENT NORMAL FORCE AND PITCHING MOMENT  
 COMPARISON FOR ARROW-WING CONFIGURATION  
 $M=0.85$

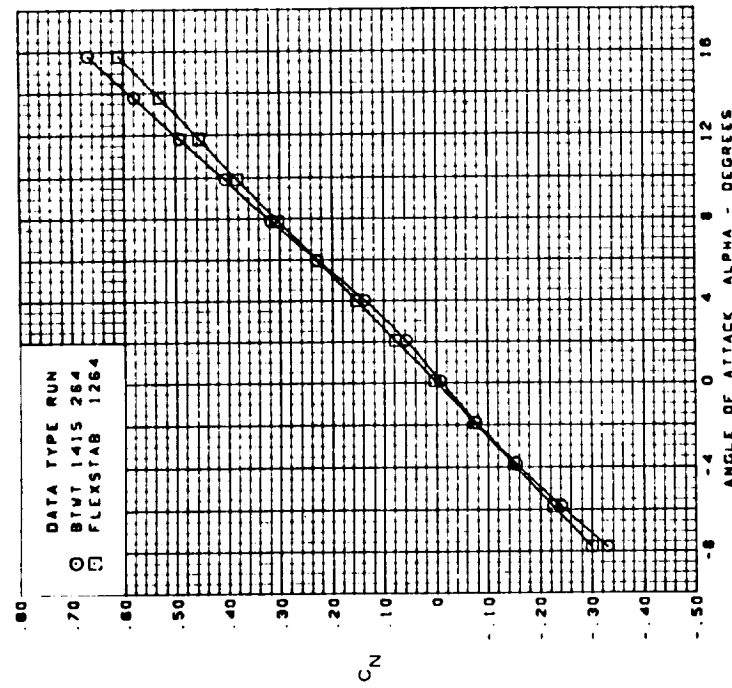
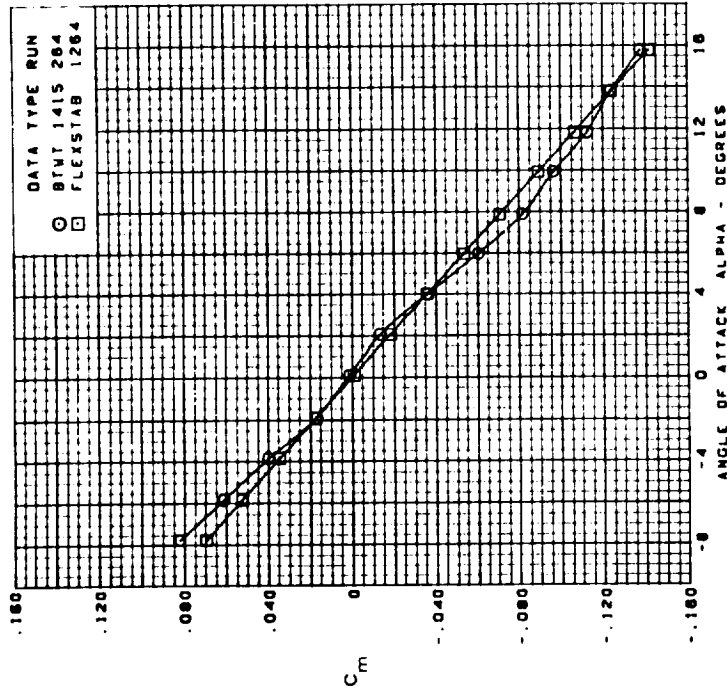


FIGURE 6.4-16.—ANALYSIS-TO-EXPERIMENT NORMAL FORCE AND PITCHING MOMENT  
 COMPARISON FOR ARROW-WING CONFIGURATION  
 M=1.05

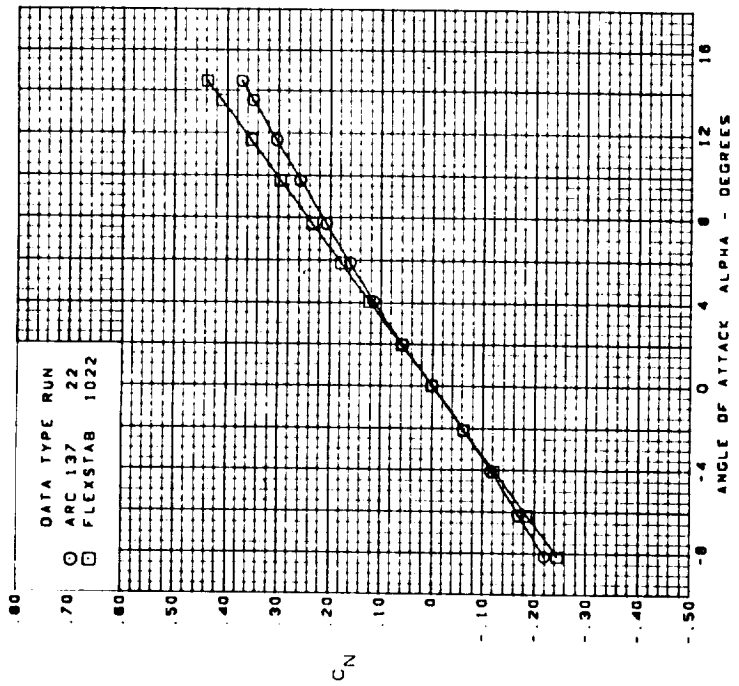
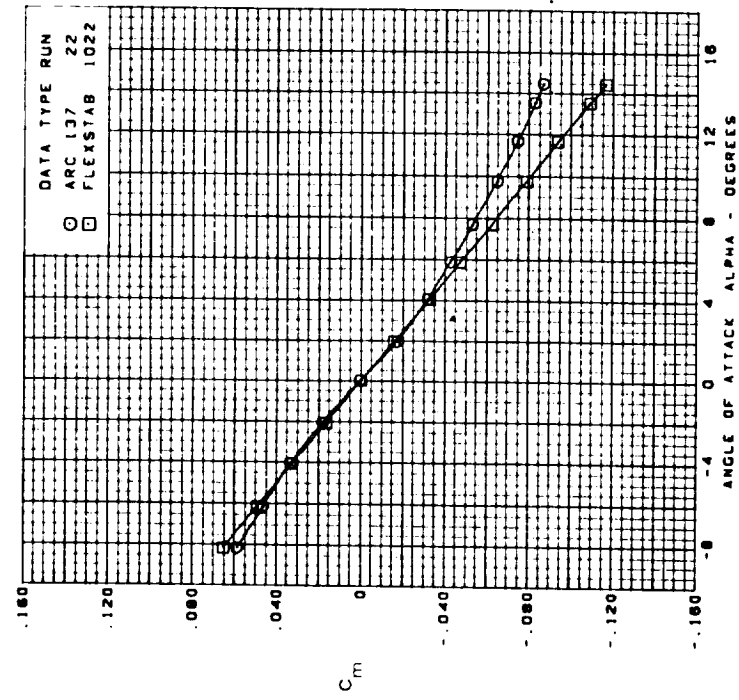


FIGURE 6.4-17.—ANALYSIS-TO-EXPERIMENT NORMAL FORCE AND PITCHING MOMENT  
COMPARISON FOR ARROW-WING CONFIGURATION  
M=2.5

## 7.0 GLOSSARY

This section contains an explanation of the technical terms and phrases used in volume IV. Also included is a list of acronyms with appropriate explanations.

**AEROCENTROID**—The geometric centroid of a Thin Body aerodynamic panel; a control point of a Slender Body (see CONTROL POINT).

**AERODYNAMIC PANEL**—A finite element of a Thin Body or an Interference Body over which the pressure is constant. There is one control point interior to each panel.

**AERODYNAMIC SINGULARITY**—A function describing a perturbation velocity field about a line or plane (that is, a source or doublet distribution on a line (line singularity) or a source or vorticity distribution on a plane) having a mathematical singularity at the line or plane.

**AIRFOIL THICKNESS**—The perpendicular distance from the camber line to the surface of an airfoil.

**ANTISYMMETRIC ELASTIC DEGREES OF FREEDOM**—A set of structural node displacement components or a structural free vibration mode shape antisymmetric in the Y-axis.

**ANTISYMMETRIC MOTION**—Translational motion that is parallel to the reference Y-axis or rotational motion that is about any line parallel to either the reference X- or Z-axis.

**CAMBER LINE**—The camber line of a two-dimensional body lies midway between the upper and lower surfaces. The camber line of a three-dimensional body is described by the centroids of the cross sections of that body.

**CAMBER SLOPES**—The slopes of the camber line.

**CHORDWISE PANEL EDGES**—The edges of Thin Body and Interference Body panels that are parallel to the reference X-axis.

**COMPRESSIBILITY EFFECTS**—The terms containing partial derivatives with respect to Mach number in the speed and yaw rate derivative calculations (see equations 6.3-14, 6.3-17, 6.3-20, and 6.3-23, vol. I).

**CONTROL EFFECTIVENESSES**—The partial derivatives of force and moment coefficients with respect to control surface deflections and deflection rates; for each structural free vibration mode, the generalized aerodynamic forces due to control surface deflections and deflection rates.

**CONTROL POINT**—The point on Thin or Interference Body panels where an aerodynamic boundary condition is satisfied. Where used in volume IV and in the program output listings, a Slender Body control point is a point on the Slender Body axis whose X-location is the X-location at which the camber slopes and surface slopes used to satisfy aerodynamic boundary conditions are evaluated.

**COPLANAR JUNCTION POINT**—The node at which the elastic axis of two consecutive Thin Body parts meet. Coplanar junction points are used only to divide a Thin Body elastic axis into parts, so that the Thin Body submatrices will not be too large. Coplanar junction Points are distinct from General Junction Points (see section 6.2 of vol. II for further details).

**COUPLED REFERENCE MOTION**—Reference motion that has at least one of the antisymmetric flight parameters (i.e.,  $V_1$ ,  $P_1$ , or  $R_1$ ) nonzero. See REFERENCE MOTION.

**DATA CARD**—Any card in a data deck. Data Control Cards and Data Comment Cards are special types of data cards. Data cards contain the user's input specifications in numeric or alphanumeric format.

**DATA CARD SET**—A related group of data cards; for example, an array of numbers usually required more than one card. The number of cards required compose a data card set.

**DATA CASE**—A complete problem description on data cards that a FLEXSTAB program will attempt to solve. A data case generally begins with the Data Control Card \$CASE and ends with the Data Control Card \$END OF CASE.

**DATA DECK**—The complete set of data cards assembled for execution by a program. A data deck consists of one or more data cases.

**DATA CONTROL CARD**—A special input data card containing a dollar sign (\$) in column one followed by descriptive words which identify key blocks of data (which immediately follow the Data Control Card). The dollar sign delimiter distinguishes this data card from all others in a data deck, making it identifiable to the user and to the computer.

**DESIGN SHAPE**—The shape of an airplane when it is flying at its design flight condition.

**ELASTIC AXIS**—Locus of shear centers of a body.

**ELASTIC SEGMENT**—A straight beam with constant stiffness properties. A Thin Body's elastic axis is approximated by a series of elastic segments.

**EXTERNAL DOWNWASH**—A downwash field experienced by the airplane that is due to some external disturbance (e.g., trailing vortices from another airplane).

**FLEXIBILITY MATRIX**—A matrix that gives displacements when premultiplied onto a force matrix.



**GENERAL JUNCTION POINT**—The node where two or more elastic axes meet. In ISIC, junction points define the beginnings and ends of elastic axes for Thin Bodies and Slender Body parts (see sec. 6.2 of vol. II for further details).

**GYROSCOPIC EFFECTS**—The moments generated by engine rotation.

**INTERFERENCE BODY**—A mathematical model used to model the interference effects between a Slender Body and nearby Thin Bodies. An Interference Body is a shell that surrounds a Slender Body in regions where there are significant wing-on-body and body-on-wing effects.

**INTERIOR STRUCTURAL NODE**—A structural node that lies between the ends of an elastic segment.

**JIG SHAPE**—The shape of an airplane when it is in the factory and supported by jigs.

**JOB**—A task submitted to a computer for processing.

**LEADING EDGE THRUST**—The leading edge thrust correction made to the drag force experienced by lifting Thin Bodies (see sec. 3.4.12, vol. I).

**LINE SINGULARITY**—See **AERODYNAMIC SINGULARITY**.

**LUMPED MASSES**—A discrete mass placed at a point to define the mass properties of a structure in a specific region. The mass distribution of a structure is defined by a distribution of lumped masses located so that the structure's first and second moments are accurately represented.

**MACH NUMBER ( $M_1$ )**—The ratio of the airplane's speed to the speed of sound of the fluid in which the airplane is flying;  $M_1 = U_1/a$ .

**MEAN SURFACES**—Cylindrical surfaces aligned with the undisturbed free stream where the surface boundary conditions are specified in a linear, first-order aerodynamic theory.

**MODAL COUPLING**—See section 6.6 in reference 8-1.

**PANEL**—An aerodynamic finite element of a Thin Body or an Interference Body over which the pressure is constant.

**PERTURBATION DELTA MACH NUMBER ( $\Delta M_1$ )**—An increment of the Mach number at which the airplane is flying. This number is used to compute the derivatives of the AIC matrices with respect to Mach number.

**PERTURBATION LOADS**—The aerodynamic loads arising from the airplane perturbation motion. See **PERTURBATION MOTION**.

**PERTURBATION MOTION**—Airplane motion that is initiated either by specifying initial values for the perturbation motion variables, or by subjecting the aircraft to a discrete gust, or by a combination of the two (see sec. 6.2, vol. I).

**PROGRAM**—A collection of subprograms designed to perform a specified function or solve a specified problem.

**REFERENCE FLIGHT CONDITION**—The steady, trimmed flight condition in which the static and dynamic stability of an aircraft is evaluated by FLEXSTAB.

**REFERENCE MOTION**—See **REFERENCE FLIGHT CONDITION**.

**REFERENCE SHAPE**—The shape of an airplane when it is in some reference flight condition.

**REFERENCE STATE**—See **REFERENCE FLIGHT CONDITION**.

**RESIDUAL-ELASTIC**—The mathematical model of an airplane which considers the structural dynamic motions of the lower frequency vibrational modes, but assumes that the higher frequency modes are in phase with the aerodynamic loads.

**RUN**—To run a program is to cause it to be executed on the computer. Running a program to solve a problem or produce real results (as opposed to debugging) is called a *production run*.

**SINGULARITY**—See **AERODYNAMIC SINGULARITY** and **LINE SINGULARITY**.

**SLENDER BODY**—A mathematical model used to define airplane components such as fuselages and nacelles. Slender Bodies are bodies of revolution with an area distribution similar to the area distribution of the body it is representing with the actual body's camber slope distribution defined at its axis of revolution.

**SLENDER BODY PART**—Refers to a Slender Body's structure; a part extends between two General Junction Points or between a General Junction Point and a free end.

**SNAIL**—A unit of mass; a snail equals the mass to which an acceleration of 1 inch/sec<sup>2</sup> would be given by the application of a 1 pound force.

**SPANWISE PANEL EDGE**—The edges of Thin Body panels that are not parallel to the reference X-axis.

**STATIC-ELASTIC**—The mathematical model of an airplane in which the air and inertia loads are considered to be in phase with the deflections. No structural dynamic effects are included.

**STICK SPEED STABILITY**—See section 5.7.1.1, volume I.

**STIFFNESS MATRIX**—A matrix that gives forces when premultiplied onto a displacement matrix.

**STIFFNESS PROPERTIES**—A body's bending and torsional properties. In the ISIC program, these include  $EI_{Y_M}$ ,  $EI_{Z_M}$ , and  $GJ$  for Slender Bodies and  $EI_{x_{nj}}$  and  $GJ$  for Thin Bodies.

**STREAMWISE PANEL EDGES**—See **CHORDWISE PANEL EDGES**.

**STRUCTURAL GEOMETRY**—Refers to the geometry created by the structural panels in the ESIC program.

**STRUCTURAL NODE**—Points on the structure at which structural forces and deflections are calculated. In the ISIC program these points always lie on elastic axes and the nodes which are not junction points are called ordinary nodes.

**STRUCTURAL PANEL**—These panels are used in the ESIC program and are either quadrilaterals or triangles with a structural node at each corner point. The structural panels are used to relate structural elastic properties to the aerocentroids.

**SURFACE SLOPE**—See **THICKNESS SLOPE**.

**SYMMETRIC MOTION**—Translational motion that is parallel to the reference X-Z plane or rotational motion about any line parallel to the reference Y-axis.

**SYMMETRIC ELASTIC DEGREES OF FREEDOM**—A set of structural node displacement components or a structural free vibration mode shape describing a deformed shape symmetric in the Y-axis.

**THICKNESS SLOPE**—The thickness slopes of a Thin Body are the slopes of the thickness distribution. The thickness slopes of a Slender Body are the slopes of the radius distribution.

**THIN BODY**—A mathematical model used to define airplane components, such as wings, horizontal stabilizers, and vertical tails. A Thin Body is defined with a planform identical to the actual body's planform in a plane parallel to the reference X-axis. Thickness and camber slopes of the actual body are defined on the plane of the Thin Body.

**THIN BODY PART**—Refers to a Thin Body's structure; a part extends between a General Junction Point and a free end, a General Junction Point and a Coplanar Junction Point, or a Coplanar Junction Point and a free end (see section 6.2 of volume II for further details).

**TRANSVERSE PANEL EDGES**—The edges of Interference Body panels that lie in planes normal to the reference X-axis.

**TRIM PARAMETERS**—The variables in the equation of motion for an airplane. These include  $\alpha$ ,  $\theta$  or  $T$ ,  $\delta e$ ,  $\beta$ ,  $\delta r$ , and  $\delta a$ .

**WING REFERENCE PLANE**—The plane defined by the Thin Body representing the wing.

## ACRONYMS

- AIC**—Aerodynamic Influence Coefficient. Relates a change in pressure at point  $i$  due to a change in incidence at point  $j$ ,  $A_{ij} = P_i/\psi_j$ . Name of a program that accepts a geometric definition from the GD program and generates aerodynamic information for input to the SD&SS program.
- ALoads**—Air Loads. A program which uses ESIC and SD&SS data to compute elastic deformation at structural nodes and resultant forces and couples at any specified point on the model due to aerodynamic loads.
- CAIC**—Correct AIC. This is the name of the AIC Matrix Correction program, a program that accepts empirical aerodynamic correction data to correct the aerodynamic influence coefficient matrix produced by the AIC program.
- CER**—Characteristic Equation Rooting. The subroutine of the SD&SS program that uses small perturbation data to calculate the dynamic stability characteristics of the airplane.
- EAPLOT**—Elastic Axis Plot. A program that accepts input from the ISIC program and generates a three-view drawing of the elastic axes of the model under consideration.
- ESIC**—External Structural Influence Coefficient. A program that accepts matrices produced by finite-element structures programs and generates structural data for the SD&SS program.
- FLEXSTAB**—Name of the aeroelastic computing system described in this report. It is derived from the key words FLEXible and STABILITY.
- GD**—Geometry Definition. A program that accepts data describing the shape of an airplane and generates data for the ISIC, ESIC, and SD&SS programs.
- GDPlot**—Geometry Definition Plot. A program that accepts data from the GD program and generates a three-view CalComp plot of the model.
- ISIC**—Internal Structural Influence Coefficient. A program that accepts data defining an airplane's structure, as described by beam theory, and generates data for the NM and SD&SS programs.
- NM**—Normal Modes. A program that accepts data from the ISIC program and generates the rigid and elastic normal modes of the structure under consideration.
- NMPlot**—Normal Modes Plot. A program that accepts data from the NM program and generates CalComp plots of the normal modes of the structure.
- PDPlot**—Pressure Distribution Plot. A program that accepts pressure distribution data from the SD&SS program and generates CalComp plots of lifting pressure coefficients versus  $x/c$  for each chordwise row of panels on each Thin Body.

**SD&SS**—**StabilDerivative and Static Stability**. A program that accepts data from the GD, ESIC or ISIC, AIC, CAIC, and NM programs and generates static and dynamic stability characteristics, steady and unsteady pressure distributions, and output data for the TH, SLOADS, and ALOADS programs.

**SLOADS**—**Structural Loads**. A program that accepts data from the SD&SS program and prints the applied loads at each structural node.

**THPLOT**—**Time Histories Plot**. A program that accepts data from the TH program and generates CalComp plots of the motion variables.



## APPENDIX A

### DART MODEL I DEMONSTRATION CASE INPUT LISTINGS

Input data deck listings for each of the twelve Dart Model I demonstration case runs are given in tables A.0-1–A.0-12. For convenience, card numbers which correspond to those used in Volume II, the User's Manual, are shown in the left hand margins of the input listings. Table A.0-13 contains the flexibility matrix for symmetric motion,  $[CS]$ , that was input to ESIC-1 on NASTAP (see sec. 3.2.5). Table A.0-14 gives the transformation matrix used to create  $[CS]$  (see sec. 3.2.5 and app. B).

TABLE A.0-1.—INPUT DECK LISTING FOR GD-1

Card number	PROGRAM	CONFIG. 01	DECK 01-01
1	\$CASE FOR GD		
2	DART MODEL 1		
3	BOEING AEROSTAFF		
4	\$GENERAL SPECIFICATIONS		
5	0.5 METERS		
6	\$SLENDER BODY DATA		
7	DART		
8	0.0		
9	1.0		
10	2.0		
11	3.0	0.0	
12	RADII		
13	1.0	3.0	
14	1.0	0.0	
16	NO CAMBER		
18	\$INTERFERENCE BODY DATA		
19	181 DART		
20	0.0		
21	2.0		
22	1.0	1.0	
25	WING		
26	85.0	0.0	
27	\$THIN BODY DATA		
28	WING		
29	1.0		
30	2.0		
31	0.0		
32	1.0		
33	0.0		
34	50.0	0.0	
36	0.0		
37	0.0		
40	0.0		
47	\$ENJ		
48	\$EXIT		

PRINT





TABLE A.0.3.—INPUT DECK LISTING FOR ISIC-1

RUN 03 , CONFIG. 01 , DECK 01-03

1	\$CASE FOR ISIC PROGRAM		
2	DART MODEL 1		
3	BOEING AEROSTAFF		
4	\$GEOMETRY TAPE DATA		
5	1.0	0.0	
6	\$OPTION		
7	RESIDUAL-ELASTIC	RESIDUAL-ELASTIC	
8	\$STRUCTURAL DATA		
9	\$JUNCTION POINTS		
10	2.0		
11	0.	1.0	
11	1.2	1.	
12	1.0		
13	2.0		
14	1.0	2.0	
15	\$SLENDER BODY		
16	\$PART 1		
17	1.0	1.0	2.0
20	\$STIFFNESS DATA		
21	1.0	31420.	31420.
22	\$LUMPED MASSES		1704.
23	1.0		
24	1.0		
16	\$PART 2		
17	3.0	2.0	0.0
18	\$COORDINATES		
19	1.5	2.5	3.0
20	\$STIFFNESS		
21	0.0	31420.	31420.
21	0.0	31420.	31420.
21	0.0	31420.	31420.
			1704.
			1704.
			1704.

TABLE A.0.3.—CONCLUDED

Card number	Command	Value 1	Value 2	Value 3	Value 4
22	\$LUMPED MASSES				
23	3.				
24	0.	0.			
27	\$THIN BODY DATA			1.	
28	2.0				
29	\$PART 1				
30	2.0				
31	\$COORDINATES				
32	0	1.0	0.0		2.0
33	\$STIFFNESS				
34	0.0	10.0	10.35		
34	1.0	10.0	10.85		
35	\$LUMPED MASSES				
36	3.				
37	2.0				
38	1.0	-0.2	0.1		0.1
37	0.				
37	0.				
44	\$MATRIX PRINT				
45	1.0	1.0	1.0	1.0	1.0
46	\$END				
47	\$EXIT				





TABLE A.0-5--CONCLUDED

Card number	STABILITY DATA	CONSTANT	C.	PRINT
34	\$SPECIFIED			
35	JIG	1.0	1.0	PRINT
36		1.0	1.0	1.0
37		0.5729578	0.0	
42	\$PERT. DATA			
58	BOTH	SPEED	PRESSURE CONTROL	LOADS
59				PRINT
60				
67				
98	\$END			
99	\$EXIT			



TABLE A.0-6.--CONCLUDED

Card number	\$STABILITY DATA				
34	SPECIFIED				
35	JIG	CONSTANT	0.	1.	PRINT
36	1.0	1.0	1.0	1.0	1.0
37	0.5729573	0.5729573	0.0		
42	\$PERT. DATA				
58	BOTH	SPEED	PRESSURE	CONTROL	LOADS
59					PRINT
60					
67					
98	\$END				
99	\$EXIT				





TABLE A.0.8.—INPUT DECK LISTING FOR SLOADS-1

Card number	1	\$CASE FOR SLOADS PROGRAM	FUN 06 , CONFIG. 01 , DECK 01--08
	2	DART MODEL 1	
	3	BOEING AEROSTAFF	
	4	L1STED	
	8	(L1)--S	
	8	(L1)--A	
	9	\$END	
	10	\$EXIT	

TABLE A.0.9.—INPUT DECK LISTING FOR ESIC-1

RUN 09 , CONFIG. 01 , DECK 01-09

Card number					
1	\$CASE FOR ESIC PRJGRAM				
2	DART MODEL 1				
3	BOEING AEROSTAFF				
4	\$GDTAPE DATA				
5	1. 0.				
6	\$CATALOG INPUT OF EXTERNAL MATRICES				
7	1.				
8					
9					
17	\$DEGREES OF FREEDOM				
18	Z				
21	\$SLENDER BODY DATA				
22	0.	10.			
23	.4	1.1	1.4	1.6	
23	2.3	2.7	3.		
24	1.				
24					
27	\$THIN BODY DATA				
28	1.2	0.	6.	1.	
29	-.2	1.	.1	1.	
29	.8	1.	.8	2.	
30	1.				
31	2.	4.			
34	\$MATRIX PRINT LIST				
35	1.	1.			
36	\$END OF CASE				
37	\$EXIT				



TABLE A.0-10.—CONCLUDED

Card number	STABILITY DATA	CONSTANT	CONTROL	LOADS	PRINT
34	\$STABILITY DATA				
35	SPECIFIED				
36	JIG	0.	1.		
37	1.0	1.0	1.0		1.0
42	0.5729579	0.5729578	0.0		
58	\$PERT. DATA				
59	SYMMETRIC SPEED	PRESSURE	CONTROL		PRINT
60					
67					
98	\$END				
99	\$EXIT				



TABLE A.0-11.--CONCLUDED

Card number	34	\$STABILITY DATA				
	35	\$SPECIFIED				
	36	\$JIG	CONSTANT	3.	1.	PRINT
	37	1.0	1.0	1.0	1.0	1.0
	42	0.5729578	0.5729578	0.0		
	58	\$PERT. DATA				
	59	\$SYMMETRIC SPEED		PRESSURE	CONTROL	LOADS
	60					PRINT
	67					
	98	\$END				
	99	\$EXIT				

TABLE A.0-12.—INPUT DECK LISTING FOR ALOADS-1

Card number							
1	\$CASE FOR ALOADS	PRJGRAM					RUN 12 , CONFIG. 01 , DECK 01-12
2	DART MODEL 1						
3	BOEING AEROSTAFF						
4	1.	1.					
5	1.5	1.	0.			1.	0.
6	1.5	2.	0.			0.	0.
7	4.	2.	1.			1.	0.
8	\$END OF CASE						
9	\$EXIT						



TABLE A.O-13. - [C<sup>S</sup>] MATRIX INPUT TO ESIC-1

	1	2	3	4	5
1	1.5277E-06	2.2915E-06	4.2011E-06	4.9650E-06	5.3469E-06
2	2.2915E-06	4.5831E-06	1.0312E-05	1.2603E-05	1.3749E-05
3	4.2011E-06	1.0312E-05	2.8262E-05	3.5901E-05	3.9720E-05
4	4.9650E-06	1.2603E-05	3.5901E-05	4.6595E-05	5.1941E-05
5	5.3469E-06	1.3749E-05	3.9720E-05	5.1941E-05	5.8243E-05
6	6.1108E-06	1.6041E-05	4.7358E-05	6.2635E-05	7.0656E-05
7	8.7842E-06	2.4061E-05	7.4093E-05	1.0006E-04	1.1410E-04
8	1.0312E-05	2.8644E-05	8.9370E-05	1.2145E-04	1.3892E-04
9	1.0694E-05	2.9790E-05	9.3189E-05	1.2680E-04	1.4513E-04
10	1.1458E-05	3.2081E-05	1.0083E-04	1.3749E-04	1.5754E-04
11	3.8192E-06	9.1661E-06	2.4443E-05	3.0554E-05	3.3609E-05
12	3.8192E-06	9.1661E-06	2.4443E-05	3.0554E-05	3.3609E-05
13	4.9650E-06	1.2603E-05	3.5901E-05	4.6595E-05	5.1941E-05
14	7.6384E-06	2.0624E-05	6.2635E-05	8.4023E-05	9.4717E-05
15	3.8192E-06	9.1661E-06	2.4443E-05	3.0554E-05	3.3609E-05
16	7.6384E-06	2.0624E-05	6.2635E-05	8.4023E-05	9.4717E-05

	6	7	8	9	10
1	6.1108E-06	8.7842E-06	1.0312E-05	1.0694E-05	1.1458E-05
2	1.6041E-05	2.4061E-05	2.8644E-05	2.9790E-05	3.2081E-05
3	4.2358E-05	7.4093E-05	8.9370E-05	9.3189E-05	1.0083E-04
4	6.2635E-05	1.0006E-04	1.2145E-04	1.2680E-04	1.3749E-04
5	7.0656E-05	1.1410E-04	1.3892E-04	1.4513E-04	1.5754E-04
6	8.6887E-05	1.4370E-04	1.7616E-04	1.8428E-04	2.0051E-04
7	1.4370E-04	2.5833E-04	3.2516E-04	3.4187E-04	3.7529E-04
8	1.7616E-04	3.2516E-04	4.1746E-04	4.4054E-04	4.8669E-04
9	1.8428E-04	3.4187E-04	4.4054E-04	4.6595E-04	5.1560E-04
10	2.0051E-04	3.7529E-04	4.8669E-04	5.1560E-04	5.7288E-04
11	3.9720E-05	6.1108E-05	7.3329E-05	7.6384E-05	8.2495E-05
12	3.9720E-05	6.1108E-05	7.3329E-05	7.6384E-05	8.2495E-05
13	6.2635E-05	1.0006E-04	1.2145E-04	1.2680E-04	1.3749E-04
14	1.1610E-04	1.9096E-04	2.3374E-04	2.4443E-04	2.6582E-04
15	3.9720E-05	6.1108E-05	7.3329E-05	7.6384E-05	8.2495E-05
16	1.1610E-04	1.9096E-04	2.3374E-04	2.4443E-04	2.6582E-04

TABLE A.0-13.—CONCLUDED

	11	12	13	14	15
1	3.8192E-06	3.8192E-06	4.9650E-06	7.6384E-06	3.8192E-06
2	9.1661E-06	9.1661E-06	1.2603E-05	2.0624E-05	9.1661E-06
3	2.4443E-05	2.4443E-05	3.5901E-05	6.2635E-05	2.4443E-05
4	3.0554E-05	3.0554E-05	4.6595E-05	8.4023E-05	3.0554E-05
5	3.3609E-05	3.3609E-05	5.1941E-05	9.4717E-05	3.3609E-05
6	3.9720E-05	3.9720E-05	6.2635E-05	1.1610E-04	3.9720E-05
7	6.1108E-05	6.1108E-05	1.0006E-04	1.9096E-04	6.1108E-05
8	7.3329E-05	7.3329E-05	1.2145E-04	2.3374E-04	7.3329E-05
9	7.6384E-05	7.6384E-05	1.2680E-04	2.4443E-04	7.6384E-05
10	8.2495E-05	8.2495E-05	1.3749E-04	2.6582E-04	8.2495E-05
11	3.7041E-02	3.7041E-02	3.1521E-02	1.8639E-02	3.7041E-02
12	3.7041E-02	4.3051E-02	3.1521E-02	1.5432E-02	3.0551E-02
13	3.1521E-02	3.1521E-02	3.4302E-02	4.0791E-02	3.1521E-02
14	1.8639E-02	1.5432E-02	4.0791E-02	1.2614E-01	3.2932E-02
15	3.7041E-02	3.0551E-02	3.1521E-02	3.2932E-02	2.6805E-01
16	3.8639E-02	3.2932E-02	9.0791E-02	1.6364E-01	2.4043E-01

16

1	7.6384E-06
2	2.0624E-05
3	6.2635E-05
4	8.4023E-05
5	9.4717E-05
6	1.1610E-04
7	1.9096E-04
8	2.3374E-04
9	2.4443E-04
10	2.6582E-04
11	6.8639E-02
12	3.2932E-02
13	9.0791E-02
14	1.6364E-01
15	2.4043E-01
16	3.5114E-01

TABLE A.0-14.—TRANSFORMATION MATRIX [T] USED TO CREATE [CS]

	1	2	3	4	5
1	0.	0.	1.0000E+00	2.0000E-01	0.
2	0.	0.	1.0000E+00	0.	0.
3	1.0000E+00	1.0000E-01	0.	0.	0.
4	1.0000E+00	-1.0000E-01	0.	0.	0.
5	0.	0.	0.	0.	1.0000E+00
6	0.	0.	0.	0.	1.0000E+00
7	0.	0.	0.	0.	0.
8	0.	0.	0.	0.	0.
9	0.	0.	0.	0.	0.
10	0.	0.	0.	0.	0.
11	0.	0.	0.	0.	0.
12	0.	0.	0.	0.	0.
13	0.	0.	0.	0.	0.
14	0.	0.	0.	0.	0.
15	0.	0.	0.	0.	0.
16	0.	0.	0.	0.	0.

	6	7	8	9	10
1	0.	0.	0.	0.	0.
2	0.	0.	0.	0.	0.
3	0.	0.	0.	0.	0.
4	0.	0.	0.	0.	0.
5	1.0000E-01	0.	0.	0.	0.
6	-1.0000E-01	0.	0.	0.	0.
7	0.	1.0000E+00	2.0000E-01	0.	0.
8	0.	1.0000E+00	-2.0000E-01	0.	0.
9	0.	0.	0.	1.0000E+00	2.0000E-01
10	0.	0.	0.	1.0000E+00	0.
11	0.	0.	0.	0.	0.
12	0.	0.	0.	0.	0.
13	0.	0.	0.	0.	0.
14	0.	0.	0.	0.	0.
15	0.	0.	0.	0.	0.
16	0.	0.	0.	0.	0.

TABLE A.0-14.—CONCLUDED

	11	12	13	14	15
1	0.	0.	0.	0.	0.
2	0.	0.	0.	0.	0.
3	0.	0.	0.	0.	0.
4	0.	0.	0.	0.	0.
5	0.	0.	0.	0.	0.
6	0.	0.	0.	0.	0.
7	0.	0.	0.	0.	0.
8	0.	0.	0.	0.	0.
9	0.	0.	0.	0.	0.
10	0.	0.	0.	0.	0.
11	1.0000E+00	0.	2.0000E-01	1.0000E+00	-5.0000E-01
12	0.	0.	0.	1.0000E+00	0.
13	1.0000E+00	0.	-1.0000E-01	0.	0.
14	0.	0.	0.	1.0000E+00	-5.0000E-01
15	0.	0.	0.	1.0000E+00	5.0000E-01
16	0.	0.	0.	1.0000E+00	5.0000E-01

	16	17	18	19
1	0.	0.	0.	0.
2	0.	0.	0.	0.
3	0.	0.	0.	0.
4	0.	0.	0.	0.
5	0.	0.	0.	0.
6	0.	0.	0.	0.
7	0.	0.	0.	0.
8	0.	0.	0.	0.
9	0.	0.	0.	0.
10	0.	0.	0.	0.
11	0.	0.	0.	0.
12	2.0000E-01	0.	0.	0.
13	0.	0.	0.	0.
14	-8.0000E-01	0.	0.	0.
15	2.0000E-01	0.	0.	0.
16	-8.0000E-01	0.	0.	0.

## APPENDIX B

### TRANSFORMATION MATRIX USED IN THE DART MODEL I ESIC STRUCTURAL DEFINITION

It was required to find a transformation matrix, [T], which related the displacements at the ESIC nodes,  $\{d\}_E$ , to the displacements and rotations corresponding to the ISIC degrees of freedom,  $\{d\}_I$ , i.e.,

$$\{d\}_E = [T] \{d\}_I.$$

The ESIC displacement vector contained the Z degree of freedom for each of the sixteen ESIC nodes (see fig. B.0-1) and therefore was of dimensions 16 x 1.  $\{d\}_E$  was ordered as follows:

$$\{d\}_E = \begin{Bmatrix} \{d\}_{E_{\text{fuselage}}} \\ \{d\}_{E_{\text{wing}}} \end{Bmatrix}$$

where

$$\{d\}_{E_{\text{fuselage}}} = \begin{Bmatrix} d_{Z_E}^1 \\ d_{Z_E}^2 \\ \cdot \\ \cdot \\ \cdot \\ d_{Z_E}^{10} \end{Bmatrix}; \quad \{d\}_{E_{\text{wing}}} = \begin{Bmatrix} d_{z_{E_n}}^{11} \\ d_{z_{E_n}}^{12} \\ \cdot \\ \cdot \\ \cdot \\ d_{z_{E_n}}^{16} \end{Bmatrix}$$

$(X, Y, Z)$  Reference Axis System  
 $(X_E, Y_E, Z_E)$  ESIC Reference Coordinate System  
 $(x_{E_n}, y_{E_n}, z_{E_n})$  ESIC Thin Body Structural Coordinate System

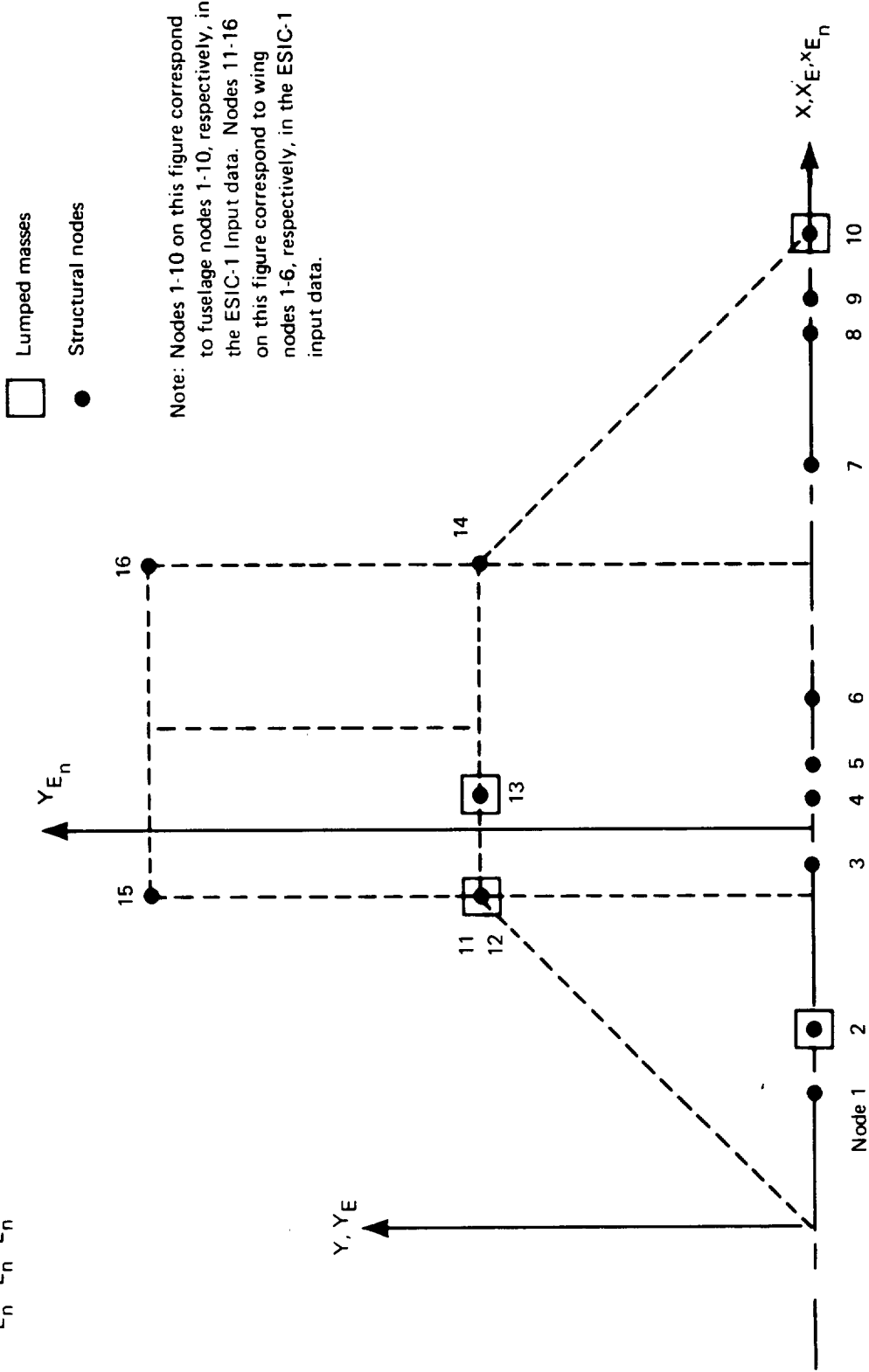


FIGURE B.0-1—ESIC STRUCTURAL REPRESENTATION—DART MODEL I

The ISIC displacement vector contained the translational and rotational degrees of freedom associated with the seven ISIC nodes and junction point 2 (see fig. B.0-2). (Note that the ISIC "node" at the nose of the fuselage is the clamped point and has no degrees of freedom associated with it.) The four fuselage nodes and General Junction Point 2 each had  $d_{Z_M}$  and  $\theta_{Y_M}$  degrees of freedom and the three wing nodes had  $d_{z_{n_i}}$ ,  $\theta_{x_{n_i}}$ , and  $\theta_{y_{n_i}}$  degrees of freedom. Thus,  $\{d\}_I$  was of dimensions  $19 \times 1$  and was ordered as follows:

$$\{d\}_I = \begin{Bmatrix} \{d\}_{I_{\text{fuselage}}} \\ \{d\}_{I_{\text{wing}}} \end{Bmatrix}$$

where

$$\{d\}_{I_{\text{fuselage}}} = \begin{Bmatrix} d_{Z_M}^{\text{JP2}} \\ \theta_{Y_M}^{\text{JP2}} \\ d_{Z_M}^1 \\ \theta_{Y_M}^1 \\ \cdot \\ \cdot \\ d_{Z_M}^4 \\ \theta_{Y_M}^4 \end{Bmatrix}; \quad \{d\}_{I_{\text{wing}}} = \begin{Bmatrix} d_{z_{n_i}}^5 \\ \theta_{x_{n_i}}^5 \\ \theta_{y_{n_i}}^5 \\ \cdot \\ \cdot \\ d_{z_{n_i}}^7 \\ \theta_{x_{n_i}}^7 \\ \theta_{y_{n_i}}^7 \end{Bmatrix}$$

Note that ISIC always orders the junction point degrees of freedom first in  $\{d\}_I$ .

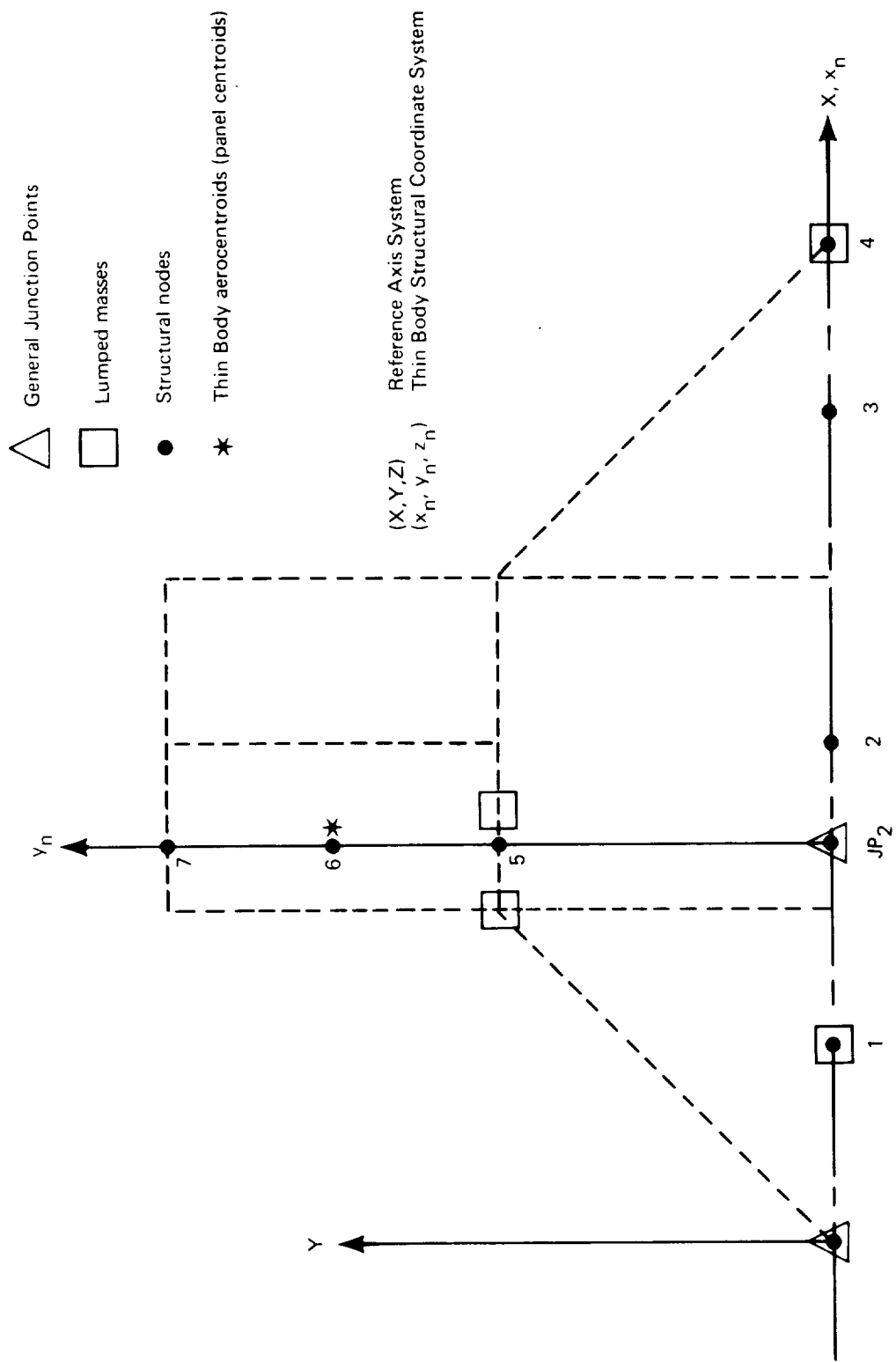


FIGURE B.0.2—ISIC STRUCTURAL REPRESENTATION—DART MODEL I



In order to form the elements of the transformation matrix, it was necessary to take into account the limitations and approximations used in the ISIC and ESIC programs. For example, consider the ISIC definition of the Dart Model I wing (figure B.0-2). It is known that the elastic displacements and rotations experienced by the Thin Body aerocentroids only depend on the displacements and rotations associated with ISIC node 6 (see fig. 6.2-7, vol. II). In the ESIC structural definition, the displacements and rotations at the aerocentroids depend on the displacements of the corner points of the structural panel to which the aerocentroids are assigned (in this case, the structural panel is defined by ESIC nodes 12, 14, 15, and 16; see fig. B.0-1). Therefore, in order to have equivalent ESIC and ISIC structural definitions, the displacements at ESIC nodes 12, 14, 15, and 16 need only depend on the displacements and rotations at ISIC node 6. For example, consider ESIC node 16 in figure B.0-3. Its Z degree of freedom,  $d_{zE_n}^{16}$ , is related to the degrees of freedom of ISIC node 6 by

$$d_{zE_n}^{16} = dz_{ni}^6 + \Delta y \theta_{x_{ni}}^6 - \Delta x \theta_{y_{ni}}^6$$

Thus, row 16 of the transformation matrix, [T], contained all zeros, with the exception of columns 14, 15, and 16, which had values of 1,  $\Delta y$ , and  $-\Delta x$ , respectively. The relationships of ESIC nodes 12, 14, and 15 with ISIC node 6 were defined similarly.

An analogous situation existed between ESIC nodes 11 and 13, and ISIC node 5. In this case, the inertia associated with the two lumped masses manifests itself through the  $d_{z_{ni}}$  and  $\theta_{y_{ni}}$  degrees of freedom of ISIC node 5. The  $d_{zE_n}$  degrees of freedom associated with the two ESIC nodes were necessary and sufficient to simulate these inertia properties in the ESIC model. (The fact that ESIC nodes 11 and 12 occupy the same physical location is only a coincidence: the same results could have been obtained by locating node 12, the structural panel corner point, elsewhere.)

As mentioned previously, General Junction Point 2 and ISIC nodes 1-4 each had  $dZ_M$  and  $\theta Y_M$  degrees of freedom. By defining two ESIC nodes (each with the  $dZ_E$  degree of freedom) for each of these ISIC nodes, the simulation of the ISIC structural definition was complete. For example, consider ESIC nodes 7 and 8 in figure B.0-3. They are related to ISIC node 3 simply by

$$dZ_E^7 = dZ_M^3 + \Delta X_1 \theta Y_M^3$$

and

$$dZ_E^8 = dZ_M^3 - \Delta X_2 \theta Y_M^3,$$

respectively. Similar relationships existed between each of the other ISIC fuselage nodes and the corresponding pairs of ESIC nodes. These relationships completely defined the remaining elements of the transformation matrix (see app. A.0-14).

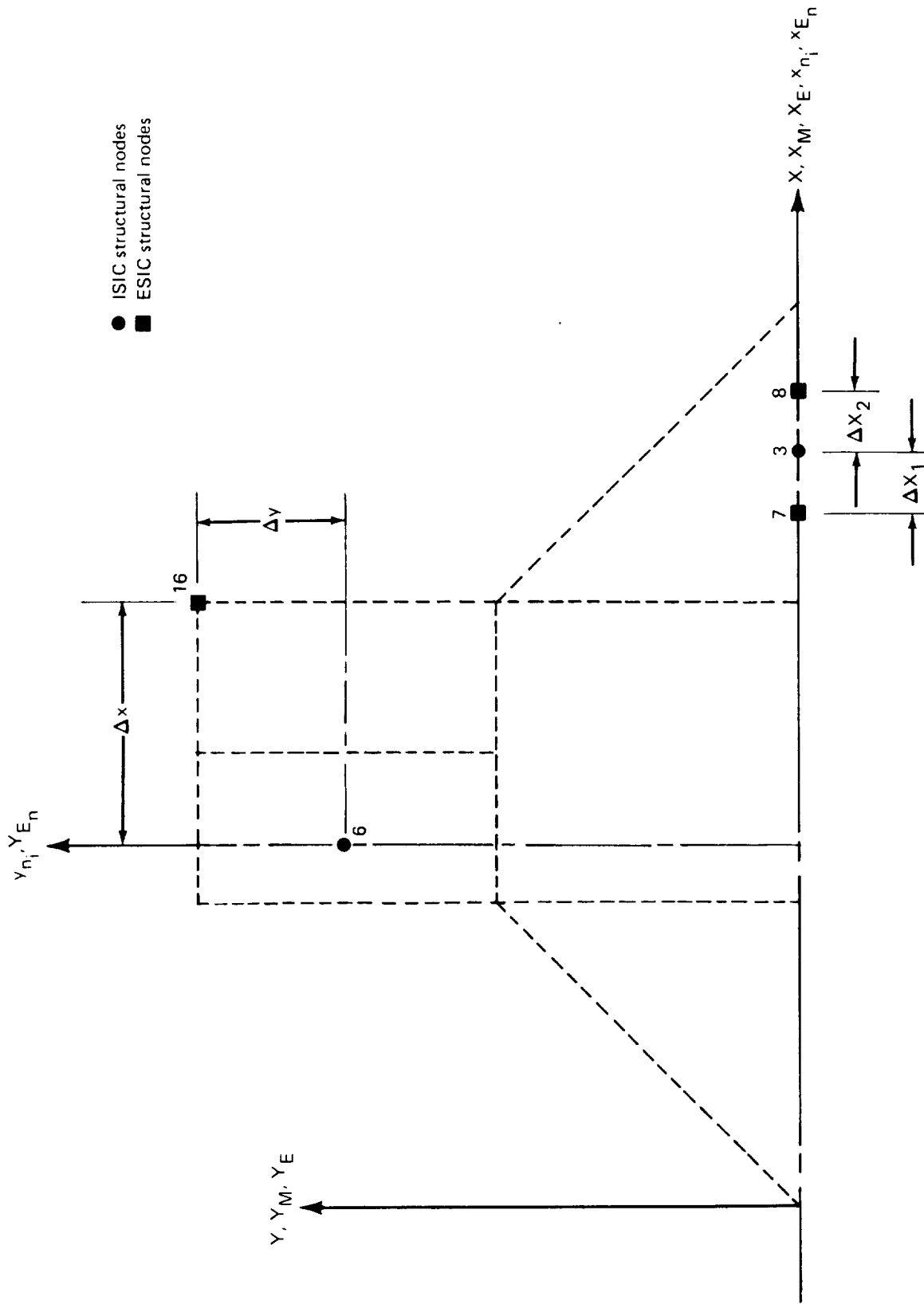


FIGURE B.0-3.—RELATIONSHIPS BETWEEN TYPICAL ESIC AND ISIC STRUCTURAL NODES—DART MODEL I

## APPENDIX C

### DEMONSTRATION CASE USAGE OF FLEXSTAB INPUT OPTIONS AND MODELING TECHNIQUES

Tables C.0-1 through C.0-8 itemizes the user convenience and solution-oriented input options used in each of the demonstration cases. Volume II field descriptors and card numbers are included. The stylized entries used in the body of these Tables have the following meanings:

Entry	Meaning
“yes”	OPTION was used
“no”	OPTION was not used
no entry (blank space)	OPTION does not apply

Table C.0-9 lists the modeling techniques used in the demonstration cases. References to the appropriate sections of Volume II are given.

TABLE C.O-1. - GD PROGRAM INPUT OPTION USAGE

INPUT OPTION	FIELD DESCRIPTOR	CARD NO.	DART MODEL I		DART MODEL II		707-320B		SST	YF-12A				
			GD-1 01-01	METERS	GD-1 02-01	METERS	GE-3A 03-01	INCHES		GD-3B 03-08	INCHES	GD-5A 05-01	INCHES	GD-5B 05-06
Linear units used	Units	5	GD-1 01-01	METERS	GD-1 02-01	METERS	GE-3A 03-01	INCHES	GD-3B 03-08	INCHES	GD-5A 05-01	INCHES	GD-5B 05-06	INCHES
<u>Slender Body Data</u>														
Specify automatic Control Point placement	NCPA	11	yes	yes	yes	yes	yes	yes	yes	yes	yes	yes	yes	yes
Specify Manual Control Point placement	NCPI	11	--	--	--	--	--	--	--	--	yes	yes	yes	yes
X-Section definition	R/A	12	RADII	RADII	RADII	AREA, RADII	AREA, RADII	AREA, RADII	AREA, RADII	RADII	RADII	RADII	RADII	RADII
X-Section interpolation	L/S <sub>BD</sub>	12	LINEAR	LINEAR	LINEAR	LINEAR, SPLINE	LINEAR, SPLINE	LINEAR, SPLINE	LINEAR, SPLINE	LINEAR	LINEAR, SPLINE	LINEAR, SPLINE	LINEAR, SPLINE	LINEAR, SPLINE
Camber line definition	RC	16	NO CAMBER	NO CAMBER	NO CAMBER	XYZ, NO CAMBER	XYZ, NO CAMBER	XYZ, NO CAMBER	XYZ, NO CAMBER	XYZ	XYZ	XYZ	XYZ	XYZ
Camber line interpolation	L/S <sub>BC</sub>	16	AUTO	EQ. SPACE	EQ. SPACE	EQ. SPACE	EQ. SPACE	EQ. SPACE	EQ. SPACE	EQ. SPACE	AUTO	INPUT	INPUT	INPUT
<u>Interference Body Data:</u>														
X-Section definition of corner points	IP	22	AUTO	Y-Z	Y-Z	Y-Z, AUTO	Y-Z, AUTO	Y-Z, AUTO	Y-Z, AUTO	Y-Z	AUTO	AUTO	AUTO	AUTO
Panel X-coordinate definition	PS	22	EQ. SPACE	EQ. SPACE	EQ. SPACE	EQ. SPACE	EQ. SPACE	EQ. SPACE	EQ. SPACE	EQ. SPACE	INPUT	INPUT	INPUT	INPUT
<u>Thin Body Data</u>														
Use "special coordinate system"	Relocate	29	--	--	--	yes	yes	yes	yes	yes	--	--	--	--
Print panel coordinates in Local Coordinate System	PrintOP	30	yes	yes	yes	yes	yes	yes	yes	yes	--	--	--	--

TABLE C.O-1.—CONCLUDED

INPUT OPTION	FIELD DESCRIPTOR	CARD NO.	DART MODEL I		DART MODEL II		707-320B		SST	YF-12A	
			GD-1 01-01	GD-2 02-01	GD-3A 03-01	GD-3B 03-08	GD-4 04-01	GD-5A 05-01		GD-5B 05-06	
Input X coordinates of panel in relative/absolute units	IX1	33	relative	relative	relative	relative	relative	relative	relative	absolute, relative	absolute, relative
Panel leading and trailing edges are constant/variable % chord	IX2	33	constant	constant	constant	constant	constant	constant	constant	variable, constant	variable, constant
<b>Airfoil sections input</b>	NAS	37	- - -	- - -	yes	yes	yes	yes	yes	yes	yes
Airfoil profile interpolation	L/SAF	37			LINEAR	LINEAR	LINEAR	LINEAR	LINEAR	LINEAR	LINEAR
Print airfoil coordinates	PrintAF	37			- - -	- - -	- - -	- - -	- - -	yes	yes
Define airfoil profile in non-streamwise (skewed) direction	AYTE	38			- - -	- - -	- - -	- - -	- - -	- - -	- - -
Input skewed airfoil coordinates in dimensional units, % chord, ratio of an arbitrary length	DIMS	38									
<b>Input airfoil coordinates in dimensional units, % chord, ratio of arbitrary length</b>	$x_i, z_i$	39			ratio	ratio	ratio	% chord		dimensional	dimensional
Twist interpolation	L/S <sub>T</sub>	40			LINEAR	LINEAR	LINEAR	LINEAR	LINEAR		

TABLE C.0-2.-AIC PROGRAM INPUT OPTION USAGE

INPUT OPTION	FIELD DESCRIPTOR	CARD NO.	DART MODEL I	DART MODEL II	707-320B	SST	YF-12A	
			AIC-1 01-02	AIC-2 02-02			AIC-3 03-02	AIC-4 04-02
Compute AIC results required for speed derivative calculations	$\Delta M_1$	4	yes	yes	yes	yes	---	---
Reference motion for steady A/D (symmetric, or symmetric + anti-symmetric)	Steady Motion <sub>REF</sub>	5	both	both	both	sym	sym	sym
Aerodynamic analysis (steady, or steady + unsteady)	Unsteady <sub>Op</sub>	6	both	both	both	both	both	study
Reference motion for unsteady A/D (symmetric, or symmetric + anti-symmetric)	Unsteady Motion <sub>REF</sub>	7	both	both	both	sym	---	---
Print AIC matrices	\$MATRIX PRINT LIST	8	---	---	---	---	---	---
Use near field- far field approximation	\$NERFAR	11	---	---	---	---	---	---

TABLE C.0.3.—ISIC PROGRAM INPUT OPTION USAGE

INPUT OPTION	FIELD DESCRIPTOR	CARD NO.	DART MODEL I	DART MODEL II	707-320B	SSI	YF-12A
			ISIC-1 01-03		ISIC-3 03-03		
Print GD data from GD tape	Print <sup>GD</sup>	5	--		--		
Data control card for elastic formulation	\$OPTION	6	yes		yes		
Structural modeling, symmetric motion	OPT-S	7	RESIDUAL-ELASTIC	N O T	RESIDUAL-ELASTIC	N O T	N O T
Structural modeling, anti-symmetric motion	OPT-A	7	RESIDUAL-ELASTIC		RESIDUAL-ELASTIC		
Junction point specification	\$JUNCTION POINT	9	yes		yes		
Slender Body mass multiplying (scale) factors used	\$SCALE FACTORS	25,26	--	E X E C U T E D	--	E X E C U T E D	E X E C U T E D
Thin Body mass multiplying (scale) factors used	\$SCALE FACTORS	39,40	--		yes		
Compute structural data required to account for gyroscopic effects	\$GYROSCOP-IC DATA	41	--		yes*		
Print structural and mass matrices	\$MATRIX PRINT LIST	44	yes		yes		

\* To account for the effects of angular momentum in the stability and control analysis gyroscopic data must also be input to the SDSS program. This was not done for this demonstration case.

TABLE C.0-4. -NM PROGRAM INPUT OPTION USAGE

INPUT OPTION	FIELD DESCRIPTOR	CARD NO.	DART MODEL I	DART MODEL II	707-320B	SST	YF-12A
			NM-1 01-04		NN-3 03-04		
Data control card for elastic formulation	\$OPTION	4	yes		yes		
Structural modeling, symmetric motion	OPT-S	5	RESIDUAL-ELASTIC	N O T	RESIDUAL-ELASTIC	N O T	N O T
Structural modeling, anti-symmetric motion	OPT-A	5	RESIDUAL-ELASTIC	E X E C U T E D	RESIDUAL-ELASTIC	E X E C U T E D	E X E C U T E D
Eigenvalues calculated	NEIG	7	yes		yes		



TABLE C.O-5.—ESIC PROGRAM INPUT OPTION USAGE

INPUT OPTION	FIELD DESCRIPTOR	CARD NO.	DART MODEL I	DART MODEL II	707-320B	SST	YF-12A	
			ESIC-1 01-09				ESIC-5A 05-03	ESIC-5B 05-08
Print GD data from GD tape	PrintGD	5	-- --	N	N	-- --	-- --	-- --
Data control card for catalog	\$CATALOG	6	yes			yes	yes	yes
Input total values of A/P mass and moments of inertia	\$MOMENT DATA	12	-- --	O T	O T	-- --	-- --	-- --
Input structural geometric data by tape	\$TAPE	15	-- --	E	E	-- --	-- --	-- --
Input structural geometric data by cards	\$DEGREES OF FREEDOM	17	yes	X E C	X E C	yes	yes	yes
Use slender Body mass multiplying (scale) factors	\$SCALE FACTORS	25	-- --	U T E D	U T E D	yes	yes	yes
Use Thin Body mass multiplying (scale) factors	\$SCALE FACTORS	32	-- --	E D	E D	yes	yes	yes
Print structural/transformation matrices	\$MATRIX PRINT LIST	34	yes			-- --	yes	yes

TABLE C.0.6.-SD&SS PROGRAM INPUT OPTION USAGE

INPUT OPTION	FIELD DESCRIPTOR	CARD NO.	DART MODEL I				707-320B	
			SDSS-1A 1-05	SDSS-1B 01-06	SDSS-1C 01-10	SDSS-1D 01-11	SDSS-3A 03-05	SDSS-3B 03-09
Steady reference motion specified	Motion <sub>REF</sub>	5	COUPLED	COUPLED	SYMMETRIC	SYMMETRIC	SYMMETRIC	SYMMETRIC
Structural model used	Elastic <sub>OP</sub>	5	STATIC-ELASTIC	STATIC-ELASTIC	STATIC-ELASTIC	RESIDUAL-ELASTIC	RIGID	
Specify steady/unsteady A/D analysis	Unsteady <sub>OP</sub>	6	UNSTEADY	UNSTEADY	UNSTEADY	UNSTEADY	steady	
Account for Thin Body thickness effects	Thickness <sub>OP</sub>	6	--	yes	--	yes	--	
Account for leading edge thrust	LE Thrust <sub>OP</sub>	6	--	yes	--	yes	--	
<b>Compute stick speed stability derivative</b>	Speed <sub>OP</sub>	6	yes	yes	yes	yes	yes	yes
Compute gust matrices for input to TH program	Gust <sub>OP</sub>	6	yes	yes	--	--	yes	yes
Specify load factor/pitch rate	Load Factor <sub>OP</sub>	6	pitch	pitch	pitch	pitch	pitch	pitch
Execute SD&SS vs. scan input data	GD Tape	7	execute	execute	execute	execute	execute	execute
Print GD data from GD tape	Print <sub>GD</sub>	7	--	--	--	--	--	--
Execute SD&SS partially vs. totally	AIC Tape	7	total	total	total	total	total	total
Input structural data by tape vs. rigid body data by cards	SIC Tape	7	tape	tape	tape	tape	tape	cards

TABLE C.0-6. - CONTINUED

INPUT OPTION	FIELD DESCRIPTOR	CARD NO.	DAKT MODEL II	SST			YF-12A	
				SDSS-4A 04-04	SDSS-4B 04-05	SDSS-4C 04-08	SDSS-5A 05-04	SDSS-5B 05-09
Steady reference motion specified	Motion <sub>REF</sub>	5	COUPLED	SYMMETRIC	SYMMETRIC	SYMMETRIC	SYMMETRIC	SYMMETRIC
Structural model used	Elastic <sub>OP</sub>	5	RIGID	STATIC-ELASTIC	STATIC-ELASTIC	STATIC-ELASTIC	STATIC-ELASTIC	STATIC-ELASTIC
Specify steady/unsteady A/D analysis	Unsteady <sub>OP</sub>	6	UNSTEADY	steady	UNSTEADY	UNSTEADY	steady	steady
Account for Thin Body thickness effects	Thickness <sub>OP</sub>	6	yes	yes	yes	yes	yes	yes
Account for leading edge thrust	LE Thrust <sub>OP</sub>	6	yes	yes	yes	yes	---	---
<b>Compute stick speed stability derivative</b>	Speed <sub>OP</sub>	6	yes	---	yes	yes	---	---
Compute gust matrices for input to TH program	Gust <sub>OP</sub>	6	---	---	---	---	---	---
Specify load factor/pitch rate	Load Factor <sub>OP</sub>	6	pitch	pitch	pitch	pitch	load	load
Execute SD&SS vs. scan input data	GD Tape	7	execute	execute	execute	execute	execute	execute
Print GD data from GD tape	Print <sub>GD</sub>	7	---	---	---	---	---	---
Execute SD&SS partially vs. totally	AIC Tape	7	total	total	total	total	total	total
Input structural data by tape vs. rigid body data by cards	SIC Tape	7	cards	tape	tape	tape	tape	tape

TABLE C.O-6. - CONTINUED

INPUT OPTION	FIELD DESCRIPTOR	CARD NO.	DART MODEL I				707-320B	
			SDSS-1A 1-05	SDSS-1B 01-06	SDSS-1C 01-10	SDSS-1D 01-11	SDSS-3A 03-05	SDSS-3B 03-09
FLEXSTAB program which generated SICTP3 tape	IN/EX_SIC	7	isic	isic	esic	esic	isic	- - -
Linear and mass units specified for SD&SS calculations	Units	8	METERS	METERS	METERS	METERS	FEET	FEET
Parameters used to specify flight conditions	ALT_OP	8	altitude & temp.	altitude & temp.	altitude & temp.	altitude & temp.	altitude & temp.	velocity & dynamic press
Set $\alpha$ to 0° for Slender Bodies off plane of symmetry	ALPHA_OP	8	- - -	- - -	- - -	- - -	- - -	- - -
Print job status messages	Print JOB	8	- - -	- - -	- - -	- - -	- - -	- - -
Print matrix operation messages	Print MAT	8	- - -	- - -	- - -	- - -	- - -	yes
Print AIC, ISIC, ESIC, or SD&SS matrices as specified	\$MATRIX PRINT	13	yes	yes	yes	yes	yes	yes
Save additional SD&SS matrices	\$SDSS MATRIX	16	- - -	- - -	- - -	- - -	- - -	- - -
Account for thrust effects or analyze for gliding flight	\$THRUST DATA	19	glide	glide	glide	glide	thrust	thrust
Account for gyroscopic effects	\$GYROSCOP-IC DATA	23	- - -	- - -	- - -	- - -	- - -	- - -
Control surface panel identification	\$CONTROL SURFACE DATA	28	yes	yes	yes	yes	yes	yes
Stability problem data	\$STABILITY DATA	34	yes	yes	yes	yes	yes	yes

TABLE C.0.6.—CONTINUED

INPUT OPTION	FIELD DESCRIPTOR	CARD NO.	DART MODEL II	SST			YP-12A	
				SDSS-4A 04-04	SDSS-4B 04-05	SDSS-4C 04-08	SDSS-5A 05-04	SDSS-5B 05-09
FLEXSTAB program which generated SICTP3 tape	IN/EX_SIC	7	SDSS-2 02-03	esic	esic	esic	esic	esic
Linear and mass units specified for SD&SS calculations	Units	8	METERS	FEET	FEET	FEET	IN/FT	IN/FT
Parameters used to specify flight conditions	ALT_OP	8	altitude & temp.	altitude & temp.	altitude & temp.	altitude & temp.	velocity & dynamic press	velocity & dynamic press
Set $\alpha$ to 0° for Slender Bodies off plane of symmetry	ALPHA_OP	8	--	yes	yes	yes	--	--
Print job status messages	Print_JOB	8	--	--	--	--	--	--
Print matrix operation messages	Print_MAT	8	--	yes	yes	yes	--	--
Print AIC, ISIC, ESIC, or SD&SS matrices as specified	\$MATRIX PRINT	13	--	yes	yes	yes	yes	yes
Save additional SD&SS matrices	\$SDSS MATRIX	16	--	--	--	--	--	--
Account for thrust effects or analyze for gliding flight	\$THRUST DATA	19	glide	thrust	thrust	thrust	thrust	thrust
Account for gyroscopic effects	\$GYROSCOPIC DATA	23	--	--	--	--	--	--
Control surface panel identification	\$CONTROL SURFACE DATA	28	yes	yes	yes	yes	yes	yes
Stability problem data	\$STABILITY DATA	34	yes	yes	yes	yes	yes	yes

TABLE C.O-6.-CONTINUED

INPUT OPTION	FIELD DESCRIPTOR	CARD NO.	DART MODEL I				707-320B	
			SDSS-LA 01-05	SDSS-LB 01-06	SDSS-1C 01-10	SDSS-1D 01-11	SDSS-3A 03-05	SDSS-3B 03-09
Type of stability problem* (specifies source of A/D co- efficients and method used to obtain trim parameters)	PROBLEM	35	SPECIFIED	SPECIFIED	SPECIFIED	SPECIFIED	CONSTANT	ITERATION
Type of shape*	SHAPE <sub>OP</sub>	36	JIG	JIG	JIG	JIG	JIG	REFERENCE
Compute thrust/flight path angle ( $\gamma$ )	Thrust <sub>OP</sub>	36	Y	Y	Y	Y	thrust	thrust
Print trim matrices	Print <sub>TRIM</sub>	36	yes	yes	yes	yes	yes	--
Input camber shape data by cards	Shape <sub>IN</sub>	37	--	--	--	--	--	--
Punch computed camber shape on cards	Shape <sub>OUT</sub>	37	--	--	--	--	--	--
Input aerocentroid position vector by cards	Disp <sub>IN</sub>	37	--	--	--	--	--	no input
Punch computed aerocentroid position vector on cards	Disp <sub>OUT</sub>	37	--	--	--	--	--	not calculated
Punch steady pressure distri- bution on cards	Press <sub>OP</sub>	37	--	--	--	--	--	yes
Compute steady structural loads for input to SLOADS or ALOADS programs	Loads <sub>OP</sub>	37	yes	yes	yes	yes	yes	--

\* see Vol. II, Table 9.2-1

TABLE C.O-6.--CONTINUED

INPUT OPTION	FIELD DESCRIPTOR	CARD NO.	DART MODEL II	SST			YF-12A	
				SDSS-4A 04-04	SDSS-4B 04-05	SDSS-4C 04-08	SDSS-5A 05-04	SDSS-5B 05-09
Type of stability problem* (specifies source of A/D coefficients and method used to obtain trim parameters)	PROBLEM	35	SPECIFIED	CONSTANT	CONSTANT	CONSTANT	CONSTANT	CONSTANT
Type of shape*	SHAPE <sub>OP</sub>	36	JIG	DESIGN	JIG	JIG	JIG	JIG
Compute thrust/flight path angle ( $\gamma$ )	Thrust <sub>OP</sub>	36	Y	thrust	thrust	thrust	thrust	thrust
Print trim matrices	Print <sub>TRIM</sub>	36	yes	yes	yes	yes	yes	yes
Input camber shape data by cards	Shape <sub>IN</sub>	37	- - -	- - -	yes	yes	yes	yes
Punch computed camber shape on cards	Shape <sub>OUT</sub>	37	- - -	yes	- - -	- - -	- - -	- - -
Input aerocentroid position vector by cards	Disp <sub>IN</sub>	37	no input	- - -	yes	yes	- - -	- - -
Punch computed aerocentroid position vector on cards	Disp <sub>OUT</sub>	37	not calculated	yes	- - -	- - -	- - -	- - -
Punch steady pressure distribution on cards	Press <sub>OP</sub>	37	- - -	not calculated	- - -	- - -	- - -	- - -
Compute steady structural loads for input to SLOADS or ALOADS programs	Loads <sub>OP</sub>	37	- - -	- - -	yes	yes	yes	yes

\* See Vol. II, Table 9.2-1

TABLE C.O-6.-CONTINUED

INPUT OPTION	FIELD DESCRIPTOR	CARD NO.	DART MODEL I					707-320B	
			SDSS-1A 01-05	SDSS-1B 01-06	SDSS-1C 01-10	SDSS-1D 01-11	SDSS-3A 03-05	SDSS-3B 03-09	
Input wind tunnel data	\$WIND TUNNEL DATA	47	- - -	- - -	- - -	- - -	- - -	- - -	yes
Obtain $C_L, C_D, C_m$ from external data input by cards	ICO <sub>OP</sub>	49	- - -	- - -	- - -	- - -	- - -	- - -	yes
Compute dynamic stability derivatives required for the dynamic equations of motion	\$PERT	58	yes	yes	yes	yes	yes	yes	yes
Perturbation motion to be analyzed	MotionPERT	59	BOTH	BOTH	SYMMETRIC	SYMMETRIC	BOTH	BOTH	BOTH
Account for effect of compressibility on speed and yaw rate derivatives	Comp <sub>OP</sub>	59	yes	yes	yes	yes	yes	yes	yes
Punch unsteady pressures on cards	Upress <sub>OP</sub>	59	- - -	- - -	- - -	- - -	- - -	- - -	- - -
Compute control derivatives	Coneff <sub>OP</sub>	59	yes	yes	yes	yes	yes	yes	yes
Compute unsteady structural loads for input to SLOADS program	Loads <sub>OP</sub>	59	yes	yes	yes	yes	yes	yes	- - -
Print perturbation stability matrices computed for input to TH program	PrintPERT	59	yes	yes	yes	yes	yes	yes	- - -
Obtain steady perturbation derivatives from external data input by cards	Steady <sub>OP</sub>	60	- - -	- - -	- - -	- - -	- - -	- - -	yes
Obtain unsteady perturbation derivatives from external data input by cards	Unsteady <sub>OP</sub>	67	- - -	- - -	- - -	- - -	- - -	- - -	yes



TABLE C.O-6.—CONTINUED

INPUT OPTION	FIELD DESCRIPTOR	CARD NO.	DART MODEL II	SST			YP-12A	
				SDSS-4A 04-04	SDSS-4B 04-05	SDSS-4C 04-08	SDSS-5A 05-04	SDSS-5B 05-09
Input wind tunnel data	\$WIND TUNNEL DATA	47	SDSS-2 02-03	---	---	---	---	---
Obtain $C_L$ , $C_D$ , $C_m$ from external $\alpha$ , $\dot{\alpha}$ , $\dot{\beta}$ data input by cards	ICO <sub>OP</sub>	49	---	---	---	---	---	---
Compute dynamic stability derivatives required for the dynamic equations of motion	\$PERT	58	yes	yes	yes	---	---	---
Perturbation motion to be analyzed	Motion PERT	59	BOTH	SYMMETRIC	SYMMETRIC	---	---	---
Account for effect of compressibility on speed and yaw rate derivatives	Comp <sub>OP</sub>	59	yes	yes	yes	---	---	---
Punch unsteady pressures on cards	Upress <sub>OP</sub>	59	---	not calculated	not calculated	---	---	---
Compute control derivatives	Coneff <sub>OP</sub>	59	yes	yes	yes	---	---	---
Compute unsteady structural loads for input to SLOADS program	Loads <sub>OP</sub>	59	---	---	---	---	---	---
Print perturbation stability matrices computed for input to TH program	Print PERT	59	yes	yes	yes	---	---	---
Obtain steady perturbation derivatives from external data input by cards	Steady <sub>OP</sub>	60	---	---	---	---	---	---
Obtain unsteady perturbation derivatives from external data input by cards	Unsteady <sub>OP</sub>	67	---	---	---	---	---	---

TABLE C.O-6.-CONTINUED

INPUT OPTION	FIELD DESCRIPTOR	CARD NO.	DART MODEL I				707-320B	
			SDSS-1A 01-05	SDSS-1B 01-06	SDSS-1C 01-10	SDSS-1D 01-11	SDSS-3A 03-05	SDSS-3B 03-09
Compute airplane dynamic stability characteristics	\$DYNAMIC ANALYSIS	73	- - -	- - -	- - -	- - -	yes	yes
Adjust computed airplane reference forces and/or obtain downwash matrices from external data input by cards	\$EXTERIOR INFLUENCE DATA	76	- - -	- - -	- - -	- - -	- - -	- - -
Input rigid body mass, C.G. location, and moments of inertia by card	\$STRUCTURAL DATA	81	- - -	- - -	- - -	- - -	- - -	yes
Adjust computed lifting and side force pressures, or forces using external data input by cards	\$PRESSURE DATA	85	- - -	- - -	- - -	- - -	- - -	- - -
Adjust panel areas used to compute forces from pressures	\$AREA RATIO	93	- - -	- - -	- - -	- - -	- - -	- - -
Specify method of selecting panels for which areas are adjusted	IP OP	94	- - -	- - -	- - -	- - -	- - -	- - -
Re-execute SD&SS for another case using the existing output saved from upstream programs	\$RECYCLE DATA	4*	- - -	- - -	- - -	- - -	yes	- - -
Data or parameter changed	Name	5*	- - -	- - -	- - -	- - -	ELASTIC OPTION	- - -
Print the AIC, ISIC, ESIC, or SD&SS matrices specified	\$MATRIX PRINT LIST	7*	- - -	- - -	- - -	- - -	yes	- - -

\*Card number in the Recycle Input Data Deck

TABLE C.O-6.-CONCLUDED

INPUT OPTION	FIELD DESCRIPTOR	CARD NO.	DART MODEL II	SST				YF-12A	
				SDSS-4A 04-04	SDSS-4B 04-05	SDSS-4C 04-08	SDSS-5A 05-04	SDSS-5B 05-09	
Compute airplane dynamic stability characteristics	\$DYNAMIC ANALYSIS	73	-- --		yes				
Adjust computed airplane reference forces and/or obtain downwash matrices from external data input by cards	\$EXTERIOR INFLUENCE DATA	76	-- --	-- --	-- --	-- --	-- --	-- --	
Input rigid body mass, C.G. location, and moments of inertia by card	\$STRUCTURAL DATA	81	yes	-- --	-- --	-- --	-- --	-- --	
Adjust computed lifting and side force pressures, or forces using external data input by cards	\$PRESSURE DATA	85	-- --	-- --	-- --	-- --	-- --	-- --	
Adjust panel areas used to compute forces from pressures	\$AREA RATIO	93	-- --	-- --	-- --	-- --	yes	yes	
Specify method of selecting panels for which areas are adjusted	IP OP	94	-- --	-- --	-- --	-- --	SELECT, ALL	SELECT, ALL	
Re-execute SD&SS for another case using the existing output saved from upstream programs	\$RECYCLE DATA	4*	-- --	-- --	-- --	-- --	yes	yes	
Data or parameter changed	Name	5*	-- --	-- --	-- --	-- --	N <sub>Z</sub> , Y <sub>1</sub>	N <sub>Z</sub> , Y <sub>1</sub>	
Print the AIC, ISIC, ESIC, or SD&SS matrices specified	\$MATRIX PRINT LIST	7*	-- --	-- --	-- --	-- --	yes	yes	

\*Card number in the Recycle Input Data Deck

TABLE C.0-7. - TH PROGRAM INPUT OPTION USAGE

INPUT OPTION	FIELD DESCRIPTOR	CARD NO.	DART MODEL I	DART MODEL II	707-320B	SST	YF-12A
			TH-1 01-07		TH-3 03-06		
Data control card	\$CASE	1	yes		yes		
Specify maximum error allowed in any integration step (forces variable step size)	\$ACCURACY CRITERIA	9	--	N O T	--	N O T	N O T
Write plot tape for THPLOT program	\$PLOT	13	--		yes		
Specify maximum roll, pitch, and yaw angles at which TH computations will stop	\$MAXIMUM EULER	15	--	E X E C U T E D	--	E X E C U T E D	E X E C U T E D
Specify initial conditions if residual-elastic representation of structure is used	\$ELASTIC PERTURBATION	17	--		yes		
Solve the equations of motion using external values of A/D coefficients and derivatives input on cards	\$TABULAR WIND TUNNEL	20	--		--		
Compute response to gust	\$GUST DATA	31	yes		yes		
Specify type of gust imposed	IDGUST	32	SQUARE, SINE		ONE-COSINE		

TABLE C.0-8. --SLOADS PROGRAM INPUT OPTION USAGE

INPUT OPTION	FIELD DESCRIPTOR	CARD NO.	DART MODEL I SLOADS-1 01-08	DART MODEL II SLOADS-3 03-07	SST	YF-12A
<b>Data control card</b>						
Specify method of selecting matrices to be printed	\$CASE Print <sub>OP</sub>	1	yes LISTED	yes LISTED		
For SELECTED method specify:						
"selected group" of matrices	Type	4				
airplane motion producing the loads	Motion <sub>OP</sub>	5				
elastic characteristics of structure resisting the loads	Elastic <sub>OP</sub>	5				
type of A/D forces producing the loads	S/U <sub>OP</sub>	5				
inclusion of gyroscopic load matrices in print out	Gyro <sub>OP</sub>	5				
					N O T E X E C U T E D	N O T E X E C U T E D

TABLE C.0-9.—MODELING TECHNIQUE USAGE

Modeling Technique	PROGRAM	Run Name	Deck Number
Subsonic Nacelle Modeling (see Fig. 4.2-6, Vol. II)	GD	GD-5A	05-01
Supersonic Nacelle Modeling (see Fig. 4.2-5, Vol. II)	GD	GD-4, GD-5B	04-01, 05-06
"Low/High-Wing" Modeling (see Fig. 4.2-4, Vol. II)	GD	GD-4	04-01
Nacelles Modeled Without Interference Bodies (see "Nacelle Definition, Sec. 3.5.1)	GD	GD-4	04-01
Z - Doublet Option (see Fig. 4.2-7, Vol. II)	SD&SS	SDSS-4A, SDSS-4B, SDSS-4C	04-04, 04-05, 04-08

## REFERENCES

- 3-1. Nyholm, R.W.: Test Report on BSWT 505, A Supersonic Wing Pressure Test of SA-1112P-1, A0.01523 Scale Model of the B2707-300 Airplane. Boeing document D6A11648-1, 1969. p. 3-93
- 3-2. Kruppa, E.A. Wahlstrom, S.; and Wedellsborg, B.: SAMECS Structural Analysis System -- Theory Document. Boeing document D6-23757-2TN, 1969.
- 3-3. Tinoco, E.N.: An Aeroelastic Analysis of the YF-12A Airplane Using the FLEXSTAB System. Paper No. 12. NASA TM X-3061 (Confidential), 1974.
- 3-4. Curtis, A.R., and Sumpter, C.D.: NASTRAN Structural Analysis of the YF-12A Airplane. Paper No. 11, NASA TM X-3061 (Confidential), 1974.
- 4-1. Augustyn, J.T.: Boeing Transonic Wind Tunnel Test No. 1246-High Speed Performance and Stability Test on a 0.035 Scale Model of the AWACS Configuration. Boeing Document D204-10449-1, 1971.
- 4-2. USAF Stability and Control Handbook. AF33(616)-6460, Douglas Aircraft Company, 1960.
- 4-3. Welles, Stanley W.: Boeing Transonic Wind Tunnel Test No. 866 - High Speed Performance and Stability Test on a 0.035 Scale Model of the 707-820 Airplane. Boeing Document D6-10847, 1965.
- 4-4. Campbell, J.P.; and McKinney, M.O.: Summary of Methods for Calculating Dynamic Lateral Stability and Response and for Estimating Lateral Stability Derivatives. NACA TR 1098, 1952.
- 6-1. The Boeing Company: An Analysis of Methods for Predicting the Stability Characteristics of An Elastic Airplane. NASA CR-73277, Prepared Under NASA Ames Contract No. NAS2-3662, 1968.
- 6-2. Lehr, Clarence: Summary of Stability Derivatives for the KC-135 and 707 Airplanes. Boeing Document D6-3938, 1959.
- 6-3. Larson, R.R.; and Page, Victor R.: Aerodynamic Data for the 707 Flight Simulator. Boeing Document D6-1154, 1957.
- 6-4. Booth, M.A.: Aerodynamic Data for the 707-320 and -420 Flight Simulator. Boeing Document D6-1154-6, 1960.
- 6-5. Holtzener, George: Analysis of 707-300C Dutch Roll Flight Test Data. Boeing Document D6-58132TN, 1966.

- 6-6. Flora, C.C. et al: Longitudinal Aerodynamic Stability and Control Data for the 2707-300 PPD and PT Airplane. Boeing Document D6A11789-1, 1970.
- 6-7. Hamilton, J.T.: Boeing Supersonic Wind Tunnel Test No. 491 – A Supersonic Test to Obtain Lateral-Directional and Longitudinal Stability and Control Characteristics on a Model 2707-300 PPD Configuration. Boeing Document D6-A11561, 1969.
- 6-8. Reichmanis, I.: The Calculation of Turbulent Skin-Friction with the Spalding and Chi Method for a Smooth Flat Plate in Subsonic and Supersonic Flow. Boeing Document D6-A11281-TN, 1968.
- 6-9. Nyholm, R.W.: Test Report on BSWT 505, A Supersonic Wing Pressure Test of SA-1112P-1, A .01523 Scale Model of the B2707-300 Airplane. Boeing Document D6-A11648-1, 1969.
- 6-10. Flora, C.C.; et al: B2707 Prototype Stability, Control and Handling Qualities. Boeing Document D6-A10627-1, 1970.
- 6-11. Perkin, B.R., and Erickson, L.L.: FLEXSTAB – A Computer Program for the Prediction of Loads and Stability and Control of Flexible Aircraft. Proceedings of the SCAR Conference, Part 1, NASA CP-001, November, 1976.
- 6-12. Manro, M.E.; Manning, K.J.R.; Halstaff, T.H.; and Rogers, J.T.: Transonic Pressure Measurements and Comparison of Theory to Experiment for an Arrow-Wing Configuration. NASA CR-2610, October, 1975.
- 6-13. Manro, M.E.: Supersonic Pressure Measurements and Comparison of Theory to Experiment for an Arrow-Wing Configuration. NASA CR-145046, November, 1976.
- 6-14. Rubbert, P.E., and Saaris, G.R.: Review and Evaluation of a Three-Dimensional Lifting Potential Flow Analysis Method for Arbitrary Configurations. AIAA Paper 72-188, 1972.
- 7-1. Etkin, B.: Dynamics of Flight. John Wiley and Sons, Inc. 1962.